UNIVERZA V LJUBLJANI

Fakulteta za elektrotehniko

Matej Reberšek

RAZISKOVALNA NAPRAVA ZA ELEKTROPERMEABILIZACIJO CELIČNE MEMBRANE

DOKTORSKA DISERTACIJA

LJUBLJANA, 2008

UNIVERZA V LJUBLJANI

Fakulteta za elektrotehniko

Matej Reberšek

RAZISKOVALNA NAPRAVA ZA ELEKTROPERMEABILIZACIJO CELIČNE MEMBRANE

DOKTORSKA DISERTACIJA

Mentor: profesor dr. Damijan Miklavčič

LJUBLJANA, 2008

ZAHVALA

Iskreno se zahvaljujem mojemu mentorju, prof. dr. Damijanu Miklavčiču, za strokovno vodstvo, koristne nasvete in konstruktivno kritiko pri nastanku doktorske disertacije.

Mateju Kranjcu se zahvaljujem za pomoč pri izdelavi in razvoju modificiranega Blumleinovega generatorja in Denisu Pavlihi za razvoj grafičnega uporabniškega vmesnika.

Urošu Flisarju se zahvaljujem za pomoč pri razvoju DC-DC pretvornika in Juretu Koselju za izdelavo napajalnega modula.

Prof. dr. Slavku Amonu in viš. znan. sod. dr. Danilu Vrtačniku za izdelavo elektrod na krovnem stekelcu.

Hvala tudi vsem sodelavcem Laboratorija za biokibernetiko na Fakulteti za elektrotehniko Univerze v Ljubljani, ki so s svojim znanjem in izkušnjami pripomogli k izboljšanju tega dela.

Zahvaljujem se mojim razumevajočim staršem, ki so mi ves čas stali ob strani.

Predvsem pa Moji Moji Katarini***

POVZETEK

Elektropermeabilizacija je metoda, pri kateri z visokonapetostnimi električnimi pulzi povečamo prepustnost celične membrane. Metoda se je izkazala za uspešno pri elektrokemoterapiji, ki je že v klinični uporabi, kot tudi pri genski elektrotransfekciji, elektrofuziji ter ostalih aplikacijah elektropermeabilizacije. Električne pulze za elektropermeabilizacijo generiramo s posebnimi napravami, ki jih imenujemo elektroporatorji. Te naprave imajo pogosto vgrajene tudi generatorje za elektroforezo, dielektroforezo ter ostale podsklope, ki jih uporabljamo ob elektropermeabilizaciji. Tako so elektropratorji zmožni generirati zelo širok spekter električnih signalov oziroma parametrov. Kljub temu raziskovalci pogosto nimajo komercialno dostopnih naprav, ki bi bile zmožne generirati za njih zanimive električne parametre, saj pogosto preizkušajo še ne preizkušene električne parametre ter njihova različna zaporedja. Razvijalci naprav za elektropermeabilizacijo smo tako primorani razvijati nove in nove naprave. Zato smo v okviru tega dela zasnovali nov celovit pristop k razvoju naprav za elektropermeabilizacijo, ki bo razvoj poenostavil in pohitril.

Nova zasnova vključuje vse do sedaj poznane električne parametre, ki se uporabljajo pri raziskavah in aplikacijah elektropermeabilizacije. Ob tem pa ne izključuje vgradnje novih funkcij in generatorjev, saj se na področju elektropermeabilizacije zelo pogosto pojavljajo potrebe po novih postopkih generiranja električnih signalov. Že vnaprej predvidena možnost nadgradnje je velika prednost pred ostalimi zasnovami naprav, ki ne predvidevajo te možnosti in je zato nadgradnja naprave skoraj enako zahtevna kot razvoj nove.

Vseh v zasnovo vključenih električnih parametrov seveda ni možno generirati z enim samim generatorjem, zato smo v zasnovi predvideli modularen pristop k razvoju naprav za elektropermeabilizacijo. Modularen pristop omogoča združevanje posameznih modulov in s tem izvedbo verzije naprave s specifičnimi generatorji pulzov. V zasnovi smo predvideli, da je za pokritje celotnega raziskovalnega

področja potrebnih vsaj pet različnih verzij naprav za elektropermeabilizacijo, zaradi nekompatibilnih elektronskih elementov in metod generiranja posameznih signalov. Za vseh teh pet verzij smo podali konceptualno zasnovo, ki predlaga skupen razvoj grafičnega uporabniškega vmesnika, nadzornega in napajalnega modula za vse izvedbe naprav. Le generatorje specifičnih signalov in izhodne module bomo razvijali za vsako izvedbo posebej. Skupni moduli so med seboj povezani s splošno uporabnimi komunikacijskimi protokoli. Tako zamenjava posameznega modula ne zahteva novega razvoja ostalih modulov. S specifičnimi generatorji pa so skupni moduli povezani s programirljivimi protokoli, ki jih po potrebi enostavno spremenimo. Tako je zamenjava specifičnih generatorjev zelo enostavna in njihova struktura poljubna.

V predlagani zasnovi so upoštevane tudi varnostne zahteve. Zasnova tako natanko določa potek galvanske ločitve izhodne napetosti od omrežne napetosti. Takšna ločitev mora biti nujno določena že v zasnovi, saj je takšna ločitev učinkovita le v primeru, da je upoštevana pri razvoju vseh vzporednih modulov. Zasnova prav tako zaradi varnosti in modularnosti naprave zahteva tokovno in napetostno zaščito vsakega napajalnega vira v napravi posebej.

V okviru predlagane zasnove smo podali tudi dva nova predloga za generiranje pravokotnih pulzov. S prvim predlogom dopolnjujemo vezavo in delovanje Blumleinovega generatorja tako, da lahko generira nanosekundne pulze spremenljive dolžine in polaritete z visoko ponavljalno frekvenco. Drugi predlog pa dopolnjuje generatorje dolgih pravokotnih pulzov, ki tako lahko generirajo dobro definirane pravokotne pulze tudi pri večjih obremenitvah generatorja.

Razvili in izdelali smo verzijo naprave kratkih visokonapetostnih pulzov, v katero smo vgradili predlagani modificirani Blumleinov generator, ki nam omogoča generiranje nanosekundnih pulzov spremenljive dolžine od 20 ns do 200 ns, amplitude od 50 V do 1000 V poljubne polaritete in ponavljalne frekvence do 1,1 MHz. V okviru razvoja prve verzije naprave smo izdelali vse skupne module, in sicer grafični uporabniški vmesnik, nadzorni in napajalni modul ter specifična modula za modificirani Blumleinov generator, in sicer zakasnilno vezje in izhodni modul.

Pri raziskavah elektropermeabilizacije so zelo pomembne tudi elektrode. Različne oblike elektrod namreč omogočajo generiranje električnih polj različnih

porazdelitev in amplitud z enakimi električnimi pulzi. Omogočajo nam tudi različne postopke dela s celicami kot tudi različne načine opazovanja celic. V delu smo zato predstavili izvedbo dveh novih komor oziroma elektrod. S predstavljenimi elektrodami na krovnem stekelcu lahko pod mikroskopom opazujemo učinke nanosekundnih električnih pulzov na biološke celice z dobro definiranim, razmeroma homogenim in zelo velikim električnim poljem, do 100 kV/cm. S predstavljeno koničasto komoro z vgrajenimi elektrodami lahko generiramo električno polje v več smereh, kar se je že izkazalo za učinkovito pri genski elektrotransfekciji in elektrofuziji. Prednost nove komore pa je predvsem zmanjšano število potrebnih pipetiranj med postopkom elektropermeabilizacije ter s tem nezaželenih poškodb celic.

Ključne besede: elektropermeabilizacija, modularni elektroporator, modificiran Blumleinov generator, elektrode na krovnem stekelcu, koničasta komora z vgrajenimi elektrodami.

ABSTRACT

Electropermeabilization is a method used to permeabilize cell membrane by means of high-voltage electric pulses. Method has been proven to be successful in electrochemotherapy, which is used in clinics, as in gene electrotransfer, electrofusion and other applications of electropermeabilization. Electric pulses for electropermeabilization are generated with special devices, i.e. electroporators. It is quite common for these devices to also have integrated generators for electrophoresis, dielectrophoresis and other components, which are used in addition to electropermeabilization. Therefore electroporators generate electrical signals with a wide range of parameters. Nevertheless researchers often do not have commercially available devices, which would generate electrical parameters required, as they by definition often try to use electrical parameters not yet tested and their various combinations. Developers of the devices for electropermeabilization are therefore often requested to develop new devices. For this reason we designed a new concept of developing high voltage devices for electropermeabilization, which will simplify and speed up the development and prototyping of electropermeabilization devices.

This new concept includes all electrical parameters up to now known, which are used in research and numerous applications of electropermeabilization. Furthermore, the concept does not exclude incorporating new functions and generators, as they are often needed in the field of electropermeabilization research and applications development. This concept allows device upgrade and thus represents great advantage with respect to other devices, which does not include this option and the improvement of the device takes almost as long as development of new one.

It is clearly not possible to generate all electrical parameters within the range of interest with the same generator. Therefore we have developed concept for modular electropermeabilization devices, which enables combining of several modules and thus realization of device version with specific pulse generators. In the concept we have foreseen that five different device versions for electropermeabilization are

necessary to cover the entire range of electrical pulse parameters of interest in the research field at the moment, because of incompatibility of electrical elements and the methods for particular signal generation. For all these five versions the conceptual plan was given that encompasses common development of graphical user interface, control and source modules. Only specific signal generators and output modules are then developed separately for each version. Common modules are interconnected with generally used communication protocols. Thus, changing of particular module does not require new development of other modules. Specific generators and common modules are interconnected via programmable protocols. These programmable protocols are changed as necessary. In this way, changing of specific generators is simplified and their structure more flexible.

The security measures and requirements are also included in the structure, which exactly defines a line of galvanic separation of output voltage from network voltage. Such separation should be included in the plan, as it is effective only if it is considered in the development of all parallel modules. Because of the security and the modularity of the device the conceptual plan also requires current and voltage protection of each power source in the device.

Two new configurations for generating square pulses were presented. The first configuration is a modified Blumlein generator, which enables generation of nanosecond pulses with variable duration and polarity with high repetition rate. The second configuration is a modified long square pulse generator, so that well defined square pulses can be generated under high load.

We have developed and constructed the device version of short high voltage pulses. In this device we have incorporated the modified Blumlein generator, which enables generation of nanosecond pulses of variable length from 20 ns to 200 ns, amplitude from 50 V to 1000 V of arbitrary polarity and repetition rate up to 1.1 MHz. Within the development of the first device version we have developed all the common modules, i.e. graphical user interface, control and source module, and specific modules for modified Blumlein generator e.g. the delay and the output module.

The interface between electropermeabilization device and sample under investigation are the electrodes. Different shapes of electrodes enable generation of

electric fields of different distributions and amplitudes with identical electrical pulses. Different shapes of electrodes also enable different cell handling protocols and different cell observation methods. For this, we have presented two new electrode chambers, i.e. electrodes on cover glass and tip electrode chamber. With electrodes on the cover glass we can observe effects of nanosecond pulses on biological cells under microscope. With these electrodes well defined, relatively homogeneous and very high (up to 100 kV/cm) electrical field can be assured. With tip electrode chamber we can generate electrical field in different directions, which has proven to be successful in gene electrotransfer and electrofusion. Advantage of this new chamber is reduced pippeting needed during electropermeabilization process i.e. minimal cell handling and thus unnecessary cell damage due to mechanical stress.

Key words: electropermeabilization, modular electroporator, modified Blumlein generator, electrodes on cover glass, tip electrode chamber.

KAZALO

1 UVOD

1.1 Elektropermeabilizacija

Elektropermeabilizacija je biofizikalen pojav, pri katerem se zaradi povečane transmembranske napetosti poveča prepustnost lipidne membrane (P_M). Transmembranska napetost (U_{TM}) mora pri tem preseči pragovno vrednost (U_P). V stanju povečane prepustnosti lahko celično membrano prehajajo tudi ioni in molekule, ki je drugače ne morejo prehajati (Slika 1.1) [Neumann et al., 1989, 1999; Weaver in Chizmadzhev, 1996; Maček-Lebar et al., 1998; Teissié et al., 1999, 2005; Mir, 2000; Gehl, 2003; Rols, 2006].

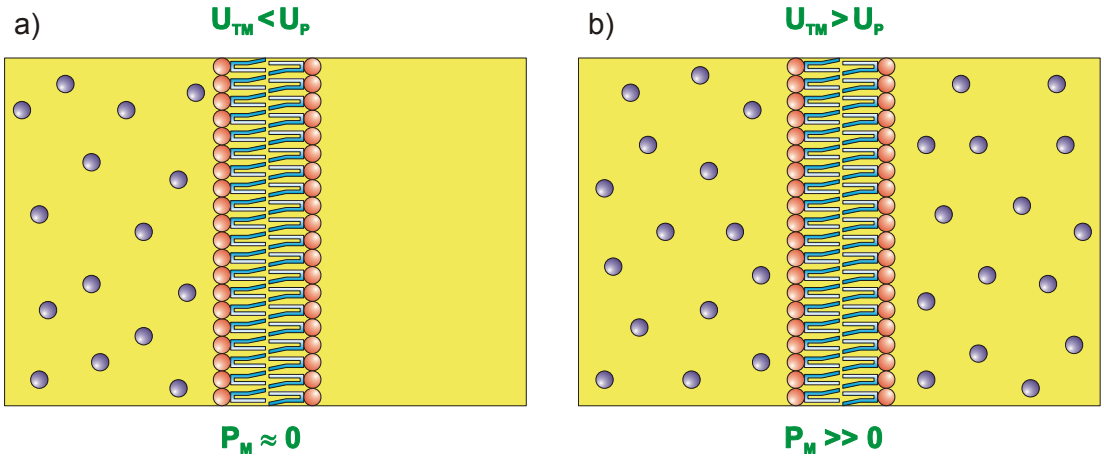

Slika 1.1 Elektropermeabilizacija lipidne membrane. Stanje pred elektropermeabilizacijo (a). Stanje po elektropermeabilizaciji (b). Lipidna membrana (oranžno – polarna glava in svetlo modro – nepolarni rep). Ioni in nekatere molekule (vijolično).

Na učinkovitost elektropermeabilizacije vplivajo številni dejavniki, ki jih razdelimo na parametre električnega polja (električna poljska jakost, trajanje posameznega električnega pulza, število pulzov, ponavljalna frekvenca pulzov, oblika pulzov in smer električnega polja) [Rols in Teissié, 1998; Vernhes et al., 1999; Kotnik et al., 2001a, 2001b, 2003; Maček-Lebar in Miklavčič, 2001; Canatella et al., 2001; Pucihar et al., 2002; Faurie et al., 2004; Reberšek et al., 2007] in druge

fizikalne ter biološke dejavnike, ki opisujejo celico in njihovo okolico (velikost in oblika celice, osmotski tlak, temperatura itd.) [Rols et al., 1992, 1994; Kotnik et al., 1997; Golzio et al., 1998; Bobrowska-Hagerstand et al., 1998; Pucihar et al., 2001]. S pravilno izbranimi parametri električnega polja lahko dosežemo, da je elektropermeabilizacija popolnoma reverzibilna. Slednje pomeni, da se po določenem času prepustnost celične membrane povrne v prvotno stanje. V nasprotnem primeru je elektropermeabilizacija ireverzibilna in celice izgubijo svojo zmožnost za preživetje [Kotnik et al., 2000]. Področji reverzibilne in ireverzibilne elektropermeabilizacije lahko določimo eksperimentalno, tako da pri različnih amplitudah elektropermeabilizacijskega pulza določimo delež elektropermeabiliziranih in delež odmrlih celic ob konstantnih ostalih parametrih pulza (Slika 1.2).

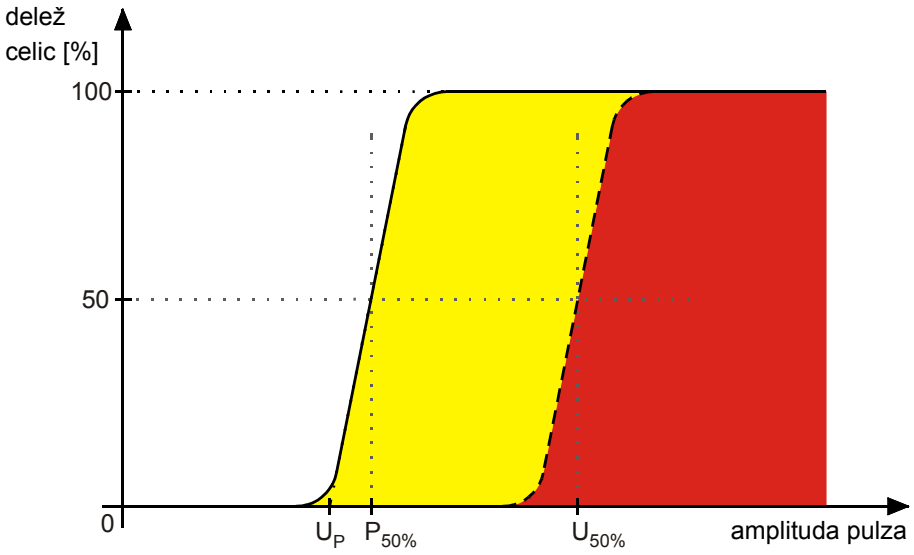

Slika 1.2 Področje reverzibilno (rumeno) in ireverzibilno (rdeče) elektropermeabiliziranih celic v odvisnosti od amplitude električnega pulza (povzeto po [Kotnik et al., 2000]). Neprekinjena črta predstavlja delež elektropermeabiliziranih celic, črtkana črta pa delež odmrlih celic.

Začetek področja reverzibilne elektropermeabilizacije celic opredelimo kot amplitudo, pri kateri delež poriranih celic doseže 50% celotne populacije ($P_{50\%}$). Mejo med reverzibilno in ireverzibilno elektropermeabilizacijo pa opredelimo kot amplitudo, pri kateri delež odmrlih celic doseže 50% celotne populacije ($O_{50\%}$). V kolenu, kjer začne elektropermeabilizacija celic močno naraščati, določimo pragovno napetost (U_P). S Schwanovo enačbo [Schwan, 1957] lahko nato iz pragovne napetosti izračunamo kritično vrednost vsiljene transmembranske napetosti. Kritična vrednost

vsiljene transmembranske napetosti se giblje nekje med 200 mV in 1000 mV ter je določena z geometrijskimi, snovnimi in fiziološkimi lastnostmi membrane celice, parametri zunanjega električnega polja in medijem, ki celico obkroža [Tsong, 1991; Teissié in Rols, 1993; Miklavčič et al., 2000].

1.1.1 Uporabnost elektropermeabilizacije in raziskovalno področje električnih parametrov

Tri desetletja po prvih objavah [Kinosita in Tsong, 1977; Teissié in Tsong, 1981; Neumann et al., 1982] se elektropermeabilizacija danes uporablja na širokem področju biomedicine. Elektropermeabilizacija se tako uporablja v elektrokemoterapiji, genski elektrotransfekciji, vstavljanju beljakovin v celično membrano, fuziji celic, vnosu zdravil preko kože, čiščenju vode, konzerviranju hrane, ablaciji tkiva, elektropermeabilizaciji organelov in lipidnih dvoslojev [Wong in Neumann, 1982; Mouneimne et al., 1989; Sixou and Teissié, 1990; Tsong, 1991; Vanbeaver et al., 1994; Mir et al., 1998; Serša et al., 1998; Miklavčič et al., 2006a].

Elektrokemoterapija je metoda za zdravljenje raka, pri kateri z elektropermeabilizacijo lokalno povečamo vnos kemoterapevtika v rakaste celice [Jaroszeski et al., 1999; Mir in Orlowski, 1999]. Optimizacija električnih parametrov je pokazala, da je za elektrokemoterapijo najbolj primernih osem elektropermeabilizacijskih pulzov dolžine 100 μs, ponavljalne frekvence 1 Hz oziroma 5 kHz in amplitude med 200 V in 1000 V [Miklavčič et al., 2006b]. Dejanska amplituda je odvisna predvsem od elektrod in ciljnega tkiva. Številne klinične študije [Mir et al., 1995; Serša et al., 1998; Heller et al., 1999; Rols et al., 2002; Serša, 2006] so pripeljale do vzpostavitve standardnih operacijskih postopkov (Standard Operating Procedures - SOP) za elektrokemoterapijo [Mir et al., 2006].

Genska elektrotransfekcija je nevirusna metoda vnosa genskega materiala v biološko celico z elektropermeabilizacijo [Neumann et al., 1989; Mir, 2000; Somiari et al., 2000; Bettan et al., 2000; Ferber, 2001; Rubanyi, 2001; Herweijer in Wolff, 2003; Prud'homme et al,. 2006]. Ob elektropermeabilizacijskem učinku električnih pulzov je za učinkovito gensko elektrotransfekcijo potreben tudi elektroforetski učinek električnih pulzov na genski material. Trenutno sta najbolj zanimivi dve različici povečanja elektroforetskega učinka električnih pulzov. Pri prvi se električni

pulzi amplitude od 400 do 600 V/cm podaljšajo (do 20 ms) [Bettan et al., 2000]. Pri drugi pa se ob elektropermeabilizacijskih pulzih (8 x 100 μs z amplitudo 1300 V/cm) uporabi tudi dolg elektroforetski pulz (1 x 100 ms z amplitudo 100 V/cm) [Šatkauskas et al., 2002].

Za vstavljanje beljakovin v celično membrano se pri celicah brez jeder uporabljajo električni pulzi z amplitudo pod pragovno vrednostjo [Mouneimne et al., 1989; Hannig et al., 1995]. Medtem ko se za celice z jedrom uporabljajo električni pulzi z amplitudo nad pragovno vrednostjo [Teissié, 1998].

Z reverzibilno elektropermeabilizacijo lahko dosežemo, da se biološke celice združijo. Metodo imenujemo elektrofuzija celic. Elektrofuzija celic je uspešna le, če med ali takoj po elektropermeabilizaciji zagotovimo stik med celicami. Stik med celicami lahko dosežemo z dielektroforezo [Pilwat et al., 1981] ali centrifugiranjem [Teissié in Rols, 1986].

Z elektropermeabilizacijo in iontoforezo ($\approx$1 mA/cm^2) lahko vnesemo zdravilne učinkovine preko kože. Elektropermeabilizacija pri tem poveča prepustnost kože, medtem ko električno polje pri iontoforezi potiska električno nabite molekule skozi kožo [Prausnitz, 1996; Vanbever et al., 1999].

Ireverzibilno elektropermeabilizacijo lahko uporabimo pri ablaciji tkiva in uničevanju mikroorganizmov pri konzerviranju hrane ali čiščenju vode [Gould, 1995; Vernhes et al., 2002]. Pri izbiri električnih parametrov za ireverzibilno elektropermeabilizacijo moramo upoštevati tudi stranske učinke, kot so elektroliza, segrevanje in poraba energije [Uemura in Isobe, 2003].

V zadnjih nekaj letih številne študije poročajo, da je možno s kratkimi pulzi (do 1 μs) in visoko električno poljsko jakostjo (nad 10 kV/cm) permeabilizirati tudi organele celice ali sprožiti celično smrt [Schoenbach et al., 2001; Smith in Weaver, 2008]. Tako se s kratkimi električnimi pulzi odpira popolnoma novo področje elektropermeabilizacije, ki pa je zaenkrat zanimivo predvsem za raziskovalce.

Prav tako je za raziskovalce zanimiva tudi elektropermeabilizacija lipidnih dvoslojev kot modela celične membrane [Abidor, 1979; Kramar et al., 2007]. Te raziskave so namreč pomemben vir informacij za boljše razumevanje elektropermeabilizacije. Za elektropermeabilizacijo lipidnega dvosloja se ponavadi

uporabljajo nizke napetosti (do 1 V), saj je celotna napetost pritisnjena neposredno na samo membrano.

Ugotovimo lahko, da je učinkovitost elektropermeabilizacije na različnih področjih uporabe v veliki meri odvisna od izbire električnih parametrov. Z izbiro le teh lahko namreč povzročimo reverzibilno ali ireverzibilno elektropermeabilizacijo, elektropermeabilizacijo lipidnega dvosloja oziroma večje ali manjše elektroforetske ali dielektroforetske učinke (Slika 1.3).

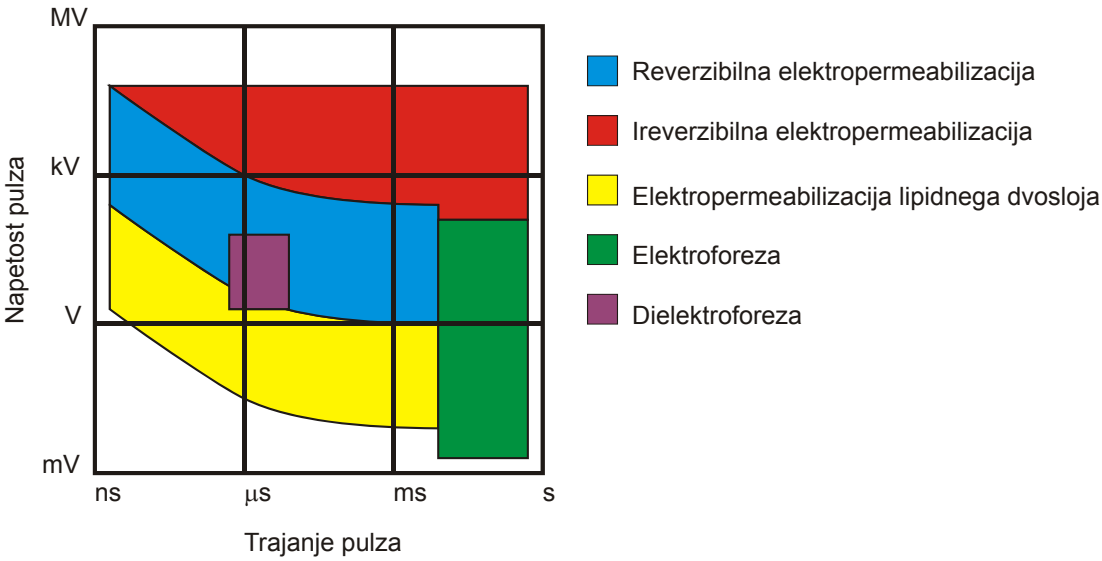

Slika 1.3 Okvirna raziskovalna področja amplitude in trajanja električnih pulzov, ki se uporabljajo pri elektropermeabilizaciji in spremljajočih učinkih.

Za reverzibilno elektropermeabilizacijo se pri dolžini pulzov 100 µs (najbolj pogosta dolžina elektropermeabilizacijskih pulzov) uporabljajo amplitude od nekaj V do nekaj 100 V, za ireverzibilno elektropermeabilizacijo od nekaj 100 V do nekaj kV in za elektropermeabilizacijo lipidnega dvosloja od nekaj 10 mV do nekaj V. S krajšanjem dolžine pulzov v nanosekundno področje se zaradi časovne konstante lipidne membrane amplitudna področja pomikajo v višje amplitude. Nasprotno pa so tipični elektroforetski pulzi dolgi nekaj ms in se uporabljajo na področju amplitude pod pragom elektropermeabilizacije. Tipični dielektroforetski pulzi pa so v frekvenčnem območju od nekaj 100 kHz do nekaj MHz in amplitude od nekaj V do nekaj 100 V.

1.2 Obstoječe izvedbe generiranja električnih signalov za elektropermeabilizacijo

Napravo, ki generira električne pulze za elektropermeabilizacijo, imenujemo elektroporator. Elektroporatorji največkrat delujejo kot napetostni viri, ki generirajo električne pulze določenih oblik. Te pulze dovedemo do celic preko elektrod, med katerimi tako vzpostavimo električno polje [Puc et al., 2004a].

Učinki posameznega električnega parametra (električna poljska jakost, trajanje posameznega električnega pulza, število pulzov, ponavljalna frekvenca pulzov, oblika pulzov in smer električnega polja) so bili v zadnjih letih obravnavani v številnih študijah [Maček Lebar in Miklavčič, 2001]. V ta namen so bili izvedeni poizkusi, v katerih so uporabili različne naprave za elektropermeabilizacijo, ki jih v nekaterih primerih ni bilo mogoče kupiti pri proizvajalcih tovrstne opreme [Defrancesco, 1997; Puc et al., 2004a]. Glavna pomanjkljivost naprav, ki jih proizvajalci nudijo na trgu, je specializiranost za konkretno, že raziskano aplikacijo elektropermeabilizacije in s tem omejitev na določene električne parametre. Zaradi takšnih omejitev naprav so bili znanstveniki v prej omenjenih študijah prisiljeni v razvoj svojih naprav, ki so zadostile potrebam njihovih poizkusov [Chang, 1989; Puc et al., 1998; Kramar, 2000; Reberšek, 2001; Petkovšek et al., 2002; Kolb et al., 2006]. Med njimi je tudi nekaj takih naprav, ki imajo zelo široko območje električnih parametrov oziroma področje uporabe [Petkovšek, 2002; Kolb et al., 2006]. Vendar kljub temu ne uspejo pokriti celotnega področja trenutno uporabnih aplikacij elektropermeabilizacije, kaj šele raziskovalno zanimivega področja.

V nadaljevanju bodo opisani trenutno najbolj zanimivi načini generiranja dolgih pulzov, kratkih pulzov in dielektroforetskih signalov, za katere bo kasneje podan tudi nov predlog izvedbe.

1.2.1 Generiranje dolgih pulzov

Za generiranje dolgih pulzov nad 1 μs najpogosteje uporabljamo različni načini vklaplanja visokonapetostnih virov in ojačevalnik s skupnim izvorom in potencialno nedoločenim vhodom [Reberšek, 2001; Petkovšek, 2004; Puc et al., 2004b].

Vklapljanje visokonapetostnega vira omogoča hitre dvižne in upadne čase pulza. Amplituda pulzev pri tem ni konstantna, ampak pada z obremenitvijo. Metoda tudi ne omogoča spreminjanja amplitude od pulza do pulza. Vklapljanje večih visokonapetostnih virov izboljša to pomanjkljivost, vendar še vedno zahteva izjemno močne in velike napetostne vire za ohranjanje amplitude pri velikih obremenitvah. Prav tako zahteva veliko število virov za natančno izbiro amplitude.

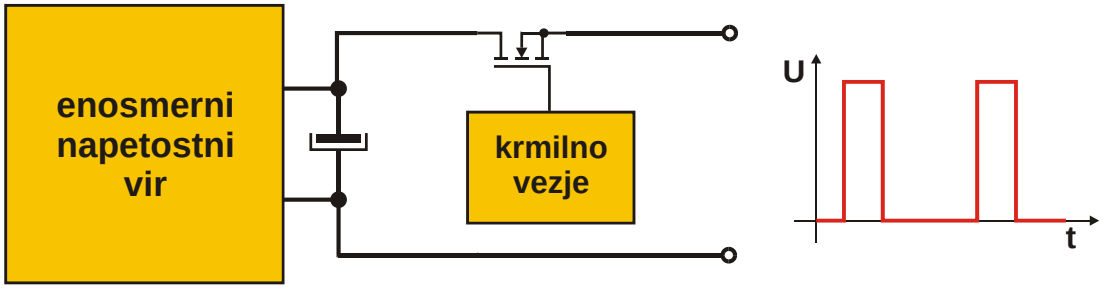

Slika 1.4 Vklapljanje visokonapetostnega vira.

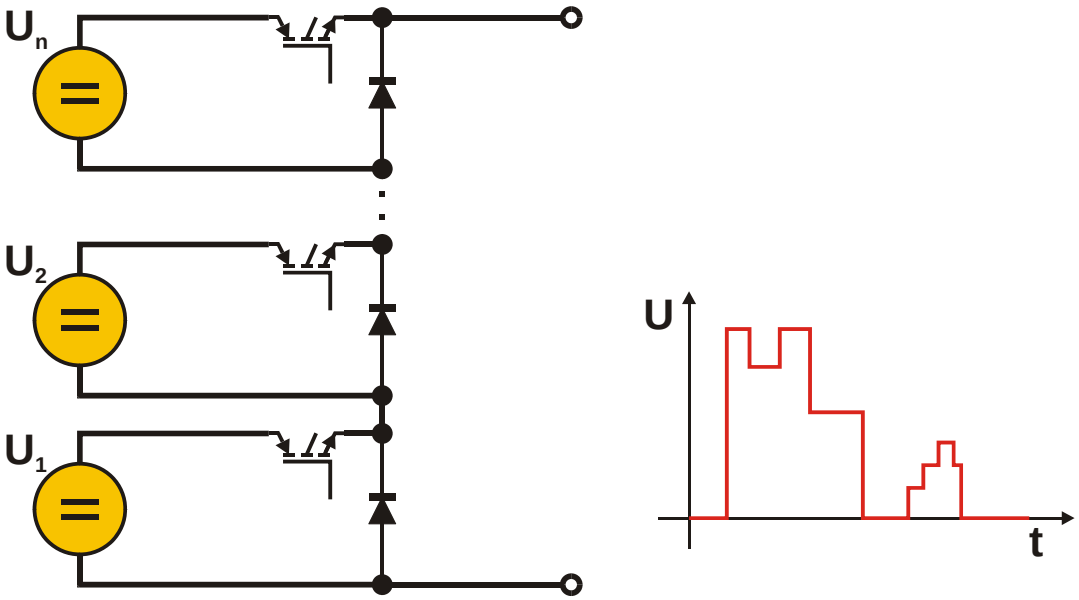

Slika 1.5 Vklapljanje visokonapetostnih virov.

Ojačevalnik s skupnim izvorom in potencialno nedoločenim vhodom ima sicer dolg dvižni in upadni čas, vendar lahko v primerjavi z različnimi načini vklapljanja visokonapetostnih virov generira izbrano amplitudo pulzov tudi pri večji obremenitvi. Lahko pa tudi razmeroma hitro zvezno spreminja amplitudo pulza, kar je potrebno pri regulaciji učinka elektropermeabilizacije [Cukjati et al., 2007].

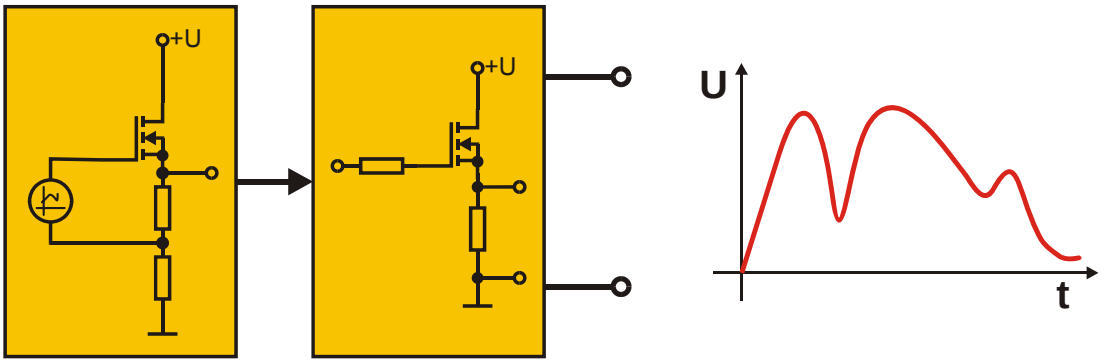

Slika 1.6 Ojačevalnik s skupnim izvorom in potencialno nedoločenim vhodom.

1.2.2 Generiranje kratkih pulzov

Za generiranje kratkih pulzov najpogosteje uporabljamo princip Blumline generatorja (Slika 1.7) [Behrend et al., 2003; Kolb et al., 2006]. Glavna slabost Blumline generatorja je nizka ponavljalna frekvenca pulzov (do 10 kHz) [Vernier et al., 2006], ker se generator polni preko nizkoprevodnega upora, in konstantna dolžina pulza, ki je odvisna od dolžine valovodne linije. Pred kratkim je bila predlagana nova konfiguracija Blumleinovega generatorja, ki omogoča generiranje nanosekundnih pulzov različnih dolžin z eno samo konstantno dolžino valovodne linije (Slika 1.8) [De Angelis et al., 2006; De Angelis et al., 2008].

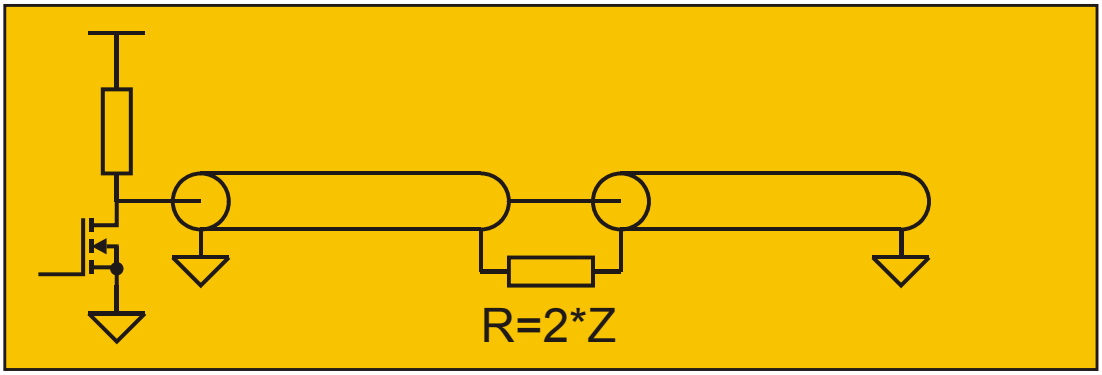

Slika 1.7 Konceptualna shema Blumleinovega generatorja.

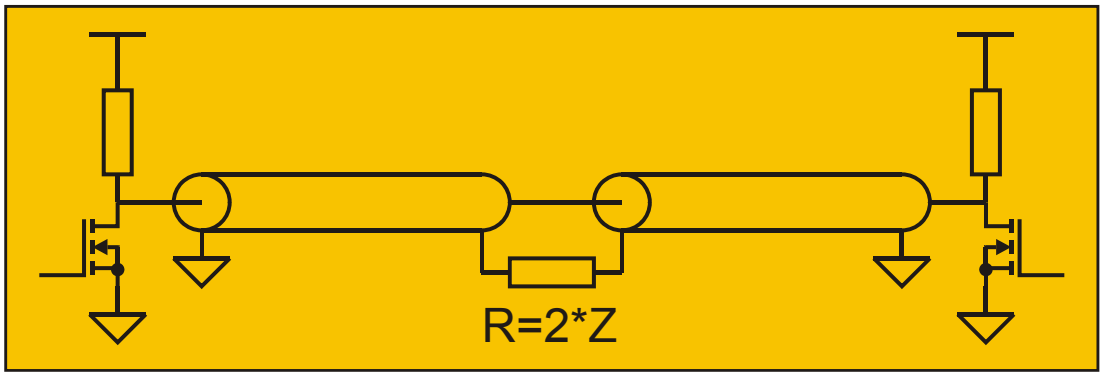

Slika 1.8 Konceptualna shema Blumleinovega generatorja z variabilno dolžino pulza.

1.2.3 Generiranje dielektroforetskih signalov

Dielektroforetske signale najpogosteje generiramo z analognimi oscilatorji, katerih signal nato napetostno in tokovno ojačamo z bipolarnim ojačevalnikom. Zato imajo ponavadi signali dolg ustalitveni čas in ozko frekvenčno območje.

1.3 Obstoječe izvedbe elektrod

Porazdelitev in jakost električnega polja med elektrodami je odvisna tudi od oblike in razdalje med elektrodami [Miklavčič et al., 2006b]. Za dve elektrodi velja, da bolj kot sta razmaknjeni, manjše je električno polje med njima. In večji kot je premer elektrod oziroma bolj kot sta elektrodi ploščati v primerjavi z razdaljo med elektrodama, bolj je polje med elektrodama homogeno. Za več elektrod so problemi podobni, bolj zahtevni [Čorović et al., 2007]. Iz naštetega sledi, da je za učinkovitost elektropermeabilizacije pomembna tudi izbira primernih elektrod.

1.3.1 Elektrode za spremembo smeri električnega polja

Med dvema elektrodama lahko obračamo zgolj polariteto električnega polja, medtem ko pri treh elektrodah lahko že obrnemo električno polje v katerokoli smer. V tem primeru potrebujemo seveda poseben generator, ki za vsako elektrodo generira točno določeno amplitudo. S posebnimi preklopnimi vezji lahko med štirimi elektrodami generiramo električno polje v štirih smereh, ne da bi pri tem spreminjali amplitudo pulza.

1.3.2 Elektrode na krovnem stekelcu

Za opazovanje učinka nanosekundnih pulzov na biološke celice najpogosteje uporabljamo elektrode na krovnem stekelcu [Sun et al., 2005; Kolb et al., 2006]. Tipičen razmik med elektrodama je 100 μm. Elektrode so ponavadi iz jekla in prilepljene na krovno stekelce s 5-40 μm lepila. Če primerjamo debelino lepila z velikostjo celice lahko ugotovimo, da so celice, ki sedimentirajo na krovno stekelce, najverjetneje že izven območja neposredno med elektrodama in zato v nehomogenem električnem polju. Električno polje na krovnem stekelcu na sredini med elektrodama, kjer najpogosteje opazujemo celice, zaradi različne debeline lepila variira tudi do 35% ob robu elektrod pa še bolj.

1.4 Izhodišče in namen naloge

Namen predlaganega dela je razvoj modularne raziskovalne naprave, katere zasnova bo omogočala uporabo njenih modulov v katerikoli obstoječi aplikaciji ali raziskavi elektropermeabilizacije. Pri razvoju modulov bomo upoštevali široko amplitudno območje (kV-mV), široko frekvenčno območje (GHz-Hz) in široko tokovno območje aplikacij (A-pA), aplikacije s pulzi različnih oblik, aplikacije s sprotnim merjenjem izhodnih parametrov in parametrov bremena ter aplikacije z večigelnimi elektrodami. Preizkusili bomo nov način generiranja kratkih in dolgih pravokotnih električnih pulzov z napetostjo do 1 kV, dolgih pravokotnih električnih pulzov z napetostjo nad 1 kV in sinusnih signalov za dielektroforezo. Tako zasnovana naprava bo s svojo prilagodljivostjo in inovativnimi rešitvami za generiranje električnih pulzov postala nepogrešljiv pripomoček raziskovalcem na področju elektropermeabilizacije, saj bo omogočala uporabo širokega območja električnih parametrov.

2 ZASNOVA RAZISKOVALNE NAPRAVE ZA ELEKTROPERMEABILIZACIJO

Preden začnemo z načrtovanjem naprave je zelo smiselno izdelati zahteve zanjo in se dodobra spoznati s tehnologijo izdelave posameznih komponent oziroma s tehnološkimi omejitvami. Včasih namreč tehnologija omejuje naše želje, včasih pa naše želje povzročijo razvoj nove tehnologije.

Želimo torej izdelati napravo, ki bo pokrila celotno raziskovalno področje električnih parametrov za elektropermeabilizacijo. To pomeni, da bo omogočala generiranje električnih pulzov z amplitudo od nekaj mV do nekaj kV, pri toku od nekaj pA do nekaj A in v frekvenčnem območju od nekaj mHz do nekaj GHz.

Vendar, ko preučimo tudi tehnološke omejitve generiranja električnih pulzov ugotovimo, da je za pokritje celotnega raziskovalnega področja elektropermeabilizacije potrebnih vsaj pet različnih verzij elektroporatorjev: verzija kratkih (do 1 μs) zelo visokonapetostnih (nad 1 kV) pulzov, verzija kratkih (do 1 μs) visokonapetostnih (do 1 kV) pulzov, verzija dolgih (nad 1 μs) zelo visokonapetostnih (nad 1 kV) pulzov, verzija dolgih (nad 1 μs) visokonapetostnih (od 5 V do 1 kV) pulzov in verzija dolgih (nad 1 μs) nizkonapetostnih (do 5 V) pulzov (Slika 2.1). Vsaj toliko različnih izvedb je potrebnih zaradi različnega načina generiranja kratkih in dolgih pulzov ter zaradi nelinearnosti elementov v različnih napetostnih in frekvenčnih območjih.

Pri kratkih pulzih je namreč dvižni čas pulza veliko krajši od časa potovanja pulza od izvora do bremena, zato je pri teh generatorjih zelo pomembna impedančna prilagoditev bremena, da ne pride do odbojev signala in s tem do podaljšanja pulza. Pri dolgih pulzih odboji niso tako pomembni, je pa bolj pomembno to, da ima lahko breme poljubno impedanco. Podobno je tudi pri električnih elementih, kjer zelo visokonapetostni (od 1 kV do 100 kV) elementi, kot so razelektritvene reže (spark gap), ne delujejo več v visokonapetostnem (od 5 V do 1 kV) območju in visokonapetostni elementi, kot so različni tranzistorji, ne delujejo v

nizkonapetostnem (do 5 V) območju, zaradi spodnje napetostne meje pri kateri začnejo delovati.

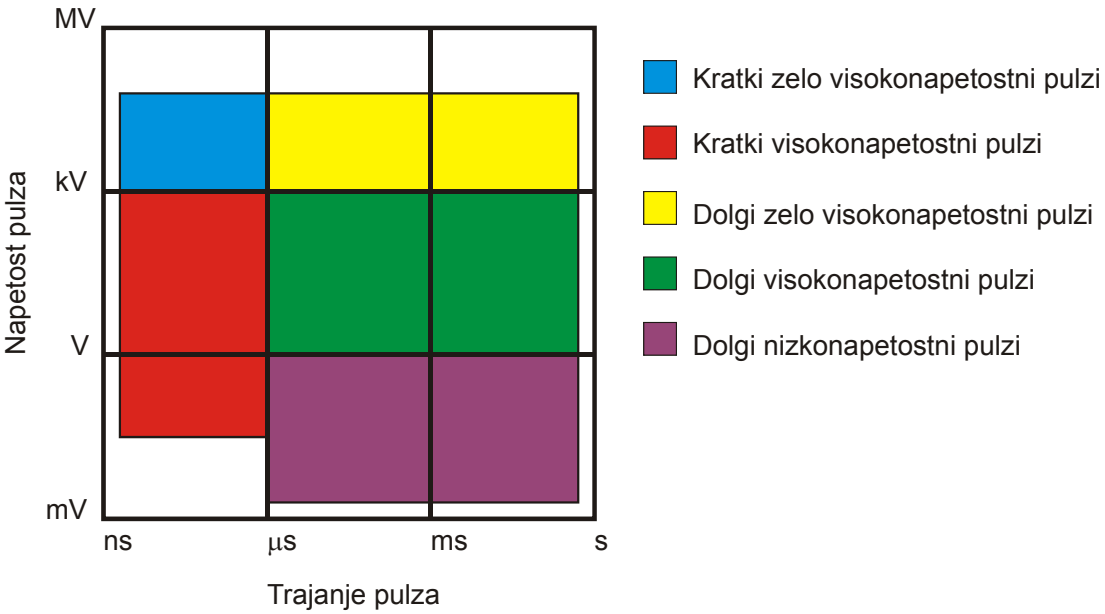

Slika 2.1 Pet različnih verzij elektroporatorjev in njihova območja amplitude in trajanja električnih pulzov. Vseh pet verzij skupaj pokriva celotno raziskovalno področje amplitude in trajanja električnih pulzov, ki se uporablja pri elektropermeabilizaciji in spremljajočih učinkih.

Poleg tega se znotraj vsakega napetostnega območja pojavi vprašanje, kako zaporedoma generirati več popolnoma različnih signalov, kot so na primer elektropermeabilizacijski, elektroforetski in dielektroforetski. Edini smiselni odgovor je, da znotraj ene verzije naredimo več generatorjev električnih pulzov, katerih delovanje nato uskladimo z kontrolno enoto. Zaradi tega smo se odločili, da začnemo našo raziskovalno napravo razvijati modularno. Vsaka enota, ki bo uporabljena v več verzijah, bo razvita samo enkrat. Pri tem imamo v mislih predvsem strojno opremo, ker bo za programsko opremo potrebno dodatno napisati za verzijo specifične aplikacije. Enote, ki bodo značilne zgolj za eno verzijo, bodo kompatibilne z vsemi enotami znotraj verzije in ne bodo obvezne, če njihove funkcije uporabnik ne potrebuje. Skupne enote bodo uporabniški grafični vmesnik, kontrolna enota in napetostni viri. Za verzijo specifične enote pa bodo predvsem generatorji različnih signalov in izhodni moduli (Slika 2.2).

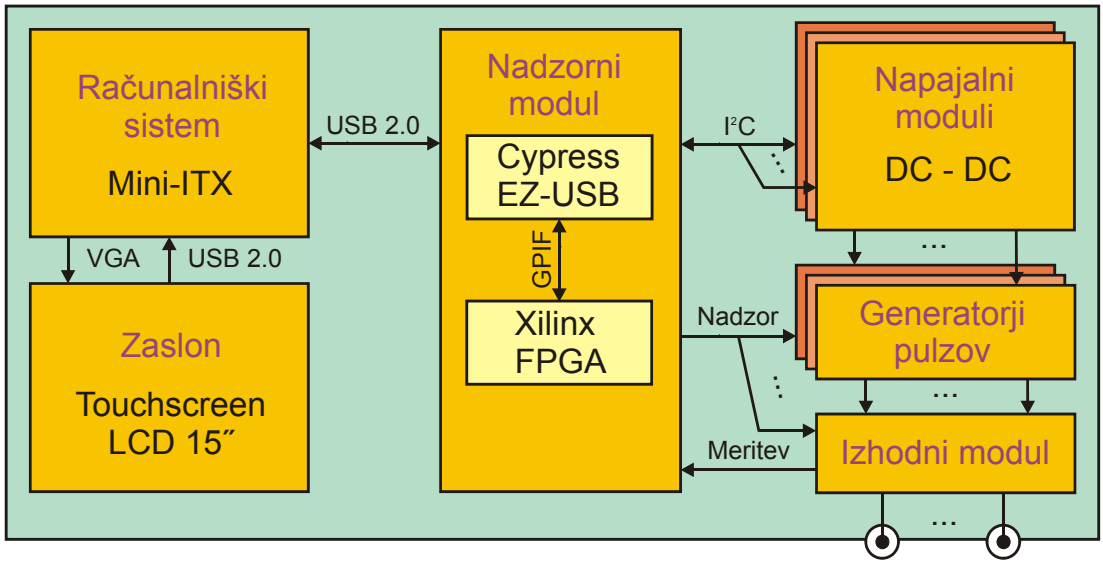

Slika 2.2 Konceptualna shema modularne zasnove raziskovalne naprave za elektropermeabilizacijo celične membrane

Uporabniški grafični vmesnik (graphical user interface - GUI) je sestavljen iz računalniškega sistema in zaslona na dotik (Touch Screen - TS). Računalniški sistem skrbi za izvajanje uporabniškega grafičnega vmesnika in nadaljnjo komunikacijo preko USB 2.0 z nadzornim modulom. Za računalniški sistem smo izbrali Mini-ITX platformo, ker ima integriranih veliko komunikacijskih protokolov, je majhna in temelji na x86 arhitekturi. Integracija komunikacijskih protokolov omogoča priklop računalniškega sistema na najrazličnejše periferne naprave brez dodatnih vmesnih enot. Tako imamo trenutno na računalniški sistem priklopljen zaslon na dotik preko VGA in USB 2.0 protokola, CompactFlash preko IDE protokola, USB ključ in nadzorni modul preko USB 2.0 protokola. V prihodnosti pa lahko po potrebi na računalniški sistem priklopimo tudi lokalno mrežo (local-area network - LAN), PCI napravo, ipd. Ker je Mini-ITX platforma majhna, zanjo ne potrebujemo veliko prostora v ohišju naprave. Ker računalniški sistem temelji na x86 arhitekturi, ga je možno brez programske spremembe enostavno zamenjati z drugo Mini-ITX ali x86 platformo in sicer v primeru, da izbrane Mini-ITX platforme ne proizvajajo več. Slednje smo med razvojem uporabniškega grafičnega vmesnika že preizkusili.

Celotna komunikacija med napravo in uporabnikom poteka preko 15" zaslona na dotik s tehnologijo površinskega akustičnega vala (surface acoustic wave - SAW). Ta tehnologija omogoča upravljanje naprave tudi z gumijastimi rokavicami, kar je v

laboratoriju potrebno. Prav tako zaradi dotičnega zaslona ne bo potrebne tipkovnice in miške, ki sta v laboratoriju z malo prostora nepriročni.

Uporabniški grafični vmesnik je napisan v programskem jeziku Visual Basic .NET Compact Framework in deluje na operacijskem sistemu Windows Embedded CE. Visual Basic .NET je splošno znan objektno orientiran programski jezik, kar pomeni, da ga veliko programerjev pozna oziroma se ga lahko vsak zelo hitro nauči. To pomeni, da je naš grafični uporabniški vmesnik dostopen za nove uporabnike, ki bi ga radi spremenili tako, da bi bil uporaben za njihov specifičen elektroporator. Operacijski sistem Windows Embedded CE je namenjen manj zmogljivim računalniškim sistemom, kakršen je tudi naš računalniški sistem. Omogoča nam popolno kontrolo nad operacijskim sistemom tudi tako, da vanj vključimo samo komponente, ki jih želimo. Tako lahko dosežemo, da se za uporabnika naprava odziva v realnem času in da je operacijski sistem nedostopen uporabniku. V operacijski sistem Windows Embedded CE smo vgradili tudi USB 2.0 gonilnik, ki smo ga razvili s pomočjo programa WinDriver (Jungo, Izrael). Ta USB 2.0 gonilnik skrbi za komunikacijo med grafičnim uporabniškim vmesnikom in nadzornim modulom.

Parametri električnih pulzov, ki jih uporabnik vnese v grafični uporabniški vmesnik se v računalniškem sistemu pretvorijo v surove strojne podatke, kar pomeni, da se lahko neposredno uporabijo za generiranje pulzov. Le tako omogočimo, da nadzorni modul kot eden najbolj obremenjenih delov naprave generira električne pulze v realnem času z realnimi amplitudami.

Nadzorni modul je sestavljen iz USB krmilnika (EZ-USB, Cypress) in programirljivega vezja (FPGA, Xilinx). Med njima poteka komunikacija preko splošno programirljivega vmesnika (General Programmable Interface – GPIF). Pri taki zasnovi nadzornega modula je večina njegovih funkcij programirljivih. Tako lahko samo s programskimi spremembami na nadzornem modulu kontroliramo vse predvidene verzije elektroporatorjev. Dana zasnova nadzornega modula omogoča tudi enostavnejši programski razvoj njegovih funkcij. USB krmilnik skrbi, da podatki iz računalniškega sistema pridejo na pravi naslov. Pri tem podatke za napajalne module usmeri preko I^2C vodila, podatke za programirljivo vezje pa preko splošno

programirljivega vmesnika. Tudi za podatke, ki gredo v obratno smer, poskrbi, da odpotujejo do prave končne točke (endpoint - EP) USB vodila.

Glavna naloga programirljivega vezja je generiranje električnih pulzov v realnem času. Zato deluje kot sinhrono sekvenčno vezje, katerega stanje definira stanje pulza (pulz, pavza...) in z istim razlogom med generiranjem električnih pulzov direktno nadzoruje generatorje pulzov in izhodni modul. Da lahko deluje v realnem času, vse potrebne parametre električnih pulzov prejme od grafičnega uporabniškega vmesnika v surovi strojni obliki že pred začetkom generiranja električnih pulzov. Prehode med stanji določajo števci stanja, ki merijo čas trajanja posameznega stanja (pulz, pavza...). Programirljivo vezje oziroma nadzorni modul na željo uporabnika predčasno ustavi generiranje pulzov ter odstrani visoko napetost z izhoda naprave. Ta funkcija je vgrajena predvsem za varnost uporabnikov v primeru nesreč in v primeru nepravilnega delovanja naprave.

Vsa nizkonapetostna vezja so napajana preko enega ATX napajalnika, medtem ko so generatorji pulzov napajani s posebnimi napajalnimi moduli. Napajalni moduli kot tudi generatorji pulzov in izhodni modul so galvansko ločeni od omrežne napetosti predvsem zaradi varnosti. Napajalni moduli delujejo kot močnostni pol-mostični DC-DC pretvornik, da lahko v najkrajšem času dosežejo želeno napetost, ki jo prejmejo v digitalni obliki preko I^2C protokola. Če je v verziji več napajalnih modulov, mora imeti vsak modul svoj I^2C naslov. Napajalni modul ima vgrajeno tudi praznilno enoto za primere, ko mora v najkrajšem času znižati napajalno napetost. To stori v primeru, ko bi visoka napetost lahko poškodovala generator pulzov ali ko uporabnik zahteva ustavitev ali izklop naprave. Napajalni moduli merijo izhodno napetost modula z namenom interne regulacije, kot tudi z namenom seznanjenja uporabnika s trenutno napetostjo modulov. Tako lahko uporabnik ali računalniški sistem preveri pravilnost delovanja napetostnih modulov.

Generatorji pulzov generirajo električne signale za elektropermeabilizacijo, elektroforezo in dielektroforezo. Ker imajo vsi ti signali skupaj preširok napetostni in frekvenčni spekter, da bi jih generirali z enim samim generatorjem, je potrebnih več generatorjev pulzov. Vsak generator ima tako svoje področje pulzov, ki jih lahko generira. Pomembno je le, da so generatorji znotraj ene same verzije med seboj kompatibilni. To pomeni, da obstaja tak električen element, ki lahko usmerja signale

vseh generatorjev. To nalogo usmerjanja izvaja izhodni modul, ki v primeru pravokotnih in bipolarnih pulzov tudi pomaga generirati pulze. V primeru, da uporabljamo več-igelne elektrode, pa izhodni modul deluje tudi kot preklopnik med elektrodami.

2.1 Zasnova verzije generatorja kratkih visokonapetostnih pulzov

Verzija kratkih visokonapetostnih pulzov omogoča generiranje nanosekundnih pulzov variabilne dolžine in polaritete ter visoke ponavljalne frekvence. Variabilno dolžino pulzov dosežemo s sinhroniziranim proženjem stikal na obeh koncih valovodnih linij Blumleinovega generatorja. Medtem, ko visoko ponavljalno frekvenco pulzov dosežemo z aktivnim polnjenjem valovodnih linij z obeh koncev Blumleinovega generatorja. Taka konfiguracija omogoča tudi generiranje bipolarnih nanosekundnih pulzov (Slika 2.3).

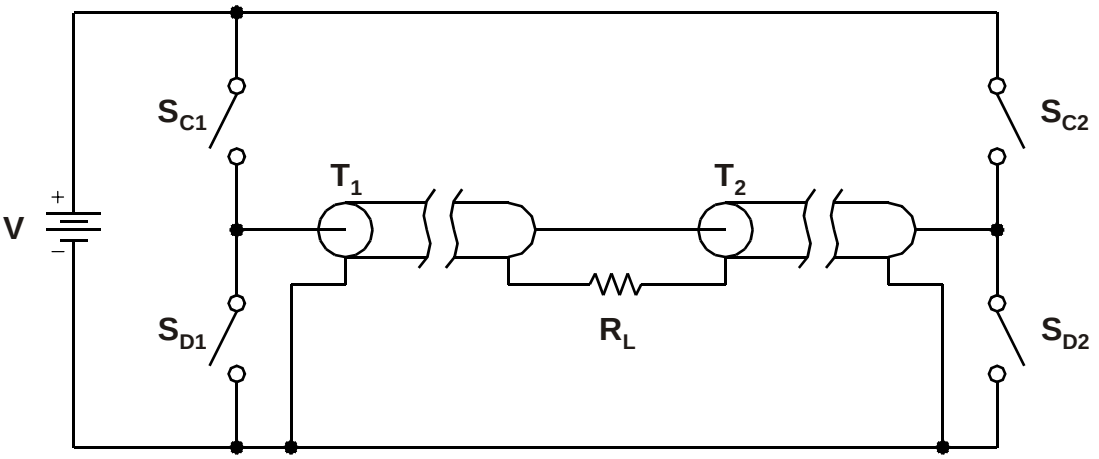

Slika 2.3 Konceptualna shema predlagane konfiguracije Blumleinovega generatorja z variabilno dolžino in polariteto ter visoko ponavljalno frekvenco nanosekundnega pulza. Pri tem sta T_1 in T_2 valovodni liniji, R_L breme, S_{C1} in S_{C2} stikali za polnjenje valovodnih linij, S_{D1} in S_{D2} stikali za praznjenje valovodnih linij ter V napetostni vir.

Preden začnemo generirati pulze z novo konfiguracijo Blumleinovega generatorja, je priporočljivo valovodni liniji bodisi sprazniti ali napolniti z visoko-ohmskima uporoma na vsaki strani generatorja. Recimo, da sta naši ekvivalentni valovodni liniji prazni. Potem lahko s polnilnima stikaloma (S_{C1} in S_{C2}) začnemo sočasno polniti valovodni liniji v Blumleinovemu generatorju. V idealnih pogojih sta

v tem primeru valovodni liniji polni v času τ, pri tem pa se na bremenu R_L ne generira električni pulz. Čas τ je enak električni dolžini posamezne valovodne linije. V primeru, da valovodni liniji ne polnimo sočasno, ampak je eno od stikal zamaknjeno za $\Delta T_1 \neq 0$, se na bremenu R_L generira pravokotni pulz. Dolžina pulza je kar enaka ΔT_1, če je $|\Delta T_1| < 2\tau$, drugače je dolžina pulza enaka 2τ. Polariteta pulza na bremenu pa je odvisna od tega, katero stikalo smo sklenili prej. Povzeto, s to prvo pravkar opisano sekvenco lahko le napolnimo valovodni liniji ali tudi generiramo visokonapetostni pulz spremenljive dolžine in polaritete. Potem, ko valovodni liniji napolnimo, lahko izklopimo stikali za polnjenje in vklopimo stikali za praznjenje (S_{D1} in S_{D2}) valovodnih linij. V idealnih pogojih čas polnjenja valovodnih linij variira med τ in 2τ ter je odvisen od ΔT_1. Od te točke naprej praznjenje valovodne linije poteka na podoben način kot polnjenje in s tem generiranje drugega, prvega ali nobenega pulza. Pri tem je lahko električni pulz ponovno variabilne dolžine in polaritete. V idealnih pogojih je tako lahko maksimalna ponavljalna frekvenca nanosekundnih pulzov pri dani konfiguraciji Blumleinovega generatorja, če generiramo pulz med polnjenjem in praznjenjem valovodnih linij, od $1/2\tau$ do $1/\tau$.

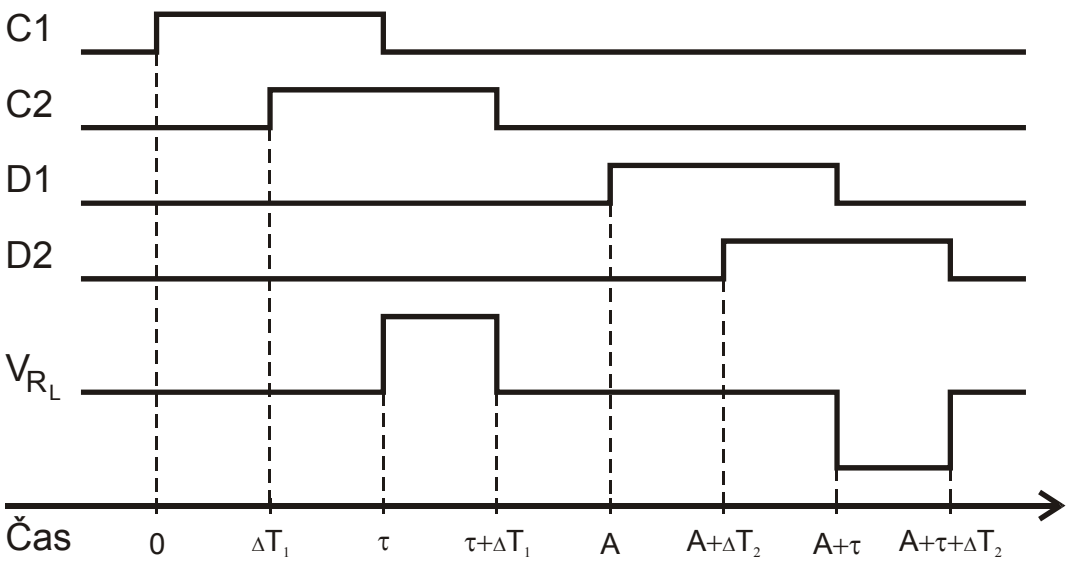

Slika 2.4 Časovni diagram generiranja nanosekundnih pulzov s predlagano konfiguracijo Blumleinovega generatorja. Pri tem so C1, C2, D1 in D2 vzbujalni signali stikal S_{C1}, S_{C2}, S_{D1} in S_{D2} ter V_{RL} napetost na bremenu R_L.

Delovanje predlagane konfiguracije Blumleinovega generatorja (Slika 2.3) smo najprej preverili s SPICE simulacijo v programu za simulacijo vezij SPICE OPUS (CACD group, Slovenija). Vsi elementi v vezju so bili pri tem idealni. V

simulaciji smo uporabili 1 kV DC napajalnik V in 100 Ω breme R_L postavljeno med valovodni liniji T_1 in T_2. Vsaka valovodna linija je imela zakasnitev τ = 100 ns in karakteristično impedanco Z_0 =50 Ω. Simulacijo smo naredili s prehodno analizo s časovnim korakom 10 ps ter simulacijskim časom 400 ns. Stikala S_{C1}, S_{C2}, S_{D1} in S_{D2} smo vzbujali s simuliranimi digitalnimi signali, kot so na Sliki 2.4 z dolžino posameznega pulza 100 ns. Zakasnitev ΔT_1 med signaloma C1 in C2 ter zakasnitev ΔT_2 med signaloma D1 in D2 sta bili 50 ns. Signal D1 je bil zakasnjen za A = 200 ns glede na signal C1.

Rezultati simulacije so potrdili naša predvidevanja o delovanju predlagane konfiguracije Blumleinovega generatorja. Ta predvidevanja so, da zakasnitev ΔT_1 definira dolžino nanosekundnega pulza ter da s predlagano konfiguracijo lahko generiramo tako bipolarne nanosekundne pulze kot tudi nanosekundne pulze z visoko ponavljalno frekvenco (Slika 2.5).

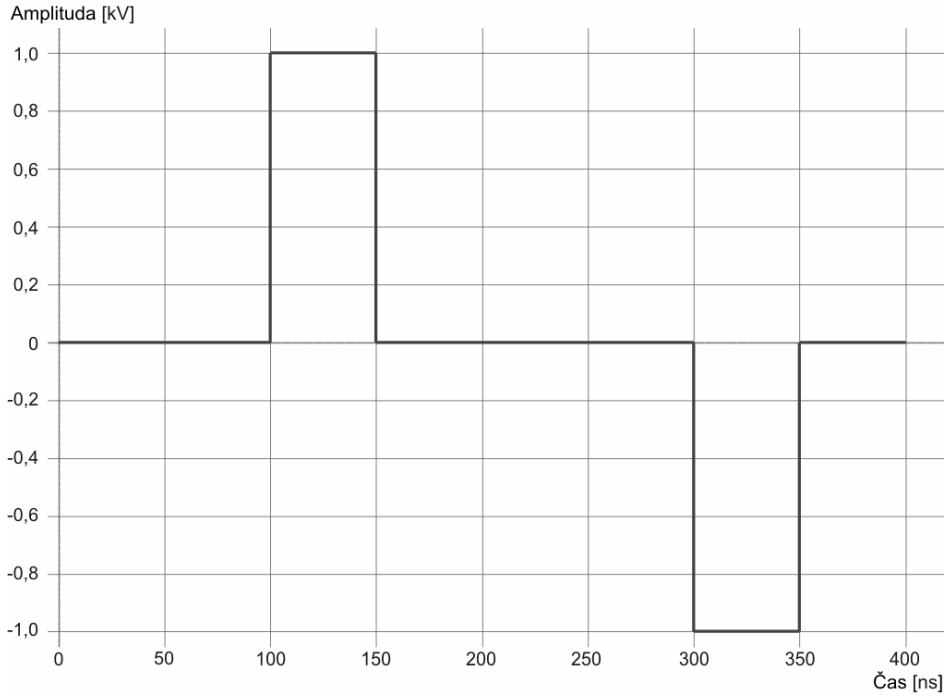

Slika 2.5 Napetost na bremenu R_L kot rezultat SPICE simulacije delovanja predlagane konfiguracije Blumleinovega generatorja.

2.2 Zasnova verzije generatorja dolgih visokonapetostnih pulzov

Verzijo generatorja dolgih visokonapetostnih pulzov smo zasnovali tako, da bo omogočala generiranje dobro definiranih pravokotnih pulzov ter pulzov poljubne oblike od 5 – 1000 V in sinusne signale od 5 – 250 V. Verzija bo omogočala obračanje polaritete kot tudi preklapljanje signalov med več-igelnimi elektrodami. V ta namen smo predlagali nov način generiranja pravokotnih pulzov, sinusnih oziroma dielektroforetskih signalov ter preklapljanja signalov med elektrodami.

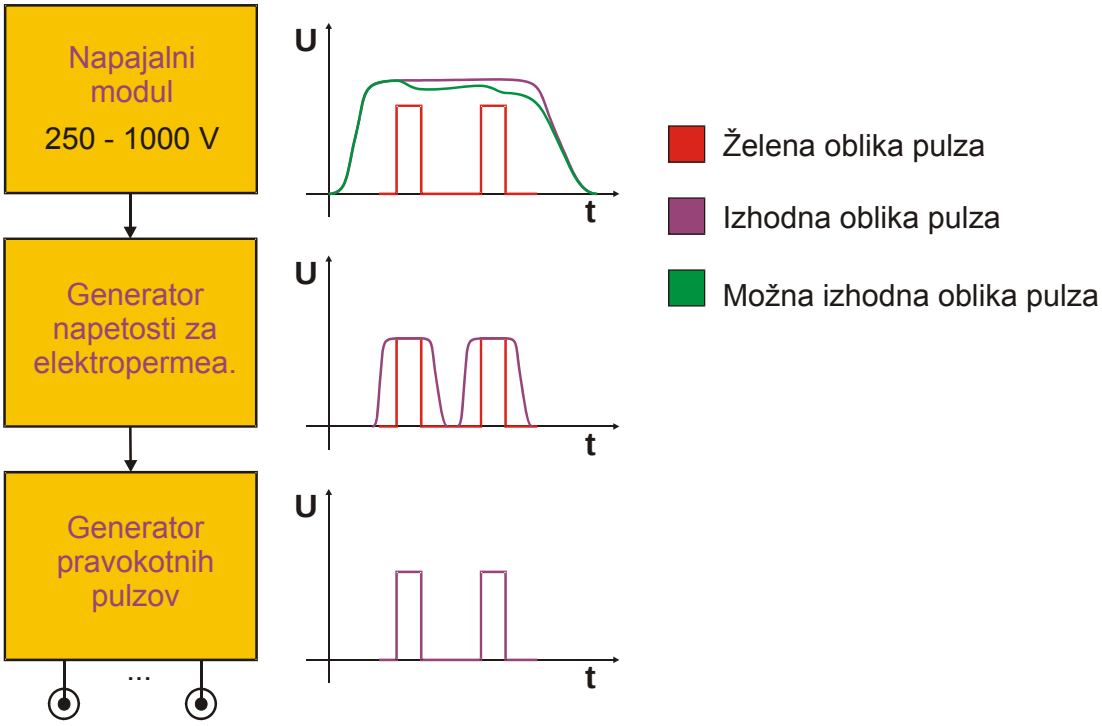

Slika 2.6 Konceptualna shema predlaganega načina generiranja dolgih pulzov. Predlagan način omogoča generiranje dobro definiranih pravokotnih pulzov tudi pri večjih obremenitvah kot tudi signale poljubnih oblik.

Predlagani način generiranja pravokotnih ter pulzov poljubnih oblik predvideva generiranje pulzov v treh korakih (Slika 2.6). V prvem koraku napajalni modul generira izhodno napetost od 50 V do 20% nad želeno amplitudo pulza. Tako velika zaloga v amplitudi omogoča generatorju, da tudi pri večjih obremenitvah še vedno generira želeno amplitudo pulza. Pri večjih obremenitvah bi se ta zaloga seveda postopoma zmanjšala, zato morata biti izhodna kapacitivnost napajalnega modula in napetostna zaloga dovolj veliki, da zdržita tudi največjo predvideno

obremenitev. Pri tem pa napetostna zaloga ne sme preseči zgornje meje, ki bi za generator pomenila močnostno preobremenitev.

V drugem koraku generator napetosti iz amplitudne zaloge izoblikuje pulze, ki imajo želeno amplitudo. Po tem koraku so pulzi še vedno nekoliko daljši od želene dolžine, zaradi dolgega dvižnega in upadnega časa generatorja napetosti. Generator napetosti lahko v tej fazi sledi poljubnim spremembam napetosti s približno 200 V/µs ter tako izoblikuje pulze poljubnih oblik. Glavni sestavni del generatorja napetosti je ojačevalnik s skupnim izvorom in potencialno nedoločenim izhodom (Slika 1.6).

V tretjem koraku stikalo v izhodnem modulu odpre in zapre pot signalu iz generatorja napetosti k elektrodam. Ker ima to stikalo kratek dvižni in upadni čas, lahko generiramo dobro časovno definirane pulze.

Prvi korak torej zagotavlja dovolj energije tudi pri večjih obremenitvah, drugi korak zagotavlja natančnost amplitude, tretji pa časovno dobro definiran signal. Na tak način lahko generiramo dobro definirane pravokotne pulze, kot tudi pulze poljubnih oblik. Predlagan način generiranja pravokotnih in pulzov poljubnih oblik je zelo primeren za elektroporator z regulacijo izhodne napetosti glede na potek elektropermeabilizacije. Elektroporator z regulacijo izhodne napetosti glede na potek elektropermeabilizacije namreč zahteva dobro definirane pravokotne pulze za oceno stopnje elektropermeabilizacije ter možnost spremembe amplitude pulza za regulacijo učinka elektropermeabilizacije [Pavlin et al., 2005; Cukjati et al., 2007]. Dobro definirani pravokotni pulzi so potrebni tudi za primerjavo rezultatov simulacij modelov elektropermeabilizacije z rezultati poizkusov.

Verzijo generatorja dolgih visokonapetostnih pulzov sestavljajo trije generatorji, katerih signale združi izhodni modul (Slika 2.7). Prvi generira pravokotne in pulze poljubnih oblik od 200 V do 1 kV za elektropermeabilizacijo, drugi od 5 V do 250 V za elektroforezo in tretji sinusne signale od 5 V do 250 V za dielektroforezo. Vsi trije generatorji so vzporedno povezani skupaj v izhodnem modulu preko zaščitnih diod, ki preprečujejo, da bi signal iz enega generatorja poškodoval drugi generator. Generatorji so nato povezani s polmostiči iz radiofrekvenčnih stikalnih tranzistorjev. Število polmostičev je enako številu izhodov naprave. Polmostiči delujejo kot elektrodni preklopniki od 5 V do 1 kV s tem, ko

določajo polariteto posamezne elektrode ter kot generatorji pravokotnih pulzov, ko z odpiranjem in zapiranjem določajo dvižni in upadni čas pravokotnih pulzov [Reberšek, 2001, 2008; Kranjc, 2006].

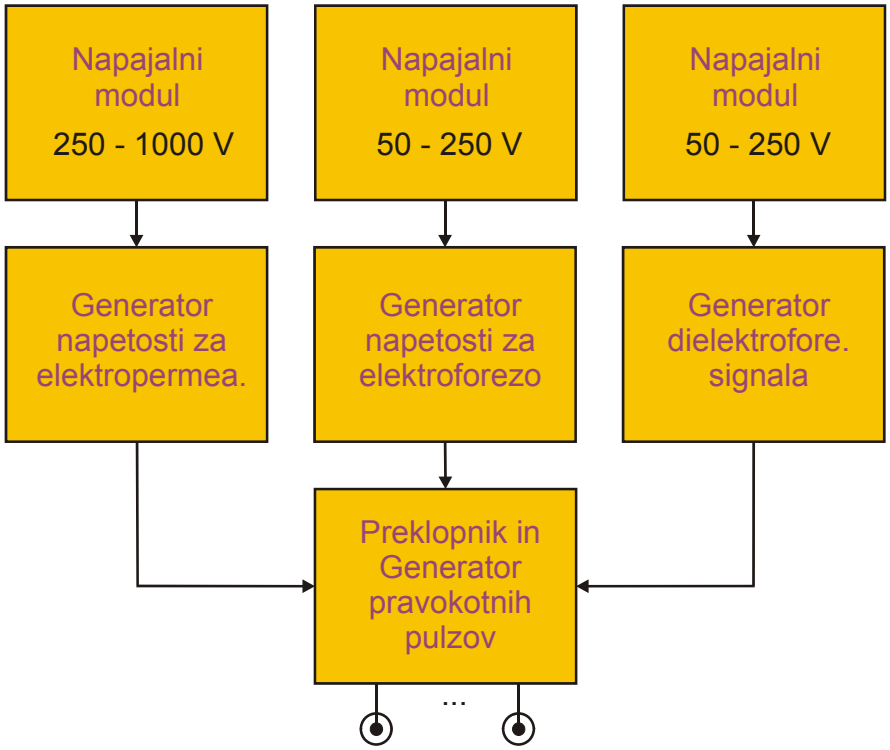

Slika 2.7 Blokovna shema predlagane modularne zgradbe verzije generatorja dolgih visokonapetostnih pulzov. Predlagana zgradba omogoča generiranje elektropermeabilizacijskih, elektroforetskih in dielektroforetskih pulzov z eno napravo na večjem številu elektrod in s tem tudi spreminjanje polaritete napetosti in orientacije električnega polja.

3 IZVEDBA NAPRAVE

V prejšnjem poglavju smo predlagali nov pristop k razvoju naprav za elektropermeabilizacijo. Predlagani pristop smo tudi praktično preizkusili z izdelavo verzije generatorja kratkih visokonapetostnih pulzov. To verzijo smo izdelali tako, da smo razvili ter vanjo vgradili vse skupne module, in sicer grafični uporabniški modul, nadzorni modul ter napajalni modul. Dodatno smo razvili še zakasnilno vezje in izhodni modul za visokonapetostne nanosekundne pulze [Kranjc, 2007] ter elektrode na krovnem stekelcu, ki so podrobneje opisane v poglavju 4.1. Elektrode na krovnem stekelcu so glavni sestavni del komore za mikroskop. Valovodni liniji sta neposredno prispajkani na komoro za mikroskop in sta zato zunaj ohišja naprave (Slika 3.1).

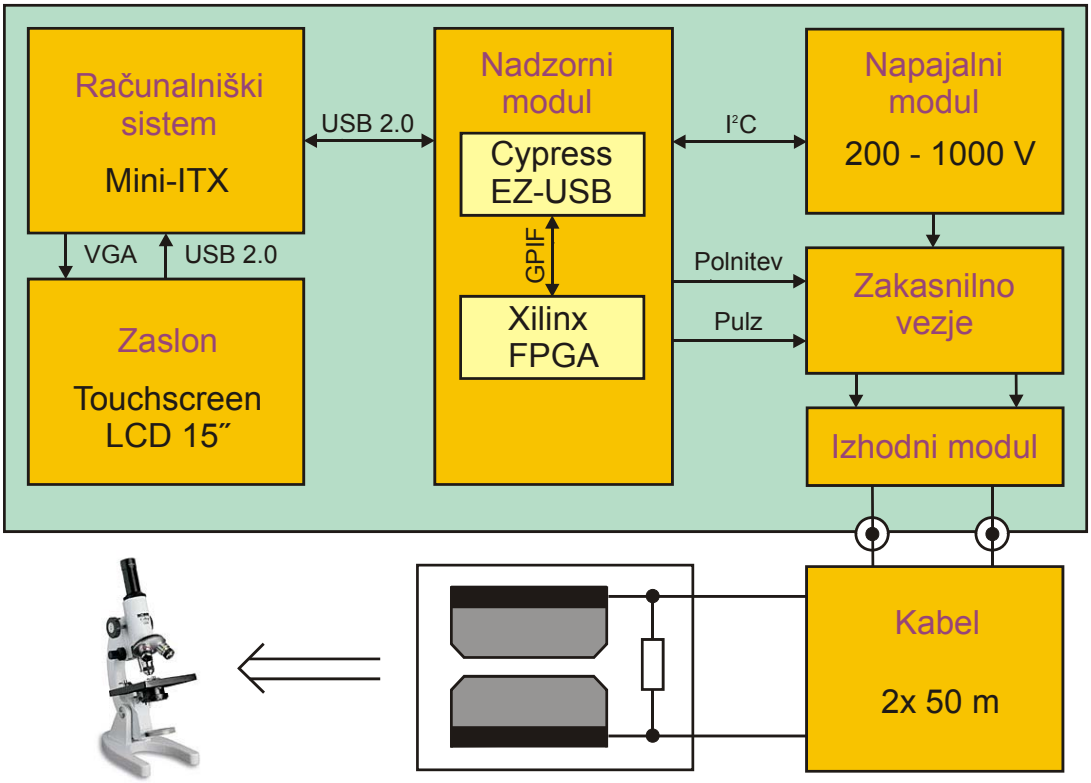

Slika 3.1 Blokovna shema predlagane modularne zgradbe verzije generatorja kratkih visokonapetostnih pulzov. Predlagana zgradba omogoča generiranje nanosekundnih pulzov različnih dolžin z visoko ponavljalno frekvenco pulzov.

3.1 Izvedba grafičnega uporabniškega vmesnika

Računalniški sistem, na katerem deluje grafični uporabniški vmesnik, smo sestavili iz Mini-ITX sistema Via Epia EN12000EG; 512 MB 533 MHz delovnega spomina; 512 MB CompactFlash kartice, ki je preko IDE vmesnika uporabljena kot trdi disk in 1 GB USB ključa. Na CompactFlash kartico smo naložili operacijski sistem, ki smo ga razvili s programskim paketom Microsoft Windows CE .NET v5.0; USB gonilnik, ki smo ga razvili v okolju Microsoft eMbedded Visual C++ s pomočjo programskega paketa Jungo WinDriver v 9.0 in aplikacijo, ki smo jo razvili v okolju Microsoft Visual Studio 2005. Na USB ključ pa se shranjujejo protokoli za poizkuse. Računalniškemu sistemu smo dodali še na dotik občutljiv zaslon EloTouch 1537L 15" IntelliTouch USB, s katerim kontroliramo delovanje celotne naprave (Slika 3.2).

Slika 3.2 Grafični uporabniški vmesnik na zaslonu občutljivem na dotik, s katerim kontroliramo delovanje verzije generatorja kratkih visokonapetostih pulzov.

Z grafičnim uporabniškim vmesnikom lahko nastavimo napetost napajalnega modula od 250 V do 1000 V, dolžino pulza od 5 ns do 200 ns, število pulzov od 1 do 100 in frekvence pulzov od 1 Hz do 100 kHz. Pod posebnim menijem SETUP lahko

nastavimo tudi potek polnjenja valovodnih linij ter strojno specifične parametre, ki določajo razmerje med nastavljenimi električnimi parametri in surovimi strojnimi podatki. S temi parametri aplikacija namreč pretvori nastavljene parametre v surove strojne podatke. Vse nastavitve skupaj lahko shranimo kot en protokol v eno od datotek na USB ključu in jih kasneje spet uporabimo. S pritiskom na gumb ARM pripravimo napravo na generiranje pulzov, s pritiskom na gumb START poženemo generiranje pulzov, s pritiskom na gumb STOP ustavimo generiranje pulzov oziroma spraznimo napajalni modul in s pritiskom na gumb SHUTDOWN izklopimo napravo.

3.2 Izvedba nadzornega modula

Nadzorni modul smo razvili in izdelali z USB krmilnikom CY7C68013-128AC (EZ-USB, Cypress; Slika 3.3) ter programirljivim vezjem XCS30V200 (SPARTAN 3, Xilinx; Slika 3.4). USB krmilnik ima vgrajen mikroprocesor 8051, ki deluje s frekvenco 48 MHz in nadzoruje celotno delovanje krmilnika. Program za USB krmilnik je napisan v programskem jeziku C v integriranem razvojnem okolju Keil µVision2. Program deluje tako, da najprej nastavi začetne nastavitve krmilnika, potem pa preide v neskončno zanko, kjer čaka na prekinitve. Prekinitve lahko sproži računalniški sistem preko USB 2.0 komunikacijskih vrat po končni točki (endpoint - EP) 0 in 1. Po končni točki 0 z zahtevkom 0x80 lahko računalniški sistem z enojnim pisanjem preko splošno programirljivega vmesnika (GPIF - General Programmable Interface) vpisuje podatke v programirljivo vezje. Po končni točki 1 pa lahko vpisuje preko I^2C vodila v napajalni modul nastavljeno napetost ali bere trenutno napetost napajalnega modula.

Programirljivo vezje je sinhronizirano z USB krmilnikom preko GPIF vmesnika s časovnim signalom IFCLK, ki ga vezje uporablja tudi za delovanje notranjih funkcij. Program za programirljivo vezje smo napisali v strojno opisnem jeziku VHDL v integriranem razvojnem okolju Xilinx ISE WebPACK 9.0. Programirljivo vezje ima vgrajena tri sinhrona sekvenčna vezja. Prvo skrbi za komunikacijo preko GPIF z USB krmilnikom. Drugo skrbi za vpis parametrov v zakasnilni vezji na zahtevo računalniškega sistema. Tretji pa skrbi za generiranje signala za polnjenje (CHARGE) in praznjenje (DISCHARGE) valovodnih linij.

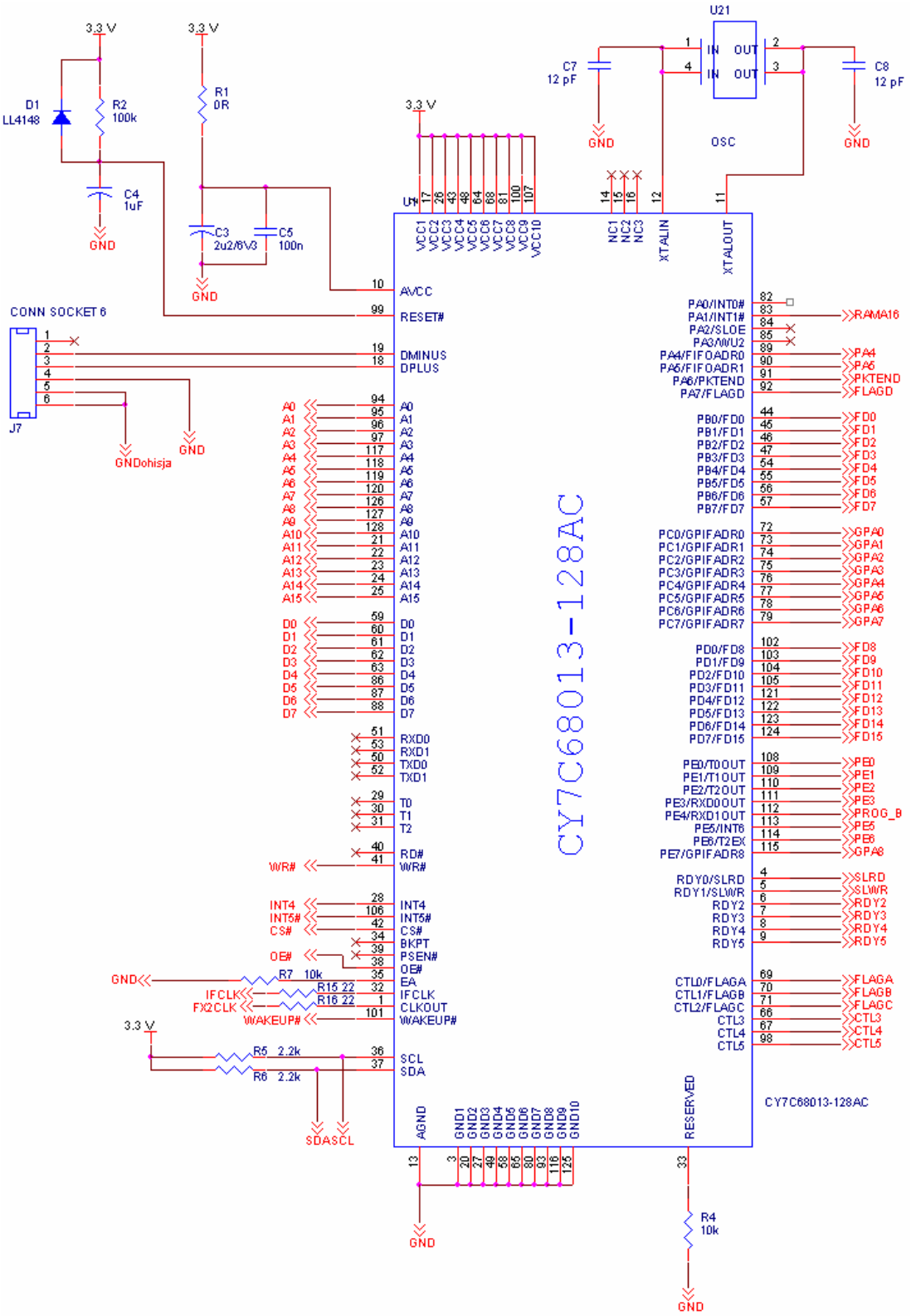

Slika 3.3 Vezalna shema USB krmilnika v nadzornem modulu. Glavna komunikacijska vrata krmilnika so USB 2.0 (D+ in D-), I^{2}C (SDA in SCL) ter GPIF (IFCLK, FD0-15, GPA0-8, RDY0-5 in CTL0-5).

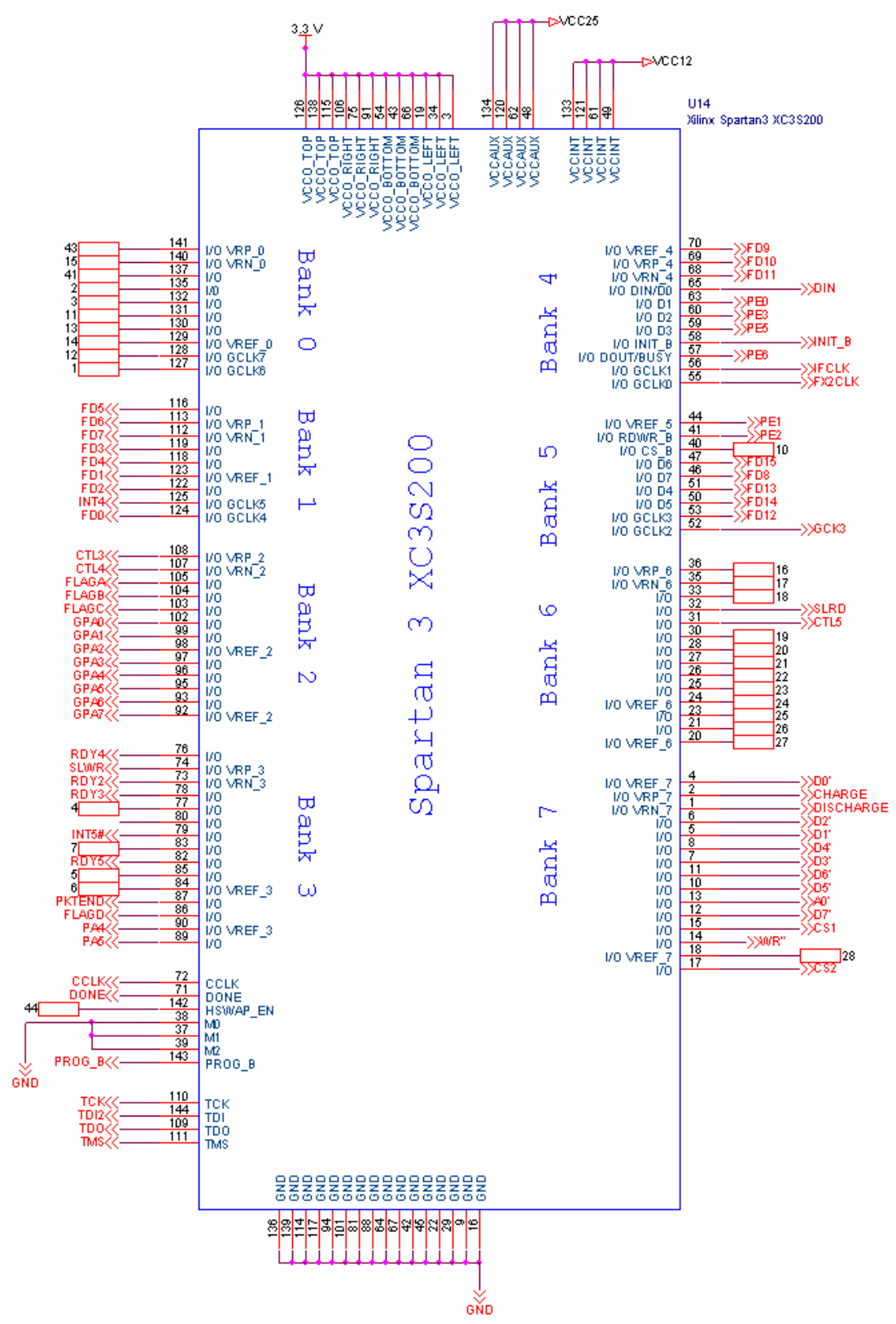

Slika 3.4 Vezalna shema programirljivega vezja v nadzornem modulu. Glavna komunikacijska vrata in povezave vezja so GPIF (IFCLK, FD0-15, GPA0-8, RDY0-5 in CTL0-5), krmiljenje zakasnilnega vezja (D0'-7', A0', WR in CS1,2) ter signala za generiranje pulzov (CHARGE in DISCHARGE).

3.3 Izvedba napajalnega modula

Delovanje napajalnega modula v celoti kontrolira mikrokontroler Microchip PIC18F45J10 (Slika 3.5). Program za mikrokontroler smo napisali v programskem jeziku za PIC mikrokontrolerje C18 v integriranem razvojnem okolju MPLAB IDE v7.41. Mikrokontroler smo sprogramirali s programatorjem in razhroščevalnikom MPLAB ICD 2 preko ICD povezave.

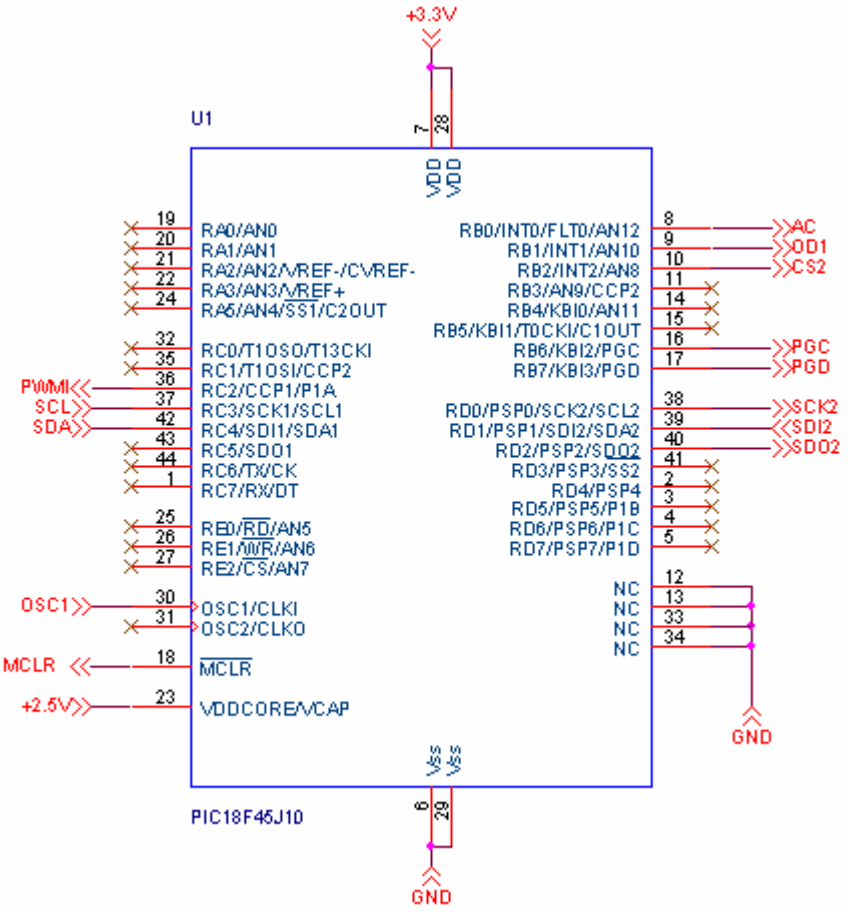

Slika 3.5 Vezalna shema mikrokontrolerja v napajalnem modulu, ki kontrolira celotno delovanje napajalnega modula. Glavna komunikacijska vrata in povezave mikrokontrolerja I^2C (SDA in SCL), SPI (SCK2, SDI2, SDO2 in CS2), ICD (MCLR, PGC in PGD) signal za priklopitev omrežne napetosti (AC), signal za praznjenje napajalnega modula (OD1) ter signal za odprtje tranzistorskega polmostiča (PWMI).

Energijo za generiranje izhodne napetosti napajalni modul dobi direktno iz omrežne napetosti (Slika 3.6). Pred poškodbami zaradi prevelikega toka ga ščiti varovalka F1 in pred poškodbami zaradi previsoke napetosti varistor RV1. Mikrokontroler lahko z relejem LS1 preko signala AC vklopi ali izklopi omrežno

napetost. Filter elektromagnetnih motenj EMI1 skrbi, da iz gladilnega vezja nazaj v omrežje uhaja čim manj elektromagnetnih motenj. NTC upor poskrbi, da ob vklopu omrežne napetosti in praznem gladilnem kondenzatorju C1 ne pride do prevelikih tokovnih sunkov. Diodni mostič BRIDGE1 nam omrežno napetost spremeni v polnovalno usmerjeno napetost, ki jo kondenzator C1 še zgladi.

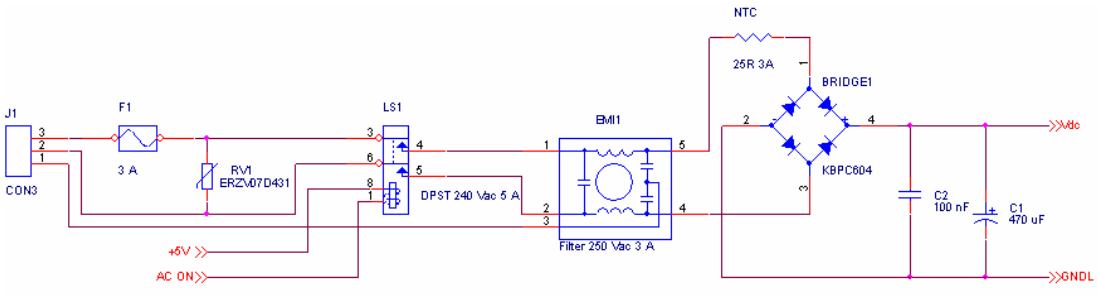

Slika 3.6 Vezalna shema varnostnega in gladilnega vezja omrežne napetosti v napajalnem modulu.

Tranzistorski polmostič, ki je zgrajen iz Q1 in Q2, zglajeno napetost razseka s frekvenco 80 kHz in jo pošlje preko transformatorja T1 (Slika 3.7). Transformirana energija se preko diode D3 in tuljave T2 usmeri v izhodni kondenzator C3 napajalnega modula. Pri tem neuporabljena energija pa se preko diod D1 in D2 vrne nazaj v gladilni kondenzator C1, tok skozi T2 se medtem zaključi preko D4. Transformator T1 galvansko loči izhodno napetost od omrežne napetosti ter tako poveča varnost naprave.

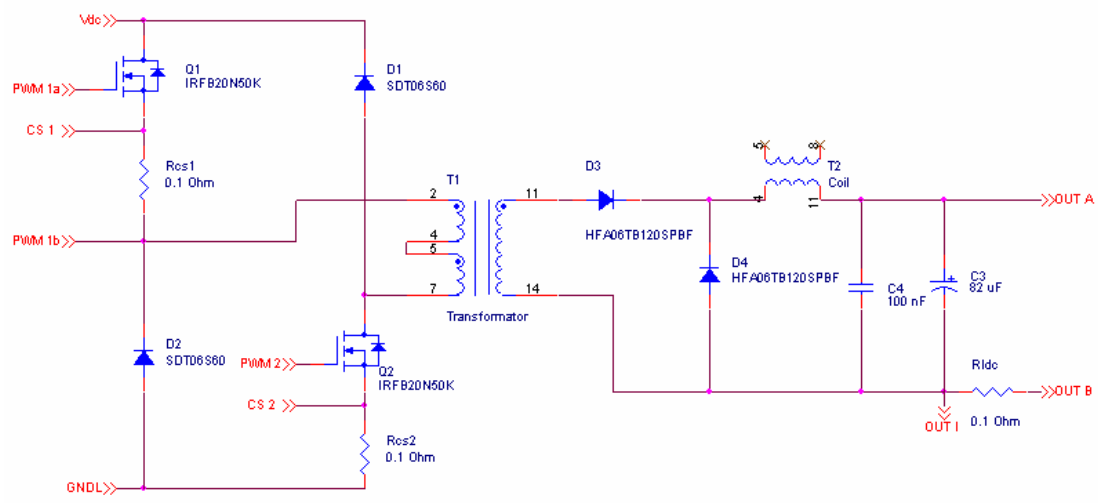

Slika 3.7 Vezalna shema izvršilnega dela polmostičnega DC-DC pretvornika v napajalnem modulu.

Za posebne primere, ko je potrebno na primer na hitro zmanjšati izhodno napetost, se uporablja posebna enota za praznjenje kondenzatorja na izhodu napajalnega modula (Slika 3.8). Ker je napetost na vhodu D med delovanjem konstantna, enota večino časa deluje kot tokovni generator. Pri visoki izhodni napetosti se tako večina energije troši na tranzistorju Q3, pri nizkih napetostih pa tudi na dveh uporih R14 in R25.

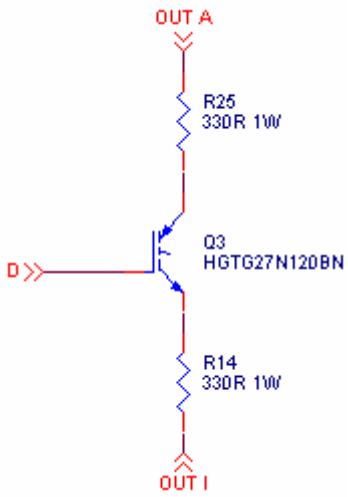

Slika 3.8 Vezalna shema enote za praznjenje napajalnega modula. Enota deluje kot tokovni generator, ki s konstantnim tokom prazni izhodni kondenzator napajalnega modula.

Za odpiranje in zapiranje tranzistorjev Q1, Q2 in Q3 (Slika 3.7 in 3.8) se uporabljajo posebni tranzistorski krmilniki U14, U15 in U16 (Slika 3.9). U14 in U15 krmilita zgornji in spodnji tranzistor v polmostiču ter imata preko tokovnih senzorjev CS 1 in CS 2 vklopljeni tokovni zaščiti, ki bi se vklopili v primeru, nasičenja jedra transformatorja T1. Tretji tranzistorski krmilnik krmili enoto za praznjenje napajalnega modula in nima vklopljene tokovne zaščite, ker že samo vezje deluje kot tokovni generator.

Program mikrokontrolerja v napajalnem modulu deluje tako, da najprej nastavi začetne nastavitve mikrokontrolerja, potem pa preide v neskončno zanko, kjer čaka na prekinitve. Prekinitve lahko sproži nadzorni modul preko I^2C protokola in interni števec, ki skrbi, da regulacija napetosti napajalnega modula poteka v realnem času. Nadzorni modul lahko med I^2C prekinitvijo vpiše želeno vrednost napetosti ali prebere dejansko vrednost napetosti na izhodnem modulu. Nadzorni modul lahko z I^2C prekinitvijo pošlje tudi dva ukaza. Ukaz 0x00 pomeni, da mora

mikrokontroler izklopiti omrežno napetost, prenehati z regulacijo in izprazniti izhodni kondenzator. Ta ukaz se izvrši ob izklopu naprave ter ob pritisku na gumb STOP. Ukaz 0x01 pa pomeni, da mora mikrokontroler izklopiti omrežno napetost in prenehati z regulacijo. Ta ukaz se izvrši, ko dalj časa ne uporabljamo naprave. Če pa prekinitev sproži interni števec, se najprej preko SPI protokola iz AD pretvornika prebere dejanska vrednost napetosti. Nato se, razen v prej omenjenih primerih, izvede regulacija napetosti. Napetostna regulacija ima dve izvršilni vezji in štiri načine delovanja za doseganje svojega cilja. Prvo izvršilno vezje je tranzistorski polmostič, ki polni izhodni kondenzator (Slika 3.7), drugo izvršilno vezje pa je enota za praznjenje izhodnega kondenzatorja (Slika 3.8). Če je izhodna napetost veliko pod želeno, potem mikrokontroler maksimalno obremeni tranzistorski polmostič ter tako zelo hitro polni izhodni kondenzator. V območju malo pod želeno napetostjo mikrokontroler napetost regulira z diskretno proporcionalno regulacijo. V okolici želene napetosti mikrokontroler preneha z regulacijo. Če pa je izhodna napetost veliko nad želeno, mikrokontroler vklopi enoto za praznjenje.

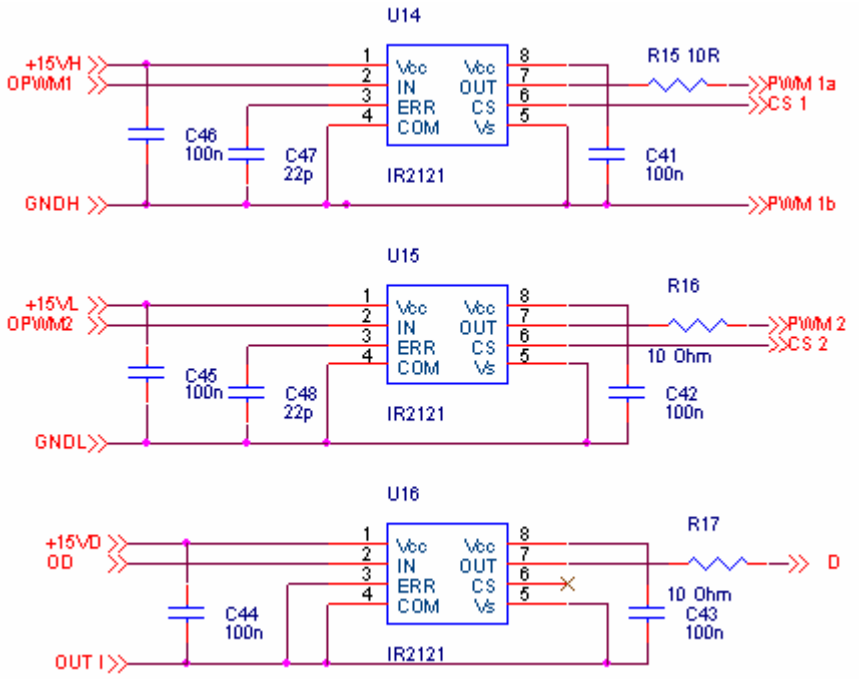

Slika 3.9 Vezalna shema tranzistorskih krmilnikov v napajalnem modulu. Prva dva krmilita polmostič DC-DC pretvornika, medtem ko tretji krmili enoto za praznjenje.

3.4 Izvedba zakasnilnega vezja

Naloga zakasnilnega vezja je, da zakasni signal polnjenja oziroma praznjenja med enim in drugim koncem valovodnih linij Blumleinovega generatorja. Naredili smo dva modula zakasnilnega vezja: enega, ki zakasni polnjenje in drugega, ki zakasni praznjenje valovodnih linij. Vsak modul ima dve zakasnilni vezji, kjer vsako vezje zakasni svoj konec valovodnih linij.

Zakasnilno vezje krmilimo z digitalnim signalom, medtem ko zakasnitev signala poteka analogno. Nadzorni modul pošlje zakasnilnemu modulu dve 8-bitni digitalni vrednosti, ki sta obratno sorazmerni z željeno zakasnitvijo signala. Dvokanalni DA pretvornik (AD5332) ter uporovna delilnika pretvorita digitalni vrednosti v dve napetosti od 0 V do 1 V (Slika 3.10). Ti dve napetosti se nato z analognim množilnikom (AD835) zmnožita s signalom polnjenja oziroma praznjenja. Dobljeni signal se nato integrira z integratorjem, ki je narejen iz operacijskega ojačevalnika (AD8099). Ker je signal polnjenja oziroma praznjenja vedno iste amplitude, je tako naklon integriranega signala premo sorazmeren z vrednostjo, ki jo je poslal nadzorni modul. Integrirani signal nato sproži Schmittov prožilnik z zakasnitvijo, ki je obratno sorazmerna naklonu integriranega signala (Slika 3.11).

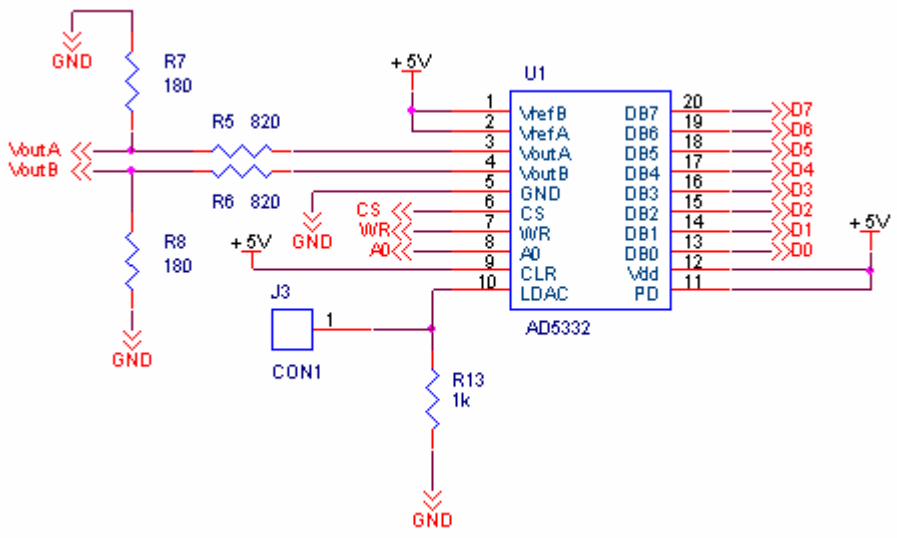

Slika 3.10 Vezalna shema dvokanalnega DA pretvornika z uporovnima delilnikoma.

Z izdelanim analognim zakasnilnim vezjem lahko poljubno zakasnimo signale med obema koncema valovodnih linij od -200 ns do +200 ns ter natančnostjo ±3 ns. Tako s predlaganim vezjem lahko generiramo nanosekundne pulze poljubne polaritete in variabilne dolžine od 30 do 200 ns ±10%.

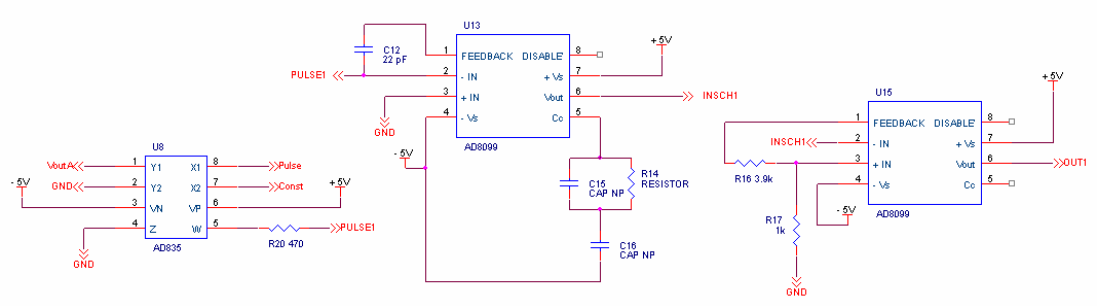

Slika 3.11 Vezalna shema analognega zakasnilnega vezja z množilnikom, integratorjem in Schmittovim prožilnikom.

3.5 Izvedba izhodnega modula

Stikala v izhodnem modulu za polnjenje in praznjenje valovodnih linij smo izdelali iz zelo hitrih radiofrekvenčnih stikalnih tranzistorjev DE275-102N06A (IXYS, ZDA). Da bi dosegli čim krajše dvižne čase stikal, jih krmilimo s posebno hitrim krmilnikom DEIC420 (IXYS, ZDA). Ob vklopu stikala steče iz krmilnika v stikalo zelo visok tok, zato morajo biti povezave med njima čim krajše in ravne. Za pokrivanje te tokovne špice je tik ob krmilniku zelo veliko majhnih in hitrih ter večjih in nekoliko počasnejših kondenzatorjev (Slika 3.12). V verzijo kratkih visokonapetostnih pulzov smo vgradili dva identična izhodna modula z enim stikalom za polnjenje in enim za praznjenje.

Med vklopom stikala za polnjenje S_C ali praznjenje S_D (Slika 2.3) se zelo hitro spremeni potencial V (Slika 3.13), kar preko parazitnega sklopa Z_P povzroči velike motnje na sicer galvansko ločenem nizkonapetostnem delu naprave. Pri predlagani konfiguraciji Blumleinovega generatorja je v primerjavi s klasično konfiguracijo parazitni sklop Z_P veliko večji zaradi direktnega stika med galvansko ločitvijo in potencialom V. Zato so tudi motnje, ki jih povzroča sprememba potenciala V, v predlagani konfiguraciji veliko večje kot v klasični konfiguraciji. V našem primeru je ob visoki napajalni napetosti Blumleinovega generatorja ali visoki ponavljalni frekvenci nanosekundnih pulzov prišlo do zaustavitve delovanja

kontrolnega oziroma zakasnilnega vezja. Zato smo morali z 10 Ω uporom med sponkama OUT (5) krmilnika DEIC420 in GATE (2) stikalnega tranzistorja DE275-102N06A (Slika 3.12) upočasniti delovanje stikalnih tranzistorjev ter tako povečati dvižne in upadne čase nanosekundnih pulzov.

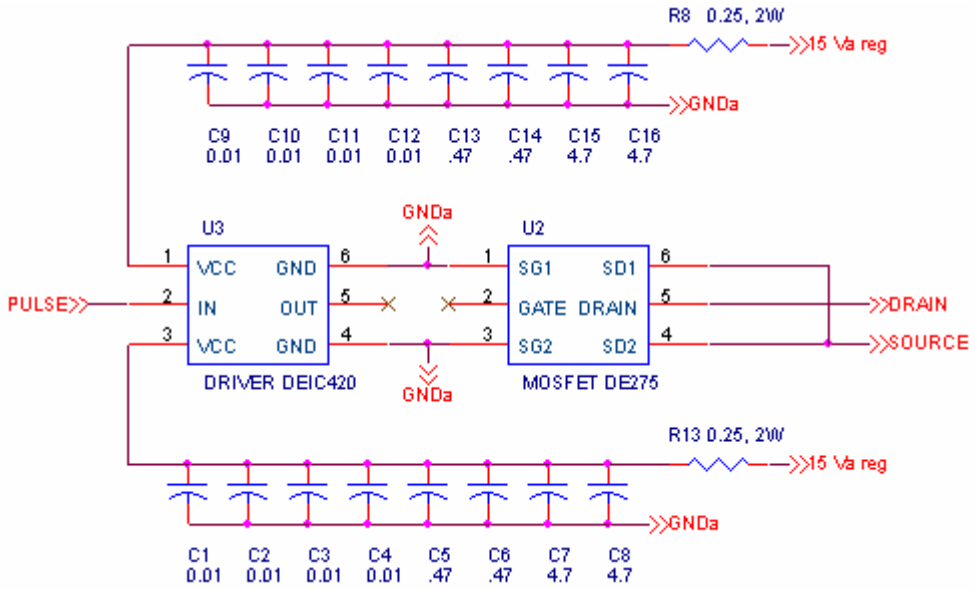

Slika 3.12 Vezalna shema radiofrekvenčnega stikalnega tranzistorja U2 in njegovega krmilnika U3 v izhodnem modulu.

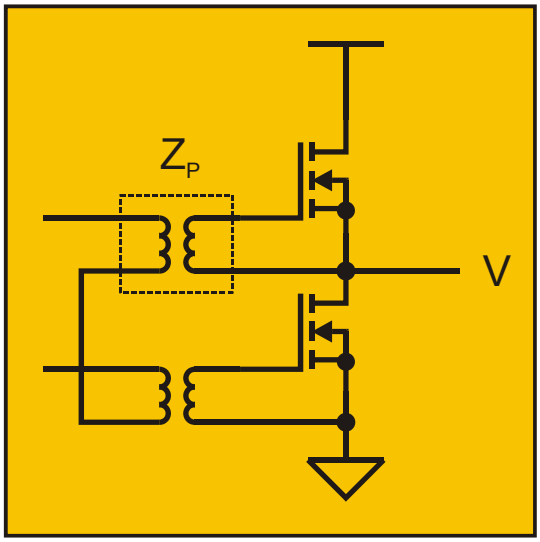

Slika 3.13 Konceptualna shema stikal in galvanske ločitve v izhodnem modulu. S črtkanim simbolom je označen parazitni sklop Z_P preko galvanske ločitve med visoko in nizkonapetostnem delu naprave.

3.6 Delovanje naprave

Mejne vrednosti električnih parametrov, ki jih lahko nastavimo v uporabniškem grafičnem vmesniku, smo izbrali glede na področje električnih parametrov, v katerem naprava deluje stabilno. Med merjenjem mejnih vrednosti in stabilnosti naprave je bila na napravo priključena komora z elektrodami na krovnem stekelcu, ki je natančneje opisana v poglavju 4.1. Z osciloskopom LeCroy waverunner LT354M ter sondo LeCroy PPE 2 kV smo izmerili izhodne signale izdelanega Blumleinovega generatorja. Izmerili smo maksimalno ponavljalno frekvenco nanosekundnih pulzov, ki je znašala 1.1 MHz, in preverili možnost generiranja bipolarnih nanosekundnih pulzov z novim Blumleinovim generatorjem (Slika 3.14). Maksimalna ponavljalna frekvenca je omejena s hitrostjo analognega zakasnilnega vezja, ki v našem primeru ne more hitreje natančno generirati dveh zaporednih nanosekundnih pulzov. Stabilnost naprave se pri maksimalni ponavljalni frekvenci pulzov in napetostih nad 300 V močno zmanjša. Pri 1000 V je naprava tako stabilna pri ponavljalni frekvenci pulzov pod 300 kHz. Za čim bolj stabilno delovanje naprave na celotnem napetostnem področju, smo omejili možnost izbire ponavljalne frekvence pulzov na 100 kHz. Preizkusili smo še ostale mejne vrednosti električnih parametrov in ugotovili, da pri vseh naprava deluje stabilno.

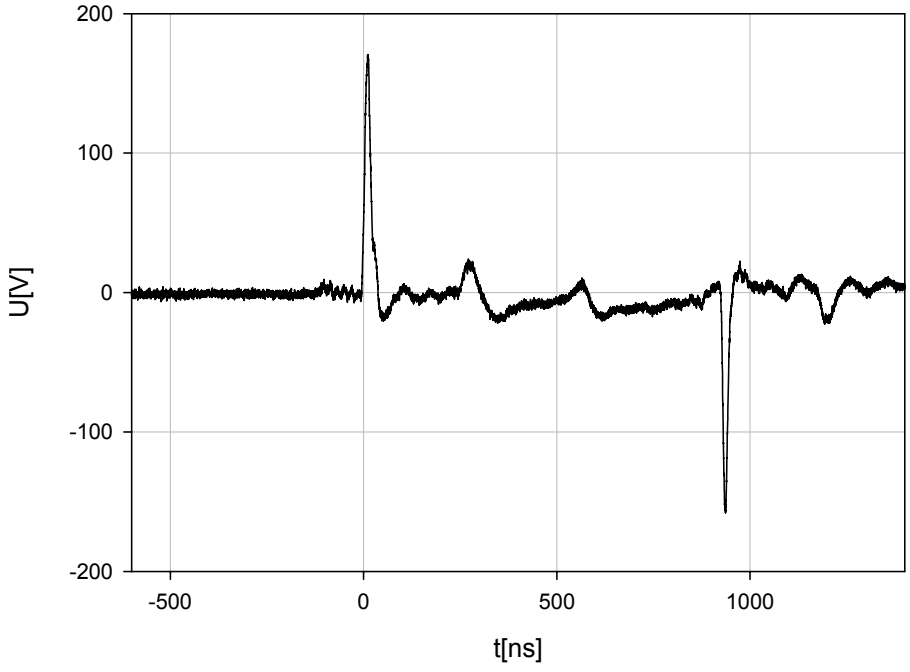

Slika 3.14 Maksimalna 1.1 MHz ponavljalna frekvenca 20 ns bipolarnih električnih pulzov pri izbrani napajalni napetosti 300 V.

Uporabnik izdelane naprave lahko spreminja napajalno napetost Blumleinovega generatorja od 250 V do 1000 V, dolžino pulza od 5 ns do 200 ns, število pulzov od 1 do 100 in frekvence pulzov od 1 Hz do 100 kHz. Delovanje naprave smo ponazorili s tremi meritvami (Slika 3.15, 3.16 in 3.17).

Pri prvi meritvi smo pri nastavljeni konstantni dolžini električnega pulza 60 ns spreminjali napajalno napetost Blumleinovega generatorja od maksimalne do minimalne s korakom 200 V in opazovali amplitudo nanosekundnega pulza na bremenu (Slika 3.15). Opazimo lahko, da je amplituda nanosekundnega pulza približno pol manjša od napajalne napetosti Blumleinovega generatorja. Zmanjšana amplituda je predvsem posledica upočasnjenega delovanja stikalnih tranzistorjev in odklona impedance bremena pri visokih frekvencah.

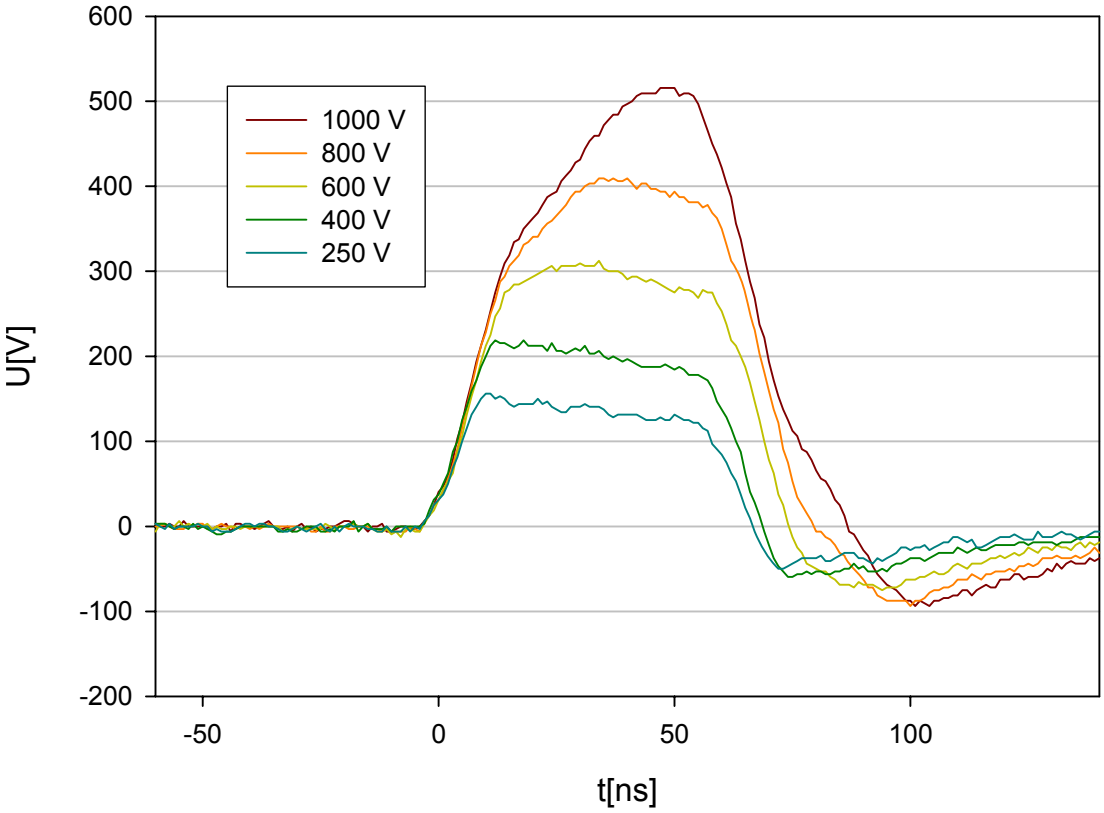

Slika 3.15 Amplituda 60 ns električnih pulzov na bremenu v odvisnosti od napajalne napetosti Blumleinovega generatorja.

Pri drugi meritvi smo pri nastavljeni konstantni napajalni napetosti Blumleinovega generatorja 400 V spreminjali nastavljeno dolžino električnih pulzov od 20 ns do 200 ns in opazovali časovni potek in dejansko dolžino nanosekundnih

pulzov (Slika 3.16). Opazimo lahko, da napaka dolžine nanosekundnih pulzov ni večja od predvidenih 10%.

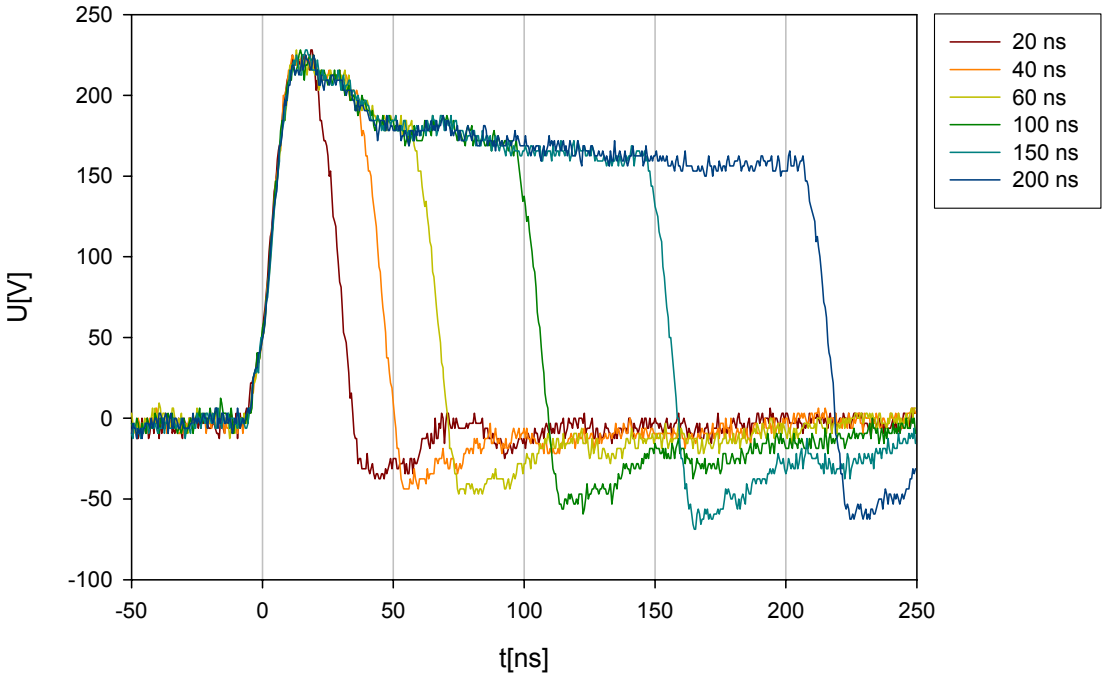

Slika 3.16 Časovni potek 200 V električnih pulzov v odvisnosti od izbrane dolžine električnih pulzov.

Pri tretji zadnji meritvi smo pri nastavljeni konstantni napajalni napetosti Blumleinovega generatorja 1000 V in dolžini električnega pulza 60 ns spreminjali ponavljalno frekvenco nanosekundnih pulzov od 1 Hz do 100 kHz in opazovali amplitudo desetega zaporednega nanosekundnega pulza. Opazimo lahko, da se maksimalna amplituda pulza med 100 Hz in 10 kHz zmanjša za okoli 10%. Zmanjšana amplituda je predvsem posledica LC filtra napajalne napetosti Blumleinovega generatorja in je enaka za vse pulze po tretjem zaporednem pulzu.

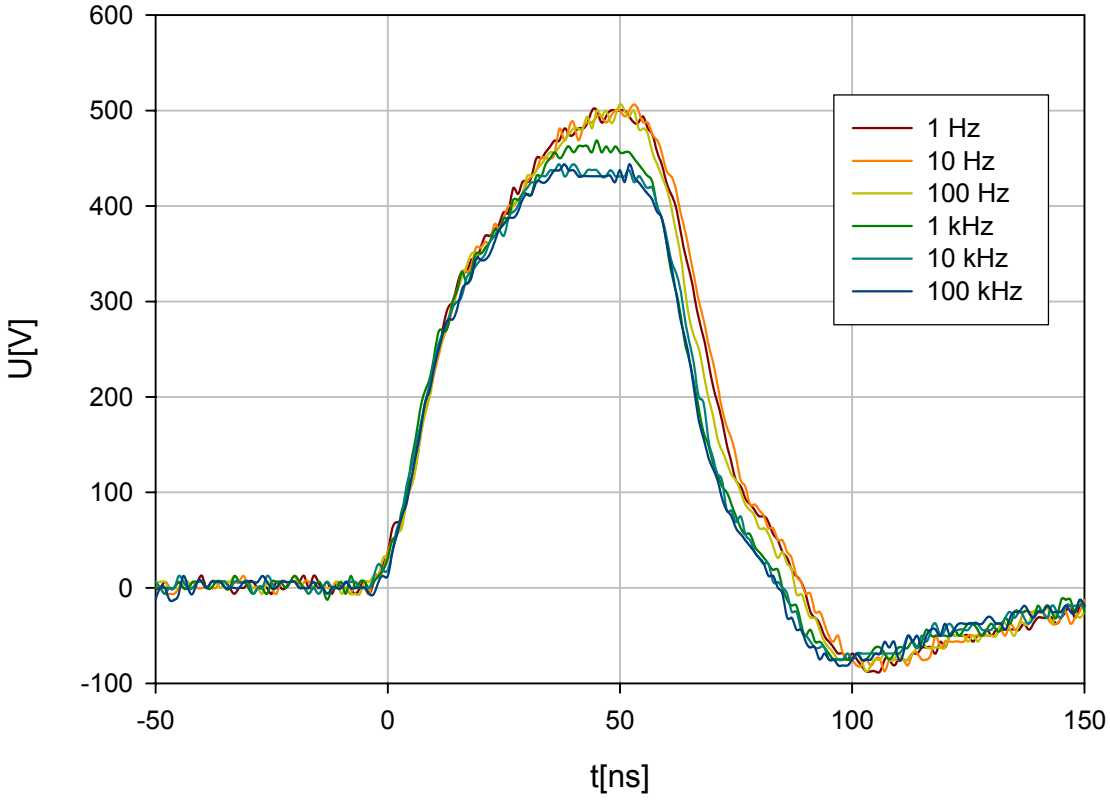

Slika 3.17 Časovni potek desetega zaporednega 60 ns električnega pulza v odvisnosti od izbrane ponavljalne frekvence pulzov. Izbrana je bila maksimalna napajalna napetost Blumleinovega generatorja 1000 V.

4 IZVEDBE ELEKTROD

V okviru te naloge smo razvili dve vrsti elektrod oziroma komor, in sicer elektrode na krovnem stekelcu ter koničasto komoro z vgrajenimi elektrodami. Prva omogoča opazovanje učinkov nanosekundnih pulzov na biološke celice pod mikroskopom. Druga pa omogoča elektropermeabilizacijo bioloških celic med postopkom pipetiranja.

4.1 Elektrode na krovnem stekelcu

Osnovno vodilo pri razvoju novih elektrod na krovnem stekelcu je bilo, da lahko samo z dobro definirano obliko elektrod točno določimo jakost električnega polja med elektrodami. Prav tako je bilo za razvoj elektrod pomembno dejstvo, da lahko samo z elektrodami tik nad krovnem stekelcem dosežemo razmeroma homogeno električno polje visoke jakosti v prostoru, kamor celice sedimentirajo med poizkusi.

Nove elektrode na krovnem stekelcu izdelamo tako, da na krovno stekelce najprej nanesemo tanko približno 100 nm plast niklja. Nanjo nanesemo še 400 nm zlata. S fotorezistom nato določimo prostor, kamor bomo nanesli še preostali del zlata ter tako določimo obliko elektrod oziroma reže. Ko na krovno stekelce nanesemo še preostale 4 μm zlata, selektivno odjedkamo fotorezist. Nato po celotni površini odjedkamo še 500 nm zlata oziroma niklja in tako dobimo elektrode direktno nanesene na krovno stekelce (Slika 4.1). Debelina reže med elektrodama je pri tem 100 μm. Elektrode pa so na vsakem koncu reže zaobljene z radijem 0.5 mm, tako da na robu ne pride do prevelike jakosti električnega polja, ki bi lahko poškodovala elektrode. Maksimalna predvidena napetost, ki se še lahko uporablja na novih elektrodah, je 1000 V. Pri tej napetosti se tik nad krovnim stekelcem vzpostavi električna poljska jakost 100 kV/cm.

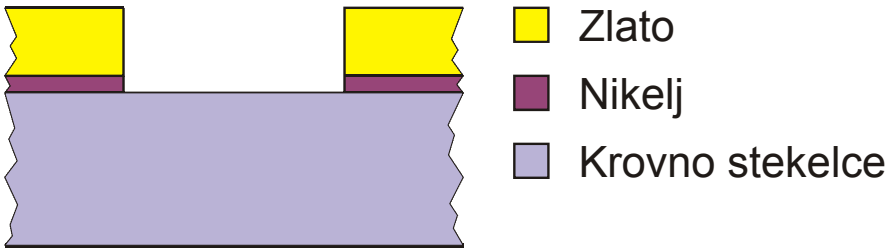

Slika 4.1 Simboličen prikaz nanosa kovine na krovno stekelce in reže med elektrodama na krovnem stekelcu. Dejanska debelina krovnega stekelca je 1 mm, debelina niklja 100 nm, debelina zlata 4 µm in širina reže 100 µm.

Komoro za mikroskop smo izdelali tako, da smo naredili tiskano vezje, ki se prilega nastavku mikroskopa. Na tiskano vezje smo nato prilepili elektrode na krovnem stekelcu. S tanko žičko in tekočo spajkalno pasto smo jih prispajkali na kontakte na tiskanem vezju. Na tiskano vezje smo prispajkali še valovodni liniji Blumleinovega generatorja ter bremenski in vzporedni (shunt) upor.

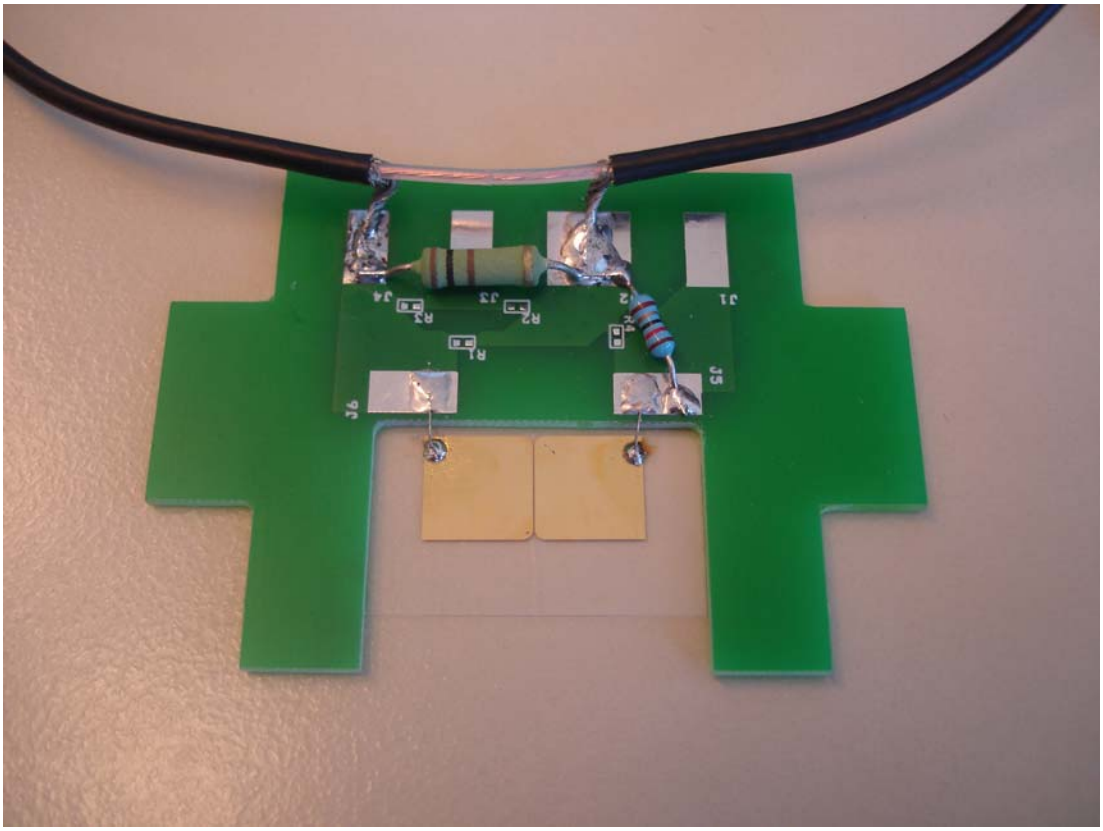

Slika 4.2 Komora za mikroskop z elektrodami na krovnem stekelcu.

4.2 Koničasta komora z vgrajenimi elektrodami

Razvili smo novo koničasto komoro za pipetor z vgrajenimi elektrodami (Slika 4.3). Poglavitna prednost pred že obstoječimi koničastimi komorami z vgrajenimi elektrodami je postavitev in oblika elektrod, ki omogočata generiranje razmeroma homogenega električnega polja med elektrodami v večih smereh in s tem večjo učinkovitost genske elektrotransfekcije in elektrofuzije. Podrobnejši opis koničaste komore, njene prednosti in prednosti vgrajenih elektrod so podane v priloženem patentu (SI22368A) in člankoma (Reberšek et al., 2007; Trontelj et al., 2008).

Slika 4.3 Koničasta komora z vgrajenimi elektrodami.

5 ZAKLJUČEK

Pri raziskavah elektropermeabilizacije uporabljamo električne signale z velikim razponom parametrov. Vseh teh signalov ni možno generirati z enim samim generatorjem. Zato smo zasnovali nov modularen pristop k razvoju naprav za elektropermeabilizacijo, ki omogoča združevanje posameznih modulov in s tem izvedbo naprave s specifičnimi generatorji pulzov. V zasnovi smo predvideli, da je za pokritje celotnega raziskovalnega področja, zaradi nekompatibilnih elektronskih elementov in metod generiranja posameznih signalov, potrebnih vsaj pet različnih verzij naprav za elektropermeabilizacijo. Za vseh teh pet verzij smo podali konceptualno zasnovo, v kateri predlagamo skupen razvoj grafičnega uporabniškega vmesnika, nadzornega in napajalnega modula za vse verzije naprav. Le generatorje specifičnih signalov in izhodne module razvijamo za vsako verzijo posebej. Predlagana modularna zasnova vključuje tudi možnost nadgradnje posamezne verzije z novimi funkcijami ali generatorji signalov. Prav ta možnost je velika prednost pred običajnimi zasnovami naprav, saj se na področju raziskav elektropermeabilizacije in razvoju novih aplikacij zelo pogosto pojavljajo potrebe po novih signalih in razširjenem območju parametrov.

V okviru doktorske disertacije smo predlagali tudi nov način generiranja kratkih in dolgih pravokotnih signalov. Nov način generiranja kratkih pravokotnih signalov omogoča generiranje nanosekundnih pulzov spremenljive dolžine in polaritete z visoko ponavljalno frekvenco. Nov način generiranja dolgih pravokotnih signalov pa omogoča generiranje pravokotnih signalov s hitrim dvižnim in upadnim časom ter konstantno amplitudo tudi pri večjih obremenitvah. Predhodni generatorji pravkar omenjenih signalov niso zmogli generirati.

Večino predlogov smo preizkusili in realizirali z izvedbo naprave kratkih visokonapetostnih pulzov. V okviru te verzije smo razvili in izdelali vse skupne module ter generator kratkih visokonapetostnih pravokotnih pulzov. Razvoj naprave je že pokazal nekatere prednosti zasnove. Tako smo med razvojem brez kakršnekoli

programske spremembe zamenjali računalniški sistem grafičnega uporabniškega vmesnika, kar podpira že v sami zasnovi upoštevano zamenljivost posameznih modulov. Prav tako smo z razvojem naprave začeli brez vnaprej natančno določenih povezav med moduli, kar potrjuje vsestranskost v zasnovi predvidenih povezav med moduli. Pokazali smo tudi, da predlagan način kratkih pravokotnih pulzov lahko generira nanosekundne pulze spremenljive dolžine od 20 ns do 200 ns, variabilne polaritete in visoke ponavljalne frekvence do 1,1 MHz.

V okviru tega dela smo razvili tudi elektrode na krovnem stekelcu, ki so se po prvih poizkusih s celicami skupaj z izvedbo naprave kratkih visokonapetostnih pulzov že izkazale kot zelo uporabne in učinkovite pri opazovanju vpliva nanosekundnih pulzov na biološke celice. Ker je debelina elektrod nekoliko manjša od višine celic, ki sedimentirajo na krovno stekelce, bi bilo v nadaljevanju zanimivo z izračunom oceniti dejansko električno polje med elektrodama. Prav tako bi bilo zanimivo z izboljšanjem tehnološkega postopka izdelave izdelati elektrode z večjo debelino. Poleg tega smo razvili in izdelali tudi koničasto komoro z vgrajenimi elektrodami, ki so se prav tako po prvih poizkusih s celicami že izkazale za zelo uporabne pri genski elektrotransfekciji in elektrofuziji.

Skupne module, ki smo jih razvili v okviru tega dela, bomo v nadaljevanju uporabili pri razvoju prihodnjih izvedb naprave. Tako bomo predvidoma porabili veliko manj časa za razvoj posamezne izvedbe naprave. Razviti skupni moduli že vključujejo zmožnost izvrševanja zelo zahtevnih funkcij, ki jih predvidevajo prihodnje izvedbe naprave. Tako lahko računalniški sistem v realnem času shranjuje 16 MBit-ov podatkov na sekundo, kakršen prenos se zahteva za shranjevanje vseh podatkov o toku in napetosti med elektropermeabilizacijo. Prav tako lahko nadzorni modul s povprečenjem diferenc toka v realnem času oceni potek elektropermeabilizacije, kar se zahteva pri regulaciji elektropermeabilizacije. Uporabniški grafični vmesnik in nadzorni modul sta univerzalna in zato primerna tudi za upravljanje ostalih podobno zahtevnih naprav.

PRISPEVKI K ZNANOSTI

V disertaciji sem predstavil naslednje izvirne prispevke k znanosti:

- **Zasnova in preizkus novega modularnega pristopa k razvoju raziskovalne naprave za elektropermeabilizacijo**

  Osnovna ideja novega pristopa je razdeljenost razvoja na posamezne module, ki so med seboj povezani z uveljavljenimi standardnimi ali programirljivimi komunikacijskimi protokoli. Izboljšave in zamenjave posameznih modulov tako ne zahtevajo strojnih izboljšav ostalih modulov. Modularni pristop k razvoju posameznih generatorjev električnih pulzov pa omogoča enostavno nadgradnjo naprave ter enostavno izdelavo naprave s točno določenimi funkcijami.

- **Zasnova in preizkus novega načina upravljanja naprav za elektropermeabilizacijo**

  Z novo zasnovo grafičnega uporabniškega vmesnika in nadzornega modula je upravljanje naprav za elektropermeabilizacijo enostavnejše in učinkovitejše. Nova zasnova omogoča prikazovanje in shranjevanje večjega števila ter hitrejše analize izmerjenih podatkov.

- **Zasnova in preizkus novega načina generiranja visokonapetostnih impulzov**

  Z aktivnim ter sinhroniziranim polnjenjem in praznjenjem obeh koncev valovodnih linij Blumleinovega generatorja lahko generiramo nanosekundne električne pulze variabilne dolžine in polaritete z visoko ponavljalno frekvenco. Predlagan način tako omogoča generiranje širšega območja električnih parametrov zanimivih za raziskovalce elektropermeabilizacije.

- **Zasnova in izdelava nove koničaste komore z vgrajenimi elektrodami**
  Uporaba predstavljene koničaste komore zmanjša število pipetiranj pri poizkusih elektropermeabilizacije, ki lahko negativno vplivajo na potek elektropermeabilizacije, elektrofuzije in genske elektrotransfekcije. V komoro so vgrajene posebne elektrode, ki omogočajo generiranje sorazmerno enakomernega električnega polja v več smereh ter s tem boljše rezultate pri elektrofuziji in genski elektrotransfekciji.

LITERATURA

Abidor, I. G., V. B. Arakelyan, L. V. Chernomordik, Y. A. Chizmadzhev, V. F. Pastushenko, M. R. Tarasevich. 1979. *246-electric breakdown of bilayer lipid membranes: i. The main experimental facts and their qualitative discussion.* Bioelectrochem. Bioenerg., 6:37–52.

Behrend, M., A. Kuthi, X. Gu, P. T. Vernier, L. Marcu, C. M. Craft, M. A. Gundersen. 2003. *Pulse generators for pulsed electric field exposure of biological cells and tissues,* IEEE Trans. Dielectr. Electr. Insul. 10:820-825.

Bettan, M., M. A. Ivanov, L .M. Mir, F. Boissiere, P. Delaere, D. Scherman. 2000. *Efficient DNA electrotransfer into tumors.* Bioelectrochemistry, 52:83-90.

Bobrowska-Hagerstand, M., H. Hagerstand, A. Iglič. 1998. *Membrane skeleton and red blood cell vesiculation at low pH.* Biochim. Biophys. Acta, 1371:123-128.

Canatella, P. J., J. F. Karr, J. A. Petros, M. R. Prausnitz. 2001. *Quantitative study of electroporation-mediated molecular uptake and cell viability*, Biophysical journal, 80:755-764.

Chang, D.C.. 1989. *Cell poration and cell fusion using an oscillating electric field,* Biophys. J., 56:641-652.

Cukjati, D., D. Batiuskaite, F. André, D. Miklavčič, L. M. Mir. 2007. *Real time electroporation control for accurate and safe in vivo non-viral gene therapy,* Bioelectrochemistry, 70:501-507.

Čorović, S., M. Pavlin, D. Miklavčič. 2007. *Analytical and numerical quantification and comparison of the local electric field in the tissue for different electrode configurations,* Biomed. Eng. Online, 6:14.

De Angelis, A., L. Zeni, G. Leone. 2006. *Blumlein configuration for variable length high-voltage pulse generation by simultaneous switch control,* Electronics letters, 42(4):205-207.

De Angelis, A., J. F. Kolb, L. Zeni, K. H. Schoenbach. 2008. *Kilovolt Blumlein pulse generator with variable pulse duration and polarity,* Rev. Sci. Instrum., 79(4): 044301.

Defrancesco, L.. 1997. *Shock jockes: a profile of 22 electroporators from 11 companies.* The scientist, 11(15):19.

Faurie, C., E. Phez, M. Golzio, C. Vossen, J. C. Lesbordes, C. Delteil, J. Teissié, M. P. Rols. 2004. *Effect of electric field vectoriality on electrically mediated gene delivery in mammalian cells*, Biochim. Biophys. Acta, 1665:92-100.

Ferber, D. 2001. *Gene therapy: Safer and virus-free?*, Science, 294:1638-1642.

Flisar, U. 2005. *Kombinirani-PFC usmernik*, Diplomsko delo, Fakulteta za elektrotehniko, Univerza v Ljubljani, Ljubljana.

Gehl, J. 2003. *Electroporation: theory and methods, perspectives for drug delivery, gene therapy and research,* Acta Physiol. Scand., 177:437-447.

Golzio, M., M. P. Mora, C. Raynaund, C. Delteil, J. Tessié, M. P. Rols. 1998. *Control by osmotic pressure of voltage-induced permeabilization and gene transfer in mammalian cells,* Biophys. J., 74:3015-3022.

Gould, G. W.. 1995. *Biodeterioration of foods and an overview of preservation in the food and dairy industries.* Int. Biodeterior. Biodegrad., 36:267-277.

Hannig, J., C. Dawkins, P. F. Tosi, C. Nicolau. 1995. *Stability and immunological reactivity of recombination membrane CD4 electroinserted into the plasma membrane of erythrocytes.* FEBS Lett., 359:9-14.

Heller, R., R. Gilbert, M. J. Jaroszeski. 1999. *Clinical applications of electrochemotherapy.* Adv. Drug Deliver. Rev., 35:119-129.

Herweijer, H., J. A. Wolff. 2003. *Progress and prospects: naked DNA gene transfer and therapy.* Gene. Ther., 10:453-458.

Jaroszeski, M. J., R. Heller, R. Gilbert. 1999. *Electrochemotherapy, electrogenetherapy and transdermal drug delivery.* Humana Press, Totowa.

Kinosita, K., T. Y. Tsong. 1977. *Formation and resealing of pores of controlled sizes in human erythrocyte membrane,* Nature, 268:438-441.

Kolb, J. F., S. Kono, K. H. Schoenbach. 2006. *Nanosecond Pulsed Electric Field Generators for the Study of Subcellular Effects,* Bioelectromagnetics J., 27(3):172-187, 2006.

Kotnik, T., F. Bobanović, D. Miklavčič. 1997. *Sensitivity of transmembrane voltage induced by applied electric fields – a theoretical analysis,* Bioelectrochem. Bioenerg., 43:285-291.

Kotnik, T., A. Maček-Lebar, D. Miklavčič, L. M. Mir. 2000. *Evaluation of cell membrane electropermeabilization by means of a nonpermeant cytotoxic agent,* Biotechniques, 28:921-926.

Kotnik, T., L. M. Mir, K. Flisar, M. Puc, D. Miklavčič,. 2001a. *Cell membrane electropermeabilization by symmetrical bipolar rectangular pulses: Part I. Increased efficiency of permeabilization,* Bioelectrochemistry, 54:83-90.

Kotnik, T., D. Miklavčič, L. M. Mir. 2001b. *Cell membrane electropermeabilization by symmetrical bipolar rectangular pulses: Part II. Reduced electrolytic,* Bioelectrochemistry, 54:91-95.

Kotnik, T., G. Pucihar, M. Reberšek, L. M. Mir, D. Miklavčič. 2003. *Role of pulse shape in cell membrane electropermeabilization,* Biochim. Biophys. Acta, 1614:193-200.

Kramar, P.. 2000. *Programska oprema za sistem za generiranje pulzov poljubnih oblik, zajem podatkov in krmiljenje merilnega sistema za poskuse na lipidnih dvoslojih.* Prešernova naloga, Fakulteta za elektrotehniko, Univerza v Ljubljani, Ljubljana.

Kramar, P., D. Miklavčič, A. Maček Lebar. 2007. *Determination of the lipid bilayer breakdown voltage by means of linear rising signal,* Bioelectrochem., 70:23–27.

Kranjc, M. 2006. *Napetostni preklopnik za mikroelektrode pri elektrogenski transfekciji,* Prešernova naloga, Fakulteta za elektrotehniko, Univerza v Ljubljani, Ljubljana.

Kranjc, M. 2007. *Metoda za generiranje nanopulzev s spreminjajočim trajanjem in visoko ponavljalno frekvenco za elektropermeabilizacijo celičnih organelov,* Diplomsko delo, Fakulteta za elektrotehniko, Univerza v Ljubljani, Ljubljana.

Maček-Lebar, A., G. Serša, M. Čemažar, D. Miklavčič. 1998. *Elektroporacija,* Medicinski razgledi. 37:339-354.

Maček-Lebar, A. 1999. *Vpliv električnih parametrov na elektroporacijo v in vitro pogojih,* Doktorska disertacija, Fakulteta za elektrotehniko, Univerza v Ljubljani, Ljubljana.

Maček-Lebar, A., D. Miklavčič. 2001. *Cell electropermeabilization to small molecules in vitro: control by pulse parameters,* Radiol. Oncol., 35(3):193-202.

Miklavčič, D., D. Šemrov, H. Mekid, L. M. Mir. 2000. *A validated model of in vivo electric field distribution in tissues for electrochemotherapy and for DNA electrotransfer for gene therapy,* Biochim. Biophys. Acta, 1523:73-83.

Miklavčič, D., N. Pavšelj, F. X. Hart. 2006a. *Electric Properties of Tissues*. Wiley Encyclopedia of Biomedical Engineering, John Wiley & Sons, New York.

Miklavčič, D., S. Čorović, G. Pucihar, N. Pavšelj. 2006b. *Importance of tumour coverage by sufficiently high local electric field for effective electrochemotherapy,* EJC supplements, 4:45-51.

Mir, L. M., S. Orlowski, J. Belehradek, J. Teissie, M.P. Rols, G. Serša, D. Miklavčič, R. Gilbert, R. Heller. 1995. *Biomedical applications of electric pulses with special emphasis on antitumor electrochemotherapy.* Bioelectrochem. Bioenerg., 38:203-207.

Mir, L. M., M. F. Bureau, R. Rangara, B. Schwartz, D. Scherman. 1998. *Long-term, high level in vivo gene expression after electric pulse-mediated gene transfer into skeletal muscle,* C. R. Acad. Sci. Paris, 321:893-899.

Mir, L. M., S. Orlowski. 1999. *Mechanisms of electrochemotherapy.* Adv. Drug Deliver. Rev., 35:107-118.

Mir, L. M. 2000. *Therapeutic perspectives of in vivo cell electropermeabilization,* Bioelectrochem., 53:1-10.

Mir, L. M., J. Gehl, G. Serša, C.G. Collins, J.R. Garbay, V. Billard, P.F. Geertsen, Z. Rudolf, G.C. O'Sullivan, M. Marty. 2006. *Standard operating procedures of the electrochemotherapy: Instructions for the use of bleomycin or cisplatin administered either systemically or locally and electric pulses delivered by the Cliniporator^{TM} by means of invasive or non-invasive electrodes,* EJC supplements, 4:14-25.

Mouneimne, Y., P.-F. Tosi, Y. Gazitti, C. Nicolau. 1989. *Electro-inserted xeno-glycophorin into red blood cell membrane,* Biochem. Bioph. Res. Co., 159(1):34-40.

Neumann, E., M. Schaefer-Ridder, Y. Wang, P. H. Hofschneider. 1982. *Gene transfer into mouse lynoma cells by electroporation in high electric fields,* EMBO J., 7(1):841-845.

Neumann, E., A. E. Sowers, C. A. Jordan. 1989. *Electroporation and Electrofusion in Cell Biology,* Plenum Press, New York.

Neumann, E., S. Kakorin, K. Toensing. 1999. *Fundamentals of electroporative delivery of drugs and genes,* Bioelectrochem. Bioenerg., 48:3-16.

Pavlin, M., M. Kandušer, M. Reberšek, G. Pucihar, F. X. Hart, R. Magjarević, D. Miklavčič. 2005. *Effect of Cell Electroporation on the Conductivity of a Cell Suspension,* Biophys. J., 88: 4378–4390.

Petkovšek, M., J. Nastran, D. Vončina, P. Zajec, D. Miklavčič, G. Serša. 2002. *High voltage pulse generation,* Electronics letters, 38(14):680-682, 2002.

Petkovšek, M. 2004. *Visokodinamični pulzni napetostni vir za in vivo elektropermeabilizacijo,* Doktorska disertacija, Fakulteta za elektrotehniko, Univerza v Ljubljani, Ljubljana.

Pilwat G., H. P. Richter, U. Zimmermann. 1981. *Giant culture cells by electric field-induced fusion.* FEBS lett., 133(1):169-174.

Prausnitz, M. R. 1996. *The effect of electric current applied to skin: A review for transdermal drug delivery,* Adv. Drug Deliver. Rev., 18:395-425.

Prud'homme, G. J., Y. Glinka, A. S. Khan, R. Draghia-Akli. 2006. *Electroporation-enhanced nonviral gene transfer for the prevention or treatment of immunological, endocrine and neoplastic diseases.* Curr. Gene Ther., 6:243-273.

Puc, M. 1998. *Naprava za klinično elektroporacijo,* Prešernova naloga, Fakulteta za elektrotehniko, Univerza v Ljubljani, Ljubljana.

Puc, M., S. Čorović, K. Flisar, M. Petkovšek, J. Nastran, D. Miklavčič. 2004a. *Techniques of signal generation required for electropermeabilization. Survey of electropermeabilization devices* Bioelectrochemistry, 64:113-124, 2004.

Puc, M. 2004b. *High performance electropermeabilization device,* Doktorska disertacija, Fakulteta za elektrotehniko, Univerza v ljubljani,.

Pucihar, G, T. Kotnik, M. Kandušer, D. Miklavčič. 2001. *The influence of medium conductivity on electropermeabilization and survival of cells in vitro.* Bioelectrochemistry, 54:107-115,

Pucihar, G., L. M. Mir, D. Miklavčič. 2002. *The effect of pulse repetition frequency on the uptake into electropermeabilized cells in vitro with possible applications in electrochemotherapy,* Bioelectrochemistry, 57:167-172.

Reberšek, M. 2001. *Elektroporacija z moduliranimi visokonapetostnimi električnimi pulzi,* Prešernova naloga, Fakulteta za elektrotehniko, Univerza v Ljubljani, Ljubljana.

Reberšek, M. 2004. *Elektrogenska transfekcija v odvisnosti od ponavljalne frekvence pulzov in orientacije električnega polja,* Diplomsko delo, Fakulteta za elektrotehniko, Univerza v Ljubljani, Ljubljana.

Reberšek, M., C. Faurie, M. Kandušer, S. Čorović, J. Teissié, M. P. Rols, D. Miklavčič. 2007. *Electroporator with automatic change of electric field direction improves gene electrotransfer in vitro,* Biomed. Eng. Online, 6:25.

Reberšek, M., S. Čorović, G. Serša, D. Miklavčič. 2008. *Electrode commutation sequence for honeycomb arrangement of electrodes in electrochemotherapy and corresponding electric field distribution,* Bioelectrochemistry, članek v tisku.

Rols, M. P., J. Teissié. 1992. *Experimental evidence for involment of the cytoskeleton in mammalian cell electropermeabilization,* Biochim. Biophys. Acta, 1111:45-50.

Rols, M. P., C. Delteil, G. Serin, J. Teissié. 1994. *Temperature effects on electrotransfection of mammalian cells.* Nucleic Acids Res., 22:540.

Rols, M. P., J. Teissié. 1998. *Electropermeabilization of mammalian cells to macromolecules: control by pulse duration,* Biophys. J., 75:1415-1423.

Rols, M. P., Y. Tamzali, J. Teissie. 2002. *Electrochemotherapy of horses. A preliminary clinical report.* Bioelectrochemistry, 55:101-105.

Rols, M. P. 2006. *Electropermeabilization, a physical method for the delivery of therapeutic molecules into cells,* Biochim. Biophys. Acta (biomembranes), 1758(3):423-428.

Rubanyi, G. M.. 2001. *The future of human gene therapy.* Mol. Aspects Med., 22:113-142.

Schwan, H. P. 1957. *Electrical properties of tissue and cell suspensions,* Adv. Biol. Med. Phys., 5:147–209.

Serša, G., B. Štabuc, M. Čemazar, B. Jančar, D. Miklavčič, Z. Rudolf. 1998. *Electrochemotherapy with cisplatin: Potentation of local cisplatin antitumor effectivness by application of electric pulses in cancer patients,* Eur. J. Cancer, 34(8):1213-1218.

Serša, G. 2006. *The state-of-the-art of electrochemotherapy before the ESOPE study; advantages and clinical uses,* EJC supplements, 4:52-59.

Schoenbach, K. H., S. J. Beebe, and E. S. Buescher. 2001. *Intracellular effect of ultrashort electrical pulses.* Bioelectromagnetics, 22:440–448.

Sixou, S., J. Teissié. 1990. *Specific electropermeabilization of leucocytes in a blood sample and application to large volumes of cells,* Biochim. Biophys. Acta, 1028:154-160.

Smith, K. C., J. C. Weaver. 2008. *Active mechanisms are needed to describe cell responses to submicrosecond, megavolt-per-meter pulses: Cell models for ultrashort pulses,* Biophys. J., 95:1547-1563.

Somiari, S., J. G. Malone, J. J. Drabick, R. A. Gilbert, R. Heller, M. J. Jaroszeski, R. W. Malone. 2000. *Theory and in vivo application of electroporative gene delivery.* Mol. Ther., 2(3):178-187.

Sun, Y., P. T. Vernier, M. Behrend, L. Marcu, M. A. Gundersen. 2005. *Electrode Microchamber for Noninvasive Perturbation of Mammalian Cells With Nanosecond Pulsed Electric Fields,* IEEE Trans. Nanobioscience, 4:277-283.

Šatkauskas, S., M. F. Bureau, M. Puc, A. Mahfoudi, D. Scherman, D. Miklavčič, L. M. Mir. 2002. *Mechanisms of in vivo DNA electrotransfer: respective contributions of cell electropermeabilization and DNA electrophoresis,* Mol. Ther., 5(2):133-140.

Teissié, J., T.Y. Tsong. 1981. *Electric field induced transient pores in phospolipid bilayer vesicles,* Biochemistry, 20:1548-1554.

Teissie, J., M. P. Rols. 1986. *Fusion of mammalian cells in culture is obtained by creating the contact between cells after their electropermeabilization.* Biochem. Biophys. Res. Commun., 140(1):258-266.

Teissié, J., M. P. Rols. 1993. *An experimental evaluation of the critical potential difference inducing cell membrane electropermeabilization,* Biophys. J., 65:409-413.

Teissie J.. 1998. *Transfer of foreign receptors to living cell surfaces: the bioelectrochemical approach.* Bioelectrochem. Bioenerg., 46:115-120.

Teissié, J., N. Eynard, B. Gabriel, M. P. Rols. 1999. *Electropermeabilization of cell membranes,* Adv. Drug Deliv. Rev., 35:3-19.

Teissié, J., M. Golzio, M. P. Rols. 2005. *Mechanisms of Cell membrane Electropermeabilization : A minireview of our present (lack of ?) knowledge,* BBA - General Subjects Special Issue : Biophysics Complex Systems, 1724(3):270-80.

Trontelj, K., M. Reberšek, D. Miklavčič. 2008a. *Koničasta komora z vgrajenimi elektrodami za elektroporacijo manjšega volumna, za elektrofuzijo in gensko transfekcijo,* Patent, Urad RS za intelektualno lastnino, Ljubljana.

Trontelj, K., M. Reberšek, M. Kandušer, V. Čurin-Šerbec, M. Šprohar, D. Miklavčič. 2008b. *Optimization of bulk cell electrofusion in vitro for production of human-mouse heterohybridoma cells*. Bioelectrochemistry. članek v tisku.

Tsong, T. Y. 1991. *Electroporation of cell membranes,* Biophys. J., 60:297-306.

Uemura, K., S. Isobe. 2003. *Developing a new apparatus for inactivating bacillus subtilis spore in orange juice with a high electric field AC under pressurized conditions.* J. Food Eng., 56:325-329.

Vanbeaver, R., N. Lecouturier, V. Preat. 1994. *Transdermal delivery of metropol by electroporation,* Pharmaceut. Res., 11:1657-1662.

Vanbever, R., V. Preat. 1999. *In vivo efficacy and safety of skin electroporation.* Adv. Drug Deliv. Rev., 35:77-88.

Vernhes, M. C., P. A. Canabes, J. Teissié. 1999. *Chinese hamster ovary cells sensitivity to localized electrical stress*. Bioelectrochem. Bioenerg., 48:17-25.

Vernhes, M. C., A. Benichou, P. Pernin, P. A. Cabanes, J. Teissie. 2002. *Elimination of free-living amoebae in fresh water with pulsed electric fields.* Wat. Res., 36:3429-3438.

Vernier, P. T., Y. H. Sun, M. A. Gundersen. 2006. *Nanoelectropulse-driven membrane perturbation and small molecule permeabilization,* BMC Cell Biology, 7(37):1-16.

Weaver, J. C., Y. A. Chizmadzhev. 1996. *Theory of electroporation: a review,* Bioelectrochem. Bioenerg., 41:135-160.

Wong, T. K., E. Neumann. 1982. *Electric field mediated gene transfer,* Biochem. Bioph. Res. Co., 107:584-587.

Spletne strani

www.cypress.com
www.ixysrf.com
www.microchip.com
www.xilinx.com

PRILOGE

Članki, katerih vsebina vključuje raziskave opisane v doktorski disertaciji

Kotnik, T., G. Pucihar, M. Reberšek, L. M. Mir, D. Miklavčič. 2003. *Role of pulse shape in cell membrane electropermeabilization,* Biochim. Biophys. Acta, 1614:193-200.

Pavlin, M., M. Kandušer, M. Reberšek, G. Pucihar, F. X. Hart, R. Magjarević, D. Miklavčič. 2005. *Effect of Cell Electroporation on the Conductivity of a Cell Suspension,* Biophys. J., 88: 4378–4390.

Reberšek, M., C. Faurie, M. Kandušer, S. Čorović, J. Teissié, M. P. Rols, D. Miklavčič. 2007. *Electroporator with automatic change of electric field direction improves gene electrotransfer in vitro,* Biomed. Eng. Online, 6:25.

Reberšek, M., S. Čorović, G. Serša, D. Miklavčič. 2008. *Electrode commutation sequence for honeycomb arrangement of electrodes in electrochemotherapy and corresponding electric field distribution,* Bioelectrochemistry, članek v tisku.

Trontelj, K., M. Reberšek, M. Kandušer, V. Čurin-Šerbec, M. Šprohar, D. Miklavčič. 2008. *Optimization of bulk cell electrofusion in vitro for production of human-mouse heterohybridoma cells*. Bioelectrochemistry. članek v tisku.

Patent, katerega vsebina vključuje raziskave opisane v doktorski disertaciji

Trontelj, K., M. Reberšek, D. Miklavčič. 2008. *Koničasta komora z vgrajenimi elektrodami za elektroporacijo manjšega volumna, za elektrofuzijo in gensko transfekcijo,* Patent, Urad RS za intelektualno lastnino, Ljubljana.

Available online at www.sciencedirect.com
SCIENCE DIRECT®
Biochimica et Biophysica Acta 1614 (2003) 193–200
BIOCHIMICA ET BIOPHYSICA ACTA
BBA
www.bba-direct.com

Role of pulse shape in cell membrane electropermeabilization

T. Kotnik[a], G. Pucihar[a], M. Reberšek[a], D. Miklavčič[a], L.M. Mir[b,*]

[a] *Faculty of Electrical Engineering, University of Ljubljana, SI-1000 Ljubljana, Slovenia*
[b] *Laboratory of Vectorogy and Gene Transfer, Institute Gustave-Roussy, UMR 8121 CNRS, 39 rue C. Desmoulins, F-94805 Villejuif, Cedex, France*

Received 19 February 2003; received in revised form 20 May 2003; accepted 26 May 2003

Abstract

The role of the amplitude, number, and duration of unipolar rectangular electric pulses in cell membrane electropermeabilization in vitro has been the subject of several studies. With respect to unipolar rectangular pulses, an improved efficiency has been reported for several modifications of the pulse shape: separate bipolar pulses, continuous bipolar waveforms, and sine-modulated pulses. In this paper, we present the results of a systematic study of the role of pulse shape in permeabilization, cell death, and molecular uptake. We have first compared the efficiency of 1-ms unipolar pulses with rise- and falltimes ranging from 2 to 100 μs, observing no statistically significant difference. We then compared the efficiency of triangular, sine, and rectangular bipolar pulses, and finally the efficiency of sine-modulated unipolar pulses with different percentages of modulation. We show that the results of these experiments can be explained on the basis of the time during which the pulse amplitude exceeds a certain critical value.

Keywords: Electropermeabilization; Electroporation; Pulse shape; Cell survival; Cell membrane permeability; Molecular uptake

1. Introduction

Electropermeabilization (also termed electroporation) is an effective method of internalization of various molecules into biological cells, with an increasing number of applications in oncology [1,2], genetics [3], immunology [4], and cell biology [5,6]. In parallel with the practical use of the method continues the quest for understanding the underlying mechanisms of the phenomenon [3,7–12].

The efficiency of electropermeabilization in vitro depends on various physical and chemical parameters, such as the molecular composition of the membrane [13,14] and osmotic pressure [15], but above all, on the parameters of electric pulses. Investigations of the role of the amplitude, number, and duration of unipolar rectangular pulses have been the subject of several comprehensive studies [16–20]. In addition, at least two studies have focused on a comparison of the efficiency of unipolar and bipolar rectangular pulses in vitro. Tekle et al. [21] compared continuous unipolar and bipolar 60-kHz rectangular waves of 400 μs total duration, and obtained a significantly better DNA transfection with a bipolar wave. Because electropermeabilization is usually not performed with continuous waves, but with sequences (trains) of separate pulses [18,22–25], our group compared the efficiency of unipolar and symmetrical bipolar rectangular pulses, in both cases delivering eight 1-ms pulses at 1-s intervals [26]. With bipolar pulses, permeabilization was achieved at lower pulse amplitudes and molecular uptake was significantly higher, while the pulse amplitude leading to cell death was practically unaltered. We also demonstrated that electrolytic contamination caused by the release of metal ions from the electrodes can be reduced considerably by the use of bipolar instead of unipolar pulses [27]. Even before these studies were published, bipolar pulses were applied successfully in electrochemotherapy [28], as well as for DNA transfection in vivo in mice [29,30].

Unlike the role of the amplitude, number, duration, and polarity of pulses, a hypothetical role of pulse dynamics, or the "pulse shape," has not yet been a subject to a broader systematic investigation.[1] One of the reasons for this is the absence of commercially available programmable genera-

* Corresponding author. Tel.: +33-1-42-11-47-92; fax: +33-1-42-11-52-45.
E-mail address: luismir@igr.fr (L.M. Mir).

[1] Unipolar and bipolar pulses should not be conceived as having different "shapes," since a bipolar pulse is a sequence of two consecutive, oppositely polarized unipolar pulses.

0005-2736/03/$ - see front matter © 2003 Elsevier B.V. All rights reserved.
doi:10.1016/S0005-2736(03)00173-1

tors of high-voltage waveforms, which confines these studies to the laboratories with access to custom-designed electronic equipment. Kinosita and Tsong [31] used linearly increasing electric fields with rates of increase from 12.5 V/cm per microsecond up to 50 V/cm per microsecond for permeabilization of erythrocytes, and concluded that field intensity at which permeabilization occurs is not affected by this rate of increase. Chang et al. reported an improved efficiency of cell permeabilization and fusion [32], as well as gene transfection [33] when a sine wave (40 kHz–1 MHz) was superimposed to a rectangular pulse. Xie and Tsong [34] compared rectangular, sine, and triangular waves with extremely long durations (1–100 s) and relatively low amplitudes (voltage-to-distance ratio 50–200 V/cm), obtaining the most efficient transfection for rectangular, less for sine, and the least for triangular waves. It is, however, uncertain (as the authors themselves agree) whether the transfection was achieved due to permeabilization itself, or rather due to subsequent electrophoresis and electroosmosis caused by the very long pulse duration. Moreover, Šatkauskas et al. [35] recently clearly demonstrated that, even though prior electropermeabilization is necessary, efficiency of DNA-electrotransfer in skeletal muscle depends critically on the electrophoretic component of the pulses.

In this paper, we present the results of a systematic study of the role of pulse shape in cell permeabilization, cell death, and uptake of exogenous molecules. Using custom-designed electronic equipment developed in our laboratory, we compared the efficiency of: (i) unipolar rectangular (trapezoidal) pulses with different rise- and falltimes, (ii) bipolar rectangular, sinusoidal, and triangular pulses, and (iii) unipolar unmodulated and sine-modulated rectangular pulses. Part (i) of the study aimed at an investigation of possible role of the first derivative of the pulse amplitude in electropermeabilization. Parts (ii) and (iii) then focused on the influence of other parameters of the pulse shape, and on the search of a plausible explanation of the obtained results, as well as of the related results published in previous studies [31–34].

2. Materials and methods

2.1. Cells

DC3F cells, a line of spontaneously transformed Chinese hamster fibroblasts [36], were grown in monolayers at 37 °C and 5% CO_2 (Universal Water Jacketed Incubator, Forma Scientific, Marietta, OH, USA). One hundred fifty-square centimeter flasks were used for general cultivation, and 60-mm petri dishes were used for cloning efficiency assays (both from TPP, Trasadingen, Switzerland). The culture medium consisted of Eagle minimum essential medium EMEM 41090 supplemented with 10% fetal bovine serum (both from Life Technologies, Rockville, MD, USA), 100 U/ml of penicillin and 125 μg/ml of streptomycin (both from Sarbach/Solvay Pharma, Brussels, Belgium).

2.2. Exposure to electric pulses

To allow for comparison with experiments using different electrode distances, the intensity of the pulses was characterized by the voltage-to-distance ratio (VDR), which was calculated as the voltage delivered to the electrodes divided by the distance between them. Since for stainless steel electrodes, the voltage drop at the electrode–electrolyte interface is very small [37], and the dimensions of the droplet in the plane parallel to the electrode plates were several times larger than the distance between the electrodes, the VDR is also a good estimate of the electric field within the droplet.

After trypsination with trypsin–EDTA (Life Technologies), cells were centrifuged for 5 min at 1000 rpm in a C312 centrifuge (Jouan, St. Herblain, France) and resuspended at 2×10^7 cells/ml in the electropermeabilization medium. Spinner minimum essential medium SMEM 21385 (Life Technologies) with electrical conductivity of 1.6 S/m was used for trapezoidal (unipolar rectangular with adjustable rise- and falltimes), bipolar rectangular, bipolar sine, and bipolar triangular pulses. These pulses were generated by an AFG 310 programmable function generator (Tektronix, Wilsonville, OR, USA), amplified with a bipolar amplifier built in the Laboratory of Biocybernetics at the Faculty of Electrical Engineering of the University of Ljubljana (the device is described in detail in Ref. [38]). The medium consisting of 250 mM sucrose, 10 mM phosphate buffer, and 1 mM $MgCl_2$ (made according to Ref. [39]) with electrical conductivity of 0.15 S/m was used for the sine-modulated pulses, which were generated by a custom-designed high-voltage waveform generator built in the same laboratory. In all experiments, the pulses were delivered through a pair of flat stainless steel electrodes 2 mm apart, between which a 50-μl droplet of the cell suspension was placed.

2.3. Determination of cell survival

The percentage of surviving cells was determined by their cloning efficiency after pulsation in the electropermeabilization medium. Subsequent to pulsation, the cells were incubated for 10 min at room temperature and then diluted by the addition of 950 μl of SMEM to prevent drying. After additional 30 min, cells were diluted in the culture medium to 100 cells/ml, and 4 ml of suspension was transferred into each 60-mm petri dish where the cells were grown for 5 days. Cells were then fixed for 15 min with 100% ethanol (Carlo Erba Reagenti, Milan, Italy) and consecutively stained for 15 min with 1% crystal violet (Sigma, St. Louis, MO, USA). Clone colonies were counted under a light microscope (Leica, Wetzlar, Germany) and normalized to the control (cells not exposed to electric pulses) to obtain the percentage of surviving cells.

2.4. Determination of cell electropermeabilization

The percentage of electropermeabilized cells was determined by their cloning efficiency after pulsation in the electropermeabilization medium containing 5 nM bleomycin (Laboratoires Roger Bellon, Neuilly-Sur-Seine, France). An intact membrane is impermeable to bleomycin, and while at 5 nM external concentration bleomycin has no effect on nonpermeabilized cells, it causes the death of electropermeabilized cells [40]. This method is highly selective and accurate, as well as affordable.

Subsequent to pulsation, the cells were incubated for 10 min at room temperature and then diluted by the addition of 950 μl of SMEM. After additional 30 min, cells were diluted in the culture medium, grown for 5 days and then fixed and stained as described above. Clone colonies were counted and normalized to the control (unpulsed cells, 5 nM bleomycin) to obtain the percentage of cells surviving the exposure to electric pulses in suspension with 5 nM bleomycin. By subtracting this percentage from 100%, the percentage of permeabilized cells was obtained.

2.5. Determination of uptake of exogenous molecules

Uptake of exogenous molecules was determined by the cell fluorescence after pulsation in the electropermeabilization medium containing 1 mM lucifer yellow (Sigma), a nonpermeant fluorescent dye. Subsequent to pulsation, cells were incubated for 10 min at room temperature and then diluted by the addition of 950 μl of SMEM. After additional 30 min, cells were diluted in 5 ml of phosphate buffer saline (PBS, Life Technologies), and extracellular lucifer yellow was then washed away by two consecutive centrifugations and resuspensions in PBS. Each centrifugation was performed for 5 min at 1000 rpm, which causes no loss of cell viability. Cells were then broken down by ultrasonication (Sonifier 250, Branson Ultrasonics, Danbury, CT, USA) and fluorescence was measured in arbitrary units on a spectrofluorometer (SFM 25, BioTek, Winooski, VT, USA). Excitation was set at 418 nm wavelength and emission was detected at 525 nm.

At pulse amplitudes which lead to the death of practically all the cells in the population, the detected uptake of lucifer yellow remains somewhat above the background (control) level. This is due to the fact that dead cells are not only those that burst or decompose due to the intense permeabilization, but also those that initially reseal, yet due to the loss of their internal constituents have no ability to form clones. Such "cellular ghosts" retain some lucifer yellow, and this results in an apparent discrepancy between the survival and uptake at high pulse amplitudes (see Figs. 2, 4, and 7).

2.6. Treatment of experimental data

All experiments were repeated three times at intervals of several days or more. For each experimental point, mean and standard deviation were determined. Voltage-to-distance ratio was used as an estimate of electric field strength of the pulses. The percentages of surviving and permeabilized cells as functions of the applied voltage-to-distance ratio (VDR) were each fitted by a two-parameter sigmoidal curve,

$$y(x) = \frac{100\%}{1 + \exp[(x_c - x)/b]},$$

where x is the VDR, y is the percentage of cells, x_c is the x-value corresponding to $y = 50\%$, and b determines the slope of the sigmoid curve. The VDR leading to the permeabilization of 50% cells was denoted as $P_{50\%}$, and the VDR causing the death of 50% cells was denoted by $D_{50\%}$.

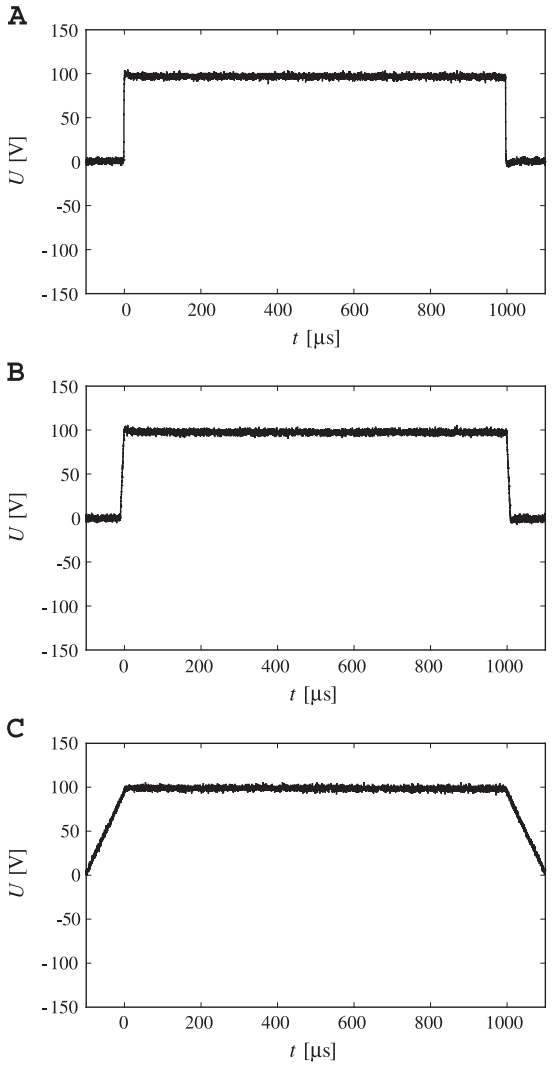

Fig. 1. The time course of a generated unipolar trapezoidal pulse of 1 ms duration, with rise- and falltimes of 2 μs (A), 10 μs (B), and 100 μs (C), and 100 V peak amplitude.

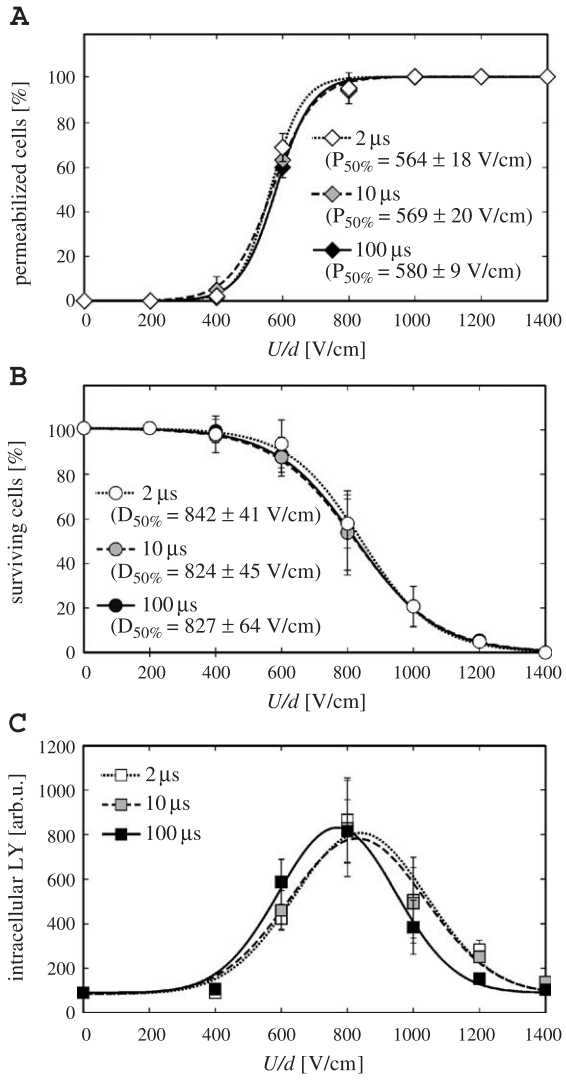

Fig. 2. The efficiency of eight unipolar trapezoidal pulses, 1 ms each, delivered in 1-s intervals, with rise- and falltimes of 2, 10, and 100 μs.

The fitting of sigmoidal curves to permeabilization and survival data is widely used, mostly on an empirical ground. However, in a recent theoretical paper [41], we showed that the two-parameter sigmoidal curves as given above are also in good agreement with the permeabilization and survival curves that would correspond to a Gaussian distribution of cell radii.

For the uptake of lucifer yellow, the intensity of fluorescence was fitted by a three-parameter Gaussian peak,

$$y(x) = y_{\max}\exp(-(x_c - x)^2/2b^2),$$

where x is again the VDR, y is the intracellular concentration of lucifer yellow, $y_{\max}$ is the maximum intracellular concentration of lucifer yellow in a given experiment, x_c is the x-value corresponding to $y = y_{\max}$, and b determines the width of the peak.

All fits were obtained by least-squares nonlinear regression using Sigma Plot 5.05 (SPSS, Richmond, CA, USA).

3. Results and discussion

3.1. Unipolar pulses with different rise- and falltimes

Fig. 1 shows the unipolar pulses with rise- and falltimes of 2, 10, and 100 μs generated by our setup, and Fig. 2 shows the percentage of electropermeabilized cells (panel A), percentage of surviving cells (panel B), and the internalized lucifer yellow (panel C) obtained with these pulses, each given as a function of voltage-to-distance ratio (VDR). In each case, eight pulses were delivered at intervals of 1 s, each pulse with the maximum VDR lasting for 1 ms (i.e., total pulse duration = risetime + 1 ms + falltime). The results shown in Fig. 2 imply that at least in the investigated range, the risetime and the falltime of the pulse do not play a detectable role in cell membrane permeabilization, which is in agreement with the results of Kinosita and Tsong [31] on erythrocytes.

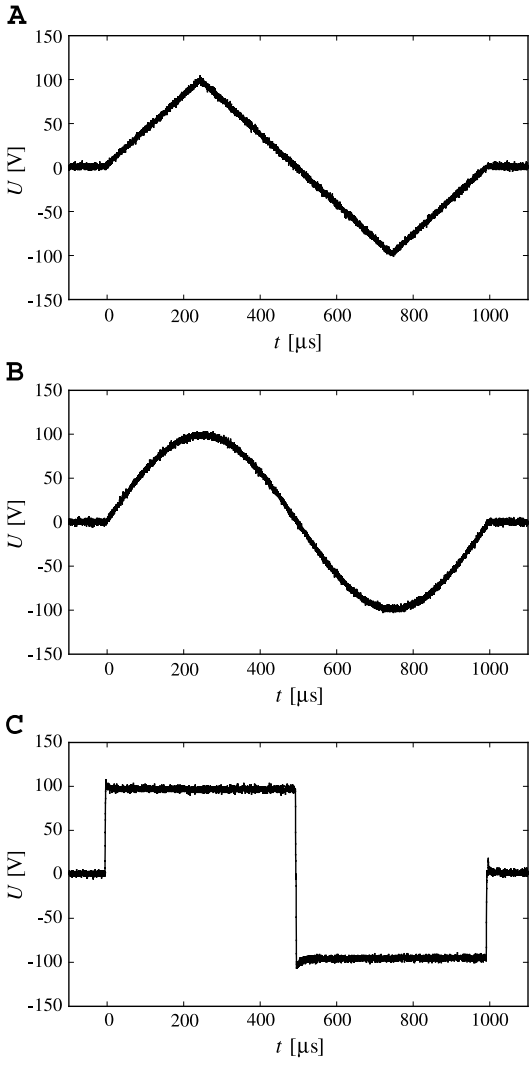

Fig. 3. The time course of a generated bipolar triangular (A), sine (B), and rectangular (C) pulse of 1 ms duration and 100 V peak amplitude.

3.2. Bipolar triangular, sine, and rectangular pulses

We previously reported on a significant difference between the efficiency of unipolar and symmetrical bipolar rectangular pulses of the same VDR and total duration [26]. In the present study, we compared the efficiency of bipolar pulses of different shapes: triangular, sine, and rectangular (Fig. 3). The results of this comparison are shown in Fig. 4, which reveals that electropermeabilization, cell death, and the peak of the uptake all occur at the lowest VDR amplitude for rectangular, and at the highest VDR amplitude for triangular pulses. In principle, these results alone could be explained by either different durations of above-critical VDR (i.e., different durations of VDR exceeding a certain critical value), or by different pulse dynamics (i.e., different values of the first derivative of the VDR with respect to time). However, the time

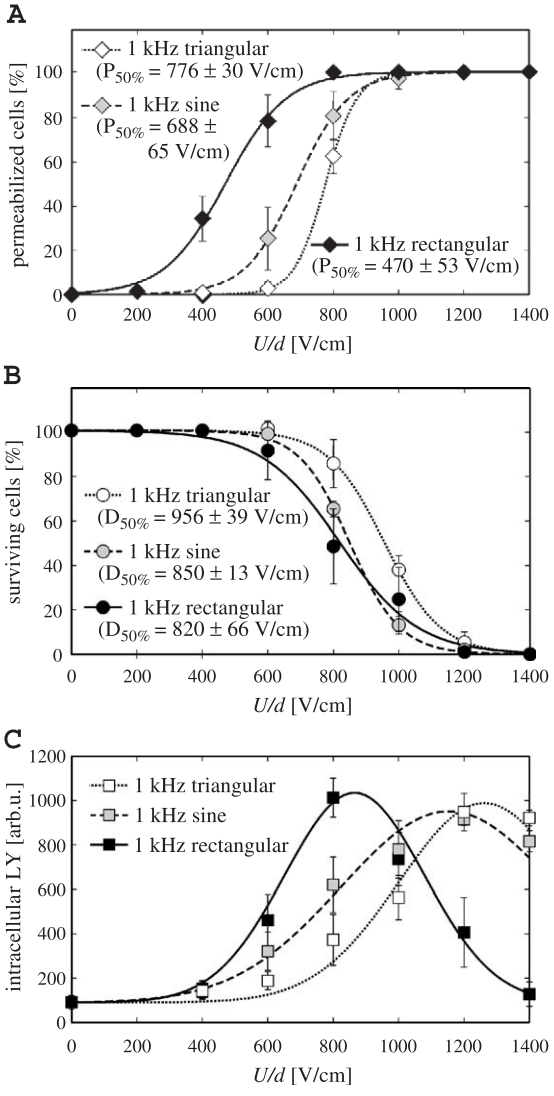

Fig. 4. The efficiency of eight symmetrical bipolar pulses, 1 ms each, delivered in 1-s intervals, for triangular, sine, and rectangular pulse shape.

Table 1
The peak VDR of 1 ms bipolar pulses of various shapes required for VDR of 470 V/cm to be exceeded without interruption for 200 and for 250 μs, compared to the experimentally determined values of $P_{50\%}$

	470 V/cm exceeded for 200 μs	470 V/cm exceeded for 250 μs	$P_{50\%}$
triangular pulse	783 V/cm	940 V/cm	776 V/cm
sine pulse	581 V/cm	665 V/cm	688 V/cm
rectangular pulse	470 V/cm	470 V/cm	470 V/cm

derivative of VDR was the only variable in the comparison of pulses with different rise- and falltimes (see Unipolar pulses with different rise- and falltimes subsection and Fig. 2), and this comparison shows no statistically significant differences. Consequently, the explanation based on pulse dynamics is unlikely, and it is plausible to attribute the results with different pulse shapes to differences in the duration of above-critical VDR. To an extent, this argument can also be supported quantitatively. In Table 1, the measured values of $P_{50\%}$ for triangular, sine, and rectangular bipolar pulses are compared to the theoretical values of the peak VDR required for the critical VDR of 470 V/cm to be exceeded without interruption for 200 μs and for 250 μs (depicted in Fig. 5). Applying durations other than these two does not provide a better agreement between the $P_{50\%}$ values and the peak VDR values, and this suggests that while the duration of above-critical VDR is indeed important for the efficiency of permeabilization, other parameters also contribute to this efficiency.

The importance of the duration of above-critical VDR is also compatible with the theory of electroporation, which attributes the increase of plasma membrane permeability to the formation of hydrophilic structures (“aqueous pores”) traversing the lipid bilayer and lined with the lipid headgroups [9]. According to this theory, considered by many as a plausible explanation of electropermeabilization, there is a threshold value of transmembrane voltage above which formation of aqueous pores becomes energetically favorable. Since the induced transmembrane voltage is proportional to the electric field [10], and thus practically proportional to the VDR (see Materials and methods section, Exposure to electric pulses subsection), this explains

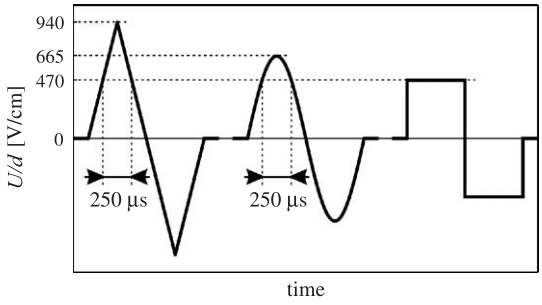

Fig. 5. The peak VDR required for a given value of VDR to be exceeded for a given duration varies with pulse shape. The figure shows the case of symmetric bipolar pulses of 1 ms duration, with VDR of 470 V/cm exceeded during 250 μs.

why an above-critical VDR is required for electropermeabilization. In addition, because the formation of aqueous pores is governed by statistical thermodynamics, the probability of formation of individual pores increases with the duration of the above-threshold transmembrane voltage, and thus with the duration of electric pulses.

3.3. Unipolar sine-modulated pulses

In the final part of this study, we compared the efficiency of unipolar unmodulated and sine-modulated rectangular pulses, the modulation at 50 kHz representing 10% or 90% of the peak VDR. The modulated pulses are shown in Fig. 6 (the unmodulated pulse is identical to the one shown in Fig. 1A), and the results of this comparison are given in Fig. 7. No statistically significant difference could be detected between an unmodulated and a 10%-modulated pulse, while with the 90%-modulated pulse, both $P_{50\%}$ and

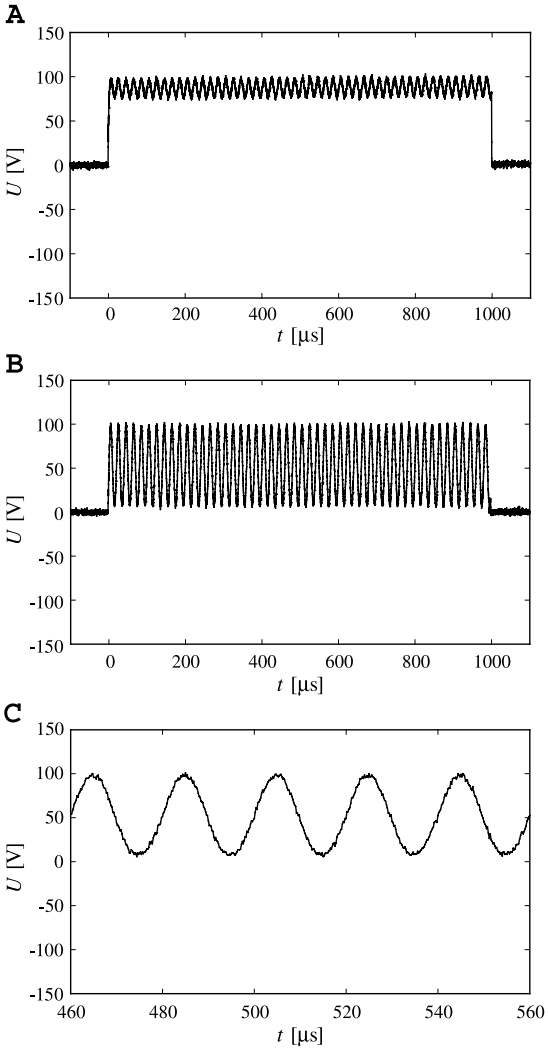

Fig. 6. The time course of a generated unipolar sine-modulated pulse of 1 ms duration and 100 V peak amplitude, with 10% modulation (A) and 90% modulation (B). The modulation frequency was 50 kHz. Panel C shows a part of the 90%-modulated signal in more detail.

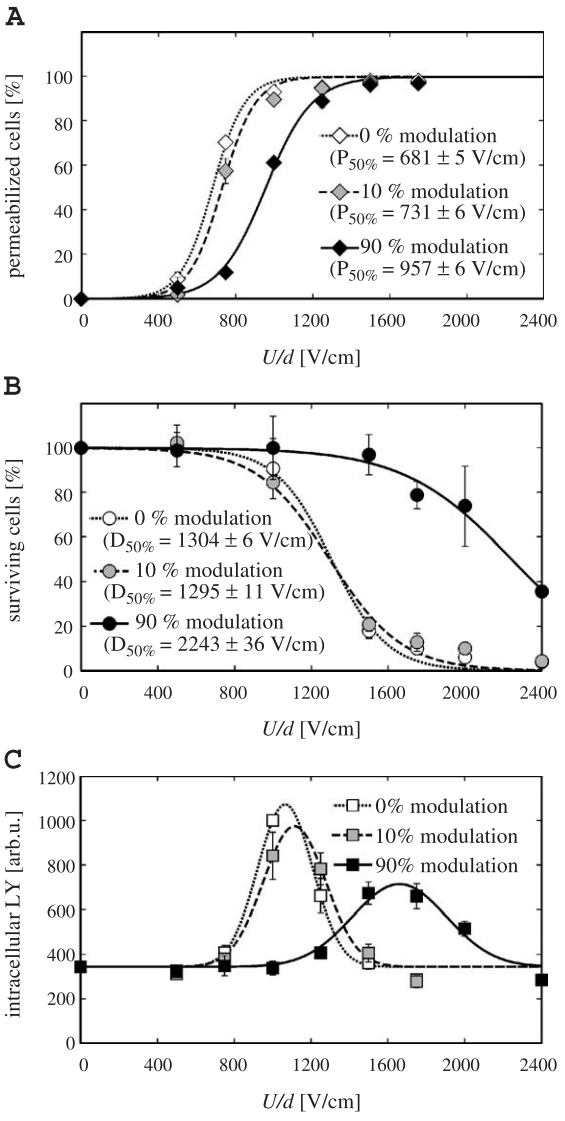

Fig. 7. The efficiency of one unipolar sine-modulated pulse of 1 ms duration, for 0% modulation (unmodulated), 10% modulation, and 90% modulation.

$D_{50\%}$ correspond to significantly higher VDRs than with either unmodulated or 10%-modulated pulse. The peak of the uptake is also rather similar for an unmodulated and a 10%-modulated pulse, while for a 90%-modulated pulse, this peak is much lower, and shifted towards much higher VDRs. These results can be explained by the same argument as the results with different waveforms (see Bipolar triangular, sine, and rectangular pulses)—namely, that the duration of the above-critical VDR has a major role in the efficiency of electropermeabilization. Despite the increase in pulse amplitude, this duration remains short for a 90%-modulated pulse, and consequently the peak of the uptake is rather low. Even at pulse amplitudes where practically all cells are permeabilized, the level of permeabilization is much lower with 90%-modulated pulses than with unmodulated or 10%-modulated pulses, which can also explain why

the value of $D_{50\%}$ is much higher with 90%-modulated pulses.

4. Conclusions

The results of this study show that among the parameters that describe the pulse shape, the time during which the pulse amplitude exceeds a certain critical value has a major role in the efficiency of electropermeabilization. As described above, this conclusion is in agreement with the theory of electroporation, considered by many as a plausible explanation of electropermeabilization. The differences in the duration of above-critical pulse amplitude can to a large extent explain the differences between various shapes of bipolar pulses, as well as the differences between pulses with different magnitude of modulation. In contrast, the time derivative of the pulse—at least in the range from several volts per microsecond up to several hundred volts per microsecond—has no detectable influence on the efficiency of electropermeabilization. This suggests that pulse generators with sub-microsecond risetimes are not a necessity for successful electropermeabilization.

Acknowledgements

This work was supported by CNRS, Institute Gustave-Roussy, University of Paris XI, IGEA Srl (Modena), and the Ministry of Education, Science and Sports of the Republic of Slovenia. Experimental work at Institute Gustave-Roussy was made possible by the Proteus program of scientific, technological and cultural co-operation between France and Slovenia. The high-voltage amplifier has been developed within the Cliniporator project (grant QLK3-1999-00484) under the framework of the 5th PCRD of the European Commission. T.K. was also a recipient of a part-time PhD scholarship of the French Government (CNOUS).

References

[1] L.M. Mir, L.F. Glass, G. Serša, J. Teissié, C. Domenge, D. Miklavčič, M.J. Jaroszeski, S. Orlowski, D.S. Reintgen, Z. Rudolf, M. Belehradek, R. Gilbert, M.P. Rols, J. Belehradek Jr., J.M. Bachaud, R. DeConti, B. Štabuc, M. Čemažar, P. Coninx, R. Heller, Effective treatment of cutaneous and subcutaneous malignant tumors by electrochemotherapy, Br. J. Cancer 77 (1998) 2336–2342.

[2] G. Serša, S. Kranjc, M. Čemažar, Improvement of combined modality therapy with cisplatin and radiation using electroporation of tumors, Int. J. Radiat. Oncol. 46 (2000) 1037–1041.

[3] E. Neumann, S. Kakorin, K. Toensing, Fundamentals of electroporative delivery of drugs and genes, Bioelectrochem. Bioenerg. 48 (1999) 3–16.

[4] J. Lukas, J. Bartek, M. Strauss, Efficient transfer of antibodies into mammalian cells by electroporation, J. Immunol. Methods 170 (1994) 255–259.

[5] Y. Bobinnec, A. Khodyakov, L.M. Mir, C.L. Rieder, B. Eddé, M. Bornens, Centriole disassembly in vivo and its effects on chromosome structure and function in vertebrate cells, J. Cell Biol. 143 (1998) 1575–1589.

[6] F. Bobanović, M.D. Bootman, M.J. Berridge, N.A. Parkinson, P. Lipp, Elementary $[Ca2^{+}]_i$ signals generated by electroporation functionally mimic those evoked by hormonal stimulation, FASEB J. 13 (1999) 365–376.

[7] T.Y. Tsong, Electroporation of cell membranes, Biophys. J. 60 (1991) 297–306.

[8] M. Hibino, H. Itoh, K. Kinosita Jr., Time courses of cell electroporation as revealed by submicrosecond imaging of transmembrane potential, Biophys. J. 64 (1993) 1789–1800.

[9] J.C. Weaver, Y.A. Chizmadzhev, Theory of electroporation: a review, Bioelectrochem. Bioenerg. 41 (1996) 135–160.

[10] T. Kotnik, F. Bobanović, D. Miklavčič, Sensitivity of transmembrane voltage induced by applied electric fields—a theoretical analysis, Bioelectrochem. Bioenerg. 43 (1997) 285–291.

[11] E. Neumann, S. Kakorin, Electrooptics of membrane electroporation and vesicle shape deformation, Curr. Opin. Colloid Interface Sci. 1 (1996) 790–799.

[12] B. Gabriel, J. Teissié, Time courses of mammalian cell electropermeabilization observed by millisecond imaging of membrane property changes during the pulse, Biophys. J. 76 (1999) 2158–2165.

[13] S. Raffy, J. Teissié, Control of lipid membrane stability by cholesterol content, Biophys. J. 76 (1999) 2072–2080.

[14] L. Tung, G.C. Troiano, V. Sharma, R.M. Raphael, K.J. Stebe, Changes in electroporation thresholds of lipid membranes by surfactants and peptides, Ann. N.Y. Acad. Sci. 888 (1999) 249–265.

[15] M. Golzio, M.P. Mora, C. Raynaud, C. Delteil, J. Teissié, M.P. Rols, Control by osmotic pressure of voltage-induced permeabilization and gene transfer in mammalian cells, Biophys. J. 74 (1998) 3015–3022.

[16] M.P. Rols, J. Teissié, Electropermeabilization of mammalian cells. Quantitative analysis of the phenomenon, Biophys. J. 58 (1990) 1089–1098.

[17] H. Wolf, M.P. Rols, E. Boldt, E. Neumann, J. Teissié, Control by pulse duration of electric-field mediated gene transfer in mammalian cells, Biophys. J. 66 (1994) 524–531.

[18] M.P. Rols, J. Teissié, Electropermeabilization of mammalian cells to macromolecules: control by pulse duration, Biophys. J. 75 (1998) 1415–1423.

[19] A. Maček-Lebar, N.A. Kopitar, A. Ihan, G. Serša, D. Miklavčič, Significance of treatment energy in cell electropermeabilization, Electro- Magnetobiol. 17 (1998) 253–260.

[20] A. Maček-Lebar, D. Miklavčič, Cell electropermeabilization to small molecules in vitro: control by pulse parameters, Radiol. Oncol. 35 (2001) 193–202.

[21] E. Tekle, R.D. Astumian, P.B. Chock, Electroporation by using bipolar oscillating electric field: an improved method for DNA transfection of NIH 3T3 cells, Proc. Natl. Acad. Sci. U. S. A. 88 (1991) 4230–4234.

[22] S.I. Sukharev, V.A. Klenchin, S.M. Serov, L.V. Chernomordik, Y.A. Chizmadzhev, Electroporation and electrophoretic DNA transfer into cells, Biophys. J. 63 (1992) 1320–1327.

[23] R. Heller, R. Gilbert, M.J. Jaroszeski, Electrochemotherapy: an emerging drug delivery method for the treatment of cancer, Adv. Drug Deliv. Rev. 26 (1997) 185–197.

[24] L.M. Mir, M.F. Bureau, J. Gehl, R. Rangara, D. Rouy, J.M. Caillaud, P. Delaere, D. Branellec, B. Schwartz, D. Scherman, High-efficiency gene transfer into skeletal muscle mediated by electric pulses, Proc. Natl. Acad. Sci. U. S. A. 96 (1999) 4262–4267.

[25] S. Kuriyama, A. Mitoro, H. Tsujinoue, Y. Toyokawa, T. Nakatani, H. Yoshiji, T. Tsujimoto, H. Okuda, S. Nagao, H. Fukui, Electrochemotherapy can eradicate established colorectal carcinoma and leaves a systemic protective memory in mice, Int. J. Oncol. 16 (2000) 979–985.

[26] T. Kotnik, L.M. Mir, K. Flisar, M. Puc, D. Miklavčič, Cell membrane electropermeabilization by symmetrical bipolar rectangular pulses:

Part I. Increased efficiency of permabilization, Bioelectrochemistry 54 (2001) 83–90.
[27] T. Kotnik, D. Miklavčič, L.M. Mir, Cell membrane electropermeabilization by symmetrical bipolar rectangular pulses: Part II. Increased efficiency of permabilization, Bioelectrochemistry 54 (2001) 91–95.
[28] I. Daskalov, N. Mudrov, E. Peycheva, Exploring new instrumentation parameters for electrochemotherapy. Attacking tumors with bursts of biphasic pulses instead of single pulses, IEEE Eng. Med. Biol. Mag. 18 (1999) 62–66.
[29] I. Mathiesen, Electropermeabilization of skeletal muscle enhances gene transfer in vivo, Gene Ther. 6 (1999) 508–514.
[30] G. Rizzuto, M. Cappelletti, D. Maione, R. Savino, D. Lazzaro, P. Costa, I. Mathiesen, R. Cortese, G. Ciliberto, R. Laufer, N. La Monica, E. Fattori, Efficient and regulated erythropoietin production by naked DNA injection and muscle electroporation, Proc. Natl. Acad. Sci. U. S. A. 96 (1999) 6417–6422.
[31] K. Kinosita, T.Y. Tsong, Voltage-induced conductance in human erythrocyte membranes, Biochim. Biophys. Acta 554 (1979) 479–497.
[32] D.C. Chang, Cell poration and cell fusion using an oscillating electric field, Biophys. J. 56 (1989) 641–652.
[33] D.C. Chang, P.Q. Gao, B.L. Maxwell, High efficiency gene transfection by electroporation using a radio-frequency electric field, Biochim. Biophys. Acta 1092 (1991) 153–160.
[34] T.D. Xie, T.Y. Tsong, Study of mechanisms of electric field-induced DNA transfection: II. Transfection by low-amplitude, low-frequency alternating electric fields, Biophys. J. 58 (1990) 897–903.
[35] S. Šatkauskas, M.F. Bureau, M. Puc, A. Mahfoudi, D. Scherman, D. Miklavčič, L.M. Mir, Mechanisms of in vivo DNA electrotransfer: respective contributions of cell electropermeabilization and DNA electrophoresis, Mol. Ther. 5 (2002) 133–140.
[36] J.L. Biedler, H. Riehm, Cellular resistance to actinomycin D in Chinese hamster cells in vitro, Cancer Res. 30 (1970) 1174–1184.
[37] F. Loste, N. Eynard, J. Teissié, Direct monitoring of the field strength during electropulsation, Bioelectrochem. Bioenerg. 47 (1998) 119–127.
[38] K. Flisar, M. Puc, T. Kotnik, D. Miklavčič, A system for cell membrane electropermeabilization with arbitrary pulse waveforms, IEEE Eng. Med. Biol. 22 (2003) 77–81.
[39] M.P. Rols, J. Teissié, Ionic-strength modulation of electrically induced permeabilization and associated fusion of mammalian cells, Eur. J. Biochem. 179 (1989) 109–115.
[40] T. Kotnik, A. Maček-Lebar, D. Miklavčič, L.M. Mir, Evaluation of cell membrane electropermeabilization by means of a nonpermeant cytotoxic agent, BioTechniques 28 (2000) 921–926.
[41] M. Puc, T. Kotnik, L.M. Mir, D. Miklavčič, Quantitative model of small molecules uptake after in vitro cell electropermeabilization, Bioelectrochemistry 60 (2003) (in press).

Effect of Cell Electroporation on the Conductivity of a Cell Suspension

Mojca Pavlin,* Maša Kandušer,* Matej Reberšek,* Gorazd Pucihar,* Francis X. Hart,† Ratko Magjarević,‡ and Damijan Miklavčič*

*University of Ljubljana, Faculty of Electrical Engineering, Ljubljana, Slovenia; †University of the South, Sewanee, Tennessee; and ‡University of Zagreb, Faculty of Electrical Engineering and Computing, Zagreb, Croatia

ABSTRACT An increased permeability of a cell membrane during the application of high-voltage pulses results in increased transmembrane transport of molecules that otherwise cannot enter the cell. Increased permeability of a cell membrane is accompanied by increased membrane conductivity; thus, by measuring electric conductivity the extent of permeabilized tissue could be monitored in real time. In this article the effect of cell electroporation caused by high-voltage pulses on the conductivity of a cell suspension was studied by current-voltage measurements during and impedance measurement before and after the pulse application. At the same time the percentage of permeabilized and survived cells was determined and the extent of osmotic swelling measured. For a train of eight pulses a transient increase in conductivity of a cell suspension was obtained above permeabilization threshold in low- and high-conductive medium with complete relaxation in <1 s. Total conductivity changes and impedance measurements showed substantial changes in conductivity due to the ion efflux in low-conductive medium and colloid-osmotic swelling in both media. Our results show that by measuring electric conductivity during the pulses we can detect limit permeabilization threshold but not directly permeabilization level, whereas impedance measurements in seconds after the pulse application are not suitable.

INTRODUCTION

A cell membrane represents a barrier to the transport of the majority of water-soluble molecules due to the hydrophobic nature of the inner part of the lipid bilayer. When a strong electric field is applied the cell membrane becomes more permeable thus enabling entrance of various molecules, which can be used as a method for introducing certain drugs or genes into the cell. The process was named electroporation because it is believed that pores are formed in the membrane due to the induced transmembrane voltage above some critical voltage (between 0.2 and 1 V), but the term electropermeabilization is used as well to stress that increased membrane permeability is observed (Neumann and Rosenheck, 1972; Zimmermann, 1982; Neumann et al., 1989; Tsong, 1991; Weaver and Chizmadzhev, 1996). After application of electric pulses the membrane completely reseals for proper selection of pulse parameters. The process of resealing takes several minutes thus allowing transport of molecules from the exterior into the cell. When the electric field is too high, for a given duration and number of pulses, physiological changes of the cell become too large to be repaired; a cell either loses too much of its content or it swells too much, which ultimately leads to cell death.

In the last decade it was shown that electroporation can be successfully used on patients, as a part of electrochemotherapy (Okino and Mohri, 1987; Mir et al., 1991; Jaroszeski et al., 1997; Mir, 2000; Serša et al., 2000) where electric pulses are used to increase locally the uptake of cytostatic drugs. In parallel it was shown that electroporation can be successfully used also for gene transfection (Wong and Neumann, 1982; Neumann et al., 1982, 1989; Sukharev et al., 1992). Electric field mediated gene transfection uses locally delivered electric pulses to transfer DNA into the cell. In contrast to more frequently used viral transfection, which has been proved to have severe side effects in some cases of in vivo gene therapy on animals and humans, electroporation presents a safer alternative method, as it does not use viral vectors (Ferber, 2001; Nebeker, 2002). Although being already an established method for in vitro gene transfection, electroporation is currently being extensively studied on animal models in vivo (Jaroszeski et al., 1999; Mir, 2000).

Until now the rate of permeabilization, survival of cells, and related efficiency of the electropermeabilization could be determined only after the application of pulses by various time-consuming methods. However, the possibility of monitoring the extent of permeabilized tissue in real time is of great importance for practical clinical use of electrochemotherapy or gene therapy. Under an assumption that the increased conductivity, which is observed in single cells, cell pellets, and cell suspensions, correlates with the extent of permeabilization, measuring electrical properties could enable observation of cell permeabilization (Kinosita and Tsong, 1977a,b, 1979; Abidor et al., 1993, 1994). Nevertheless, the complex structure of a tissue makes the interpretation of such measurements difficult. For these reasons it is important to verify this hypothesis on a dense suspension of cells, which represent a more controllable and homogeneous sample than tissue.

Only a few studies have been performed to assess changes of the electrical properties of cells in suspensions or pellets

Submitted July 5, 2004, and accepted for publication January 24, 2005.

Address reprint requests to Prof. Dr. Damijan Miklavčič, University of Ljubljana, Faculty of Electrical Engineering, Trzaska 25, 1000 Ljubljana, Slovenia. Tel.: 386-1-4768-456; Fax: 386-1-4264-658; E-mail: damijan@svarun.fe.uni-lj.si.

0006-3495/05/06/4378/13 $2.00

doi: 10.1529/biophysj.104.048975

due to electroporation. The first measurements of the electrical properties were done on erythrocytes 20 years ago (Kinosita and Tsong, 1977a,b, 1979). Increased conductivity was observed above the threshold electric field, which after the pulse returned to its initial value. On a longer timescale, however, conductivity of a cell suspension was increased due to the ion efflux. The observed increase in conductivity correlated with the hemolysis of the cells. These observations were confirmed on pellets of different cell lines by Abidor and co-workers as well (Abidor et al., 1993, 1994), where a similar nonlinear current voltage relationship and fast resealing after the pulse was observed. In another study (Hibino et al., 1991, 1993) a decrease of the induced transmembrane voltage was detected on a part of the cell indicating increased membrane permeability for ions in that region of the membrane. Using microsecond and nanosecond pulses also increased conductivity was observed (Garner et al., 2004). Recently it was suggested (Davalos et al., 2000, 2002; Pliquett et al., 2004) that measurement of conductivity could enable online observation and control of tissue electroporation.

In this article we present measurements of electrical conductivity of a dense cell suspension in typical electroporation experiments. Conductivity of cells in a suspension was measured by current-voltage measurements during and impedance measurement before and after the application of high-voltage pulses. In parallel we determined the percentage of permeabilized and survived cells, and extent of osmotic swelling. The effect of different parameters (e.g., cell volume fraction, number of pulse, medium conductivity,. . .) on the conductivity of a cell suspension was studied and measured changes were compared to theoretical estimates. Previous studies focused on experiments with one or two pulses at most, however, for more efficient permeabilization several pulses have been proved to be more successful (Kotnik et al., 2000; Canatella et al., 2001). Thus, our interest was to also determine conductivity changes during a train of successive pulses. We analyzed how conductivity changes are related to the percentage of permeabilized cells in view of possible application of such measurements for online monitor of cell electroporation. Finally, we discuss how our observations agree with the current theoretical models of electroporation and which processes might contribute to the observed increase of bulk conductivity of a cell suspension.

MATERIALS AND METHODS

Current-voltage and impedance measurements

The experimental setup for current-voltage and impedance measurements is shown in Fig. 1. To generate high-voltage square pulses a high-voltage generator (prototype developed at the Laboratory of Biocybernetics, Faculty of Electrical Engineering, University of Ljubljana) was used. Impedance amplitude $|Z|$ and phase angle-φ before and after pulses were measured with impedance meter (HP4274A, Houston, TX). For every sample first impedance was measured after which the system switched electrodes to the high-voltage pulse generator and pulses were delivered. The second impedance measurement was carried out 2–3 s after the train of pulses and the third measurement 10 s after the second measurement. Impedance was measured at 10 different frequencies from 100 Hz to 100 kHz and altogether lasted 4 s.

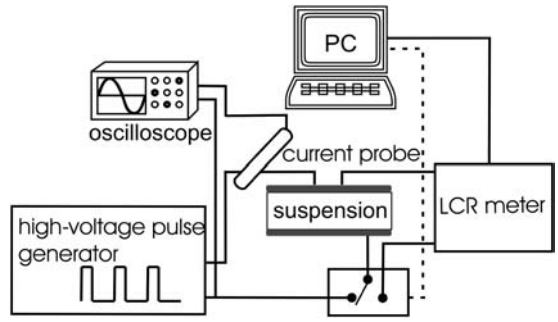

FIGURE 1 A schematic diagram of the system for electroporation and current-voltage and impedance measurements. The cell suspension (100 μl) was placed between the electrodes. First, impedance was measured then the system switched electrodes to the high-voltage pulse generator and pulses were delivered. Two to three seconds after the pulses, impedance was measured for the second time and after another 10 s for the third time. For each pulse application, voltage, and current were traced on oscilloscope and stored for further analysis.

During the pulses the electric current was measured with a current probe (LeCroy AP015, New York, NY) and both current and voltage were measured and stored on the oscilloscope (LeCroy 9310 C Dual, 400 MHz). Pulse amplitudes were varied to produce applied electric field E_0 between 0.4 and 1.8 kV/cm. We used a train of eight square pulses of 100-μs duration with 1 Hz repetition frequency except where stated otherwise. The memory segmentation function was used to obtain high time resolution during the pulses and only 100 μs after the pulses were recorded. Parallel aluminum plate electrodes (Eppendorf cuvettes) with 2-mm distances between the electrodes when the whole range of amplitude were used and 4-mm distances in experiments where two volume fractions of cells were used. For every set of parameters a reference measurement on medium with no cells was also performed.

Cells and medium

Mouse melanoma cell line, B16F1, was used in experiments. Cells were grown in Eagle's minimum essential medium supplemented with 10% fetal bovine serum (Sigma-Aldrich Chemie GmbH, Deisenhofen, Germany) at 37°C in a humidified 5% CO_2 atmosphere in the incubator (WTB Binder, Labortechnik GmbH, Seelbach, Germany). For all experiments the cell suspension was prepared from confluent cultures with 0.05% trypsin solution containing 0.02% EDTA (Sigma-Aldrich Chemie GmbH). From the obtained cell suspension trypsin and growth medium were removed by centrifugation at 1000 rpm at 4°C (Sigma-Aldrich Chemie GmbH) and the resulting pellet was resuspended in medium and again centrifuged. Two media were used for electroporation: a high-conductive medium Spiner's modification of Eagle's minimum essential medium (SMEM) (Life Technologies, Paisey, UK) having conductivity σ_0 (25°C) = 1.58 S/m that does not contain calcium and a low-conductive medium that contained phosphate buffer with 250 mM sucrose, PB σ_0 (25°C) = 0.127 S/m. Cell suspensions having cell volume fractions $f = 0.15$ (5×10^7 cells/ml) and $f = 0.3$ (1×10^8 cells/ml) were used in the experiments.

Permeabilization and viability experiments

Cell permeabilization was determined by the uptake of the cytostatic drug bleomycin and cell survival by the cell ability to survive the application of

electric pulses. It was shown that bleomycin at 5 nM external concentration penetrates only the permeabilized cells thus it can be used as an indicator of membrane permeabilization. The method is described in detail by Kotnik and co-workers (Kotnik et al., 2000). A 100-μl droplet of a cell suspension was placed between electrodes. Bleomicyn was added (5 nM external concentration) immediately after pulse application (never >60 s after the end of pulse application) to determine permeabilization. We used two amplitudes of the applied electric pulses, under permeabilization threshold (0.4 kV/cm) and above the threshold (0.94 kV/cm) for cells suspended in SMEM medium, and one amplitude for PB medium (0.94 kV/cm) for which two different volume fractions were used. For each pulse amplitude, a train of eight rectangular pulses with duration of 100 μs and repetition frequency 1 Hz was applied and a control consisting of cells that were not exposed to an electric field was prepared. All cells were incubated at room temperature for 30 min to allow resealing of membrane and were plated at a concentration of 250 cells per petri dish for clonogenic assay. Colonies were grown in the same conditions as described above for cell culturing and after five days colonies were fixed with methanol (Merck KGaA, Darmstadt, Germany) and stained with crystal violet (Sigma-Aldrich Chemie GmbH). Visible colonies were counted and results were normalized to the control (cells with added 5 nM bleomycin not exposed to electric field). The percentage of survived colonies was subtracted from 100 percent to obtain the percentage of bleomycin uptake. Three different sample data were pooled together to obtain average and standard deviation. Each experiment was repeated twice on two separate days. Cell survival was determined as described above for the cell permeabilization but without addition of bleomycin. Results were expressed as a percentage of the cell survival.

Both results of permeabilization and survival were compared to the results obtained with the same procedure in similar conditions but with lower cell density (2×10^7/ml) obtained from our previous study. Results are plotted against the local electric field E rather than applied electric field $E_0 = U/d$ because for a high density of cells the local field experienced by each cell is smaller than the applied field due to the interaction between the cells (Susil et al., 1998; Canatella et al., 2001; Pavlin et al., 2002a). The scaling factor E/E_0 was taken from our previous study (Pavlin et al., 2002a), where the decrease of the field (and induced transmembrane voltage) due to the neighboring cells was calculated to be 1% for $f = 0.05$ and 9% for $f = 0.3$.

Measurements of cells swelling

In separate experiments we exposed cells to pulses ($E_0 = 0.4, 0.95, 1.43$ kV/cm) in an observation chamber under the inverted phase contrast microscope (Zeiss 200, Axiovert, Jena, Germany). As in other measurements a train of eight 100-μs pulses with 1-Hz repetition frequency was used. The images were recorded (MetaMorph imaging system, Visitron, Puchheim, Germany) during the train of pulses and after the pulses up to 600 s after the first pulse. Three experiments for each, SMEM and PB medium, were made on three different days. For every parameter the area of five cells was measured from which an average was obtained. From this the changes in cells volume fraction was determined.

Theoretical analysis: calculation of the conductivity of a suspension of permeabilized cells

For theoretical analysis we used an analytical model that relates the change in the membrane conductivity with the change of the effective conductivity of a cell suspension (Pavlin and Miklavčič, 2003). The induced transmembrane voltage for a nonpermeabilized spherical cell exposed to the external electrical field E can be derived from the Laplace equation. Except in very low-conductive medium, the solution can be approximated with

$$U_m = 1.5\,ER\cos\theta\,, \tag{1}$$

where we assume that the cell membrane is almost nonconductive compared to the external medium. R is the cell radius and θ is the angle between direction of the electric field and the point vector on the membrane.

When the induced transmembrane voltage exceeds the threshold voltage, the part of the cell membrane where U_m exceeds U_c is permeabilized. The permeabilized part of the cell membrane can be therefore defined by the critical angle θ_c, where $U_c = 1.5\,ER\cos\theta_c$. This permeabilized part of the cell membrane is in the model described by the increased membrane conductivity σ_m, whereas other parts of the cell membrane have zero conductivity. The potential around such permeabilized cell oriented parallel to the electric field is calculated with the Laplace equation and by using a dipole approximation the equivalent conductivity σ_p of a single cell is calculated. From this, using the Maxwell equation (Maxwell, 1873; Pavlin et al., 2002b)

$$\frac{\sigma_e - \sigma}{2\sigma_e + \sigma} = f\frac{\sigma_e - \sigma_p}{2\sigma_e + \sigma_p}\,, \tag{2}$$

the effective conductivity σ of a suspension of permeabilized cells is obtained, where f is the volume fraction of the cells and σ_e the conductivity of the external medium. The model takes into account the anisotropic nature of permeabilization, i.e., that only part of the membrane is permeabilized, and incorporates this in the calculation of the effective conductivity. The model allows calculation of the change of the effective conductivity ($\sigma - \sigma_0$), which depends on different parameters: the cell volume fraction f, average membrane conductivity of the permeabilized area σ_m, critical angle of permeabilized area θ_c, and conductivities of the external medium and cytoplasm, σ_e and σ_i, respectively. A more detailed description of the model is described in our previous article (Pavlin and Miklavčič, 2003).

RESULTS

In the presented study we performed experiments where conductivity of a cell suspension was measured in parallel with the extent of cell permeabilization and cell survival. We used low-conductive medium typically used in in vitro conditions and high-conductive medium that is more representative for in vivo conditions. In addition, different volume fractions and pulse repetition frequencies were used to establish their effect on the conductivity changes.

Measured data were analyzed in terms of ''instant'' conductivity $\sigma(t) = I(t)/U(t)\ d/S$, the ratio between current and voltage at a given time point, where d is the distance between the electrodes, and S the surface of the sample volume at the electrodes. We obtained time-dependent conductivity of cell suspension σ for a train of eight 100-μs pulses and applied electric field between 0.4 and 1.8 kV/cm, as shown in Fig. 2. Because our goal was to determine the difference in the conductivity of permeabilized and nonpermeabilized cells, only the difference in the initial and final level was analyzed and not the dynamic behavior. The initial value of conductivity at the start of each pulse σ_0^N was determined 3 μs after the start of the pulse, so that transient effects were not taken into account. The conductivity at the end of each pulse σ^N was determined and from this the change in the conductivity during the N^{th} pulse was obtained: $\Delta\sigma^N = \sigma^N - \sigma_0^N$. With σ_0 we denote the initial conductivity at the start of the first pulse $\sigma_0 = \sigma_0^1$.

Fig. 3 represents conductivity changes $\Delta\sigma^1/\sigma_0$ during the first 100-μs pulse for cells in SMEM medium (*a*) and cells in

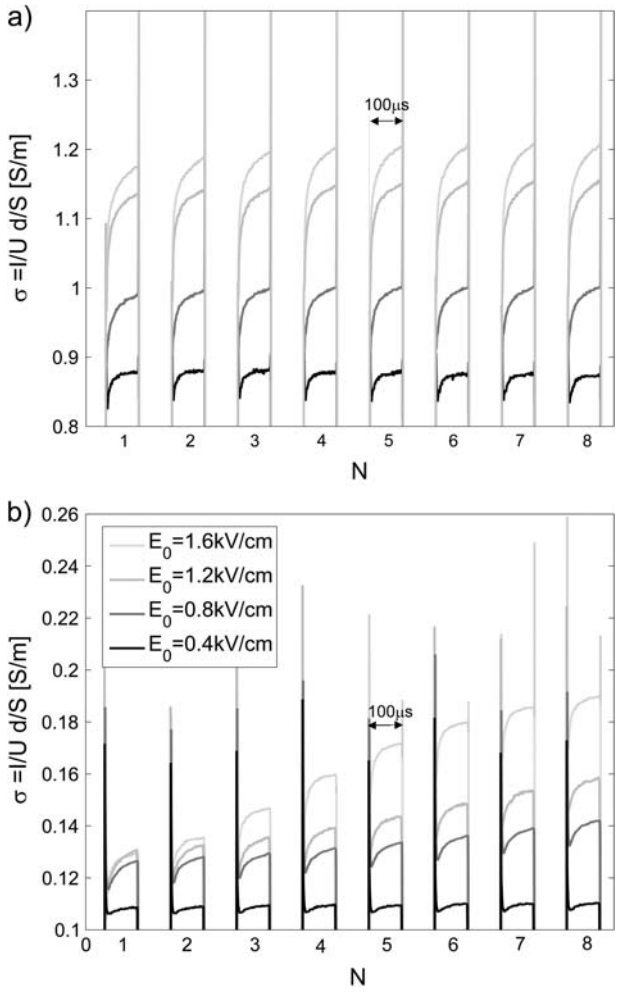

FIGURE 2 Measured time-dependent conductivity $\sigma(t) = I(t)/U(t)\ d/S$ during a train of eight 100-μs pulses, 1-Hz repetition frequency for (*a*) cells in high-conductive SMEM medium and (*b*) cells in low-conductive PB medium for different applied electric fields $E_0 = U/d$. The memory segmentation function of the oscilloscope was used to obtain high time resolution during the pulses, and only 100 μs after the pulse were recorded. Legend in panel *b* applies also to panel *a*.

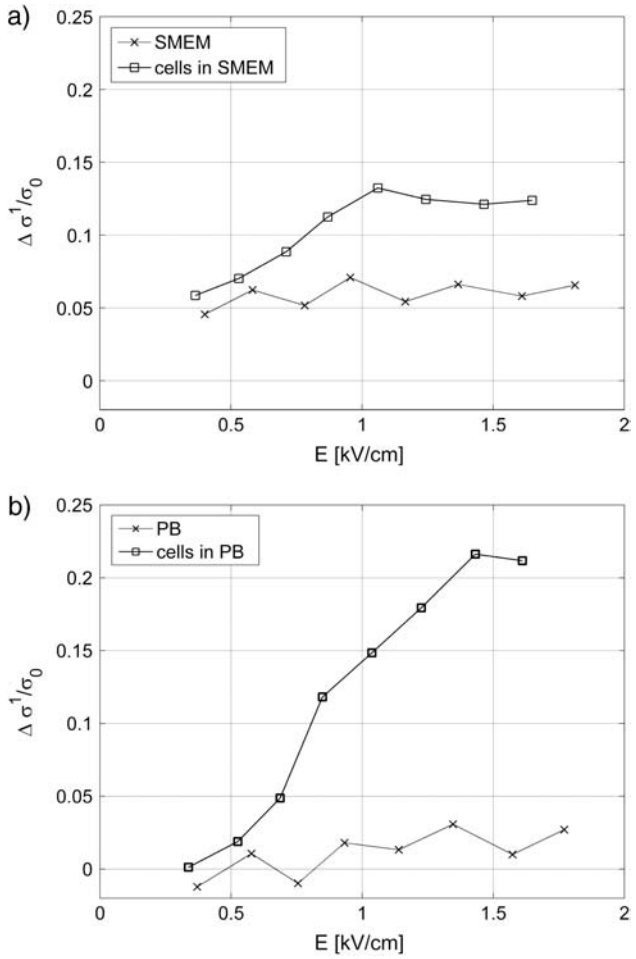

FIGURE 3 Conductivity change after the first pulse of the train of 8 × 100-μs pulses $\Delta\sigma^1$ normalized to initial conductivity in (*a*) cells in SMEM medium and (*b*) cells in PB medium, cells in medium (*solid line*), reference measurement on medium without the cells (*dotted line*). The results are shown for local electric field E, where $E/E_0 = 0.91$ ($f = 0.3$).

PB medium (*b*) for $E_0 = U/d = [0.4–1.8]$ kV/cm, electrode distance was 2 mm. In analysis all data are represented for the local electric field E obtained from the applied electric field E_0 by taking into account the decrease of the electric field due to the neighboring cells.

For cells in both media, an increase in conductivity change during first pulse $\Delta\sigma^1/\sigma_0$ is observed for E above 0.5 kV/cm, which reaches the maximum (12%) around 1 kV/cm in SMEM medium and at 1.4 kV/cm (25%) in PB medium. Very similar field dependence is obtained for all pulses in both media, where a dramatic increase in conductivity is observed above 0.5 kV/cm. The reference measurements in pure SMEM and PB media show constant $\Delta\sigma^1/\sigma_0$ that can be attributed to electrode processes and Joule heating. Conductivity changes $\Delta\sigma^N/\sigma_0$ during consecutive pulses in PB (see Fig. 8 *b*) and SMEM media are approximately constant at 1-Hz repetition frequency and even when a train of 24 pulses was applied, the increase in the conductivity during the pulses surprisingly remained constant.

In Fig. 4 percentage of permeabilized and survived cells in SMEM medium after application of 8 × 100 μs pulses (E = 0.84 kV/cm) is shown. Results in dense suspensions ($f = 0.3$) are compared to previous measurements performed using the same experimental protocol but with lower cell density (f = 0.05). We can see good agreement with the permeabilization curve for a lower density of cells. The permeabilization curve for PB medium is similar to the curve for SMEM medium because we have shown previously that permeabilization curves for SMEM and PB medium are similar (Pucihar et al., 2001). Similar agreement of measurements for high density with results for lower density of cells was obtained also for PB medium where at $E = 0.84$ kV/cm 92% of permeabilization is achieved with survival being 100%.

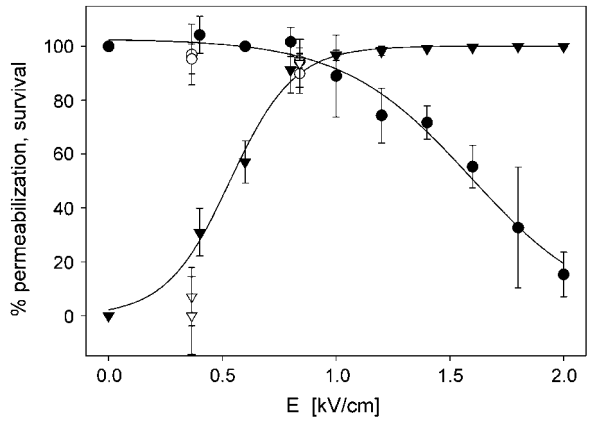

FIGURE 4 Permeabilization (▼) and survival rate (●) of B16F1 cells in SMEM medium for electroporation experiments with 8 × 100-μs pulses, 1-Hz repetition frequency (lines show fitted sigmoid function). Experiments where high density of cells $f = 0.3$ (*open symbols*) are compared with the permeabilization and survival curves obtained in experiments with lower cell density $f = 0.05$ (*solid symbols*).

Comparing Figs. 3 and 4 it can be seen that transient conductivity changes $\Delta\sigma^1/\sigma_0$ increase above 0.5 kV/cm agrees with permeabilization curve shown in Fig. 4. Percentage of permeabilized cells reaches maximum at 1 kV/cm similarly as conductivity changes in SMEM, whereas in PB medium maximum conductivity increase is obtained at 1.4 kV/cm.

In Fig. 5 relative changes of the initial level of conductivity $(\sigma_0^N - \sigma_0)/\sigma_0$ in PB medium for consecutive pulses are shown. It can be seen that the initial level starts to increase again for $E > 0.5$ kV/cm, which can be explained with the efflux of ions (mostly K^+ ions) from the cytoplasm into the medium through membrane pores due to the concentration gradient, indicating that the cell membrane is permeabilized above 0.5 kV/cm. In high-conductive SMEM medium the

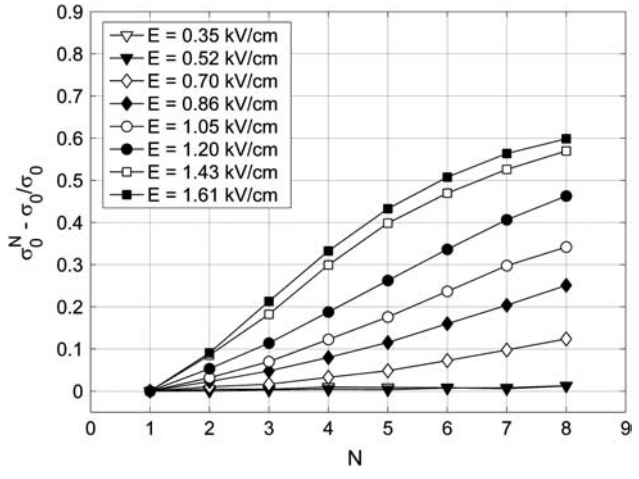

FIGURE 5 The relative change of the initial level of conductivity in PB medium for consecutive pulses: $(\sigma_0^N - \sigma_0)/\sigma_0$, where σ_0^N is the initial level at the start of the N^{th} pulse is shown.

increase of the initial conductivity $(\sigma_0^N - \sigma_0)/\sigma_0$ is solely due to Joule heating as almost the same values are obtained for medium alone (results not shown). For higher electric fields the efflux of ions in PB increases up to 1.4 kV/cm where it reaches maximum, similarly as transient conductivity changes during a single pulse. Up to $E = 1.0$ kV/cm the conductivity increases approximately linearly with time but starts to reach saturation level at higher electric field due to a decrease of the concentration gradient of the ions. This is expected because the total duration of the train of eight pulses at 1 Hz is 7 s and the time constant for diffusion of ions is few seconds. In Appendix B we theoretically analyzed the efflux of ions through the permeabilized membrane and obtained an exponential rise to a maximum. Deviation from this behavior is due to different simplifications of the model and statistical variation of cell sizes that are consequently permeabilized above different critical electric fields.

Another interesting parameter is the total conductivity change $\Delta\sigma_{tot} = \sigma^8 - \sigma_0$, which we define as the difference between the final conductivity at the end of the eight pulse and the initial conductivity. In Fig. 6 the total conductivity changes after the application of a train of eight 100-μs pulses are presented for the same experiments as shown in Fig. 3. For the low-conductive medium a steady increase of the total conductivity change is observed above 0.5 kV/cm, corresponding to both ion efflux from the cell interior and the increased conductivity. The conductivity changes in low-conductive medium without cells are negligible.

In contrast, in high-conductive medium the difference between the total change in conductivity for cells in a suspension and the total conductivity change for pure medium is less pronounced. This can be attributed to substantial Joule heating during 8 × 100-μs pulses, which can be calculated theoretically when neglecting the heat dissipation:

$$\frac{\Delta\sigma_{temp}}{\sigma_0} = \alpha\Delta T, \quad \Delta T = N\, t_E E_0^2 \frac{\sigma}{\rho c_p}, \tag{3}$$

where T is temperature of the suspension, α is constant of the conductivity temperature dependence, t_E is length of the pulse, ρ the density, c_p specific heat capacity of the suspension, and N number of pulses. The above equation gives for $\alpha = 0.017/°C$ (SMEM medium) a temperature increase of ~3°C after eight pulses for $E_0 = 1$ kV/cm. From this theoretical calculation of the conductivity change due to Joule heating for 8 × 100-μs pulses gives $\Delta\sigma^8_{temp}/\sigma_0 \cong 0.048 (\Delta\sigma^1_{temp}/\sigma_0 \cong 0.006)$. But during a single 100-μs pulse in pure medium a change of $\Delta\sigma^1/\sigma_0 \cong 0.04$ is observed (see Fig. 3 *a*), which is evidently not only due to Joule heating but also due to some other effects (electrode processes, anomalous heating), which has been observed by other authors (Pliquett et al., 1996).

Another important process that significantly affects mainly the results obtained in high-conductive medium (because the total changes are smaller) is colloid-osmotic swelling of cells, which increases the effective volume fraction of the cells and

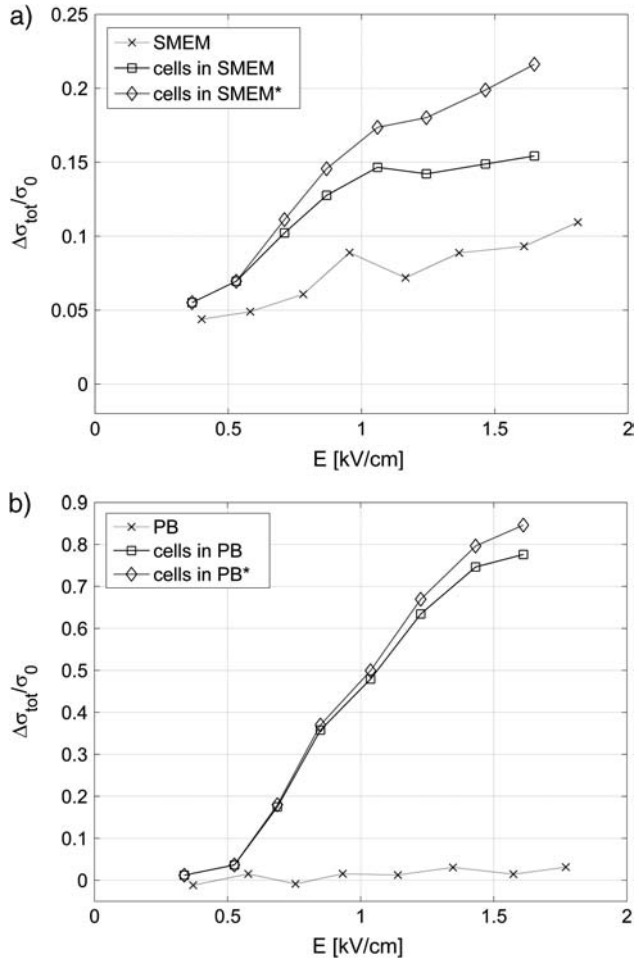

FIGURE 6 The total conductivity change $\Delta\sigma_{tot} = \sigma^8 - \sigma_0$ after the application of 8 × 100-μs pulses (same experiment as in Fig. 3) in (*a*) cells in SMEM medium and (*b*) cells in PB medium, cells in medium (*solid line*), reference measurement (*dotted line*) on pure medium (×). Note the difference in scale between panels *a* and *b*. In Fig. 6 *a* measured total conductivity change (□) and total conductivity change corrected for the increased cell size due to the colloid-osmotic swelling (◇) $\Delta\sigma'_{tot}/\sigma_0 = \Delta\sigma_{tot}/\sigma_0 - \Delta\sigma_{swell}/\sigma_0$ is shown.

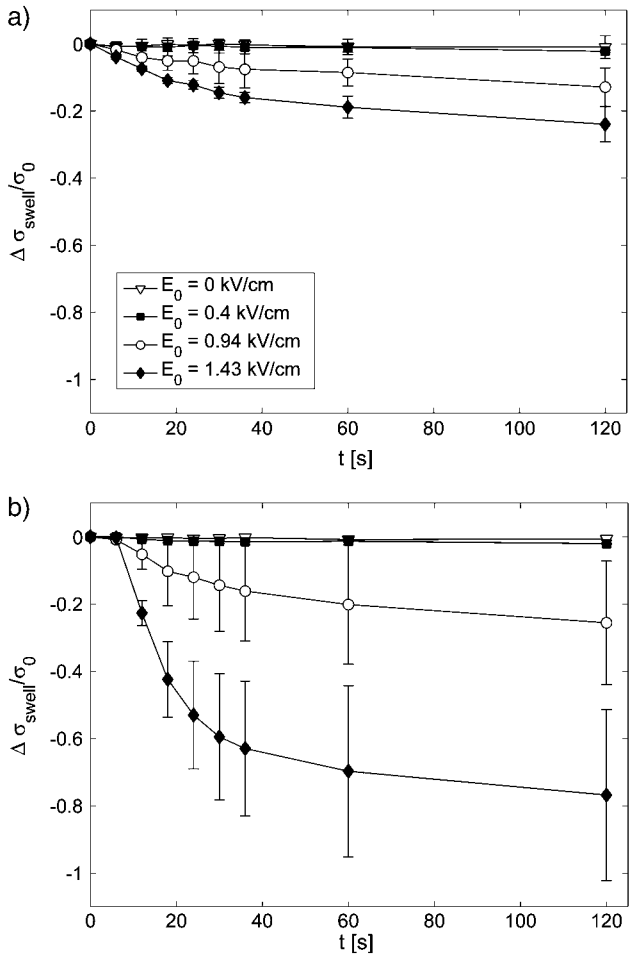

FIGURE 7 The effect of colloid-osmotic swelling on the bulk conductivity for different applied electric field strengths E_0 and control ($E_0 = 0$ kV/cm); time $t = 0$ s, start of the first pulse; $t = 7$ s, end of the pulsation. The changes of cells volume fractions due to the increased cell sizes were transformed into the conductivity change $\Delta\sigma_{swell}/\sigma_0$ in (*a*) SMEM and (*b*) PB medium.

consequently decreases the conductivity (see Fig. 7). In Fig. 6 *a* we compare the total conductivity changes (*open squares*) and total conductivity changes corrected for the increased cell size due to the colloid-osmotic swelling (*) $\Delta\sigma'_{tot}/\sigma_0 = \Delta\sigma_{tot}/\sigma_0 - \Delta\sigma_{swell}/\sigma_0$. We can see that when the increase in cell size is taken into account the total change after the eight pulses shows a similar strong increase above the threshold field as in the low-conductive medium.

Measurements of colloid-osmotic swelling

It was shown in several experiments that cells swell during electroporation and consequently a drop in the conductivity of the cell suspensions and pellets after the pulses was observed (Kinosita and Tsong, 1977b; Abidor et al., 1993, 1994). Swelling of permeabilized cells is caused due to the difference in the permeabilities of ions and larger molecules (macromolecules) inside the cell, which results in an osmotic pressure that drives water into the cells and leads to cell swelling.

To determine the dynamics and the extent of cell swelling for our experimental conditions we made additional experiments where images of cells during and after pulse application were recorded. The results of the measurements of the cell sizes during and after the pulses are shown in Fig.7 where the changes in the volume fraction were transformed into changes of conductivity $\Delta\sigma_{swell} / \sigma_0(\Delta f)$ according to Eq. 2. The corrected curve in Fig. 6 *a* was obtained by extracting the $\Delta\sigma_{swell} / \sigma_0$ due to cell swelling at $t = 7$ s, which corresponds to the time point at the end of the eight pulse.

The time constant of colloid-osmotic swelling is a few tens of seconds; this is in agreement with the time constant for efflux of ions, which is between 10 and 20 s (see Fig. 5).

Impedance measurements

From impedance measurements before and after application of pulses, the change of the real part of the impedance was calculated. From the impedance spectrum only the results at 100-kHz frequency were used due to the large scattering of data at lower frequencies. From the real part of the impedance we calculated bulk conductivity: $\sigma = 1/\mathrm{Re}(Z)\ d/S$. For each sample we present values of the conductivity change $\Delta\sigma/\sigma_0$ at the two time points: $t_1 = 14$ s and $t_2 = 28$ s after the first pulse.

Impedance measurements in all experiments showed reproducibly decrease in conductivity in SMEM medium above permeabilization threshold and increase in conductivity in PB medium. Results of the experiments with the 8×100-μs pulses for $E = 0.35$–1.6 kV/cm are given in Table 1. We can observe steady increase in conductivity in PB medium for higher fields whereas in SMEM medium conductivity is decreased after the pulses. We can explain these values by considering all the effects that contribute to post-pulse conductivity: efflux of ions in PB medium, Joule heating in SMEM medium, and osmotic swelling: $\Delta\sigma_{\mathrm{imp}}/\sigma_0 = \Delta\sigma_{\mathrm{efflux}}/\sigma_0 + \Delta\sigma_{\mathrm{swell}}/\sigma_0 + \Delta\sigma_{\mathrm{temp}}/\sigma_0$. For example, in PB medium at 1 kV/cm is $\Delta\sigma_{\mathrm{imp}}/\sigma_0\ (14\ \mathrm{s}) = 0.47$, which can be obtained from extrapolating the values of the initial conductivity changes from Fig. 5 at $t = 7$ s ($N = 8$) to $t = 14$ s, which gives approximately $\Delta\sigma_{\mathrm{efflux}}/\sigma_0 + \Delta\sigma_{\mathrm{swell}}/\sigma_0 \cong 0.5$. Here the first term efflux of ions dominates because from Fig. 7 *b* we obtain $\Delta\sigma_{\mathrm{swell}}/\sigma_0\ (14\ \mathrm{s}) \cong -0.05$. At higher fields osmotic swelling drastically decreases conductivity up to -0.4, however, the efflux of ions in PB is so large that after the pulse $\Delta\sigma_{\mathrm{imp}}/\sigma_0\ (14\ \mathrm{s})$ increases up to $+0.7$, which is also the saturation level of the changes of the initial level. On the other hand in SMEM medium there is no net efflux of ions, therefore, mostly osmotic swelling contributes to reducing of bulk conductivity, which results in negative values of $\Delta\sigma_{\mathrm{imp}}/\sigma_0$; e.g., at 1 kV/cm we obtain $\Delta\sigma_{\mathrm{imp}}/\sigma_0\ (28\ \mathrm{s}) = -0.04$, which can be explained by contributions of cell swelling $\Delta\sigma_{\mathrm{swell}}/\sigma_0 \cong -0.07$ (see Fig. 7 *a*) and Joule heating $\Delta\sigma_{\mathrm{temp}}/\sigma_0 \cong +0.035$ whereas efflux of ions in high-conductive SMEM medium is negligible.

The effect of the repetition frequency on the measured increase in conductivity

Fig. 8 summarizes the effect of the repetition frequency on the conductivity changes in low-conductive PB medium. In Fig. 8 *a* the initial level of conductivity is shown for consecutive pulses and it can be seen that for frequencies above 10 Hz (100-ms pause between the pulses) very small changes of the initial level are obtained, which agrees with previous observation that the diffusion time constant is around a few seconds. In Fig. 8 *b* absolute changes of conductivity $\Delta\sigma(t)$ during the first, third, and the fifth pulse are compared for different frequencies.

We can observe that for 1 Hz the consecutive pulses are almost identical and that relaxation of the conductivity is complete in one second, however, for higher frequencies each consecutive pulse is smaller than the previous pulse and the time course of the second part of the pulse is different. This indicates that relaxation in milliseconds after the pulse is not complete and that the conductivity does not relax to its initial level but constantly increases. In SMEM medium (results not shown) we also obtained complete relaxation at 1 Hz and difference in pulse shapes for consecutive pulses at 1 kHz. The initial level of conductivity increased between the pulses almost twice as in pure medium at 1 kHz, whereas at 1 Hz no difference between pure medium and cells was observed, which similarly as in PB medium shows that time constant of conductivity relaxation is in the millisecond range.

In Fig. 9 changes of conductivity after the first pulse $\Delta\sigma^1$ for two volume fractions are shown at $E = 0.84$ kV/cm, electrode distance was 4 mm. The measured values for cells in SMEM medium are corrected for the changes in the medium alone. The lines represent results of the theoretical model described in the Materials and Methods section. Membrane conductivity was fitted to the measured data in high- and low-conductive medium to obtain the equivalent conductivity $\sigma_{\mathrm{p}} = 0.0495$ and 0.0209 S/m, respectively. Then the dependence of the relative changes on the electric field were obtained from finite elements models of permeabilized cells for different critical angles and by this a scaling factor was determined between equivalent conductivity σ_{p} when $\theta_{\mathrm{c}} = 54°$ (at 0.84 kV/cm) and σ'_{p} when $\theta_{\mathrm{c}} = 90°$. From the equivalent conductivity σ'_{p} [0.053 S/m, 0.0226 S/m] of a single cell σ_{m} for $\theta_{\mathrm{c}} = 90°$ can be obtained from the Pauly-Schwan equation:

TABLE 1 The changes of the real part of the impedance 14 and 28 s after the first pulse transformed into the conductivity change $\Delta\sigma_{\mathrm{imp}}/\sigma_0$ for cells in SMEM and PB medium

$\Delta\sigma_{\mathrm{imp}}/\sigma_0$	$E = 0.35$ kV/cm	$E = 0.52$ kV/cm	$E = 0.7$ kV/cm	$E = 0.86$ kV/cm	$E = 1.05$ kV/cm	$E = 1.2$ kV/cm	$E = 1.43$ kV/cm	$E = 1.61$ kV/cm
SMEM $t_1 = 14$ s	−0.002	−0.025	−0.010	−0.0136	−0.026	−0.030	−0.023	−0.032
SMEM $t_2 = 28$ s	0.000	−0.061	−0.017	−0.022	−0.040	−0.043	−0.033	−0.042
PB $t_1 = 14$ s	0.010	0.027	0.24	0.40	0.47	0.58	0.66	0.70
PB $t_2 = 28$ s	0.015	0.041	0.33	0.48	0.54	0.63	0.70	0.73

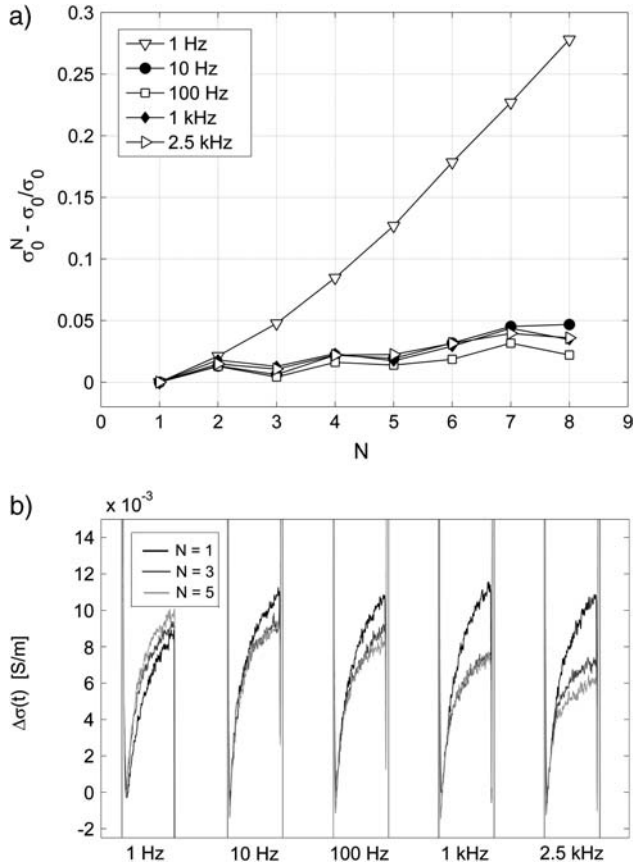

FIGURE 8 Effect of the repetition frequency on the conductivity changes in PB medium. Pulses 8×100 μs with repetition frequencies from 1 Hz to 2.5 kHz were used, $E = 0.84$ kV/cm. (*a*) Relative change of the initial level of the conductivity σ_0^N is shown. (*b*) The time-dependent conductivity changes $\Delta\sigma(t)$ of the first, third, and fifth pulse with respect to the first pulse (all initial levels are set to zero) are compared for different frequencies.

$$\sigma_p' = \sigma_m \frac{2(1-\nu)\sigma_m + (1+2\nu)\sigma_i}{(2+\nu)\sigma_m + (1-\nu)\sigma_i} \quad \nu = (1-d/R)^3, \quad (4)$$

where R is the cell radius and d the thickness of the membrane. In this way we obtained average membrane conductivity of the permeabilized part to be $\sigma_m = 3.5 \times 10^{-5}$ S/m (SMEM) and $\sigma_m = 1.4 \times 10^{-5}$ S/m (PB).

Under the assumption that that the number and size of the pores remain constant for different electric field strengths, the average membrane conductivity of the permeabilized area σ_m does not depend on E. Therefore, E governs only the area of the permeabilized surface given by (Schwister and Deuticke, 1985)

$$S_c = S_0(1 - E_c/E), \quad (5)$$

and by this the dependency of the cell equivalent conductivity on E.

In Fig. 10 the theoretical curve of the dependency of the conductivity increase due to the increased surface of permeabilized area for different E is shown where the critical angle θ_c is defined by the applied electric field and the critical voltage U_c. We numerically calculated the equivalent conductivity of a single cell σ_p (θ_c) and the bulk conductivity of a suspension of permeabilized cells for different critical angles as described in our previous work (Pavlin and Miklavčič, 2003) and in Materials and Methods. From this field-dependent conductivity changes $\Delta\sigma/\sigma_0$ (E) were calculated for constant membrane conductivity or taking into account the nonohmic behavior of the conductivity inside the pore using Eq. A.7, as shown in Fig. 10. Values of membrane conductivity were obtained from fitted values of our experimental data shown in Fig. 9. Critical electric field strength in both media was set to 0.5 kV/cm according to our experimental results (see Figs. 3 and 4).

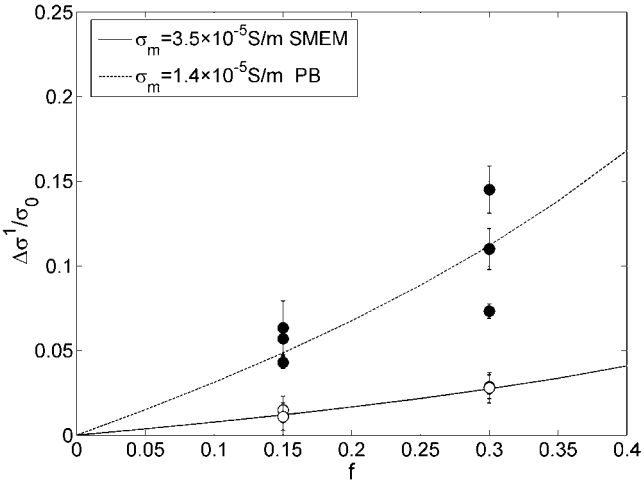

FIGURE 9 Absolute change in conductivity during the first pulse $\Delta\sigma^1$ is shown. Each error bar represents three sample data pooled together, obtained for a train of eight 100-μs pulses of 0.84 kV/cm in SMEM medium (○) and PB medium (●). The conductivity changes in pure SMEM medium were subtracted from the measured value obtained for cells in SMEM. The lines represent values of the theoretical model (see the Materials and Methods section) where membrane conductivity was fitted to obtain the best agreement with measured data.

DISCUSSION

The aim of our study was to analyze the effect of high-voltage pulses on the electrical properties of cells in a suspension and to analyze how these changes correspond to the level of membrane permeabilization. We performed current and voltage measurements during the train of eight high-voltage pulses and impedance measurements before and after the application of pulses in a dense suspension of cells. At the same time we determined the percentage of permeabilized cells and cell survival. In additional experiments the extent of colloid-osmotic swelling was also determined.

We observed a transient increase in conductivity during electric pulses for electric fields above 0.5 kV/cm ($U_m = 450$

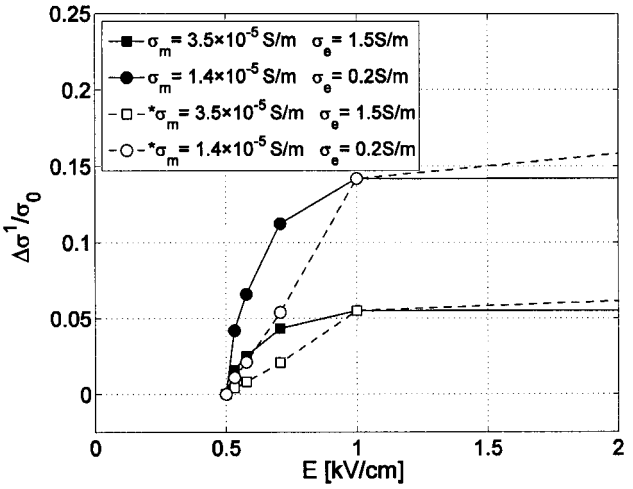

FIGURE 10 The theoretical curve of the dependency of the conductivity increase on the electric field due to the increased permeabilized surface area according to the theoretical model (see Appendix). Field-dependent conductivity change calculated theoretically for high conductive medium (*squares*) and low conductive medium (*circles*), $f = 0.3$, under an assumption of constant membrane conductivity of the permeabilized area (*solid line*) or *taking into account the nonohmic behavior of the conductivity inside the pore using Eq. A.7 (*dashed line*) is shown. Values for membrane conductivity σ_m were chosen as obtained from experiments shown in Fig. 9 at $E = 0.84$ kV/cm), threshold electric field in both cases was set to 0.5 kV/cm according to our experimental results.

mV) both in low- and high-conductive medium after which the pulse conductivity relaxed almost to the initial level. Our results are in agreement with the results of other groups obtained on single cells (Chernomordik et al., 1987; Ryttsen et al., 2000), cell suspensions (Kinosita and Tsong, 1977a,b; 1979), and cell pellets (Abidor et al., 1993; 1994) where also a transient increase in conductivity above a threshold electric field was observed. The threshold electric field at which the increased conductivity is observed in our experiments corresponds to the permeabilization threshold for the uptake of molecules for both media for several pulses. We obtained similar results for dense and dilute suspensions for permeabilization and survival, in agreement with Canatella et al. (2001) where it has been shown that the cell density itself does influence permeabilization only by affecting the local electric field. For tissue electroporation in general, however, there are several effects that contribute to non-homogeneous molecules uptake due to differences in cell state, solute concentration, and local electric field (Canatella et al., 2004).

The saturation of the conductivity in high-conductive medium, which is reached at the same electric field (around 1 kV/cm) as the permeabilization level (see Figs. 3 and 4) for eight pulses, agrees with the theoretical model where the field strength determines the permeabilized area and the membrane conductivity is assumed to be constant or having conductivity of the pore dependent on the electric field (see Appendix A) as shown in Fig. 10. In low-conductive medium maximum increase in conductivity is reached at higher electric field as permeabilization (and as described by the theoretical model) indicating that conductivity of permeabilized area is also increased due to increase in number or size of the pores, as has been suggested in some theoretical descriptions of pore evolution during the electric pulses (Chernomordik et al., 1987; Glaser et al., 1988). The changes of the initial level of conductivity obtained in the low-conductive medium (see Fig. 5) clearly show an increase of the overall level of the conductivity above 0.5 kV/cm, as well as saturation of conductivity increase at 1.4 kV/cm indicating that permeable structures in the membrane are present, which enable ions to leak from the cytoplasm into the external medium.

When analyzing the total increase in conductivity after the eight pulses (see Fig. 6) and the impedance several seconds after the pulses, we obtained that the change in conductivity consists of several contributions: i), a transient increase in conductivity during each pulse, which is observed above the threshold electric field and drops back to the initial level in less than a second; ii), a decrease in conductivity caused by colloid-osmotic swelling due to osmotic imbalance when the cell membrane is permeabilized, which is again observed only above the threshold field; swelling decreases the relative conductivity for a few percent in seconds after the application of pulses and up to 80% on the order of minutes; iii), increase in conductivity due to Joule heating by a few percent in high-conductive medium; and iv), efflux of ions from the cell interior, which is observed in low-conductive medium above the threshold electric field. All these contributions have to be taken into account when measuring the conductivity in cell suspensions as well as in tissue, where except for the efflux of ions, both the Joule heating and swelling of cells could affect the results considerably. Altogether our experiments on cell suspensions indicate that only measurements during the pulses or very shortly after the pulses relate to permeabilization, whereas impedance measurements several seconds later detect predominantly other effects. Because of higher density of cells in tissue and consequently lesser cell swelling due to cell-cell contacts (Abidor et al., 1993; 1994) the impedance measurements in tissue could give more information compared to measurements in cell suspensions.

Fitting the measured values of the conductivity changes to our theoretical model gives us an approximate membrane conductivity at the end of the 100-μs pulse $\sigma_m = [1.4–3.5] \times 10^{-5}$ S/m, which is smaller than the membrane conductivity determined on sea urchin eggs $\sigma_m = [1–4] \times 10^{-4}$ S/m (Hibino et al., 1991) or a magnitude lower than the values obtained on erythrocytes by Kinosita and Tsong (1977a, 1979) ($\sigma_m = 5 \times 10^{-4}$ –5×10^{-3} S/m). This discrepancy can be explained by different experimental procedures and differences between the cell types. Comparison of theoretical curves in Fig. 10 and permeabilization

dependence on the electric field suggest that electric field affects mostly the surface of the permeabilized area and consequently increased conductivity as well as fraction of permeabilized cells. Of course, the surface area of the permeabilized part of the cell membrane depend on the number as well as on the size of the pores, which both are time dependent. But in this article we limited our analysis only on the change of the conductivity and surface area of pores at the end of one pulse. A complementary theoretical analysis of the conductivity changes caused by membrane electroporation on CHO cell pellets was published recently (Schmeer et al., 2004). Authors analyze also the dynamic behavior and the size of the pores and obtain similarly that the conductivity changes during the pulses are transient whereas the conductivity increase between the pulses in a low conductive medium is due to the ion efflux.

In Appendix A, we estimate the fraction of surface area of the pores $f_p = S_{por}/S_0$ from obtained membrane conductivity that gives us $f_p \approx 10^{-5}$–10^{-4}. This is substantially less than the values obtained on sea urchin eggs (Hibino et al., 1991) $f_p \approx 10^{-4}$–10^{-3} and CHO cells $f_p \approx 10^{-4}$ (Neumann et al., 1998) or values that were obtained by electrooptical measurements on vesicles $f_p \approx 10^{-4}$ (Tönsing et al., 1997). We further estimated fraction of pores from ion efflux between the pulses in low-conductive medium (see Appendix B) and obtained $f_p \approx 10^{-7}$–10^{-6} that is approximately two orders of magnitude lower than the fraction of pores calculated from the membrane conductivity during the pulses.

Our results are in agreement with fast relaxation of the conductivity and with results of other authors (Kinosita and Tsong, 1977a, 1979; Hibino et al., 1991, 1993) where the conductivity of the membrane dropped for an order of magnitude in the millisecond range. The results support the hypothesis of the existence of two types of pores: short-lived pores, which are created during the pulse and transiently increase conductivity, and long-lived pores that contribute to increased permeability for ions and molecules in minutes after the pulses.

The results obtained in both low-conductive and high-conductive medium show that the conductivity changes during each pulse do not ''remember'' previous pulses for 1-Hz repetition frequency, similarly as observed by other authors on planar bilayer membranes (Chernomordik et al., 1987; Macek-Lebar et al., 2002a) and cells (Chernomordik et al., 1987; Kinosita and Tsong, 1979), where for a 1-s pause between the pulses the second pulse started from the same level as the first one. When repetition frequency is increased above 1 kHz, relaxation is not complete and the initial level of conductivity for consecutive pulses increases. This is in agreement with the results of other authors where at 1-kHz repetition frequency the second pulse started from much higher level (Chernomordik et al., 1987; Kinosita and Tsong, 1979), except for slightly faster relaxation in our experiments. It is also interesting to note that even after application of three series of 24 pulses of 1 Hz in low-conducting medium the dynamic behavior and conductivity change during each pulse remained the same.

One possible explanation for fast relaxation of conductivity is that the number and diameter of short-lived conductive pores is decreased to a level where their contribution to the conductivity is negligible, whereas some of them are still present and can later participate in formation of the long-lived transport pores that have long resealing time and are large enough to facilitate transport of molecules. Only a few long-lived pores could suffice for a substantial uptake of molecules, however, their contribution to the increase in conductivity would be negligible; e.g., from our data for the efflux of ions the membrane conductivity 10^{-6} S/m gives an increase in conductivity on the order of 0.1%, which is not measurable, but the corresponding fraction of pores gives approximately $N = 100$ pores having a radius of 1 nm (from the literature approximately the size of a hydrophilic metastable pore) and large enough for the transport of molecules of a few kilodaltons such as bleomycine (1.5 kDa).

This is in accordance with the theoretical predictions of the electroporation theory that the size distribution of the pores is changed after the pulse (Weaver and Chizmadzhev, 1996) due to the resealing of smaller pores while a small number of larger long-lived pores remain in the membrane. Long-lived permeable state of the cell membrane is not yet fully explained even though several hypotheses exist such as existence of metastable hydrophilic pores (Weaver and Chizmadzhev, 1996; Neumann et al., 1989; Smith et al., 2004; Leontiadou et al., 2004), coalescence of pores (Sugar and Neumann, 1984), or presence of small defects in the lipid bilayer (Teissie and Ramos, 1998). Also specific cell structures could be important for the creation of long-lived permeable structures and could lead to difference in resealing dynamics between lipid bilayers and cells like involvement of cytoskeletal network (Rols and Teissie, 1992; Teissie and Rols, 1994), membrane proteins (Weaver and Chizmadzhev, 1996), or anisotropic inclusions in the membrane (Fošnarič et al., 2003; Kandušer et al., 2003).

Another possible explanation of the fast relaxation of conductivity could be, that only a smaller part of the increased conductivity can be attributed to the conductive pores and that the larger part is a result of some related process (e.g., release of bound charges in the vicinity of a pore due to the very strong local electric field) with relaxation around 1 ms. This process remains, however, to be identified and explained.

When analyzing if transient conductivity changes reflect the level of permeabilization we identified the major discrepancy between permeabilization and conductivity changes when a train of pulses was analyzed, which has not been studied in previous reports. Our results indicate that the increase in conductivity is observed above the threshold electric field for permeabilization. This on one hand suggests that permeabilization could be detected with measurements of conductivity. On the other hand, almost identical transient

conductivity changes for consecutive pulses are observed, indicating that the conductivity increase is not necessarily related to the formation of the long-lived ''transport'' pores. The results further show that conductivity changes and the conductivity threshold do not depend on number of pulses, in contrast to cell permeabilization (detected usually as a transport of certain molecules), which depends on the duration and the number of pulses (Rols and Teissie, 1990; Kotnik et al., 2000; Canatella et al., 2001; Macek-Lebar et al., 2002b). This can be partially explained by the fact that electric current depends on different ion properties (mobility, concentration, and charge) and is governed by the electric field, whereas for small and especially noncharged molecules transport is governed mostly by diffusion (Puc et al., 2003). Hence, increased conductivity and permeabilization are not necessarily directly linked. It was also shown (Rols and Teissie, 1990) that when the number of pulses (or pulse duration) is increased, the threshold level reaches a certain limit threshold that cannot be decreased any further. So it is possible that with conductivity measurements we actually detect this limit threshold, which then explains why the conductivity threshold is equal for one or several pulses.

To summarize, conductivity measurements during the pulses give information about increased membrane permeability whereas impedance measurements several seconds after pulse application are not suitable due to fast relaxation of conductivity changes, colloid-osmotic swelling, and ions leakage. By measuring electric conductivity we can detect limit permeabilization threshold above which the electroporation process (uptake) occurs. However, conductivity changes are similar for a single or several pulses in contrast to considerable increase in permeabilization for several pulses, thus the transient conductivity changes, i.e., short-lived pores are related to permeabilization (long-lived pores) only indirectly and the relationship between the transient pores and long-lived permeable structures in the membrane remains to be explained. So, our results suggest that conductivity measurements can be used to optimize the voltage but not to control cell permeabilization in vitro in general, e.g., varying all pulse parameters. For application of conductivity measurements for online monitoring of cell electroporation relationship between permeabilization for a single and several pulses should be known, which is feasible because usually a certain protocol is chosen with constant number of pulses, and only the electric field is varied to achieve optimum efficiency. In such case the use of conductivity measurements for online control of the electroporation could be readily applied.

APPENDIX A: CALCULATION OF THE FRACTION OF SURFACE AREA OF PORES

Here we present the estimation of the fraction of the surface area of pores in the cell membrane from the increased membrane conductivity (similar derivation was first presented by Hibino). We assume that the specific conductance of the permeabilized area of a cell is approximately the sum of the conductance of N_p pores having radius r_p:

$$G_p = N_p \pi r_p^2 \frac{\sigma_{por}}{d} = S_{por} \frac{\sigma_{por}}{d}, \tag{A.1}$$

where we neglect the very small conductance of nonpermeabilized cell membrane, S_{por} represents the surface of all conducting pores. On the other hand this conductance is equal to the average membrane conductance of the permeabilized area as obtained from our measurement and from the theoretical model:

$$G_p = \overline{G}, \tag{A.2}$$

thus

$$S_{por} \frac{\sigma_{por}}{d} = S_c \frac{\sigma_m}{d}, \tag{A.3}$$

where S_c represents the total permeabilized surface of one cell (the area exposed to above-threshold transmembrane voltage), which is described by Eq. 5 and σ_m the average membrane conductivity of permeabilized area as defined in the theoretical model.

Conductance of the pore in a 1:1 electrolyte is given by (Glaser et al., 1988)

$$G_{por} = G_0 \frac{\exp(\beta U_m) - 1}{\frac{\beta U_m}{d} \int_0^d \exp\left[\beta U_m \frac{d-x}{d} + w(x)\right] dx} = G_0 \rho,$$
$$G_0 = N_p \pi r_p^2 \frac{\sigma_{0por}}{d}, \tag{A.4}$$

where $\beta = e / kT$ and $w(x) = W(x) / kT$ where e is the electron charge, U_m is the transmembrane voltage, and $W(x)$ the energy of an ion inside the pore due to the interactions of the ion with the pore walls (Parsegian, 1969; Glaser et al., 1988). Parameter ρ is a scaling factor, which reduces the conductivity of the ions inside the pores (σ_{por}), compared to the bulk approximation $\sigma_{0por} \approx (\sigma_e + \sigma_i)/2$ in the limit of very large pores when interactions are negligible. For a trapezoid shape of $w(x)$ we obtain from Eq. A.4 that when the transmembrane voltage is small $n\beta U_m \ll w_0$

$$\rho = \exp[-0.43(w_0 - n\beta U_m)], \tag{A.5}$$

and when the transmembrane voltage is large, e.g., for $\beta U_m \gg w_0$ ($U_m \gg 25$mV) we get

$$\rho = \frac{1}{\left(1 + \frac{n\beta U_m}{w_0 - n\beta U_m}\right) \exp(w_0 - n\beta U_m) - \frac{n\beta U_m}{w_0 - n\beta U_m}}, \tag{A.6}$$

where n is the relative size of the entrance region of the pore, and was estimated to be ~0.15 (Glaser et al., 1988). W_0 is the energy of an ion inside

TABLE 2 Values of used parameters

n	e/kT	σ_i	U_m	R	d
0.15	40 V^{-1}	0.5 S/m	900 mV	9.5 μm	5 nm
E	E_c	w_0	ρ	σ_m	D
0.84 kV/cm	0.5 kV/cm	2.5–5	0.22–0.57	1.4–3.5 $\times 10^{-5}$ S/m	2.5 $\times 10^{-5}$ cm^2/s

center of a pore and was estimated to be a few kT (Glaser et al., 1988). Thus, the fraction of pores f_p of the total membrane surface is approximately:

$$f_p = \frac{S_{por}}{S_0} = \frac{(1 - E_c/E)S_{por}}{S_c} \approx \frac{(1 - E_c/E)\sigma_m}{\sigma_{por}} \approx \frac{(1 - E_c/E)\sigma_m}{\rho\sigma_{0por}}, \quad (A.7)$$

where ρ is obtained from Eq. A.4. To estimate fraction of pores in our case for the membrane conductivity $\sigma_m = [1.4–3.5] \times 10^{-5}$ at $E = 0.84$ kV/cm we can use approximation Eq. A.6 because $U_m \gg 450$ mV. Inserting values of parameters (see Table 2) into Eq. A.7 $(1 - E_c / E) = 0.404$ and Eq. A.6 $w_0 =$ 2.5–5 we obtain for fraction of pores after 100-μs pulse being $f_p = 10^{-5}$–10^{-4}.

APPENDIX B: EFFLUX OF IONS

From the efflux of ions in the low conductivity medium (see Fig. 5) the fraction of the surface area of pores can be estimated. Here we assume that all conductivity increase on the order of seconds can be attributed to the efflux of ions (also some other process could be involved). Because by far the largest concentration difference between internal and external concentration is for K^+ ions ($c_e \approx 0$ mM, $c_i = 142$ mM) only this ion will be considered in the following analysis and their contribution to the external conductivity.

The diffusion of ions through the membrane is governed by Nernst-Planck equation

$$\frac{dn_e(x,t)}{dt} = -D\,S\frac{dc(x,t)}{dx} - \frac{zF}{RT}D\,S\,c(x,t)\frac{d\Psi(x,t)}{dx}, \quad (A.8)$$

where n_e is the number of mol in the external medium, D is the diffusion constant (2×10^{-5} cm^2/s), c the molar concentration, S the total transport surface $S = N\,S_{por}$ of N permeabilized cells, and Ψ the electric potential. In general D and S depend on time, electric field strength, and number of pulses, but here we will assume that they are approximately constant. The diffusion of ions is a slow process compared to the duration of the electric pulses, thus we can assume that the major contribution to efflux of ions occurs without the presence of the electric field. When there is no external electric field present, $\Delta\Psi$ is small (around 20 mV) because only the imbalance of the electric charges due to concentration gradient contributes (i.e., the reversal potential); therefore, the second term in Eq. A.8 can be neglected. By replacing the concentration gradient with $(c_e - c_i)/d$ we obtain:

$$\frac{dc_e(t)}{dt} = -\frac{DS}{dV_e}[c_e(t) - c_i(t)], \quad (A.9)$$

where V_e represent the external volume. In the above equation, we neglect spatial changes of the concentration and assume that they are approximately constant. We further neglect the volume fraction changes during the pulses and by taking into account that the sum of ions inside and outside remains constant, the equation further simplifies:

$$\frac{dc_e(t)}{dt} = -\frac{DS}{dVf(1-f)}\left(c_e(t) - fc_i^0\right), \quad (A.10)$$

where c_i^0 is the initial internal concentration of K^+ ions. Solution of the above equation is an exponential increase to maximum $c_e^k = f\,c_i^0$

$$c_e(t) = c_e^k\left[1 - \exp\left(-\frac{t}{\tau}\right)\right], \quad (A.11)$$

with a time constant

$$\tau = \frac{S_p}{S_0}\frac{3D}{d\,Rf(1-f)}. \quad (A.12)$$

From the time constant τ the fraction of pores can be estimated:

$$f_p \approx \frac{1}{\tau}\frac{d\,Rf(1-f)}{3D'}, \quad D' = D\exp(-0.43\,w_0), \quad (A.13)$$

where we again take into account that the effective diffusion constant D' of K^+ ions inside the pore differs from that in bulk. From Fig. 5 we obtain that for $E = 0.84$ kV/cm the time constant for conductivity changes is ≈ 22 s. Using Eq. A.12 for $w_0 = 2.5$–5 we obtain for diffusion time constants being between 8 s ($E = 1.6$ kV/cm) and 42 s ($E = 0.7$ kV/cm) fraction of the pores in PB medium $f_p = 10^{-7}$–10^{-6}.

The authors thank D. Kovaćić (Faculty of Electrical Engineering and Computer Science, University of Zagreb), M. Puc, and K. Flisar (both Faculty of Electrical Engineering, University of Ljubljana) who developed the measuring system that enabled us this research and Prof. J. Trontelj (Faculty of Electrical Engineering, University of Ljubljana) who kindly borrowed the LCR meter. M. Pavlin also thanks B. Valič (Faculty of Electrical Engineering, University of Ljubljana) for his help and V. B. Bregar for his valuable suggestions and comments.

This research was supported by the Ministry of Education, Science and Sports of the Republic of Slovenia under the grants Z2-6503 and SLO-CRO grant Monitoring of the Efficiency of Electrochemotherapy by Means of Bioimpedance Measurements, and the European Commission under the grant Cliniporator QLK3-99-00484 within the fifth framework.

REFERENCES

Abidor, I. G., A. I. Barbul, D. V. Zhelev, P. Doinov, I. N. Bandarina, E. M. Osipova, and S. I. Sukharev. 1993. Electrical properties of cell pellets and cell fusion in a centrifuge. *Biochim. Biophys. Acta.* 1152:207–218.

Abidor, I. G., L.-H. Li, and S. W. Hui. 1994. Studies of cell pellets. II. Osmotic properties, electroporation, and related phenomena: membrane interactions. *Biophys. J.* 67:427–435.

Canatella, P. J., M. M. Black, D. M. Bonnichsen, C. McKenna, and M. R. Prausnitz. 2004. Tissue electroporation: quantification and analysis of heterogeneous transport in multicellular environments. *Biophys. J.* 86: 3260–3268.

Canatella, P. J., J. F. Karr, J. A. Petros, and M. R. Prausnitz. 2001. Quantitative study of electroporation-mediated molecular uptake and cell viability. *Biophys. J.* 80:755–764.

Chernomordik, L. V., S. I. Sukarev, S. V. Popov, V. F. Pastushenko, A. V. Sokirko, I. G. Abidor, and Y. A. Chizmadzev. 1987. The electrical breakdown of cell and lipid membranes: the similarity of phenomenologies. *Biochim. Biophys. Acta.* 902:360–373.

Davalos, R. V., Y. Huang, and B. Rubinsky. 2000. Electroporation: bioelectrochemical mass transfer at the nano scale. *Microscale Thermophys. Eng.* 4:147–159.

Davalos, R. V., B. Rubinsky, and D. M. Otten. 2002. A feasibility study for electrical impedance tomography as a means to monitor tissue electroporation for molecular medicine. *IEEE Trans. Biomed. Eng.* 49:400–403.

Ferber, D. 2001. Gene therapy: safer and virus-free? *Science.* 294:1638–1642.

Fošnarič, M., V. Kralj-Iglič, K. Bohinc, A. Iglič, and S. May. 2003. Stabilization of pores in lipid bilayers by anisotropic inclusions. *J. Phys. Chem. B.* 107:12519–12526.

Garner, A. L., N. Y. Chen, J. Yang, J. Kolb, R. J. Swanson, K. C. Loftin, S. J. Beebe, R. P. Joshi, and K. H. Schoenbach. 2004. Time domain dielectric spectroscopy measurements of HL-60 cell suspensions after microsecond and nanosecond electrical pulses. *IEEE Trans. Plasma. Sci.* 32:2073–2084.

Glaser, R. W., S. L. Leikin, L. V. Chernomordik, V. F. Pastushenko, and A. V. Sokirko. 1988. Reversible electrical breakdown of lipid bilayers: formation and evolution of pores. *Biochim. Biophys. Acta.* 940:275–287.

Hibino, M., H. Itoh, and K. Jr. Kinosita. 1993. Time courses of cell electroporation as revealed by submicrosecond imaging of transmembrane potential. *Biophys. J.* 64:1789–1800.

Hibino, M., M. Shigemori, H. Itoh, K. Nagayama, and K. Jr. Kinosita. 1991. Membrane conductance of an electroporated cell analyzed by submicrosecond imaging of transmembrane potential. *Biophys. J.* 59: 209–220.

Jaroszeski, M. J., R. Gilbert, and R. Heller. 1997. Electrochemotherapy: an emerging drug delivery method for the treatment of cancer. *Adv. Drug Deliv. Rev.* 26:185–197.

Jaroszeski, M. J., R. Heller, and R. Gilbert. 1999. Electrochemotherapy, Electrogenetherapy and Transdermal Drug Delivery: Electrically Mediated Delivery of Molecules to Cells. Humana Press, Totowa, NJ.

Kandušer, M., M. Fošnarič, M. Šentjurc, V. Kralj-Iglič, H. Hägerstrand, A. Iglič, and D. Miklavčič. 2003. Effect of surfactant polyoxyethylene glycol (C12E8) on electroporation of cell line DC3F. *Colloids Surf. A.* 214:205–217.

Kinosita, K., and T. Y. Tsong. 1977a. Voltage-induced pore formation and hemolysis of human erytrocytes. *Biochim. Biophys. Acta.* 471:227–242.

Kinosita, K., and T. Y. Tsong. 1977b. Formation and resealing of pores of controlled sizes in human erythrocyte membrane. *Nature.* 268:438–441.

Kinosita, K., and T. Y. Tsong. 1979. Voltage-induced conductance in human erythrocyte. *Biochim. Biophys. Acta.* 554:479–497.

Kotnik, T., A. Maček-Lebar, D. Miklavčič, and L. M. Mir. 2000. Evaluation of cell membrane electropermeabilization by means of a nonpermeant cytotoxic agent. *Biotechniques.* 28:921–926.

Leontiadou, H., A. E. Mark, and S. J. Marrink. 2004. Molecular dynamics simulations of hydrophilic pores in lipid bilayers. *Biophys. J.* 86:2156–2164.

Macek-Lebar, A., G. Sersa, S. Kranjc, A. Groselj, and D. Miklavcic. 2002b. Optimisation of pulse parameters in vitro for in vivo electrochemotherapy. *Anticancer Res.* 22:1731–1736.

Macek-Lebar, A., G. C. Troiano, L. Tung, and D. Miklavčič. 2002a. Interpulse interval between rectangular voltage pulses affects electroporation threshold of artificial lipid bilayers. *IEEE Trans. Nanobiosc.* 1:116–120.

Maxwell, J. C. 1873. Treatise on Electricity and Magnetism. Oxford University Press, London, UK.

Mir, L. M. 2000. Therapeutic perspectives of in vivo cell electropermeabilization. *Bioelectrochemistry.* 53:1–10.

Mir, L. M., S. Orlowski, J. Belehradek, Jr., and C. Paoletti. 1991. Electrochemotherapy potentiation of antitumour effect of bleomycin by local electric pulses. *Eur. J. Cancer.* 27:68–72.

Nebeker, F. 2002. Golden accomplishments in biomedical engineering, 50 years of the IEEE EMBS and the emergence of a new discipline. *IEEE Eng. Med. Biol. Mag.* 21:17–47.

Neumann, E., and K. Rosenheck. 1972. Permeability changes induced by electric impulses in vesicular membranes. *J. Membr. Biol.* 10:279–290.

Neumann, E., M. Schaefer-Ridder, Y. Wang, and P. H. Hofschneider. 1982. Gene transfer into mouse lyoma cells by electroporation in high electric fields. *EMBO J.* 1:841–845.

Neumann, E., A. E. Sowers, and C. A. Jordan. 1989. Electroporation and Electrofusion in Cell Biology. Plenum Press, New York, NY.

Neumann, E., K. Toensing, S. Kakorin, P. Budde, and J. Frey. 1998. Mechanism of electroporative dye uptake by mouse B cells. *Biophys. J.* 74:98–108.

Okino, M., and H. Mohri. 1987. Effects of a high-voltage electrical impulse and an anticancer drug on in vivo growing tumors. *Jpn. J. Cancer Res.* 78:1319–1321.

Parsegian, A. 1969. Energy of an ion crossing a low dielectric membrane: solutions to four relevant electrostatic problems. *Nature.* 221:844–846.

Pavlin, M., and D. Miklavčič. 2003. Effective conductivity of a suspension of permeabilized cells: a theoretical analysis. *Biophys. J.* 85:719–729.

Pavlin, M., N. Pavšelj, and D. Miklavčič. 2002a. Dependence of induced transmembrane potential on cell density, arrangement and cell position inside a cell system. *IEEE Trans. Biomed. Eng.* 49:605–612.

Pavlin, M., T. Slivnik, and D. Miklavčič. 2002b. Effective conductivity of cell suspensions. *IEEE Trans. Biomed. Eng.* 49:77–80.

Pliquett, U., R. Elez, A. Piiper, and E. Neumann. 2004. Electroporation of subcutaneous mouse tumors by rectangular and trapezium high voltage pulses. *Bioelectrochemistry.* 62:83–93.

Pliquett, U., E. A. Gift, and J. C. Weaver. 1996. Determination of the electric field and anomalous heating caused by exponential pulses with aluminum electrodes in electroporation experiments. *Bioelectrochem. Bioenerg.* 39:39–53.

Puc, M., T. Kotnik, L. M. Mir, and D. Miklavčič. 2003. Quantitative model of small molecules uptake after in vitro cell electropermeabilization. *Bioelectrochemistry.* 60:1–10.

Pucihar, G., T. Kotnik, M. Kanduser, and D. Miklavčič. 2001. The influence of medium conductivity on electropermeabilization and survival of cells in vitro. *Bioelectrochemistry.* 54:107–115.

Rols, M. P., and J. Teissie. 1990. Electropermeabilization of mammalian cells: quantitative analysis of the phenomenon. *Biophys. J.* 58:1089–1098.

Rols, M. P., and J. Teissie. 1992. Experimental evidence for the involvement of the cytoskeleton in mammalian cell electropermeabilization. *Biophys. J.* 1111:45–50.

Ryttsen, F., C. Farre, C. Brennan, S. G. Weber, K. Nolkrantz, K. Jardemark, D. T. Chiu, and O. Orwar. 2000. Characterization of single-cell electroporation by using patch-clamp and fluorescence microscopy. *Biophys. J.* 79:1993–2001.

Schmeer, M., T. Seipp, U. Pliquett, S. Kakorin, and E. Neumann. 2004. Mechanism for the conductivity changes caused by membrane electroporation of CHO cell-pellets. *Phys. Chem. Chem. Phys.* 6:5564–5574.

Schwister, K., and B. Deuticke. 1985. Formation and properties of aqueous leaks induced in human erythrocytes by electrical breakdown. *Biochim. Biophys. Acta.* 816:332–348.

Serša, G., T. Čufer, M. Čemazar, M. Reberšek, and Z. Rudolf. 2000. Electrochemotherapy with bleomycin in the treatment of hypernephroma metastasis: case report and literature review. *Tumori.* 86:163–165.

Smith, K. C., J. C. Neu, and W. Krassowska. 2004. Model of creation and evolution of stable electropores for DNA delivery. *Biophys. J.* 86:2813–2826.

Sugar, I. P., and E. Neumann. 1984. Stochastic model for electric field-induced membrane pores electroporation. *Biophys. Chem.* 19:211–225.

Sukharev, S. I., V. A. Klenchin, S. M. Serov, L. V. Chernomordik, and Y. A. Chizmadzhev. 1992. Electroporation and electrophoretic DNA transfer into cells. The effect of DNA interaction with electropores. *Biophys. J.* 63:1320–1327.

Susil, R., D. Šemrov, and D. Miklavčič. 1998. Electric field-induced transmembrane potential depends on cell density and organization. *Electro. Magnetobiol.* 17:391–399.

Teissie, J., and C. Ramos. 1998. Correlation between electric field pulse induced long-lived permeabilization and fusogenicity in cell membranes. *Biophys. J.* 74:1889–1898.

Teissie, J., and M. P. Rols. 1994. Manipulation of cell cytoskeleton affects the lifetime of cell-membrane electropermeabilization. *Ann. N. Y. Acad. Sci.* 720:98–110.

Tönsing, K., S. Kakorin, E. Neumann, S. Liemann, and R. Huber. 1997. Annexin V and vesicle membrane electroporation. *Eur. Biophys. J.* 26: 307–318.

Tsong, T. Y. 1991. Electroporation of cell membranes. *Biophys. J.* 60:297–306.

Weaver, J. C., and Y. A. Chizmadzhev. 1996. Theory of electroporation: a review. *Bioelectrochem. Bioenerg.* 41:135–160.

Wong, T. K., and E. Neumann. 1982. Electric field mediated gene transfer. *Biochem. Biophys. Res. Commun.* 107:584–587.

Zimmermann, U. 1982. Electric field-mediated fusion and related electrical phenomena. *Biochim. Biophys. Acta.* 694:227–277.

BioMedical Engineering OnLine

BioMed Central

Research

Open Access

Electroporator with automatic change of electric field direction improves gene electrotransfer *in-vitro*

Matej Reberšek[1], Cécile Faurie[2], Maša Kandušer[1], Selma Corović[1], Justin Teissié[2], Marie-Pierre Rols[2] and Damijan Miklavčič*[1]

Address: [1]University of Ljubljana, Faculty of Electrical Engineering, Tržaška 25, SI-1000 Ljubljana, Slovenia and [2]Institut de Pharmacologie et de Biologie Structurale du CNRS UMR 5089, 205, route de Narbonne, 31077 Toulouse cedex, France

Email: Matej Reberšek - matej.rebersek@fe.uni-lj.si; Cécile Faurie - faurie.cecile@laposte.net; Maša Kandušer - masa.kanduser@fe.uni-lj.si; Selma Corović - selma.corovic@fe.uni-lj.si; Justin Teissié - justin.teissie@ipbs.fr; Marie-Pierre Rols - marie-pierre.rols@ipbs.fr; Damijan Miklavčič* - damijan.miklavcic@fe.uni-lj.si

* Corresponding author

Published: 2 July 2007

BioMedical Engineering OnLine 2007, **6**:25 doi:10.1186/1475-925X-6-25

Received: 26 February 2007
Accepted: 2 July 2007

This article is available from: http://www.biomedical-engineering-online.com/content/6/1/25

Abstract

Background: Gene electrotransfer is a non-viral method used to transfer genes into living cells by means of high-voltage electric pulses. An exposure of a cell to an adequate amplitude and duration of electric pulses leads to a temporary increase of cell membrane permeability. This phenomenon, termed electroporation or electropermeabilization, allows various otherwise non-permeant molecules, including DNA, to cross the membrane and enter the cell. The aim of our research was to develop and test a new system and protocol that would improve gene electrotransfer by automatic change of electric field direction between electrical pulses.

Methods: For this aim we used electroporator (EP-GMS 7.1) and developed new electrodes. We used finite-elements method to calculate and evaluate the electric field homogeneity between these new electrodes. Quick practical test was performed on confluent cell culture, to confirm and demonstrate electric field distribution. Then we experimentally evaluated the effectiveness of the new system and protocols on CHO cells. Gene transfection and cell survival were evaluated for different electric field protocols.

Results: The results of *in-vitro* gene electrotransfer experiments show that the fraction of transfected cells increases by changing the electric field direction between electrical pulses. The fluorescence intensity of transfected cells and cell survival does not depend on electric field protocol. Moreover, a new effect a shading effect was observed during our research. Namely, shading effect is observed during gene electrotransfer when cells are in clusters, where only cells facing negative electro-potential in clusters become transfected and other ones which are hidden behind these cells do not become transfected.

Conclusion: On the basis of our results we can conclude that the new system can be used in *in-vitro* gene electrotransfer to improve cell transfection by changing electric field direction between electrical pulses, without affecting cell survival.

1. Background

Gene therapy is an experimental method used in clinics proven to be successful in *in-vitro* and *in-vivo* conditions. For gene therapy, DNA or RNA molecules are transferred into living cells to replace, change or silence gene expression. Consequently cells change their biological nature in therapeutical purposes [1,2]. Effective and potentially safe transfer of DNA molecules into living cells has been a goal of scientific research for many years. This research is now divided into two main fields: viral and non-viral gene delivery. Viral vectors are considered to provide the highest effectiveness of DNA transfer, but they are often associated with immune responses [3] and insertional mutagenesis [4-6]. That is why non-viral methods of DNA transfer are being sought for [7-9].

An exposure of a cell to adequate amplitude and duration of electric pulses leads to temporary increase of cell membrane permeability while preserving cell viability. This phenomenon, termed electroporation or electropermeabilization, allows various otherwise non-permeant molecules to cross the membrane and enter the cell. Both *in-vitro* and *in-vivo*, reversible electropermeabilization allows for internalization of a wide range of substances [10,11]. When DNA molecules are transferred into cells by electropermeabilization, this method is called gene electrotransfer. Gene electrotransfer is therefore a non-viral method used to transfer DNA molecules into living cells by means of high-voltage electric pulses [11-16]. Being extensively investigated, gene electrotransfer is becoming more and more effective and therefore gaining importance as a non-viral gene therapy method [7,9].

Electropermeabilization of the cell occurs in the area of cell membrane facing negative and positive electro-potential regarding intercellular potential [17,18]. However, DNA molecules do not spontaneously interact with mammalian cell membrane but are driven to the membrane by electrophoretic forces. Therefore, negative DNA molecules only interact with the cell membrane facing negative electro-potential. Thus, only one side of cell membrane is susceptible for transfer of DNA molecules. Any increase in the susceptible area for transfer of DNA molecules therefore increases the effectiveness of transfection [19,20].

Changing the electric field direction between electrical pulses presumably increases the area of successful electropermeabilization [21] and therefore increases susceptible area for transfer of DNA molecules. This method is especially effective for cells *in-vivo* and also for plated cells *in-vitro*, because their cell shapes and their orientations in the electric field are important for successful electropermeabilization [22-24]. Changing the polarity of electric field during the electric pulse delivery is also important for gene electrotransfer as it allows interaction of DNA molecules on both sides of the cell membrane perpendicular to direction of electric field (changing the electric field polarity corresponds to changing the electric field direction for 180°). Changing the electric field direction between electrical pulses therefore improves the efficiency of gene electrotransfer indirectly by increasing the area of successful electropermeabilized membrane, or directly by interaction of DNA molecules with the cell membrane on both sides.

The protocol that defines changes of electric field direction between electrical pulses is referred to as the electric field protocol. Researchers who had already investigated influence of electric field protocol on the gene electrotransfer did not use any of the existing systems for automatic change of electric field direction between electrical pulses. That is because they did not have any electrodes which would allow delivery of electric field protocols with relatively homogeneous electric field intensity. Because of that they had to change the electric field direction by rotating the electrodes manually, which however is not always possible [20]. Nevertheless similar research, with or without such automatic system, had also been done in electrochemotherapy, but predominantly with the aim of improving electric field distribution including its homogeneity [21,25].

The aim of our research was to develop and test new system and protocol which would improve gene electrotransfer by automatic change of electric field direction between electrical pulses. For this we chose an electroporator, which can control at least four electrodes. In addition, we designed new electrodes made of four cylindrical rods that provides as homogeneous electric field distribution as possible. We calculated the distribution of electric field numerically for given electrode design and electric field protocol. New system and protocols were tested experimentally on Chinese Hamster Ovary cells. *In-vitro* gene transfection and cell survival were evaluated for different electric field protocols by fluorescence microscopy. A shading effect, previously not yet described in scientific literature was observed during our research.

2. Methods

A new system for gene electrotransfer was developed which consists of an electroporator (EP-GMS 7.1, Fig. 1a) and specially designed new electrodes (E-S 4.1, Fig. 1b). Both were developed at the University of Ljubljana, Faculty of Electrical Engineering. The EP-GMS 7.1 electroporator was already used and described in previously reported studies [26,27]. The main advantage of this electroporator is the ability to automatically change the electric field direction between electrical pulses at various frequencies, without rotation or movement of electrodes.

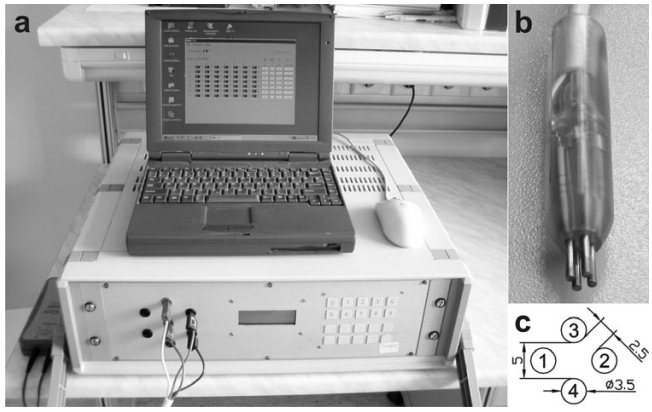

Figure 1
A new system for gene electrotransfer. Photograph of the electroporator EP-GMS 7.1 (a), photograph of the electrodes E-S 4.1 (b) and electrodes E-S 4.1 geometry design (c). Electrodes are numbered. Their diameter is 3.5 mm. Electrodes 1 and 2 or 3 and 4 are opposite electrodes and are 5 mm apart. Adjacent electrodes are 2.5 mm apart, which is a half distance between opposite electrodes.

2.1 Electroporator (EP-GMS 7.1) and electrodes (E-S 4.1)

The user defines electrical parameters of applied electric pulse through the interface of the electroporator (EP-GMS 7.1) on a personal computer (PC). Parameters are then transferred to the executive part of the electroporator. After this transfer the electroporator is ready to generate defined electric pulses in predefined directions.

Electroporator (EP-GMS 7.1) generates from 1 to 32 square electric pulses from 80 to 400 V, duration from 10 to 1000 μs and repetition frequency from 0.1 to 5000 Hz. Particularity of this electroporator is an embedded electrode commutator which controls up to seven electrodes. This commutator applies one of three possible states to each of the electrodes: positive, negative or high impedance state. Electrode state change is accomplished within 12 ms thus the electric field direction between the electrodes can be changed.

The electrodes (E-S 4.1) were designed as four cylindrical rods that allow delivery of electric field in different directions and at the same time providing relatively homogeneous electric field distribution. Delivery of electric field in all directions can be achieved by two sinusoidal signals phase shifted for 90°, which are delivered on two pairs of opposite electrodes (e.g. 1–2 and 3–4, Fig. 1c). However, for that different electroporator should be used, which allows delivery of such sinusoidal signals.

The electrodes are made of stainless steel; their diameter is 3.5 mm, adjacent electrodes are 2.5 mm apart, opposite electrodes are 5 mm apart, their length is 18 mm (Fig. 1c). Electrodes are connected to 4-wire cable and fixed with polyester resin, which assures constant distance between the electrodes and also protects the user against high-voltage.

Four different electric field protocols were used with this new system (electroporator and electrodes) in our experiments: single polarity (SP), both polarities (BP), orthogonal single polarity (OSP) and orthogonal both polarities (OBP; Fig. 2). When SP electric field protocol is used, single polarity electric pulses are applied between two opposite electrodes (Fig. 2a). When BP electric field protocol is used, both polarities electric pulses are applied between two opposite electrodes (Fig. 2b). When OSP electric field protocol is used, single polarity electric pulses are applied alternately between two pairs of opposite electrodes (Fig. 2c). And when OBP electric field protocol is used, both polarities electric pulses are applied alternately between two pairs of opposite electrodes (Fig. 2d).

2.2 Electric field intensity

Electric field intensity between the electrodes during the electric pulse delivery was calculated numerically by means of finite-elements method (Fig. 3a–c) [28] and a quick practical test was performed to confirm the correct-

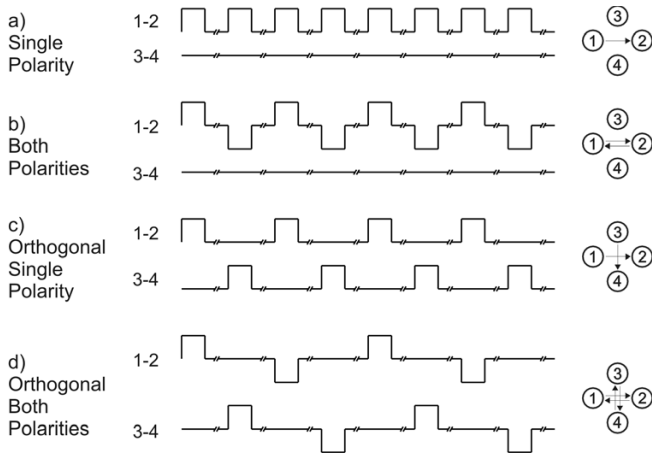

Figure 2
Electric field protocols. In single polarity (SP) electric field protocol direct electric pulses are applied between two opposite electrodes. While in both polarities (BP) electric field protocol alternating electric pulses are applied between two opposite electrodes. In orthogonal single polarity (OSP) electric field protocol direct electric pulses are applied between both opposite pairs of electrodes. While in orthogonal both polarities (OBP) electric field protocol alternating electric pulses are applied between both opposite pairs of electrodes. Signals in the middle represent applied voltage to the electrodes. Symbols on the right represent electric field protocols in which arrows represent directions of electric field in the centre between the electrodes.

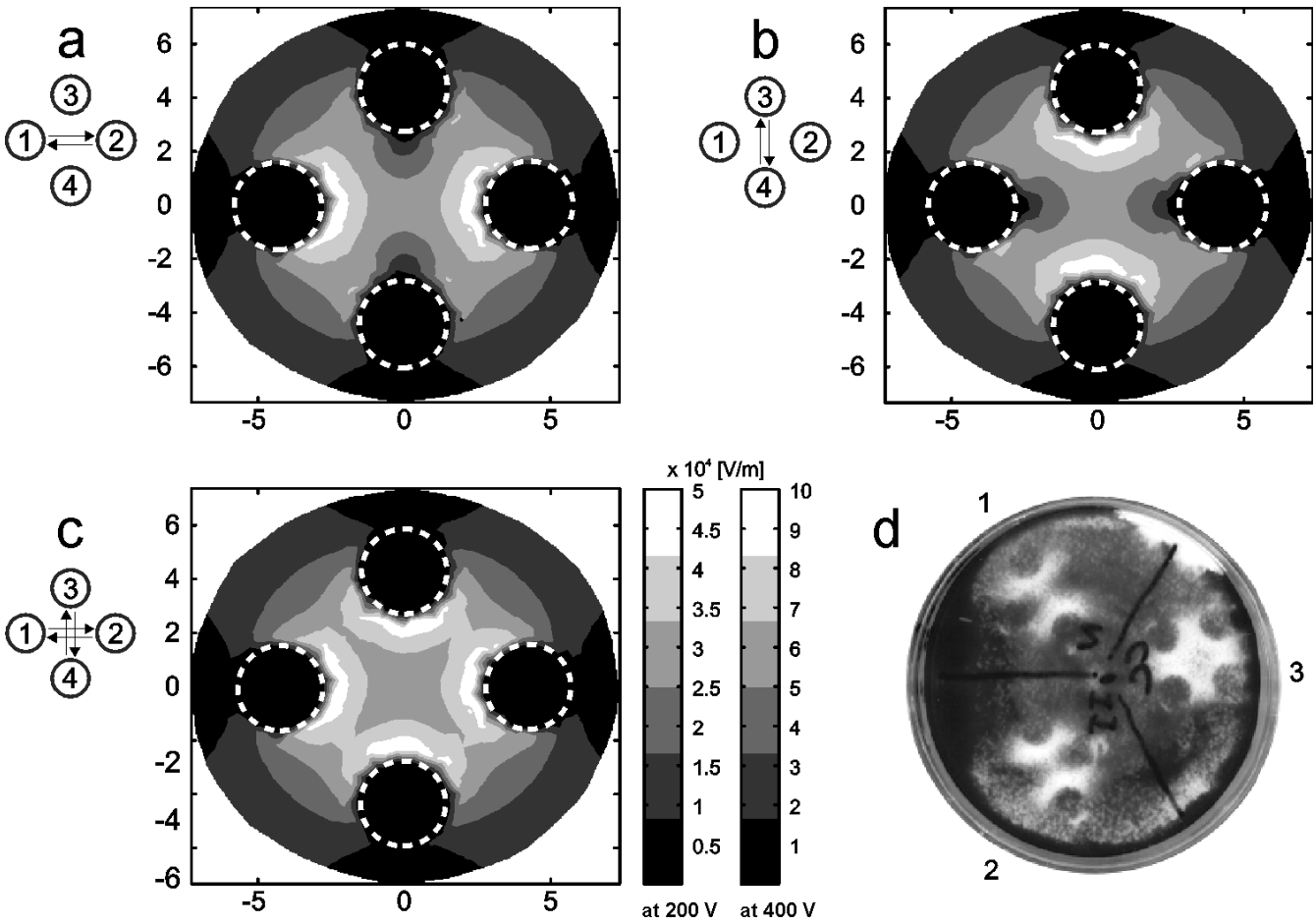

Figure 3

Calculated electric field intensity between the electrodes. Calculated electric field intensity between the electrodes during the electric pulse delivery of 200 V (+100 V, -100 V) and 400 V (+200 V, -200 V), when electrical pulses are applied between electrodes 1 and 2 (a) and when they are applied between electrodes 3 and 4 (b). Calculated local maxima of electric field intensity between the electrodes in orthogonal single polarity (OSP) and orthogonal both polarities (OBP) electric field protocol (c). Dashed circles represents position of electrodes. Symbols on the left represent electric field protocols. Electric field intensity scale is given for 200 V and 400 V. Experimental electric field intensity between the electrodes E-S 4.1 during the electric pulse delivery (d), when electrical pulses are applied between electrodes 1 and 2 (d1) and when they are applied between electrodes 3 and 4 (d2). Experimental local maxima of electric field intensity between the electrodes, when electrical pulses are applied between electrodes 1 and 2 and between electrodes 3 and 4 (d3). A train of eight electric pulses with amplitude of 400 V (+200 V, -200 V), duration 1 ms and repetition frequency 1 Hz was applied.

ness of calculations and demonstrate electric field intensity distribution (Fig. 3d).

A three-dimensional finite-elements model of an electroporation medium in culture dish with inserted electrodes (E-S 4.1) was designed using software package EMAS (ANSOFT Corporation, USA). Applied voltage was modelled as Dirichlet's boundary condition on the surface which presents the cross-section of electrode and cell suspension. Electro-potential of disconnected electrodes was defined as zero, because our model is symmetrical and disconnected electrodes are always in the middle between the connected electrodes. Electro-potential of disconnected electrodes was also defined as zero, to satisfy the conditions that electrodes are a lot more conductive then electroporation medium and that the sum of current through the entire surface to disconnected electrodes is always zero. Electroporation medium was mathematically separated from surrounding area by Neuman's boundary condition:

$$J_N = 0, \quad (1)$$

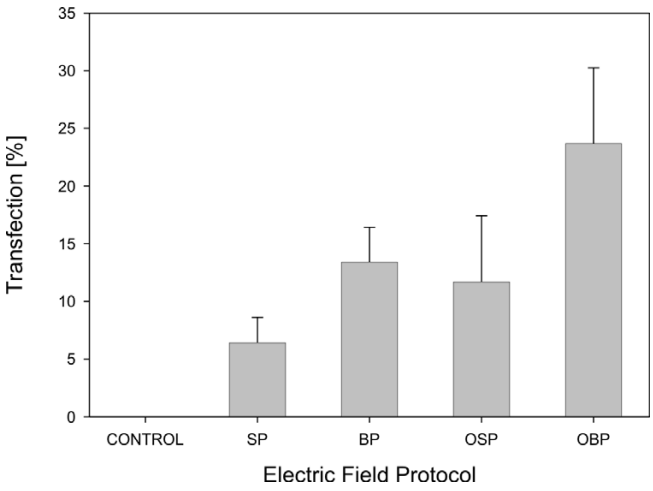

Figure 4

Fraction of transfected CHO cells. Fraction of transfected CHO cells after gene electrotransfer experiment in different electric field protocol. Cells were exposed to a train of eight pulses with amplitude of 200 V, duration 1 ms and repetition frequency 1 Hz. Results were obtained by means of fluorescence microscopy. Each value in the graph represent mean of four independent experiments, ± standard deviation. Electric field protocols result in different fraction of transfected cells (ANOVA: P = 0.002).

where J_N is the normal electric current density [A/m^2]. Electroporation medium was modelled as a constant i.e. independent of electric field applied, passive, homogeneous and isotropic volume conductor in the quasi-stationary electric current field. A condition in such structure is described by Laplace's equation:

$$\Delta\phi = 0, \qquad (2)$$

where ϕ is electric potential [V]. Results of electric field intensity obtained by such linear model are scalable by applied voltage ratio (Fig. 3).

To calculate the electric field intensity, when electrical pulses are applied between electrodes 1 and 2 (Fig. 3a), boundary conditions on the surface of the electrode 1 were set to +100 V and on the electrode 2 to -100 V. Electrodes 3 and 4 were in this case set to 0 V and thus defined as disconnected. Calculation of electric field intensity, when electrical pulses are applied between electrodes 3 and 4 (Fig. 3b), was done in the similar way as calculation of electric field intensity, when electrical pulses are applied between electrodes 1 and 2. Local maxima of both electric field intensities (Fig. 3c) were calculated to evaluate effectiveness of OSP and OBP electric field protocol [29].

Results of calculations have shown that electric field intensity in the space between the electrodes is very homogeneous compared to electric field intensity between two cylindrical rods, because of the two additional rods, which are highly conductive with respect to electroporation medium, are equalizing the distances between the equipotential lines in the space between the electrodes.

Quick practical test was performed on confluent cell culture in plastic culture dish. To confirm and demonstrate electric field distribution, plastic culture dish was separated into three sections (Fig. 3d). A train of eight electric pulses with amplitude of 400 V (+200 V, -200 V), duration 1 ms and repetition frequency 1 Hz was applied to kill the cells exposed to highest electric field intensity. In the first section electric pulses were applied between electrodes 1 and 2 (Fig. 3d1). In the second section electric pulses were applied between electrodes 3 and 4 (Fig. 3d2). In the third section electric pulses were applied between electrodes 1 and 2 and between electrodes 3 and 4 (Fig. 3d3). After 24 hours, killed cells were washed out and living cells were fixed in plastic culture dish with methanol for 10 minutes and stained with crystal violet.

2.3 Cells, cell survival and gene electrotransfer

Chinese Hamster Ovary (CHO; European Collection of Cell Cultures, Great Britain) cells were used. Cells in suspension were cultured in Eagle's Minimum Essential Medium (MEM; Sigma, USA) supplemented with 10 % Foetal Calf Serum (FCS; Sigma, USA). When cell suspension density reached 2 × 10^6 cells/ml, it was diluted with culture medium. For experiments, 5 × 10^5 cells were plated in a plastic culture dish (growth surface: 9.2 cm^2, diameter: 40 mm, height: 11 mm; TPP, Switzerland) and grown in the incubator (37°C, 5% CO_2) for 24 hours. During that time they attached to the surface of the culture dish and started to divide.

For gene electrotransfer experiments, plasmid DNA pEGFP-C1 (Clontech, USA; 4649 base pairs), which expresses green fluorescent protein (GFP, excitation 488 nm, emission 507 nm) under promoter cytomegalovirus, was added in concentration 40 μg/ml to the electroporation medium (10 mM phosphate buffer K_2HPO_4/KH_2PO_4, 1 mM MgCl, 250 mM sucrose; pH: 7.4, conductivity: 0.14 S/m). Culture medium was removed and 100 μl drop of electroporation medium containing plasmids was placed between electrodes. A train of eight electric pulses with amplitude of 200 V (+100 V, -100 V), duration 1 ms and repetition frequency 1 Hz was applied according to previous results [19,20]. Four different electric field protocols were used as described previously in subsection 2.1: single polarity (SP), both polarities (BP), orthogonal single polarity (OSP) and orthogonal both polarities

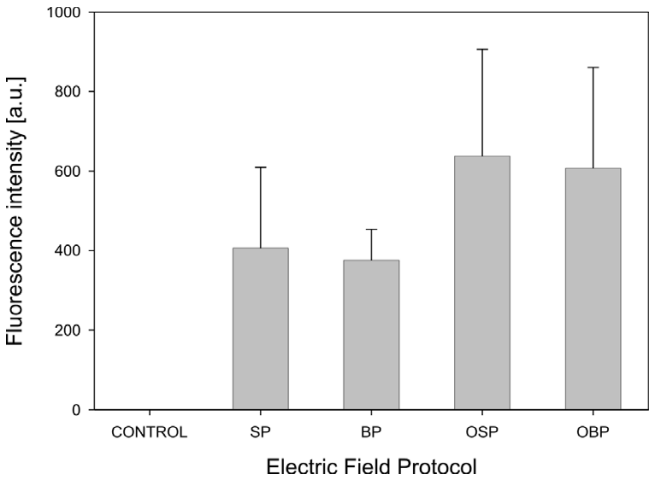

Figure 5

Fluorescence intensity of transfected CHO cells. Fluorescence intensity of transfected CHO cells after gene electrotransfer experiment in influence of electric field protocol. Cells were exposed to a train of eight pulses with amplitude of 200 V, duration 1 ms and repetition frequency 1 Hz. Results were obtained by means of fluorescence microscopy. Each value in the graph represent mean of four independent experiments, ± standard deviation. Different electric field protocols did not result in different level of fluorescence intensity (ANOVA: P = 0.246).

(OBP) (Fig. 2), to determine gene expression. In the control, cells were not exposed to electric pulses.

After electroporation, cells were left for 15 min at room temperature for cell membrane resealing. Then 2 ml of culture medium was added and culture dishes were then placed into incubator (37°C, 5% CO_2). 24 hours after electroporation, cells were investigated under inverted fluorescence microscope (Axiovert 200, Zeiss, Germany). Five photos of phase contrast and fluorescence images were taken per sample randomly in the area in the centre between the electrodes with cooled CCD camera (12 bit; VisiCam, Germany). Objective magnification was 20× and approximately 100 cells per image were observed. For fluorescence imaging, excitation wavelength 425 nm (Polycome IV, Visitron Systems, Germany), dichroic mirror (460 DCLP; Chroma, USA) and emission filter (D505/40 m; Chroma, USA) were used.

MetaMorph (Version 5.0r7, Universal Imaging Corporation, USA) was used for image analysis. The fraction of transfected cells was calculated as the ratio between transfected cells and all viable cells in a given treatment. The fluorescence intensity of transfected cells related to quantity of GFP inside the transfected cells was quantified on acquired images by MetaMorph. The fraction of cell survival was calculated as the ratio between viable cells in treatment and viable cells in control, which were not treated with electric pulses. Independent experiments of gene electrotransfer were repeated four times. Results (the fraction of transfected cells, the fluorescence intensity of transfected cells and the fraction of cell survival) are given in a form of bar graphs (SigmaPlot 9.0, Systat, USA), where every point represents the mean of four independent experiments and the error bars indicate the standard deviation (Fig. 4, 5). Statistical tests One way analysis of variance (One Way ANOVA) were performed on all results (SigmaStat 3.1, Systat, USA). Bonferroni t-test was performed on results if there was indication of a statistically significant difference between different electric field protocols used.

To visualize interaction of DNA with cell membrane immediately after application of electric pulses, we stained plasmid DNA pEGFP-C1 with thiazole orange homodimer dye (TOTO-1, excitation 514 nm, emission 533 nm; Molecular Probes, USA). Plasmid DNA pEGFP-C1 was mixed with TOTO-1 by base pair to dye ratio of 5 and placed on ice for 1 hour [30]. Electropermeabilization procedure was the same as for gene electrotransfer, except that only two different electric field protocols were used as described previously in subsection 2.1: single polarity (SP) and both polarities (BP; Fig. 2), to determine areas of DNA interaction with cell membranes (Fig. 6a, b). Up to 5 minutes after electropermeabilization photos of phase contrast and fluorescence images of cells were taken under inverted fluorescence microscope (Fig. 7, 8). For fluorescence imaging excitation wavelength 480 nm (Polycome IV, Visitron Systems, Germany), dichroic mirror (Q505LP; Chroma, USA) and emission filter (HQ535/50m; Chroma, USA) were used.

3. Results

Effects of four different electric field protocols: single polarity (SP), both polarities (BP), orthogonal single polarity (OSP) and orthogonal both polarities (OBP) on *in-vitro* gene electrotransfer were evaluated by determining the fraction of transfected cells (Fig. 4) and the fluorescence intensity of transfected cells (Fig. 5). At the same time also the fraction of cell survival was determined.

The results of our *in-vitro* gene electrotransfer experiments show that the fraction of transfected cells increases by changing the electric field direction between electrical pulses. This increase is almost quadrupled at OBP electric field protocol with respect to SP electric field protocol. The largest fraction of transfected cells was observed at OBP electric field protocol and was 24 % (Fig. 4). One way ANOVA indicates that there is a statistically significant difference between different electric field protocols (P = 0.002). Bonferroni t-test indicates that there is a statistically significant difference in comparison of OBP ver-

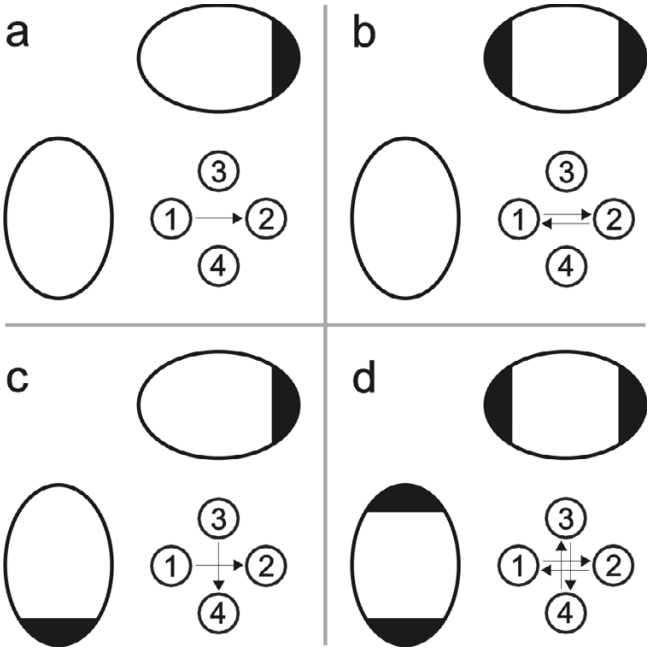

Figure 6
Schematic drawing of competent areas for DNA interaction with cell membrane. Schematic drawing of competent cell membrane areas for DNA interaction with cell membrane in influence of electric field protocols: single polarity (a), both polarities (b), orthogonal single polarity (c) and orthogonal both polarities (d). Black areas represent regions of permeabilized membrane where DNA interacts with cell membrane.

sus SP electric field protocol (P = 0.001) and OBP versus OSP electric field protocol (P = 0.023).

The fluorescence intensity of transfected cells does not however depend on electric field protocol (Fig. 5). One way ANOVA indicated that there is no difference between the electric field protocols (P = 0.246), although transfected cells exposed to orthogonal polarities show higher intensity.

Cell survival after electric pulses applied at 200 V is in the range 96 – 102 % at all four electric field protocols (data not shown). One way ANOVA indicated that there is no difference between the electric field protocols and control (P = 0.963).

Visualization of interaction between DNA and cell membrane showed that DNA molecules interact with the cell membrane facing negative electro-potential (Fig. 7). If SP electric field protocol is used, DNA interacts with cell membrane only from one side of the cell (Fig. 7a) whereas if BP electric field protocol is used, DNA interacts with cell membrane from two sides of the cell (Fig. 7b).

Shading effect is observed when cells are in clusters (Fig. 8). In such clusters we can observe that cells facing negative electro-potential are shading other cells so that DNA molecules can not interact with them (Fig. 8c). Therefore if SP electric field protocol is used the cells in clusters, which are exposed to one side of negative electro-potential during SP electric field protocol, interacts with DNA molecules (III and V, partially: I; Fig. 8c1) and the cells, which are hidden behind this cells in clusters, does not interact with DNA molecules (II and IV, partially: I; Fig. 8c1). And if BP electric field protocol is used the cells in clusters, which are exposed to one of both sides of negative electro-potential during BP electric field protocol, interacts with DNA molecules (VI and VIII, partially VII; Fig. 8c2) and the cells, which are hidden behind this cells in clusters from both sides, does not interact with DNA molecules (partially: VII; Fig. 8c2).

4. Discussion and Conclusion

The aim of our research was to develop and test new system and protocol which would improve gene electrotransfer by automatic change of electric field direction between electrical pulses. For this we chose electroporator with embedded electrode commutation circuit, which controls up to seven electrodes and applies one of three possible states to each of the electrodes: positive, negative or high impedance. Although any other electroporator could be used for such experiments. Since previous observations already demonstrated that homogeneity of electric field distribution affects the effectiveness of electropermeabilization [29,31], we developed electrodes that allow as homogeneous electric field distribution as possible.

An ideal homogeneous electric field distribution can only be achieved between two infinite flat electrodes. In practice we achieve a very close approximation to such electric field distribution if we use sufficiently large flat parallel electrodes that are relatively close to each other. But between two parallel electrodes only two directions of electric field are possible. To generate electric field in more that two directions we need to use more electrodes. We could use four plate electrodes, but in this case we get very inhomogeneous electric field distribution between the electrodes, since the current predominantly flows through the metal of the adjacent electrodes and less through the sample (cells suspension or tissue). That is why in the development of new electrodes (E-S 4.1) we focused on conductivity between opposite electrodes and between adjacent electrodes. Our hypothesis in the development of electrodes was that the most homogeneous electric field distribution between four cylindrical electrodes is achieved when conductivity between opposite electrodes is twice the sum of conductivity between adjacent electrodes (Fig. 1c).

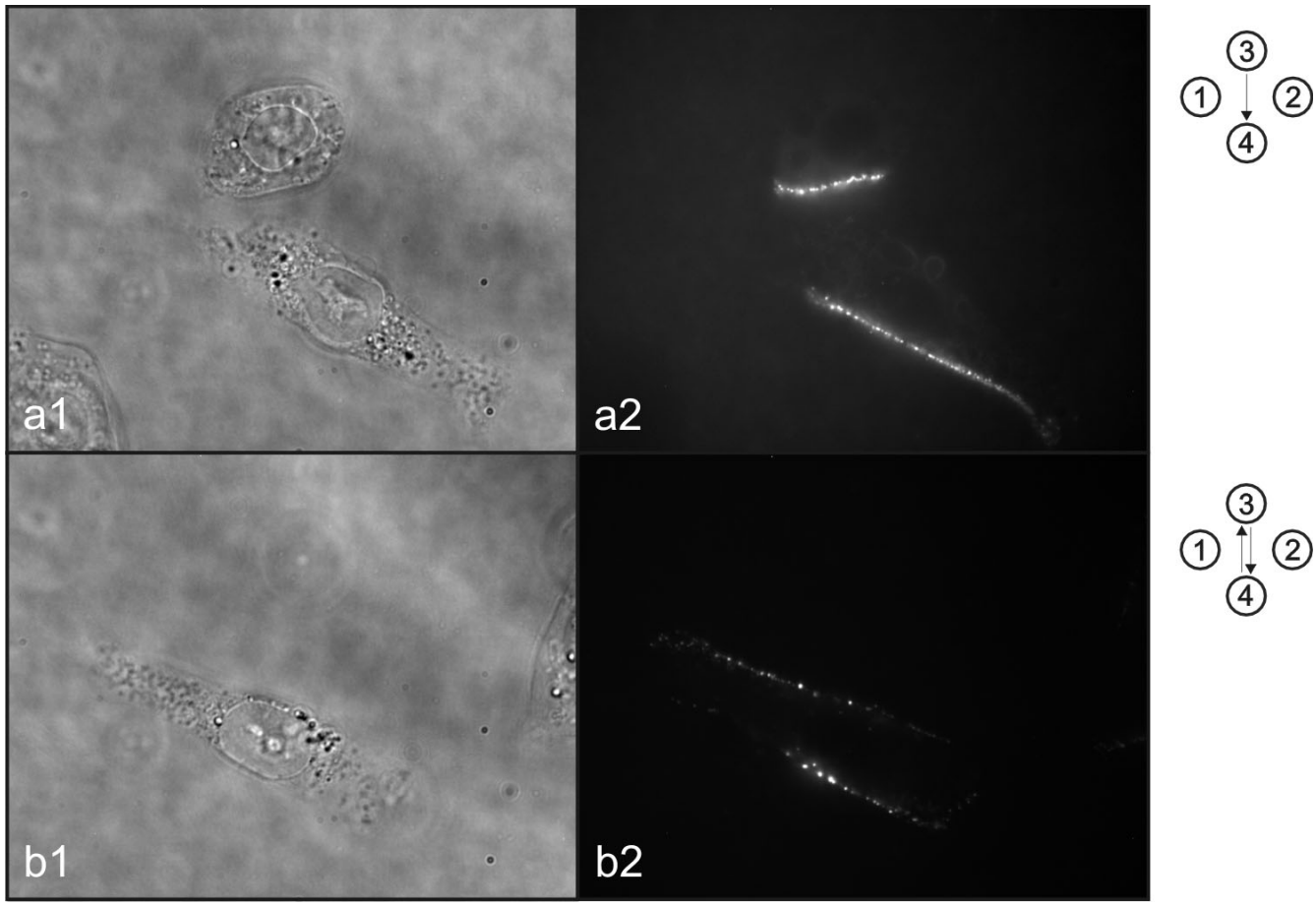

Figure 7
Visualization of interaction between DNA and cell membrane. Visualization of interaction between DNA and cell membrane after single polarity electric field protocol (a) and both polarities electric field protocol (b). Photos of phase contrast (1) and fluorescence (2) images were taken under inverted fluorescence microscope. Symbols on the right represent electric field protocol used.

To evaluate homogeneity of electric field between the electrodes, we designed a three-dimensional finite-elements model of an electroporation medium in culture dish with inserted electrodes. Calculations of electric field intensity in this model showed that the electric field distribution is relatively homogeneous between the electrodes for all four different electric field directions (Fig. 3). Results of calculations have also shown that orthogonal single polarity (OSP) and orthogonal both polarities (OBP) electric field protocols are efficient only in the space between the electrodes, because only there the electric field direction can be rotated for 90°. In addition, a quick practical test was performed to confirm the correctness of calculations and demonstrate electric field intensity distribution (Fig. 3d). In this test, cell survival was depended on electric field intensity. At highest electric field intensity all cells where killed and at low electric field intensity all cells survived. Good agreement was obtained between calculated and experimental data.

In the next step we experimentally evaluated effectiveness of new system and electric field protocols to improve *in-vitro* gene electrotransfer on Chinese Hamster Ovary cells. Results show that changing the electric field direction between electrical pulses increases the fraction of transfected cells (Fig. 4), with no statistically significant influence on fluorescence intensity of transfected cells (Fig. 5) and cell survival. Therefore, the results obtained in our research support previous observations that changing the electric field direction between electrical pulses improves gene electrotransfer with no significant effect on cell survival [20,32].

Plated cells are of various shapes and often elongated. Because of this, their orientation in electric field is impor-

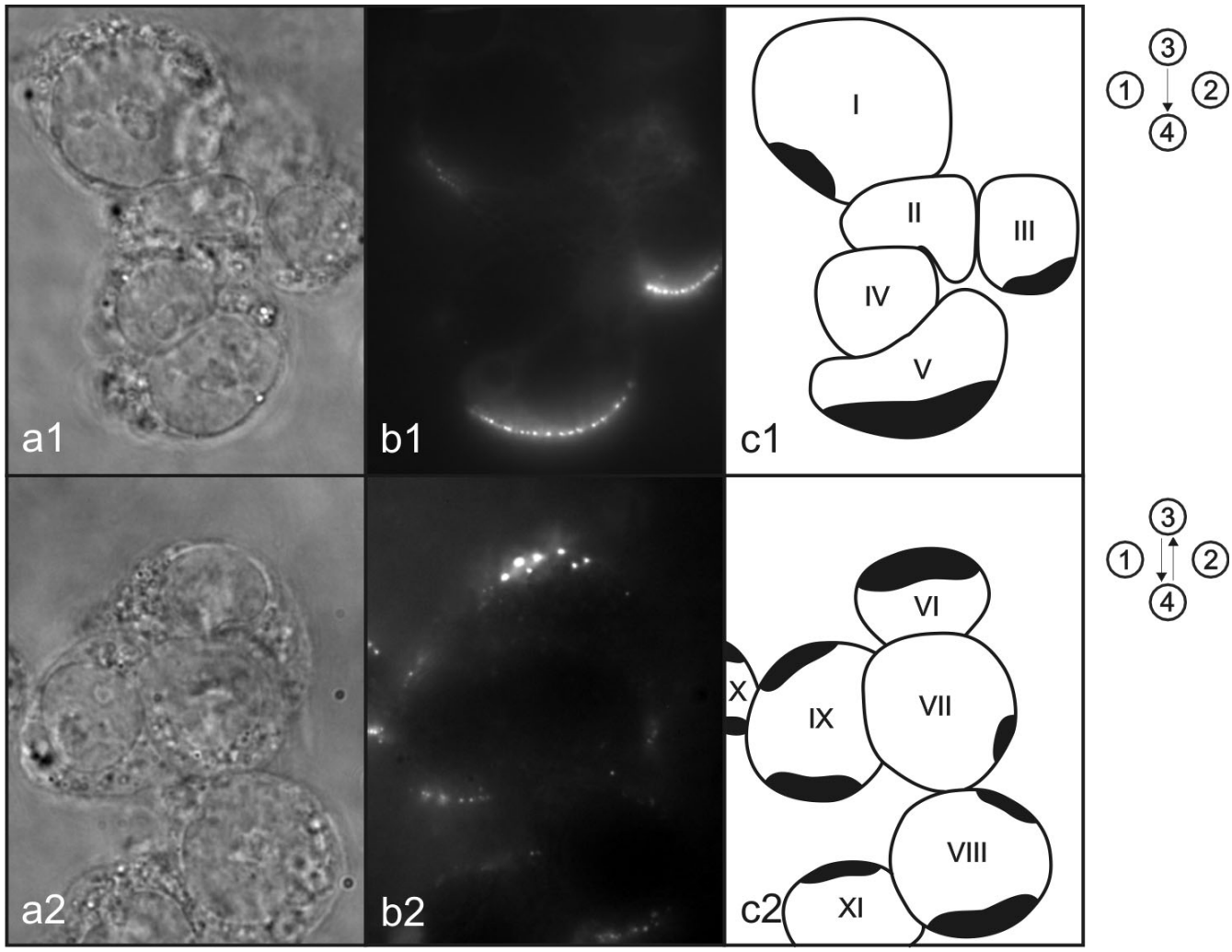

Figure 8
Shading effect. Photos of phase contrast (a) and fluorescence (b) images were taken under inverted fluorescence microscope. Symbolic picture (c) was made for better representation of the observed shading effect. Drawn shapes represent cells and black areas represent regions of permeabilized membrane where DNA interacts with cell membrane. Symbols on the right represent electric field protocol used.

tant [23]. If they are elongated in the direction of electric field, they have higher probability to be permeabilized and that DNA interacts with this part of the membrane (Fig. 6a, b). If we change the direction of electric field during electric pulse delivery, cumulatively more cells are elongated in the direction of electric field and therefore DNA interacts with the membranes of more cells (Fig. 6c, d). Consequently there are more transfected cells (Fig. 4).

We observed another effect during our research i.e. a shading effect, which is also important for efficient gene electrotransfer of plated cells. Shading effect is observed during gene electrotransfer when cells are in clusters, where only cells facing negative electro-potential in clusters become transfected and other ones which are hidden behind these cells do not become transfected (Fig. 8c1). And if we change electric field direction between electrical pulses, cumulatively more cells face negative electro-potential (in case of inhomogeneous electric field distribution the direction of electric field is not always the same as direction towards electrodes, therefore the term facing electro-potential is used instead of the term facing electrodes) in cluster and more cells in cluster become transfected (Fig. 8c2). Therefore changing electric field direction between electrical pulses improves fraction of transfected cells in clusters, which is another reason why it is advisable to use orthogonal both polarities (OBP) electric field protocol instead of single polarity (SP) electric field protocol.

For each electric field protocol we used the same cumulative number of pulses (Fig. 2). Thus, if we used more directions of electric field during electric pulse delivery, fewer pulses were delivered in each direction. Therefore from each direction a lower "degree" of membrane permeabilization is obtained and less DNA interacts with the cell membrane. But overall, our results indicate that fluorescence intensity of transfected cells is not affected when using our protocols.

Cell survival was also not significantly affected by electric pulse application, which is important for gene transfection as damaged cells difficultly express genes [33]. This means that our protocol is also appropriate for cells which are valuable, such as human primary cells, which are taken directly from a donor or patient [34].

On the basis of our results we can conclude that although homogeneity of electric field distribution between the newly designed electrodes presented in this paper is not as good as between two parallel plate electrodes, the results of gene electrotransfer are improved. By automatic change of electric field direction, electric pulses can be delivered at precise frequencies, which enables new experiments for better understanding of DNA interaction with cell membrane. In addition, the new system can be used wherever manual rotating is not possible, like in case of multiple electrodes, when they are used with different electric field direction between electrical pulses. Such an embedded electrode commutator is being built in the Cliniporator device [35]. In conclusion, the main advantage of the new system and electric field protocol is that it can be used in *in-vitro* gene electrotransfer to improve fraction of transfected cells without affecting fluorescence intensity of transfected cells and cell survival by using automatic orthogonal both polarities electric field protocol.

Acknowledgements

The authors want to thank French-Slovenian Scientific Cooperation (PROTEUS and PICS Programme), Slovenian Research Agency (ARRS), Paul Sabatier University in Toulouse and French Association against Myopathies (AFM) for supporting this study.

References

1. Murphy DB, Epstein SL: **Guidance for industry: guidance for human somatic cell therapy and gene therapy.** CBER FDA, Rockville; 1998.
2. Cavazzana-Calvo M, Thrasher A, Mavilio F: **The future of gene therapy.** *Nature* 2004, **427:**779-781.
3. Lehrman S: **Virus treatment questioned after gene therapy death.** *Nature* 1999, **401:**517-518.
4. Williams DA, Baum C: **Gene therapy – new challenges ahead.** *Science* 2003, **302:**400-401.
5. Hacein-Bey-Abina S, Von Kalle C, Schmidt M, McCormack MP, Wulffrat N, Leboulch P, Lim A, Osborne CS, Pawliuk R, Morillon E, Sorensen R, Forster A, Fraser P, Cohen JI, de Saint Basile G, Alexander I, Wintergerst U, Frebourg T, Aurias A, Stoppa-Lyonnet D, Romana S, Radford-Weiss I, Gross F, Valensi F, Delabesse E, Macintyre E, Sigaux F, Soulier J, Leiva LE, Wissler M, Prinz C, Rabbitts TH, Le Deist F, Fischer A, Cavazzana-Calvo M: **LMO2-associated clonal T cell proliferation in two patients after gene therapy for SCID-X1.** *Science* 2003, **302:**415-419.
6. Davé UP, Jenkins NA, Copeland NG: **Gene therapy insertional mutagenesis insights.** *Science* 2004, **303:**333.
7. Ferber D: **Gene therapy: safer and virus-free?** *Science* 2001, **294:**1638-1642.
8. Herweijer H, Wolff JA: **Progress and prospects: naked DNA gene transfer and therapy.** *Gene Ther* 2003, **10:**453-458.
9. Prud'homme GJ, Glinka Y, Khan AS, Draghia-Akli R: **Electroporation-enhanced nonviral gene transfer for the prevention or treatment of immunological, endocrine and neoplastic diseases.** *Curr Gene Ther* 2006, **6:**243-273.
10. Neumann E, Sowers AE, Jordan CA: **Electroporation and electrofusion in cell biology.** Plenum Press, New York; 1989.
11. Mir LM: **Therapeutic perspectives of *in vivo* cell electropermeabilization.** *Bioelectrochemistry* 2000, **53:**1-10.
12. Neumann E, Schaefer-Ridder M, Wang Y, Hofschneider PH: **Gene transfer into mouse lynoma cells by electroporation in high electric fields.** *EMBO J* 1982, **7:**841-845.
13. Wolf H, Rols MP, Boldt E, Neumann E, Teissié J: **Control by pulse parameters of electric field-mediated gene transfer in mammalian cells.** *Biophys J* 1994, **66:**524-531.
14. Heller R, Jaroszeski M, Atkin A, Moradpour D, Gilbert R, Wands J, Nicolau C: ***In vivo* gene electroinjection and expression in rat liver.** *FEBS lett* 1996, **389:**225-228.
15. Neumann E, Kakorin S, Tœnsing K: **Fundamentals of electroporative delivery of drugs and genes.** *Biochem Bioenerg* 1999, **48:**3-16.
16. Gehl J: **Electroporation: theory and methods, perspectives for drug delivery, gene therapy and research.** *Acta Physiol Scand* 2003, **177:**437-447.
17. Kinosita K, Itoh H, Ishiwata S, Hirano K, Nishizaka T, Hayakawa T: **Dual-view microscopy with a single camera: real-time imaging of molecular orientations and calcium.** *J Cell Biol* 1991, **115:**67-73.
18. Gabriel B, Teissié J: **Time courses of mammalian cell electropermeabilization observed by millisecond imaging of membrane property changes during the pulse.** *Biophys J* 1999, **76:**2158-2165.
19. Golzio M, Teissie J, Rols MP: **Direct visualization at the single-cell level of electrically mediated gene delivery.** *Proc Natl Acad Sci USA* 2002, **99:**1292-1297.
20. Faurie C, Phez E, Golzio M, Vossen C, Lesbordes JC, Delteil C, Teissié J, Rols MP: **Effect of electric field vectoriality on electrically mediated gene delivery in mammalian cells.** *Biochim Biophys Acta* 2004, **1665:**92-100.
21. Serša G, Жемажар M, Šemrov D, Miklavčič D: **Changing electrode orientation improves the efficacy of electrochemotherapy of solid tumors in mice.** *Bioelectrochem Bioenerg* 1996, **39:**31-66.
22. Kotnik T, Miklavčič D: **Analytical description of transmembrane voltage induced by electric fields on spheroidal cells.** *Biophys J* 2000, **79:**670-679.
23. Valič B, Golzio M, Pavlin M, Schatz A, Faurie C, Gabrile B, Teisssié J, Rols MP, Miklavčič D: **Effect of electric field induced transmembrane potential on spheroidal cells: theory and experiment.** *Eur Biophys J* 2003, **32:**519-528.
24. Phez E, Faurie C, Golzio M, Teisssié J, Rols MP: **New insights in the visualization of membrane permeabilization and DNA/membrane interaction of cells submitted to electric pulses.** *Biochim Biophys Acta* 2005, **1724:**248-254.
25. Gilbert RA, Jaroszeski MJ, Heller R: **Novel electrode designs for electrochemotherapy.** *Biochim Biophys Acta* 1997, **1334:**9-14.
26. Kotnik T, Pucihar G, Reberšek M, Mir LM, Miklavčič D: **Role of pulse shape in cell membrane electropermeabilization.** *Biochim Biophys Acta* 2003, **1614:**193-200.
27. Pavlin M, Kandušer M, Reberšek M, Pucihar G, Hart FX, Magjarević R, Miklavčič D: **Effect of cell electroporation on the conductivity of a cell suspension.** *Biophys J* 2005, **88:**4378-4390.
28. Šemrov D, Miklavčič D: **Numerical modeling for *in vivo* electroporation.** *Meth Mol Med* 2000, **37:**63-81.
29. Šemrov D, Miklavčič D: **Calculation of the electrical parameters in electrochemotherapy of solid tumours in mice.** *Comput Bio Med* 1998, **28:**439-448.
30. Rye HS, Yue S, Wemmer DE, Quesada MA, Haugland RP, Mathies RA, Glazer AN: **Stable fluorescent complexes of double-stranded**

DNA with bis-intercalating asymmetric cyanine dyes: properties and applications. *Nucleic Acids Res* 1992, **20:**1803-1812.
31. Miklavčič D, Beravs K, Šemrov D, Žemažar M, Demšar F, Serša G: **The importance of electric field distribution for effective *in vivo* electroporation of tissues.** *Biophys J* 1998, **74:**2152-2158.
32. Tekle E, Astumian RD, Chock PB: **Electroporation by using bipolar oscillating electric field: an improved method for DNA transfection of NIH 3Ts cells.** *Proc Natl Acad Sci USA* 1991, **88:**4230-4234.
33. Rols MP, Delteil C, Golzio M, Teisssié J: **Control by ATP and ADP of voltage-induced mammalian-cell-membrane permeabilization, gene transfer and resulting expression.** *Eur J Biochem* 1998, **254:**382-388.
34. Grossman M, Raper SE, Kozarsky K, Stein EA, Engelhardt JF, Muller D, Lupien PJ, Wilson JM: **Successful *ex vivo* gene therapy directed to liver in a patient with familial hypercholesterolaemia.** *Nat Genet* 1994, **6:**335-341.
35. Marty M, Serša G, Garbay JR, Gehl J, Collins CG, Snoj M, Billard V, Geertsen PF, Larkin JO, Miklavčič D, Pavlović I, Paulin-Košir SM, Žemažar M, Morsli N, Soden DM, Rudolf Z, Robert C, O'Sullivand GC, Mir LM: **Electrochemotherapy – An easy, highly effective and safe treatment of cutaneous and subcutaneous metastases: Results of ESOPE (European Standard Operating Procedures of Electrochemotherapy) study.** *EJC supplements* 2006, **4:**3-13.

Bioelectrochemistry xxx (2008) xxx-xxx

Contents lists available at ScienceDirect

Bioelectrochemistry

journal homepage: www.elsevier.com/locate/bioelechem

Electrode commutation sequence for honeycomb arrangement of electrodes in electrochemotherapy and corresponding electric field distribution

Matej Reberšek [a], Selma Čorović [a], Gregor Serša [b], Damijan Miklavčič [a,*]

[a] University of Ljubljana, Faculty of Electrical Engineering, Tržaška 25, SI-1000 Ljubljana, Slovenia
[b] Institute of Oncology, Department of Experimental Oncology, Zaloška 2, SI-1000 Ljubljana, Slovenia

ARTICLE INFO

Article history:
Received 30 April 2007
Received in revised form 28 February 2008
Accepted 1 March 2008
Available online xxxx

Keywords:
Electrode commutation sequence
Electroporation
Finite-elements method
Multiple electrodes

ABSTRACT

Electrochemotherapy is a treatment based on combination of chemotherapeutic drug and electroporation. It is used in clinics for treatment of solid tumours. For electrochemotherapy of larger tumours multiple needle electrodes were already suggested. We developed and tested electrode commutation circuit, which controls up to 19 electrodes independently. Each electrode can be in one of three possible states: on positive or negative potential or in the state of high impedance. In addition, we tested a pulse sequence using seven electrodes for which we also calculated electric field distribution in tumour tissue by means of finite-elements method. Electrochemotherapy, performed by multiple needle electrodes and tested pulse sequence on large subcutaneous murine tumour model resulted in tumour growth delay and 57% complete responses, thus demonstrating that the tested electrode commutation sequence is efficient.

1. Introduction

Electroporation is a phenomenon that occurs in cell membranes when cells are exposed to sufficiently high electric field [1–4]. Molecules, such as some drugs or nucleic acids, which otherwise are unable to cross cell membrane may then enter cells. This phenomenon is used in combination with some chemotherapeutic drugs e.g. bleomycin and cisplatin for tumour treatment, which is known as electrochemotherapy [5–7]. It is used in clinics for transfer of chemotherapeutic drugs in tumour cells by means of short high voltage electric pulses applied to the tumour [8,9].

Generators of electrical pulses for electroporation are named electroporators. For small tumours electric pulses are delivered to the tissue usually via two metal (plate) electrodes [10,11]. Electrochemotherapy of small tumours is already well investigated and good results are obtained with a single pair of electrodes. To achieve good electrochemotherapy the entire volume of the tumour needs to be effectively permeabilized [12]. On larger tumours pair of electrodes should be repositioned or higher voltage should be used [13]. However, repositioning of electrodes is not practical since positions and amplitudes should be pre-calculated to achieve effective permeabilization over the whole tumour. Moreover, electroporators certified for clinical use do not generate electric pulses with amplitudes over a few kV [14]. Therefore, multiple needle electrodes were suggested for effective tissue permeabilization in electrochemotherapy, i.e. to cover the whole tumour with sufficiently high electric field. Such electrodes allow for treatment of larger tumours and at the same time using lower pulse voltages [15,16].

Electronic circuits which commutate electric pulses between the electrodes are named electrode commutation circuits. Honeycomb and square arrangements of electrodes were mainly suggested proposed as multiple needle arrangements, which theoretically enable the use of infinite arrays of needle electrodes with finite electrode commutation circuit [17]. Therefore the design of electrode commutation circuit does not depend on the number of electrodes but only on the maximum voltage applied and current to be delivered through the electrodes.

The aim of our study was to develop electrode commutation circuit and test its efficiency *in vivo* by performing electrochemotherapy with multiple needle electrodes on larger tumours, which with a single pair of electrodes cannot be achieved. For this we developed an electrode commutation circuit, which commutates the usual electroporation single output signal from an electroporator to multiple electrodes. We used seven-needle electrodes, for which we suggested and tested an effective electrode commutation sequence for tissue electroporation. We also calculated the corresponding electric field distribution in tumour tissue by means of finite elements method (FEM) in 3D model taking into account the increase of tissue conductivity due to electroporation in order to demonstrate also theoretically that the entire tumour volume is exposed to sufficiently high electric field leading to tissue permeabilization and efficient electrochemotherapy.

* Corresponding author. Tel.: +386 1 4768 456; fax: +386 1 4264 658.
E-mail address: damijan.miklavcic@fe.uni-lj.si (D. Miklavčič).

1567-5394/$ – see front matter © 2008 Elsevier B.V. All rights reserved.
doi:10.1016/j.bioelechem.2008.03.001

2. Materials and methods

2.1. Electroporator (EP-GMS 7.1) with embedded electrode commutation circuit

Both electroporator (EP-GMS 7.1) and embedded electrode commutation circuit for multiple electrodes were developed at the University of Ljubljana, Faculty of Electrical Engineering. The EP-GMS 7.1 electroporator was already used in previously reported studies [18–20]. The main advantage of this electroporator is the ability to automatically commutate electrical pulses between electrodes with embedded electrode commutation circuit.

The user defines electrical parameters of applied electric pulse through the interface of the electroporator (EP-GMS 7.1) on a personal computer (PC). These parameters are then transferred to the executive part of the electroporator. After this transfer the electroporator is ready to generate defined electric pulses in defined sequence.

Electroporator (EP-GMS 7.1) generates square electric pulses from 80 to 530 V, duration from 10 to 1000 μs, repetition frequency from 0.1 to 5000 Hz and from 1 to 32 pulses. Particularity of this electroporator is an embedded electrode commutation circuit which consists of controlling part and executive part (Fig. 1).

The commutation control (Fig. 1) is compatible with external bus interface of microprocessor MCF5204 (FreeScale, USA) or with any other similar 16-bit bus interfaces. Computer board based on microprocessor MCF5204 is a part of EP-GMS 7.1 and it can be controlled by personal computer (PC) via serial port (RS-232). The commutation control works like parallel input–output unit (PIO), which can control up to 38 relays in the executive part of the electrode commutation circuit which corresponds to 19 electrodes. The commutation control registers the time of last command and thus estimates the position of relays. This is necessary due to relatively long switching time of relays. Commutation control functions are designed on Field Programmable Gate Array (FPGA, XCS30-VQ100, Xilinx, USA).

Each executive module (Fig. 1) consists of fourteen relays TRK1703 (Iskra, Slovenia), which with their positions define states of seven electrodes. The first half of relays defines the polarity of electrodes, while the second part defines the impedance state of the electrodes. Each of the electrodes can thus be in one of three possible states: positive, negative or in high impedance. Positive state means that electrode is connected to positive potential of electroporator, negative state means that electrode is connected to negative potential of electroporator and high impedance state means that electrode is disconnected from electroporator. This concept and design of commutating the electroporation signal allows no possibility to short-circuit electroporator.

Maximal voltage of electroporation signal which can be connected to the executive module is 1 kV. Maximal continuous current is 3 A per executive module and 2 A per electrode. Maximal pulse current of maximum duration 10 ms and more than nine times longer pause is 30 A per executive module and 10 A per electrode. Electric (galvanic) separation between the commutation control and electroporation signal is more than 4 kV.

Because of the presence of high voltage and high electric current in the executive module the distance between the contacts and the weight of the anchor in relays is very large. Therefore the switching time of such a relay is relatively long. With proper selection of relays and especially with adequate driving circuit we achieved switching time of 6 ms (Fig. 2). The relay is driven by high voltage Darlington transistors and paralleled by a zener diode. This allowed for optimization of the relay turning off time. The fastest would be without the diode but sooner or later this would result in the transistors break down. Due to ageing and variations in elements, the time reserved for switching was extended to 12 ms. Embedded electrode commutation circuit can therefore automatically commutate electrical pulses between electrodes with frequencies up to 83 Hz.

2.2. Electric field in tumour tissue during the electroporation process

A three-dimensional finite-elements model of tumour tissue (cylinder; diameter: 15 mm, length: 6 mm; Fig. 3) with inserted seven-needle electrodes (honeycomb arrangement; diameter of needles: 0.5 mm, distance between two neighbouring needles: 5.5 mm) was built according to specifications of *in vivo* electrochemotherapy experiment using software package EMAS (ANSOFT Corporation, USA). Applied voltage (±265 V) was modelled as Dirichlet's boundary condition on the surface which presents the cross-section of electrode and

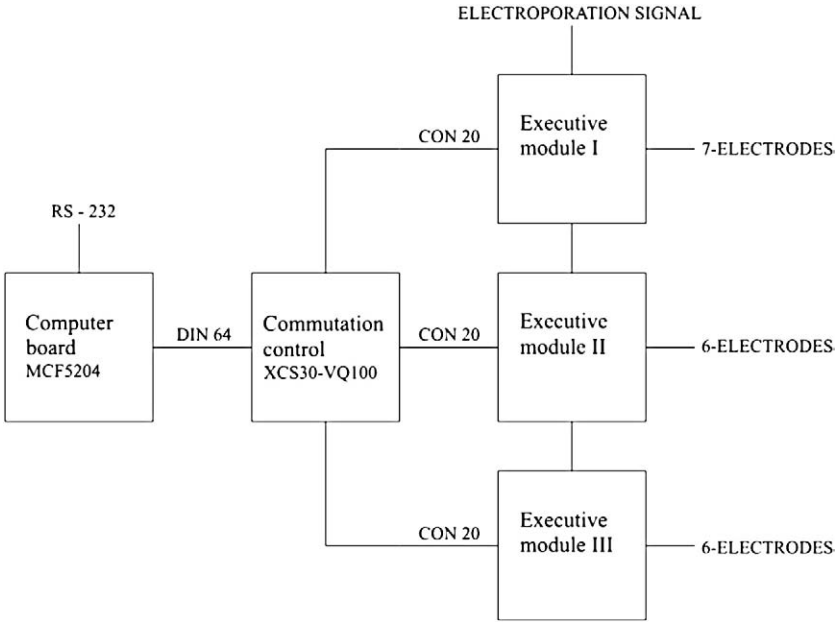

Fig. 1. Block scheme of electrode commutation circuit, which commutates electroporation single output signal from an electroporator to up to 19 independent electrodes. Electrode commutation circuit consists of controlling part (Commutation control XCS30-VQ100) and executive part (three Executive modules) and it can be controlled by personal computer (PC) over serial port (RS-232) on computer board MCF5204.

Please cite this article as: M. Reberšek, et al., Electrode commutation sequence for honeycomb arrangement of electrodes in electrochemotherapy and corresponding electric field distribution, Bioelectrochemistry (2008), doi:10.1016/j.bioelechem.2008.03.001

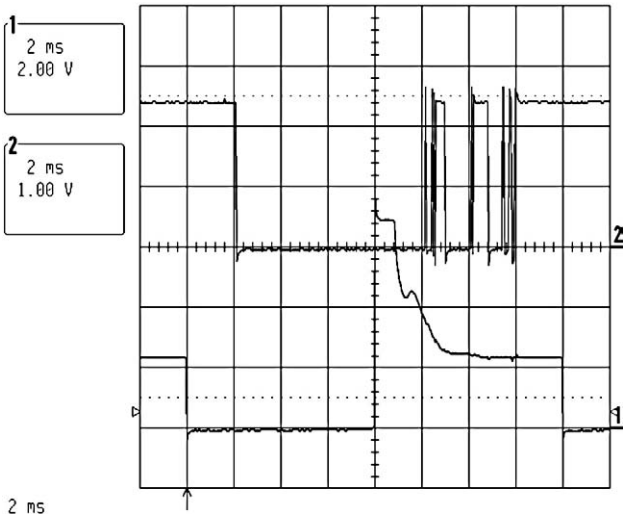

Fig. 2. Switching time of relay Iskra TRK1703. Signal 1 represents negative driving voltage for relay and signal 2 represents the commutation of relay. Signal 2 shows us that coil releases or pulls the anchor in 2 ms and that the anchor then bounces on the contact for 4 ms. Therefore the whole switching time is about 6 ms.

tumour tissue. Dirichlet's boundary condition was also set on the surface of disconnected (high impedance) electrodes to satisfy the conditions, that electrodes are a lot more conductive then tumour tissue. Electropotential of disconnected electrodes was defined as zero, because our model is symmetrical and disconnected electrodes were always in the middle between the connected electrodes. Tumour tissue was mathematically separated from surrounding area by Neuman's boundary condition:

$$J_N = 0, \tag{1}$$

where J_N is the normal electric current density [A/m^2]. The distribution of the electric field intensity in tumour tissue for given electrode geometry was calculated numerically by means of finite-elements method [21]. Tumour tissue was modelled as a quasi-stationary passive and isotropic volume conductor in the quasi-stationary electric current field. A condition in such structure is described by Laplace's equation:

$$\Delta\phi = 0, \tag{2}$$

where ϕ is the electric field potential [V].

Due to a functional dependency of tumour tissue conductivity on electric field intensity, a sequence analysis application for modelling of electrical properties changes during electroporation process was used. In each static model of the sequence analysis tissue conductivity was determined based on electric field distribution in previous model of the sequence analysis:

$$\sigma(k) = f(E(k-1)), \tag{3}$$

where σ is the tissue conductivity [S/m], E is the electric field intensity [V/m], k is the sequential number of static model in the sequence analysis and f functional dependency of tumour tissue conductivity on electric field intensity, which was obtained from previously reported studies [22,23].

In *in vivo* electrochemotherapy experiment we used an electrode commutation sequence as presented on Fig. 4. In the commutation sequence used first (Fig. 4b) all outer electrodes were activated and neighbouring needles were of the opposite polarity (±265 V), while the middle electrode was in high impedance state (0 V in the finite-elements model). After the commutation the second part (Fig. 4c) was delivered in which all outer electrodes were positive (+265 V) and the inner electrode was negative (−265 V).

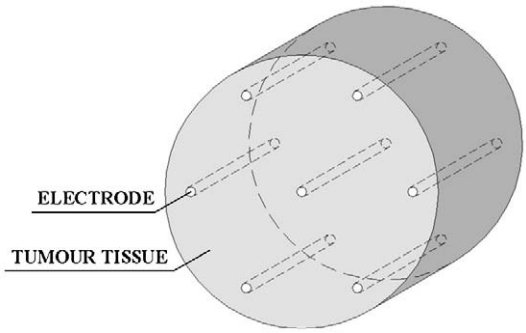

Fig. 3. A geometry of 3D-model of multiple needle electrodes inserted into the tumour tissue. Tumour tissue is in the shape of a cylinder with a diameter of 15 mm and length of 6 mm. Inserted seven-needle electrodes are in honeycomb arrangement with a diameter of 0.5 mm and the distance between two neighbouring needles is 5.5 mm.

The course of electrical conductivity changes inside the model of the tumour tissue due to electroporation is presented in Fig. 5b, with corresponding distribution of electric field intensity presented in Fig. 5a. The electric field intensity and the specific conductivity are given in *XY* cross-section (Z=2 mm plane) of the three-dimensional finite-elements model. First part of electric field intensity and electrical conductivity is presented on Fig. 5a1-3 and b1-3, while second part of electrode commutation sequence is presented on Fig. 5a4 and b4.

2.3. Electrochemotherapy

In vivo electrochemotherapy experiment was performed at the Department of Experimental Oncology, Institute of Oncology, Ljubljana, Slovenia in accordance with ethical provisions for research on animals.

In experiment subcutaneous SA-1 fibrosarcoma syngeneic to A/J mice was initiated by injection of 5×10^5 cells into the left flank of the animal. SA-1 cell suspension was cultivated in Eagle Minimal Essential Media with 10% of Foetal Calf Serum (MEM, FCS; Sigma, ZDA). Ten days after subcutaneous injection of cells, the tumours were large enough (volume≈300 mm^3, diameter≈12 mm) for electroporation with multiple needle electrodes.

During the electrochemotherapy animals were anaesthetized with ketamin and rompun (2 μl of ketamin+8 μl of 0.9% physiological solution and 0.5 μl of rompun+9.5 μl of 0.9% physiological solution per gram of mouse). Animals were divided into four experimental groups: control, chemotherapy (CT), electric pulses (EP) and electrochemotherapy (ECT). In each experimental group 7 mice were treated independently. In all experimental groups multiple needle electrodes were inserted into the tumour. Animals in CT and ECT experimental

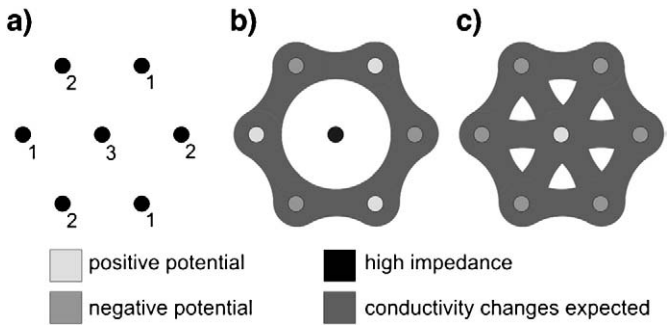

Fig. 4. Electrode commutation sequence of two parts for honeycomb arrangement of electrodes. Position of the electrodes and its numeration (a). States of the electrodes in the first part of electrode commutation sequence (b). States of the electrodes in the second part of electrode commutation sequence (c).

Please cite this article as: M. Reberšek, et al., Electrode commutation sequence for honeycomb arrangement of electrodes in electrochemotherapy and corresponding electric field distribution, Bioelectrochemistry (2008), doi:10.1016/j.bioelechem.2008.03.001

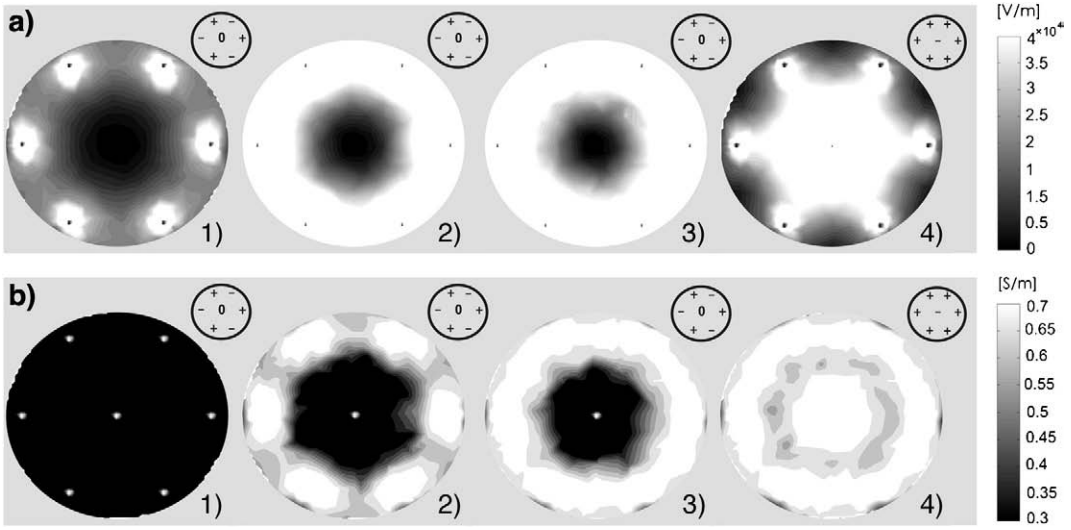

Fig. 5. Electric field intensity [V/m] (a) and electrical conductivity [S/m] (b): the sequence analysis was not applied (1), the first static model in the first part (2), the final static model in the first part (3) and the final static model in the second part of the electrode commutation sequence (4).

groups were injected intravenously with 100 μg of bleomycin. Tumours in experimental groups EP and ECT were exposed to electric pulses (2 intervals×8 square pulses, duration 100 μs, amplitude 530 V and pulse repetition frequency of 100 Hz). Pulses in the ECT group were delivered 3–4 min after the bleomycin injection.

Each day after the treatment on day 0 cranial/caudal, dorsal/ventral and medial/lateral diameters of the tumours were measured. Volumes of tumours were then modelled and calculated as spheroids. Results are given in form of scatter graphs (SigmaPlot 9.0, Systat, USA), where each point represents the mean volume of tumours in each experimental group and the error bars indicate the standard error of the mean (Fig. 6).

3. Results

Electric field intensity (Fig. 5a) in tumour tissue and consecutive tumour tissue conductivity changes (Fig. 5b) were calculated for suggested electrode commutation sequence (Fig. 4) by means of finite-elements method. In Fig. 5a1 and b1 sequence analysis was not yet applied. Fig. 5a2 and b2 represents first static model of sequence analysis. And Fig. 5a3,4 and b3,4 represents final static model of sequence analysis. In the first part of electrode commutation sequence (all outer electrodes are activated and neighbouring needles are of the opposite polarity, while the middle electrode is in high impedance state; Fig. 4b) when sequence analysis was not yet applied electric field intensity was strong only around outer electrodes (Fig. 5a1). When sequence analysis was applied electric field intensity (Fig. 5a2) and tumour tissue conductivity (Fig. 5b2) quickly iterated to its final value, which was obtained with insignificant numerical error in only four steps (Fig. 5a3 and b3). Strong electric field intensity around outer electrodes distributed around all outer part of tumour tissue (Fig. 5a3). We can see that after the first part of electrode commutation sequence all outer part of tumour tissue changed its conductivity which can also be considered as it was electroporated while the tumour tissue around the middle electrode remained unchanged i.e. not porated (Fig. 5b3). In the second part of electrode commutation sequence (all outer electrodes are positive and the inner electrode is negative; Fig. 4c) electric field intensity was particularly strong around inner electrode (Fig. 5a4) also because outer tumour tissue was already electroporated.

After completed electrode commutation sequence tumour tissue was thus well electroporated (Fig. 5b4), which was demonstrated also by electrochemotherapy effectiveness (Fig. 6). The suggested electrode

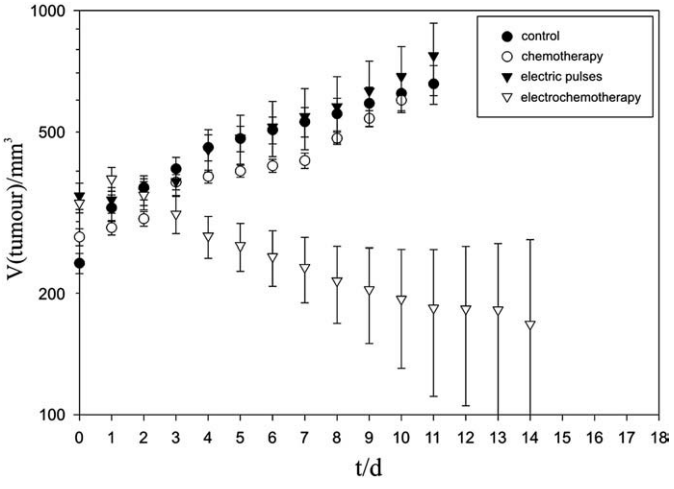

Fig. 6. Tumour growth after electrochemotherapy (ECT) on day 0 and three standard control groups for ECT: control, chemotherapy (CT) and electric pulses (EP). Each symbol represents an average tumour volume and standard error in specific experimental group.

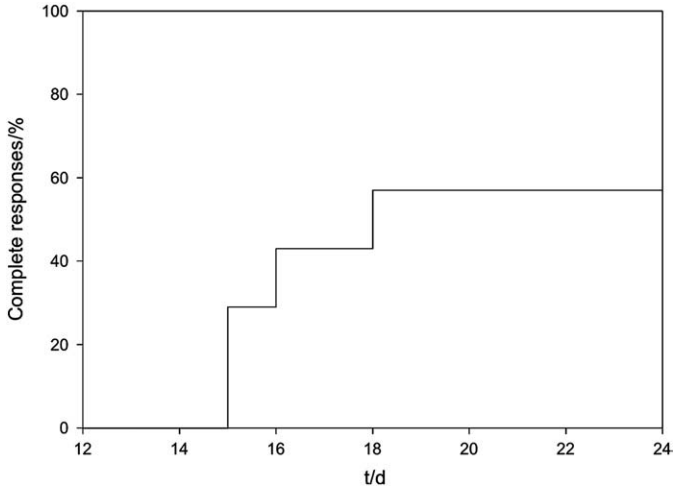

Fig. 7. Complete responses of tumour treatment on A/J mice after electrochemotherapy (ECT) on day 0. Tumours were observed for 3 months after day 0.

Please cite this article as: M. Reberšek, et al., Electrode commutation sequence for honeycomb arrangement of electrodes in electrochemotherapy and corresponding electric field distribution, Bioelectrochemistry (2008), doi:10.1016/j.bioelechem.2008.03.001

commutation sequence for honeycomb arrangement of seven-needle electrodes was evaluated in *in vivo* electrochemotherapy (ECT) experiment on larger tumours. Three standard experimental groups for evaluating ECT were used: control, chemotherapy (CT) and electric pulses (EP). Tumours in these experimental groups were not retarded in growth and animals were sacrificed after 10 days due to large tumours. In ECT group where tumours were subjected to the electrochemotherapy on day 0, tumours were however significantly reduced in volume and delayed in growth. In addition, 57% (4/7) complete responses were obtained (Fig. 7).

4. Discussion and conclusion

The aim of our study was to develop and test an effective *in vivo* electrochemotherapy on larger tumours by means of multiple needle electrodes. We thus developed and tested an electrode commutation circuit, which commutates the usual single output electroporation signal between the seven-needle electrodes used in our study. We suggested and tested experimentally by performing electrochemotherapy an effective electrode commutation sequence for tissue electroporation. Results of electrochemotherapy show a significant reduction in tumour volume, delay in growth and 57% complete responses (Fig. 6 and 7). We also calculated corresponding electric field distribution in tumour tissue taking into account an increase of tissue conductivity due to electroporation. Results of calculations show that large volume of tumour tissue is successfully electroporated by using suggested electrode commutation sequence (Fig. 5b4).

Electroporation is a dynamic process, meaning that tissue properties are changing during the constant voltage pulse from 0.3 to 0.7 S/m [22,23]. Electric field intensity below the reversible threshold value does not permeabilize the cell membranes and therefore no changes in conductivity are expected. When the electric field intensity exceeds reversible threshold cell membrane is permeabilized and tissue conductivity increases. The membrane permeabilization is reversible for electric field intensities below irreversible threshold.

The main purpose of the modelling was to foresee electroporated tissue in treated tumours. We thus had to take into account the influence of electric field intensity on tumour tissue conductivity and that changes in tumour tissue conductivity retroact on electric field distribution. Therefore sequence analysis was used to take into account such retroactivity. Results obtained with this application describe a sequence of static models, where each of them describes the process at one discrete interval. Each discrete interval relates to a real yet undetermined time interval. If we compare first (Fig. 5b2) and the last (Fig. 5b3) result of sequence analysis iteration we can see such retroactivity in results of tumour tissue conductivity. These results demonstrate that larger volume of electroporated tumour tissue is expected if sequence analysis is applied. Such expectations are in agreement with electrochemotherapy results (Figs. 6 and 7).

In *in vivo* electrochemotherapy experiment multiple needle electrodes in honeycomb arrangement were used, because such arrangement of electrodes is preferable in electrochemotherapy as better coverage of tumour tissue with electric field distribution can be achieved with single amplitude of electric pulses. For such electrodes an effective and short pulse electrode commutation sequence for electroporation is required. In our study we used a combination of two parts, which are presented on Fig. 4. Such sequence of voltage pulses application is quick, because it is delivered in only two parts and therefore suitable for clinical use where patients are subjected to muscle contraction and painful sensations. It is also effective as the conductivity changes expected due to tissue permeabilization are favouring electric field distribution through all the area between the electrodes.

Embedded electrode commutator, which was developed and used in our study, has been proven to be effective and was therefore built in the Cliniporator device [24]. Moreover, such electrode commutator is relatively easy to construct due to simple design and can be used for any other single output electroporator. On the basis of our experimental and numerical results we can conclude that suggested electrode commutation sequence for honeycomb arrangement of electrodes can be efficiently used in electrochemotherapy. Given output amplitude allows for treatment of larger tumours using multiple needle electrodes without repositioning of electrodes.

Acknowledgments

This research was in part supported by IGEA S.r.l., Carpi (MO) Italy and by the Ministry of Higher Education, Science and Technology of the Republic of Slovenia. Authors thank also Alenka grošel and Simona Kranjc (both Institute of Oncology, Ljubljana, Slovenia) for their contribution at electrochemotherapy experiment. The seven-needle electrodes were kindly provided to us by Dr. Lluis M. Mir, IGR and CNRS, Villejuif, France.

Appendix A. Supplementary data

Supplementary data associated with this article can be found, in the online version, at doi:10.1016/j.bioelechem.2008.03.001.

References

[1] E. Neumann, M. Schaefer-Ridder, Y. Wang, P.H. Hofschneider, Gene transfer into mouse lynoma cells by electroporation in high electric fields, EMBO J. 7 (1982) 841–845.
[2] E. Neumann, S. Kakorin, K. Toensing, Fundamentals of electroporative delivery of drugs and genes, Bioelectrochem. Bioenerg. 48 (1999) 3–16.
[3] L.M. Mir, Therapeutic perspectives of *in vivo* cell electropermeabilization, Bioelectrochemistry 53 (2001) 1–10.
[4] J. Teissie, M. Golzio, M.P. Rols, Mechanisms of cell membrane electropermeabilization: a minireview of our present (lack of?) knowledge, BBA — General Subjects Special Issue: Biophysics Complex Systems, vol. 1724, 2005, pp. 270–280.
[5] L.M. Mir, S. Orlowski, Mechanisms of electrochemotherapy, Adv. Drug Deliv. Rev. 35 (1999) 107–118.
[6] J. Gehl, Electroporation: theory and methods, perspectives for drug delivery, gene therapy and research, Acta Physiol. Scand. 177 (2003) 437–447.
[7] G. Sersa, The state-of-the-art of electrochemotherapy before the ESOPE study; advantages and clinical uses, Eur. J. Cancer Suppl. 4 (2006) 52–59.
[8] R. Heller, R. Gilbert, M.J. Jaroszeski, Clinical applications of electrochemotherapy, Adv. Drug Deliv. Rev. 35 (1999) 119–129.
[9] L.M. Mir, J. Gehl, G. Sersa, C.G. Collins, J.R. Garbay, V. Billard, P.F. Geertsen, Z. Rudolf, G.C. O'Sullivan, M. Marty, Standard operating procedures of the electrochemotherapy: Instructions for the use of bleomycin or cisplatin administered either systemically or locally and electric pulses delivered by the Cliniporator™ by means of invasive or non-invasive electrodes, Eur. J. Cancer Suppl. 4 (2006) 14–25.
[10] L.M. Mir, L.F. Glass, G. Sersa, J. Teissie, C. Domenge, D. Miklavcic, M.J. Jaroszeski, S. Orlowski, D.S. Reintgen, Z. Rudolf, M. Belehradek, R. Gilbert, M.P. Rols, J. Jr Belehradek, J.M. Bachaud, R. DeConti, B. Stabuc, M. Cemazar, P. Coninx, R. Heller, Effective treatment of cutaneous and subcutaneous malignant tumours by electrochemotherapy, Br. J. Cancer 77 (1998) 2336–2342.
[11] J. Gehl, L.M. Mir, Determination of optimal parameters for *in vivo* gene transfer by electroporation, using a rapid *in vivo* test for cell permeabilization, Biochem. Biophys. Res. Commun. 261 (1999) 337–380.
[12] D. Miklavcic, S. Corovic, G. Pucihar, N. Pavselj, Importance of tumour coverage by sufficiently high local electric field for effective electrochemotherapy, Eur. J. Cancer Suppl. 4 (2006) 45–51.
[13] M. Cemazar, D. Miklavcic, L. Vodovnik, T. Jarm, Z. Rudolf, R. Stabuc, T. Cufer, G. Sersa, Improved therapeutic effect of electrochemotherapy with cisplatin by intratumoral drug administration and changing of electrode orientation for electropermeabilization on EAT tumor model in mice, Radiol. Oncol. 29 (1995) 121–127.
[14] M. Puc, S. Corovic, K. Flisar, M. Petkovsek, J. Nastran, D. Miklavcic, Techniques of signal generation required for electropermeabilization. Survey of electropermeabilization devices, Bioelectrochemistry 64 (2004) 113–124.
[15] R.A. Gilbert, M.J. Jaroszeski, R. Heller, Novel electrode designs for electrochemotherapy, Biochim. Biophys. Acta 1334 (1997) 9–14.
[16] L.H. Ramirez, S. Orlowski, D. An, G. Bindoula, R. Dzodic, P. Ardouin, C. Bognel, J. Belehradek, J.N. Munck, L.M. Mir, Electrochemotherapy on liver tumours in rabbits, Br. J. Cancer 77 (1998) 2104–2111.
[17] G.A. Hoffman, Methods in molecular medicine, Ch. Instrumentation and electrodes for *in vivo* electroporation, Humana Press, New York, 2000, pp. 37–61.
[18] T. Kotnik, G. Pucihar, M. Rebersek, L.M. Mir, D. Miklavcic, Role of pulse shape in cell membrane electropermeabilization, Biochim. Biophys. Acta 1614 (2003) 193–200.
[19] M. Pavlin, M. Kanduser, M. Rebersek, G. Pucihar, F.X. Hart, R. Magjarevic, D. Miklavcic, Effect of cell electroporation on the conductivity of a cell suspension, Biophys. J. 88 (2005) 4378–4390.
[20] M. Rebersek, C. Faurie, M. Kanduser, S. Corovic, J. Teissie, M.P. Rols, D. Miklavcic, Electroporator with automatic change of electric field direction improves gene electrotransfer in vitro, Biomed. Eng. Online 6 (2007) 1–11.

Please cite this article as: M. Reberšek, et al., Electrode commutation sequence for honeycomb arrangement of electrodes in electrochemotherapy and corresponding electric field distribution, Bioelectrochemistry (2008), doi:10.1016/j.bioelechem.2008.03.001

[21] D. Semrov, D. Miklavcic, Numerical modeling for *in vivo* electroporation, Meth. Mol. Med. 37 (2000) 63–81.
[22] D. Sel, D. Cukjati, D. Batiuskaite, T. Slivnik, L.M. Mir, D. Miklavcic, Sequential finite element model of tissue electropermeabilization, IEEE Trans. Biomed. Eng. 52 (2005) 816–827.
[23] N. Pavselj, Z. Bregar, D. Cukjati, D. Batiuskaite, L.M. Mir, D. Miklavcic, The course of tissue permeabilization studied on a mathematical model of a subcutaneous tumor in small animals, IEEE Trans. Biomed. Eng. 52 (2005) 1373–1381.
[24] M. Marty, G. Sersa, J.R. Garbay, J. Gehl, C.G. Collins, M. Snoj, V. Billard, P.F. Geertsen, J.O. Larkin, D. Miklavcic, I. Pavlovic, S.M. Paulin-Kosir, M. Cemazar, N. Morsli, D.M. Soden, Z. Rudolf, C. Robert, G.C. O'Sullivand, L.M. Mir, Electrochemotherapy — an easy, highly effective and safe treatment of cutaneous and subcutaneous metastases: results of ESOPE (European Standard Operating Procedures of Electrochemotherapy) study, Eur. J. Cancer Suppl 4 (2006) 3–13.

Please cite this article as: M. Reberšek, et al., Electrode commutation sequence for honeycomb arrangement of electrodes in electrochemotherapy and corresponding electric field distribution, Bioelectrochemistry (2008), doi:10.1016/j.bioelechem.2008.03.001

Bioelectrochemistry xxx (2008) xxx-xxx

Contents lists available at ScienceDirect

Bioelectrochemistry

journal homepage: www.elsevier.com/locate/bioelechem

Optimization of bulk cell electrofusion in vitro for production of human–mouse heterohybridoma cells

Katja Trontelj [a], Matej Reberšek [a], Maša Kandušer [a], Vladka Čurin Šerbec [b,c], Marjana Šprohar [b], Damijan Miklavčič [a,*]

[a] University of Ljubljana, Faculty of Electrical Engineering, Tržaska 25, SI-1000 Ljubljana, Slovenia
[b] Blood Transfusion Centre of Slovenia, Šlajmerjeva 6, SI-1000 Ljubljana, Slovenia
[c] University of Ljubljana, Faculty of Chemistry and Chemical Technology, Aškerčeva 5 SI-1000, Ljubljana, Slovenia

ARTICLE INFO

Article history:
Received 11 December 2007
Received in revised form 14 May 2008
Accepted 2 June 2008
Available online xxxx

Keywords:
Electrofusion
Electropermeabilization
Electric field direction
Heterohybridoma

ABSTRACT

Cell electrofusion is a phenomenon that occurs, when cells are in close contact and exposed to short high-voltage electric pulses. The consequence of exposure to pulses is transient and nonselective permeabilization of cell membranes. Cell electrofusion and permeabilization depend on the values of electric field parameters including amplitude, duration and number of electric pulses and direction of the electric field. In our study, we first investigated the influence of the direction of the electric field on cell fusion in two cell lines. In both cell lines, applications of pulses in two directions perpendicular to each other were the most successful. Cell electrofusion was finally used for production of human–mouse heterohybridoma cells with modified Koehler and Milstein hybridoma technology, which was not done previously. The results, obtained by cell electrofusion, are comparable to usually used polyethylene glycol mediated fusion on the same type of cells.

1. Introduction

The ability to fuse two different types of cells allows for creation of a third type of cells that are polynuclear and display hybrid characteristics of the two original types of cells. Cell fusion has been used for transfer of foreign receptors into the membrane of the living cell [1,2] and was also demonstrated as an important process in tissue regeneration in cell transplantation [3–5]. The later offers possibilities for targeted cell therapy for organ regeneration. In addition, hybrid cells can be useful especially in biotechnology for production of monoclonal antibodies [6,7] and in biomedicine for the production of hybrid cell vaccines for immunotherapy of cancer [8].

Hybridoma technology is the most often used procedure for producing monoclonal antibodies [12]. The critical step within this procedure is fusion of myeloma cells with B-lymphocytes to form hybridoma cells, which grow in culture and produce these important biological molecules. Myeloma cells are "fusion partner" cells that grow in culture and lymphocytes are the cells that produce antibodies. After fusion, cells are plated in HAT selection media to obtain only cells that are constituted from both types of cells. In some cases, where mouse or hen cells are used, fusion with polyethylene glycol [9] and electrofusion give good results [10,11], however the use of human lymphocytes is favored. The use of human lymphocytes would give us human monoclonal antibodies, which are more valuable than mouse monoclonal antibodies for use in human therapy.

Also promising are hybrid cells made of dendritic cells and autologus tumor cells. These hybrid cells could be used as a vaccine in cancer immunotherapy. Dendritic cells are most powerful antigen presenting cells that activate naive T lymphocytes to generate cytotoxic effectors (cytotoxic T lymphocytes). Hybrid autologus tumor–dendritic cells would thus express specific tumor antigens and be able to activate T cell mediated responses [8]. Due to low efficiency of fusion by means of polyethylene glycol, it is however not possible to produce hybrid cells in sufficient quantities for the therapy with this method. Hybrid cells must therefore be further grown in the culture, thus it is difficult to obtain sufficient number of cells for therapy in adequately short time.

Fusion of human cells is however most often unsuccessful. The compromise for hybridoma technology is fusing human cells or human B-lymphocytes with mouse or hen myeloma cells, respectively. The efficiency of such fusion with polyethylene glycol is however not good enough for efficient production of monoclonal antibodies. The alternative procedure for obtaining human monoclonal antibodies or hybrids of dendritic and autologus tumor cells, that can be more efficient than polyethylene glycol, is cell electrofusion. For cancer immunotherapy, investigators suggested that electrofusion is an effective method [13]; justified to be used in clinical trials besides previously used fusion by means of polyethylene glycol [14]. For production of human monoclonal antibodies from hybrids made of

* Corresponding author. Tel.: +386 1 4768456; fax: +386 1 4264658.
E-mail address: damijan.miklavcic@fe.uni-lj.si (D. Miklavčič).

1567-5394/$ – see front matter © 2008 Elsevier B.V. All rights reserved.
doi:10.1016/j.bioelechem.2008.06.003

human lymphocytes and mouse or even human fusion partner cell lines, no such comparative study of both fusion techniques (polyethylene glycol and electrofusion) has been done before.

Cell electrofusion is a simple and safe method that does not introduce any substances in the cell suspension so it can be safely used in all clinical applications, which is clearly an advantage over chemical or viral methods. Furthermore, electrofusion effectiveness can be further improved by optimizing electrical parameters that affect its efficiency. Cells fuse only when they are brought into their fusogenic state. This fusogenic state seems to correlate well with the permeabilized state of the membrane [15]. To achieve cell fusion we must have cells with permeabilized membranes in close contact. Therefore, in order to achieve the highest fusion yield, we must choose values of electrical parameters, which cause membrane permeabilization and good survival of fusion partner cells.

The most important and known electrical parameters governing membrane electropermeabilization are pulse amplitude, which enlarges permeabilized area and pulse duration and number of pulses, which enlarge the density of membrane defects [16]. Another way of enlarging the permeabilized area without reducing the survival of the cells that has not been studied until lately is changing electric pulse direction [17]; i.e. delivering electrical pulses in different directions to the cells. From the theory of electroporation [18,19] and already performed experiments [20,21] it follows that applying pulses to cells in different directions causes permeabilization of different areas of the cell membrane. Application of pulses in different directions thus increases the total permeabilized area of the membrane.

It was demonstrated that a prerequisite for cell fusion is that membranes of both cell fusion partners in contact are in their fusogenic state [22]. Contact between cells after exposing them to electric pulses in electrofusion is most often established by centrifugation of cells in suspension. Since in centrifugation contacts between cells create randomly between already electroporated cells, increased permeabilized area should increase the probability of creating adequate contact between membranes in fusogenic state of two neighboring cells.

In our study, we therefore first investigated the influence of the electric field direction on electropermeabilization and subsequent electrofusion in two cell lines (B16F1 and CHOK1, respectively). In the second part of our study, electrofusion was used for the first time for production of human–mouse heterohybridoma cells with modified Koehler and Milstein hybridoma technology [12] and compared to the most often used polyethylene glycol mediated cell fusion.

2. Materials and methods

2.1. Cells

In the first part of our work, we used two adherent cell lines. Chinese hamster ovary cells (CHOK1) were grown in HAM medium with added 10% Fetal Calf Serum (both from Sigma, USA). Mouse melanoma cells (B16F1) were grown in Eagle's Minimum Essential Medium (EMEM) with added 10% Fetal Calf Serum (both from Sigma, USA). After trypsinization, cells were centrifuged for 5 min at 1000 rpm at 4 °C and resuspended in isoosmolar low conductance (pulsing medium) to obtain 5×10^6 cells/ml. This medium with pH 7.4 consists of 250 mM sucrose, 10 mM phosphate (K_2HPO_4/KH_2PO_4) and 1 mM $MgCl_2$ as was previously described elsewhere [23].

For production of heterohybridoma in the final part of our study, we used human spleen lymphoblasts and NS1—mouse myeloma cells—as fusion partners. Lymphoblasts were isolated and frozen in liquid nitrogen. One week before the experiment, they were thawed and kept in DMEM medium with added 13% Fetal Calf Serum (both from Sigma, USA). HAT-sensitive NS1 myeloma cells were also cultured in DMEM medium with added 13% Fetal Calf Serum. The myeloma cells were used for fusion when they were in exponential growth phase.

2.2. Electropermeabilization

A 100 µl droplet of cells suspended in the pulsing medium ($\approx5\times10^5$ cells) was taken and placed between four cylinder stainless steel electrodes [17] of diameter 2 mm, which were positioned in corners of a quadrant with a distance between the opposite electrodes $d=5$ mm. The entrapped droplet wetted all four electrodes and thus formed electric contact between all four of them (Fig. 1a).

Cells were exposed to three different combinations of 6 or 10 pulses with the amplitude of 400 or 500 V. In all experiments, pulses were 100 µs long and their repetition frequency was 77 Hz. Each combination of the pulses was further used in three different pulsing sequences (Fig. 1b) which resulted in different electric field directions of the pulses (same direction, opposite directions and two directions perpendicular to each other).

After exposure of cells to electric pulses, cell suspension was transferred by micropipette from the place between the electrodes to the 24-microtiter plate holes. Propidium iodide (Sigma, USA) was used to determine the degree of permeabilization of cells [24]. This nonpermeant fluorescent dye was added to the cell suspension before electroporation in quantity that gave 0.01 mM concentration of propidium iodide in the cell suspension.

Propidium iodide enters the cells when they are permeabilized as described earlier [24] and binds on cell's DNA. When bound, its fluorescence increases 1000 times. Propidium iodide is toxic and eventually enters in nonpermeabilized cells as well so all the measurements must be finished in less than 30 min after the addition of the dye.

Permeabilization was determined as the ratio between the number of fluorescent cells and the total number of cells in the field of view. We observed cells under the inverted fluorescent microscope Axiovert 200 (Zeiss, Germany). Phase contrast and fluorescence images of the same areas were taken between 5 and 9 min after the electroporation with digital IMAGO CCD camera VISICAM 1280 (Visitron, Germany) with the resolution 1280×1024 pixels and were analyzed with Meta Morph 5.0 (Visitron, Germany). Excitation was set at 510 nm

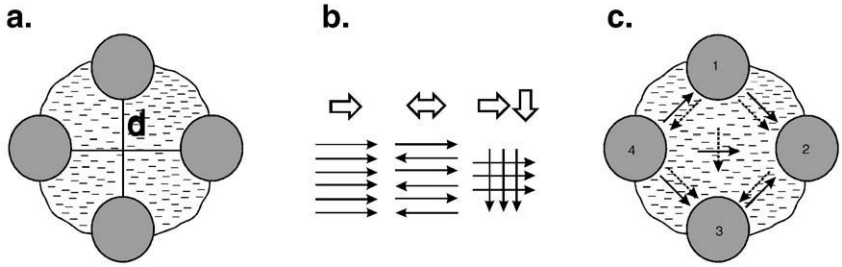

Fig. 1. a) Schematic of electrodes and the drop of cell suspension between them. b) Directions of pulsing sequences: pulses in same directions (⇨), pulses in opposite directions (⇔) and pulses in two directions perpendicular to each other (⇨ ⇩). c) At treatments with pulses in perpendicular directions, pulses were applied between opposite electrodes. Resulting electric field is depicted with dashed arrows (for pulses applied between electrodes 1 and 3) and solid arrows (for pulses applied between electrodes 2 and 4).

Please cite this article as: K. Trontelj, et al., Optimization of bulk cell electrofusion in vitro for production of human–mouse heterohybridoma cells, Bioelectrochemistry (2008), doi:10.1016/j.bioelechem.2008.06.003

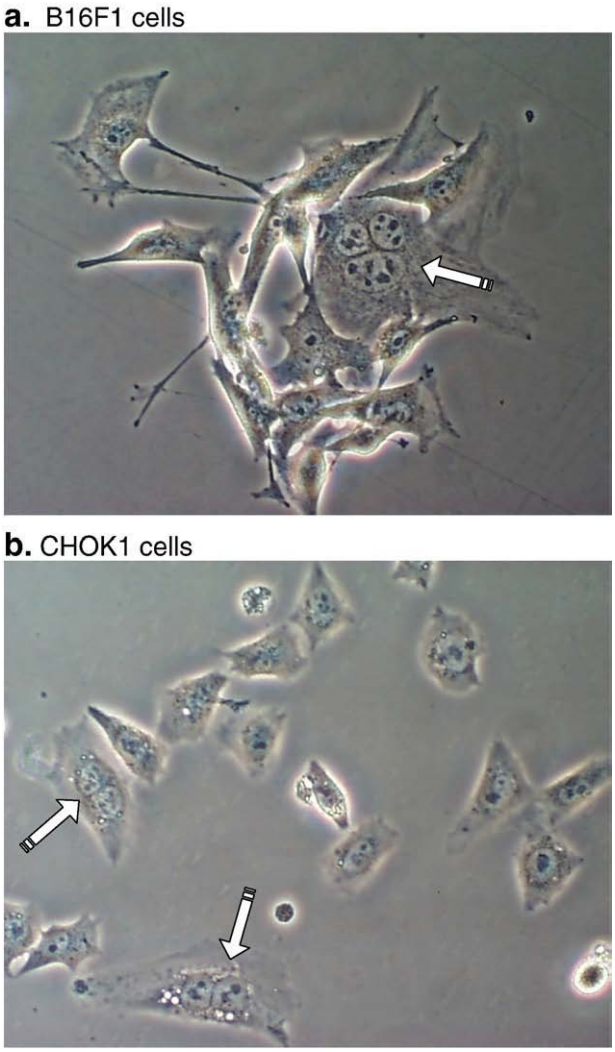

Fig. 2. Phase contrast pictures with 20× magnification a) B16F1 cells, cell marked with an arrow has three nuclei. b) CHOK1 cells: cells, marked with arrows have two nuclei.

wavelength and emission detected between 565 nm and 595 nm (Rhodamin filter BP 580/30).

2.3. Electrofusion

For electrofusion, we used the protocol where contact between cells was established by means of centrifugation as previously described [25,26]. After exposing cells to electric field (see Section 2.2), cell suspension was transferred by micropipette to a centrifuge tube and in a centrifuge in less than 20 s after the electroporation. The electroporated cells were centrifuged 5 min at 525 rpm at 4 °C. Next 10 min cells in centrifuge tubes were incubated at 37 °C and 5% CO_2. After this procedure, cells were placed in Petri dishes and incubated at 37 °C and 5% CO_2 for 24 h.

We observed adhered cells with inverted optical microscope CK40 (Olympus, Japan). Images were taken from live cells in the medium or from cells fixed first with absolute methanol and dyed with Giemsa dye. For each experiment, we counted at least 400 cells. All experiments were repeated three times.

Fusion yield FY was calculated as a number of nuclei in multinucleated cells divided by number of all nuclei.

$$\mathrm{FY} = \frac{\text{number of nuclei in multinucleated cells}}{\text{number of all nuclei}} \quad (1)$$

FY values can be from zero to one. Zero means there are no polynucleated cells, at one all cells would be polynucleated. In the next step, we considered the survival of the cells (S) in each treatment. We defined number of nuclei in control treatment (no electric pulses) as 100% (all cells survive). We determined the survival S in different treatments according to this number. Actual fusion yield FY* was then calculated considered cell survival, thus correcting FY.

$$\mathrm{FY}^* = \mathrm{FY} \cdot S[\%] \quad (2)$$

FY* values can be from zero to one, because FY is between zero and one and survival S is between zero and hundred percent, but FY* is always smaller than FY since S is smaller than 100%. Furthermore, in practical use of fused cells, we are usually not interested in their nuclei number but in the yield of functional fused cells. Namely some fused cells can contain large (>2) number of nuclei, which reduces the number of cells obtained. On the picture 2a, B16F1 cell with three nuclei can be seen and on the picture 2b, two CHOK1 cells with two nuclei can be seen.

We thus considered the average number of nuclei in the polynucleated cells for different treatments, so called index of

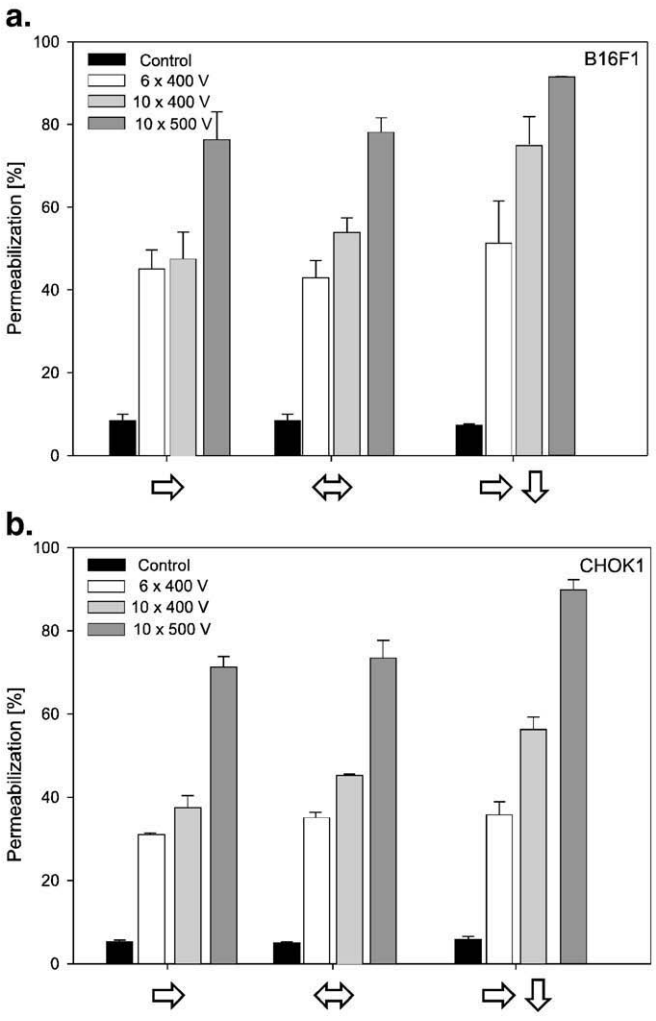

Fig. 3. Permeabilization of a) B16F1 and b) CHOK1 cells. Cells were pulsed in suspension. The length of square-wave pulses was 100 μs and repetition frequency of pulses was 77 Hz. Numbers of pulses applied were 6 and 10. The pulse amplitudes were 400 V and 500 V. Three different combinations of pulse directions were used: pulses applied in same directions (⇨), pulses applied in opposite directions (⇔) and pulses applied in two directions perpendicular to each other (⇨ ⇩). Values are given as a mean ± SD.

Please cite this article as: K. Trontelj, et al., Optimization of bulk cell electrofusion in vitro for production of human–mouse heterohybridoma cells, Bioelectrochemistry (2008), doi:10.1016/j.bioelechem.2008.06.003

polynucleation I_P. To obtain the yield of fused cells we calculated FY** as

$$FY^{**} = FY^{*} \cdot 2/I_P \quad (3)$$

I_p in ideal situation of the fusion would be two, meaning that each cell fused with one another cell resulting in all polynucleated cells having two nuclei. If the number of nuclei is higher than two, FY** is smaller than FY*. FY** is thus the most conservative estimate of fusion yield taking into account also survival and index of polynucleation (Fig. 2).

2.4. Hybridoma technology

For production of heterohybridoma, we used human spleen lymphoblasts and mouse myeloma NS1 cells. We mixed both cells in the ratio of 1:1 in the pulsing medium at the same concentration as for CHOK1 or B16F1 cells (5×10^6 cells/ml) and then fused them by using the same protocol as for CHOK1 or B16F1 cells.

After exposing cells to the electric field, as we described in Section 2.2, the cell suspension was transferred by micropipette to a centrifuge tube and into a centrifuge in less than 20 s after the electroporation. The electroporated cells were centrifuged for 5 min at 525 rpm at 4 °C. Next 10 min cells in centrifuge tubes were incubated at 37 °C and 5% CO_2.

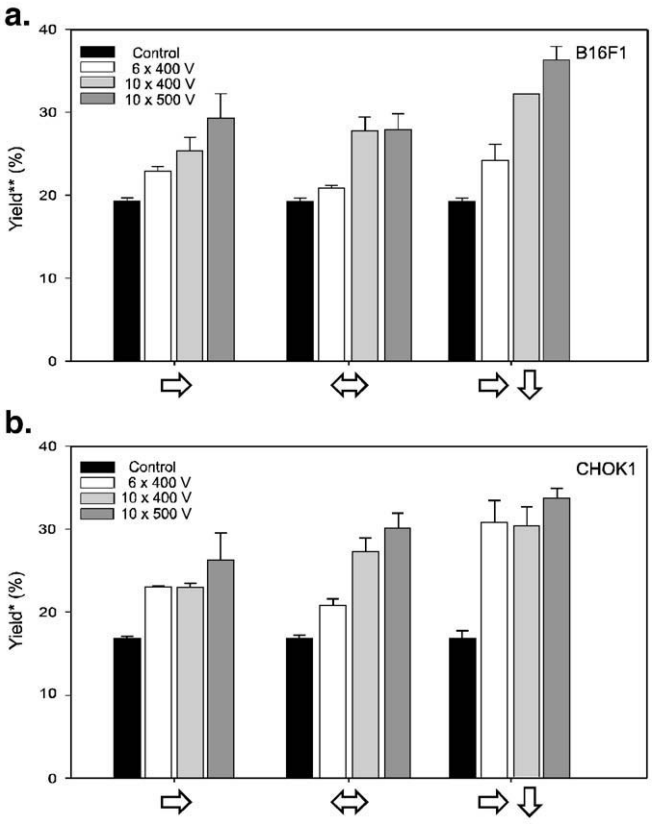

Fig. 4. Fusion yield of a) B16F1 and b) CHOK1 cells. Note: FY** is given for B16F1 and FY* is given for CHOK1. Cells were pulsed in suspension. The length of square-wave pulses was 100 μs and frequency of pulses was 77 Hz in all experiments. Numbers of pulses applied were 6 and 10. The pulse amplitudes were 400 V and 500 V. Three different combinations of pulse directions were used: pulses applied in same directions (⇨), pulses applied in opposite directions (⇔) and pulses applied in two directions perpendicular to each other (⇨ ⇩). Fusion yield presented is corrected for survival and polynucleation of cells in each treatment for B16F1 cells and for survival only for CHOK1 cells. Values are given as a mean±SD.

Table 1
Survival of B16F1 and CHOK1 cells in the experiments of cell fusion

Survival of cells [%]		6 pulses, 100 μs, 400 V	10 pulses, 100 μs, 400 V	10 pulses, 100 μs, 500 V
B16F1	⇨	101.8±0.02	103.6±0.05	104.1±0.1
	⇔	95.0±0.1	103.5±0.2	96.7±0.1
	⇨ ⇩	91.9±0.1	92.1±0.1	86.9±0.1
CHOK1	⇨	90.2±0.1	98.8±0.3	87.9±0.1
	⇔	85.1±0.2	86.5±0.2	84.1±0.2
	⇨ ⇩	82.6±0.1	80.3±0.1	77.2±0.2

Values are given as a mean±SD.

After the electrofusion procedure, cells were resuspended in DMEM medium with 13% FCS and transferred in units of 5×10^4 cells to the 96-well culture plates.

After 24 h, HAT selection medium was added and replaced with HT medium after two weeks. About 3 weeks later heterohybridomas were counted under inverted microscope and transferred into conventional 24-well culture plates for growing.

Results (permeabilization and fusion yield) are given in a form of multiple bar graphs (SigmaPlot 9.0, Systat, USA) where every point represents the mean of three independent experiments and the error bars indicate the standard deviation (Figs. 3 and 4). Statistical test, One way analysis of variance (One way ANOVA), was performed on all results (SigmaStat 3.1, Systat, USA). Bonferroni *t*-test was performed on results if there was indication of a statistically significant difference between different electric field protocols used.

3. Results

3.1. Electropermeabilization

The permeabilization of cell membrane and the percentage of permeabilized cells in suspension are increased with an increase in the pulse amplitude and with the number of pulses as expected and described before, and can be seen in Fig. 3a and b (pulses delivered in the same directions). The effect of electric field direction is however more interesting because its role in cell electrofusion has not been extensively studied yet.

Pulsing cells in two opposite directions caused almost no difference in permeabilization in comparison to pulsing cells in one direction while permeabilization is increased for the same pulse amplitude and number of pulses by using pulses in two perpendicular directions ($p<0.001$). The effects of the observed parameters were similar for both cell lines under investigation, the B16F1 and CHOK1 cells (Fig. 3a and b).

3.2. Electrofusion

The fusion yield FY was generally increased with an increase in the pulse amplitude and in the number of pulses (Fig. 4) although number of pulses and pulse amplitudes were chosen close together so that the

Table 2
Polynucleation index for fusion of B16F1 and CHOK1 cells

Polynucleation index [I_P]		6 pulses, 100 μs, 400 V	10 pulses, 100 μs, 400 V	10 pulses, 100 μs, 500 V
B16F1	⇨	2.3±0.2	2.2±0.2	2.2±0.1
	⇔	2.3±0.2	2.2±0.2	2.2±0.1
	⇨ ⇩	2.2±0.1	2.3±0.1	2.2±0.1
CHOK1	⇨	2.1±0.05	2.1±0.1	2.1±0.05
	⇔	2.1±0.1	2.0±0.1	2.1±0.02
	⇨ ⇩	2.4±0.2	2.2±0.2	2.3±0.2

Values are given as a mean±SD.

Please cite this article as: K. Trontelj, et al., Optimization of bulk cell electrofusion in vitro for production of human–mouse heterohybridoma cells, Bioelectrochemistry (2008), doi:10.1016/j.bioelechem.2008.06.003

Table 3
Results of fusion of human lymphoblasts and myeloma cells

Pulse amplitude [V]	Number of pulses	Length of pulses [μs]	Wells seeded	Wells where clones appeared	Viable hybridoma
400	6	100	27	/	/
400	10	100	27	/	/
500	10	100	70	21 [30%]	5
500	10	200	18	6 [33%]	1
500	10	500	27	2 [7%]	/

differences were small. In control samples (without electrical pulses delivered), we observed polynucleated cells that are always present in the cell culture. For CHO cells there was approximately 17% and for B16F1 cells 19% of inherently polynucleated cells.

The fusion yields shown are multiplied with the cell survival (Table 1) according to Eq. (2) in order to take into account also the cell survival. Survival of CHOK1 cells was consistently lower than the survival of B16F1 cells for about 10%.

For each pulse combination, we also evaluated index of polynucleation—i.e. the average number of nuclei in one polynucleated cell (Table 2). The level of polynucleation was between 2.0 and 2.4; it was the same in both cell lines and did not depend on different protocols used. When we took into account the level of polynucleation (Eq. (3)), most of the significant differences between treatments for CHOK1 cells were no longer present. The differences in fusion yield between treatments with different number of pulses remained noticeable also when we took into account the level of polynucleation.

3.3. Hybridoma technology

In our present work, we also used electrofusion to produce human–mouse heterohybridoma cells from human lymphocytes and mouse myeloma cell line NS1 with modified Koehler and Milstein hybridoma technology. We were able to obtain viable human–mouse heterohybridoma in amounts that are comparable to those obtained by fusing the same cells by means of polyethylene glycol (data not published).

We used the treatment procedures that worked best on B16F1 and CHOK1 cells (pulses in two directions perpendicular to each other) and also treatments with prolonged pulses (Table 3). Our results show that treatments with pulse amplitudes of 400 V are suboptimal for making lymphocytes fusogene and treatments with ten pulses 500 μs long were probably too strong for myeloma cells to survive.

4. Discussion

In our present study, we examined the effect of different electric pulse parameters on electropermeabilization and electrofusion in two cell lines. We were especially interested in the effect that the direction of the electric field might have on cell fusion. Even though we intentionally worked at suboptimal conditions in order to be able to detect expected differences with changing the direction of electric field, fusion yield obtained in our study was comparable to the fusion yield obtained by means of electrofusion by other researchers [27–29]. At optimal values of studied parameters, the values of fusion yields, after the subtraction of the polynucleated cells in control samples, are approaching 20%.

The effect of the electric field direction on fusion yield is similar as for permeabilization of cells. We did not observe the difference between pulsing cells in one direction and pulsing cells in two opposite directions. Fusion yield is however increased when pulsing cells in two perpendicular directions for the same pulse amplitude and number of pulses.

We observed consistently lower survival of CHOK1 cells than of B16F1 cells for about 10%. Since B16F1 cells are somewhat larger than CHOK1 cells, the difference in the survival is not due to the cell size effect on the sensitivity of the cells to the electric field. It was shown that B16F1 cells are less sensitive to electric field due to their biological properties [30]. The other reason is probably also the larger sensitivity of CHOK1 cells to mechanical and other manipulation.

The level of polynucleation was between 2.0 and 2.4 and did not depend on different protocols used. The level of polynucleation is however important, because obtaining cells with huge number of nuclei reduces the number of polynucleated cells and additionally large cells are less likely to survive and divide. The ideal level of polynucleation values therefore should not be much higher than 2.

The observed effects due to different parameters used, were similar for both investigated cell lines although the differences were more pronounced for the B16F1 cell line (Fig. 4). For CHOK1 cells we have shown only the FY*, because at the FY** level significant differences between different treatments were not apparent, while for the B16F1 cells the differences remained visible also when we further took into account the level of polynucleation.

The degree of permeabilization and fusion yield was higher at treatments with higher pulse amplitude and larger number of pulses. This effect of pulse amplitude and number is in agreement with Teissie and Ramos, 98 [15]. In their study, they observed a strong correlation between permeabilization and fusion.

In our study, we focused on observing differences between the treatments delivering pulses in different directions. We obtained the highest fusion yield when delivering pulses in two directions perpendicular to each other, while the effect of using pulses in two opposite directions was not significantly different when compared to delivering pulses in the same direction. That was expected and it is in agreement with the theory of electroporation [17,18] and experiments done by others [20,31].

The differences between different electric protocols used, however, are not large. The reason for that in our opinion is in the design of the electrodes. Only part of the cells in suspension drop was actually exposed to the pulses in claimed directions. This effect is most obvious when pulses are applied in two directions perpendicular to each other. Large outer part of the cell suspension is actually exposed only to the field in the same or in two opposite directions (Fig. 1c). The design of the electrodes has since been improved in order to resolve this problem [32].

In our study, we also noticed that survival for treatments, where the electric field direction was changed, was lower than in the treatments where pulses were applied in only one direction. The reason for that is probably in the fact that in the case of changing electric field more cells is in close proximity to an energized electrode and therefore a high electric field. In our design of new electrodes, we have predicted the possibility of covering the surface of the electrodes with the filler material, which would conduct the electric current in the same range as our medium and on the other hand, it would function as a mechanical barrier between the cells and the electrode surface. This barrier would exclude cells from the proximity of the electrode surface and thus reduce the number of cells being killed while applying electric field. As it was suggested already by Schmeer [33].

The advantage of our method of detection of fused cells by counting nuclei after 20 to 24 h is that we count only the cells that actually survived. This is important, because only cells that actually survive and divide are useful in obtaining hybrid cells for monoclonal antibodies or hybrid autologus tumor–dendritic cells production. On the other hand, this method has a drawback that nuclei in fused cells can also fuse [34]. Therefore, in estimation of fusion yield we depended also on cell and nuclei sizes, which are not linearly dependent on nuclei number in the cell and therefore cannot be relied on completely.

In the second part of our study, we used electrofusion technique in hybridoma technology for fusion of smaller human lymphoblasts with

Please cite this article as: K. Trontelj, et al., Optimization of bulk cell electrofusion in vitro for production of human–mouse heterohybridoma cells, Bioelectrochemistry (2008), doi:10.1016/j.bioelechem.2008.06.003

larger mouse myeloma cells NS1 as fusion partners. The yield of heterohybridomas is never as good as the yield of mouse–mouse or human–human hybridomas due to the chromosome loss [12]. We succeeded in producing heterohybridomas in the amounts that are comparable to those previously obtained by the means of polyethylene glycol.

Furthermore, we used electrical conditions that were the most successful in the first part of our study. This can be useful for comparing the results but was not necessarily optimal for fusion of human lymphoblasts with NS1 cells. Lymphoblasts are namely approximately twice smaller in diameter than NS1 cells and are therefore less prone to electropermeabilization under the same conditions than larger NS1 cells. For permeabilization of lymphoblasts, we would need higher pulse amplitude or number of pulses than for permeabilization of myeloma NS1 cells [35]. On the other hand, it was shown in the case of primary and transformed human amnion cells that primary cells are more sensitive to electric field than transformed cells [36]. Since lymphoblasts are primary cells, they could be more sensitive to electric field even though they are of smaller size.

In our experiments, we observed that after exposure to electric pulses myeloma cells were in bad shape. That makes us believe that they were seriously damaged by exposure to electric pulses. At the same time, treatments with longer pulses, higher pulse amplitude or more pulses were needed for obtaining hybridoma (Table 3). This supports our conclusion that lymphoblasts were fusogenic only after treatments with longer pulses, larger pulse amplitude or more pulses. We expect that pulses with even larger amplitude could be more successful due to enlarged area of permeabilized membrane [37] but current electrode design and pulse generator limitations did not allow us to use them. If we could use larger amplitudes, we would most probably encounter a problem of viability of the NS1 cells, which were permeabilized at the same time with the lymphoblasts. Therefore, we suggest raise of myeloma cells fraction from half as used in our study to 90% or separate permeabilization of different types of cells and consequent fusion in order to achieve optimal fusogenicity and survival of both fusion partner cells.

Acknowledgements

This research was in part supported by the Agency for Research (ARRS) of the Republic of Slovenia, the Proteus program of scientific, technological and cultural cooperation between CNRS (project no. 5386), France and Ministry for research and higher education (Proteus program), Slovenia and the PICS program between CNRS (project no. 3212), France and Ministry for research and higher education (PICS program), Slovenia. We thank Dr. Justin Teissie for valuable discussion of procedures and results.

References

[1] R. Heller, R.J. Grasso, Transfer of human membrane surface components by incorporating human cells into intact animal tissue by cell-tissue electrofusion in vivo, Biochim. Biophys. Acta 1024 (1990) 185–188.
[2] J. Teissie, Transfer of foreign receptors to living cell surfaces: the bioelectrochemical approach, Bioelectrochemistry and Bioenergetics 46 (1998) 115–120.
[3] X. Wang, H. Willenbring, Y. Akkari, Y. Torimaru, M. Foster, M.A. Dhalimy, E. Lagasse, M. Finegold, S. Olson, M. Grompe, Cell fusion is the principal source of bone-marrow-derived hepatocytes, Nature 422 (2003) 897–901.
[4] G. Vassilopoulos, P.R. Wang, D.W. Russell, Transplanted bone marrow regenerates liver by cell fusion, Nature 422 (2003) 901–904.
[5] M. Alvarez-Dolado, R. Pardal, J.M. Garcia-Verdugo, J.R. Fike, H.O. Lee, K. Pfeffer, C. Lois, S.J. Morrison, A. Alvarez-Buylla, usion of bone-marrow-derived cells with Purkinje neurons, cardiomyocytes and hepatocytes, Nature 425 (2003) 968–973.
[6] P. Kufer, R. Lutterbuese, P.A. Baeuerle, A revival of bispecific antibodies, Trends Biotechnol. 22 (2004) 238–244.
[7] Martin J. Glennie, Peter W.M. Johnson, Clinical trials of antibody therapy, Immunology oday 21 (2000) 403–410.
[8] T.H. Scott-Taylor, R. Pettengell, I. Clarke, G. Stuhler, M.C. La Barthe, P. Walden, A.G. Dalgleish, Human tumor and dendritic cell hybrids generated by electrofusion: potential for cancer vaccines, Biochim. Biophys. Acta 1500 (2000) 265–279.
[9] E. Harlow, D. Lane, Antibodies — Laboratory Manual, Cold Spring Harbor Laboratory, 1988.
[10] L.H. Li, M.L. Hensen, Y.L. Zhao, S.W. Hui, Electrofusion between heterogeneous-sized mammalian cells in a pellet: potential applications in drug delivery and hybridoma formation, Biophys. J. 71 (1996) 479–486.
[11] S.W. Hui, The application of electroporation to transfect hematopoietic cells and to deliver drugs and vaccines transcutaneously for cancer treatment, Technol. Cancer Res. Treat. 1 (2002) 373–384.
[12] M.A. Ritter, H.M. Ladyman, Monoclonal Antibodies, Production, Engineering and Clinical Application, Cambridge University Press, 1995.
[13] P.A. Elder, P.T. Gaynor, J.G. Lewis, P.S. Bodger, L.M. Bason, Generation of monoclonal progesterone antibodies by electrofusion techniques, Bioelectrochem. Bioenerg. 43 (1997) 35–40.
[14] M. Lindner, V. Schirrmacher, Tumour cell–dendritic cell fusion for cancer immunotherapy: comparison of therapeutic efficiency of polyethylen-glycol versus electro-fusion protocols, Eur. J. Clinic. Inv. 32 (2002) 207–217.
[15] J. Teissie, C. Ramos, Correlation between electric field pulse induced long-lived permeabilization and fusogenicity in cell membranes, Biophys. J. 74 (1998) 1889–1898.
[16] C. Ramos, J. Teissie, Tension–voltage relationship in membrane fusion and its implication in exocytosis, FEBS Lett. 465 (2000) 141–144.
[17] M. Reberšek, C. Faurie, M. Kandušer, S. Čorović, J. Teissie, M.P. Rols, D. Miklavčič, Electroporator with automatic change of electric field direction improves gene electrotransfer *in-vitro*, Biomed. Eng. (OnLine) 6 (2007).
[18] B. Valič, M. Golzio, M. Pavlin, A. Schatz, C. Faurie, B. Gabriel, J. Teissie, M.P. Rols, D. Miklavčič, Effect of electric field induced transmembrane potential on spheroidal cells: theory and experiment, Eur. Biophys. J. 32 (2003) 519–528.
[19] T. Kotnik, L.M. Mir, K. Flisar, M. Puc, D. Miklavčič, Cell membrane electropermeabilization by symmetrical bipolar rectangular pulses Part I, Increased efficiency of permeabilization, Bioelectrochemistry 54 (2001) 83–90.
[20] D. Miklavčič, Electrodes and corresponding electric field distribution for effective in vivo electroporation, in: T. Kotnik, D. Miklavčič (Eds.), Medicon 2001, 2001, pp. 5–9.
[21] C. Faurie, E. Phez, M. Golzio, C. Vossen, J.C. Lesbordes, C. Delteil, J. Teissie, M.P. Rols, Effect of electric field vectoriality on electrically mediated gene delivery in mammalian cells, Biochim. Biophys. Acta 1665 (2004) 92–100.
[22] G.B. Melikyan, L.V. Chernomordik, Electrofusion of lipid bilayers, in: E. Neumann, A.E. Sowers, C.A. Jordan (Eds.), Electroporation and Electrofusion in Cell Biology, Plenum Press, New York, 1989, pp. 181–192.
[23] C. Blangero, J. Teissie, Ionic modulation of electrically induced fusion of mammalian-cells, J. Membr. Biol. 86 (1985) 247–253.
[24] M.P. Rols, J. Teissie, Flow cytometry quantification of electroporation, in: M. Jaroszeski, R. Heller (Eds.), Methods in Molecular Biology: Flow Cytometry Protocols, Humana Press, 1998, pp. 141–148.
[25] J. Teissie, M.P. Rols, Fusion of mammalian cells in culture is obtained by creating the contact between cells after their electropermeabilization, Biochem. Biophys. Res. Commun. 140 (1986) 258–266.
[26] A.E. Sowers, A long-lived fusogenic state is induced in erythrocyte ghosts by electric pulses, J. Cell Biol. 102 (1986) 1358–1362.
[27] C. Ramos, D. Bonenfant, J. Teissie, Cell hybridization by electrofusion on filters, Anal. Biochem. 302 (2002) 213–219.
[28] M.P. Rols, J. Teissie, Ionic-strength modulation of electrically induced permeabilization and associated fusion of mammalian cells, Eur. J. Biochem. 179 (1989) 109–115.
[29] M.P. Rols, J. Teissie, Modulation of electrically induced permeabilization and fusion of Chinese hamster ovary cells by osmotic pressure, Biochemistry 29 (1990) 4561–4567.
[30] M. Kanduser, M. Sentjurc, D. Miklavcic, Cell membrane fluidity related to electroporation and resealing, Eur. Biophys. J. 35 (2006) 196–204.
[31] B. Gabriel, J. Teissie, Mammalian cell electropermeabilization as revealed by millisecond imaging of fluorescence changes of ethidium bromide in interaction with the membrane, Bioelectrochem. Bioenerg. 47 (1998) 113–118.
[32] K. Trontelj, M. Reberšek, D. Miklavčič, The tip electrode chamber for small volume electroporation, electrofusion and gene transfection, PCT/SI2007/000036.
[33] M. Schmeer, Elektrische Kenngrossen für die elektroporative Wirkstoff-Einschleusung und den DNA-Transfer in Zentrifugal-Aggregate von CHO-Zellen als Gewebemodell, PhD Thesis. Bielefeld, Bielefeld University, 2004, p 103.
[34] D.J. Prockop, C.A. Gregory, J.L. Spees, One strategy for cell and gene therapy: harnessing the power of adult stem cells to repair tissues, PNAS 100 (2003) 11917–11923.
[35] S. Sixou, J. Teissie, Specific electropermeabilization of leucocytes in a blood sample and application to large volumes of cells, Biochim. Biophys. Acta 1028 (1990) 154–160.
[36] S. Kwee, B. Gesser, J.E. Celis, Electroporation of human cultured cells grown in monolayers Part 3. Transformed cells and primary cells, Bioelectrochem. Bioenerg. 28 (1992) 269–278.
[37] C. Ramos, J. Teissie, Electrofusion: a biophysical modification of cell membrane and a mechanism in exocytosis, Biochimie 82 (2000) 511–518.

Please cite this article as: K. Trontelj, et al., Optimization of bulk cell electrofusion in vitro for production of human–mouse heterohybridoma cells, Bioelectrochemistry (2008), doi:10.1016/j.bioelechem.2008.06.003

(19) REPUBLIKA SLOVENIJA
Urad RS za intelektualno lastnino

(10) SI 22368 A

(12) PATENT

(21) Številka prijave: 200600250

(22) Datum prijave: 25.10.2006

(51) Int. Cl. (2006)
A61N 1/30

(45) Datum objave: 30.04.2008

(72) Izumitelji: TRONTRLJ Katja, Ponova vas 79, 1290 Grosuplje, SI;
REBERŠEK Matej, Orehova ulica 13, 1241 Kamnik, SI;
MIKLAVČIČ Damjan, Benedikova 20, 4000 Kranj, SI

(73) Imetnik: UNIVERZA V LJUBLJANI FAKULTETA ZA ELEKTROTEHNIKO,
Tržaška cesta 16, 1000 Ljubljana, SI

(74) Zastopnik: ITEM d.o.o. Zastopniška pisarna za patente in blagovne znamke, Resljeva 16, 1000 Ljubljana, SI

(54) KONIČASTA KOMORA Z VGRAJENIMI ELEKTRODAMI ZA ELEKTROPORACIJO MANJŠEGA VOLUMNA, ZA ELEKTROFUZIJO IN GENSKO TRANSFEKCIJO

(57) Predmet tega izuma je aparat za elektroporacijo s pipetrom, priprava z več elektrodami z minimiziranim nehomogenim električnim poljem in kompaktnim polnilcem za elektrodne komore za minimiziranje nehomogenega električnega polja. Koničasta komora z vgrajenimi elektrodami je označena s tem, da je odprtina (5) pozicionirana v sredini ohišja (1) in vzdolžni smeri skozi ohišje (1) in da je od dveh do šest elektrod (2) nameščenih paralelno in simetrično v notranjost površine ohišja (1) in vzdolžno k odprtini (5) in da delno segajo v navedeno odprtino (5) ter da imata navedeni elektrodi (2) konektorje (3) za povezavo z zunanjostjo. Opisana je tudi koničasta komora z vgrajenimi elektrodami, pri kateri je kompaktni polnilec (6) vstavljen v navedeno odprtino (5) z luknjo (7), in je v vzdolžni smeri ohišja (1) in kompaktnega filtra (6) nameščenih od dveh do šest elektrod (2) paralelno in simetrično v notranjost stičišča površin ohišja (1) in kompaktnega polnilca (6) ter imata navedeni elektrodi (2) konektorje (3) za povezavo z zunanjostjo.

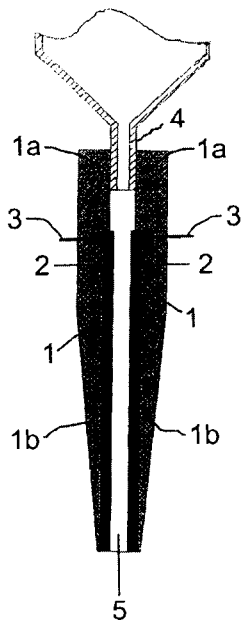

SI 22368 A

KONIČASTA KOMORA Z VGRAJENIMI ELEKTRODAMI ZA ELEKTROPORACIJO MANJŠEGA VOLUMNA, ZA ELEKTROFUZIJO IN GENSKO TRANSFEKCIJO

PODROČJE IZUMA

Predmet tega izuma je aparat za elektroporacijo s pipetrom, priprava z več elektrodami z minimiziranim nehomogenim električnim poljem in kompaktnim polnilcem za komore z vgrajenimi elektrodami za minimiziranje nehomogenega električnega polja.

Ta izum se nanaša na koničasto komoro z vgrajenimi elektrodami za elektroporacijo manjšega volumna, za elektrofuzijo in gensko transfekcijo. Izum spada na področje elektroporacije bioloških celic v suspenziji in, natančneje, na področje tehnik ter priprav za elektroporacijo s ciljem, električno permeabilizirati celično membrano ter, posledično, vstaviti z elektriko katerokoli aktivno farmacevtsko - kemično ali biološko aktivno - substanco, in ciljem genske transfekcije ter celične fuzije. Rezultat izuma so elektrode za hitro in učinkovito elektroporacijo majhnih in kontroliranih volumnov celičnih suspenzij, ki obdržijo svojo visoko sposobnost rasti zaradi minimalnih mehanskih ukrepov in možnosti uporabe električnih impulzov v različnih smereh, s čimer se poveča membransko območje elektroporirane celice in s tem učinkovitost elektroporacije brez bistvene izgube glede preživetja celice.

OZADJE IZUMA

Uporaba elektroporacije

Elektroporacija (imenovana tudi elektropermeabilizacija) celic se aplicira za različne namene, ki uporabljajo permeabilizirano stanje celične membrane.

Električna vsaditev ali električna ekstrakcija predstavljata uvedbo ali ekstrakcijo različnih molekul, kot so zdravila, proteini ali geni, v celice. Vsaditevmajhnih molekul se učinkovito

doseže z uporabo nekaj kratkih pravokotnih impulzov visoke napetosti. Ta način se sedaj učinkovito uporablja v elektrokemoterapiji za uvajanje zdravil v celice tumorja *in situ* pacientov. Elektroekstrakcija se uporablja za ekstrakcijo izdelkov iz kvasa pri postopkih, ki potekajo v nasprotni smeri toka.

Genska elektrotransfekcija *in vitro* ter *in vivo* predstavlja vsaditev plazmidov, ki vsebujejo ustrezni genski material, v celice. DNK je velika molekula, za katero je bilo ugotovljeno, da se jo lahko uspešno vsadi z uporabo eksponencialno razpadajočih impulzov ali kombinacijo krajših impulzov visoke napetosti in daljših impulzov nizke napetosti.

Drugi sorodni postopek je elektrofuzija celic. Sestoji iz dveh stopenj . Ena stopnja povzroči fuzogenizacijo membran s pomočjo elektroporacije, s pomočjo druge pa dosežemo tesne kontakte med celicami. Le-te lahko zagotovimo ali pred elektroporacijo ali kmalu po le-tej (v prvih nekaj minutah), dokler so membrane še v fuzogenem stanju

Mehanska obdelava

Pri veliki večini obstoječih metod za elektroporacijo celic v suspenziji se uporabljata ali komora ali kiveta ali pretočni sistem z enim parom ali več pari ploščatih elektrod. Celična suspenzija ali celice, gojene na podlagi, položimo med elektrodi in čez njiju spustimo napetostni impulz. Celice v suspenziji se ponavadi pipetirajo v elektrodnih komorah ali kivetah ali zunaj enih izmed njih.

Te navedbe predstavljajo mehansko obdelavo, ki je povezana z dvema problemoma. Prvi je občutna izguba volumna, drugi pa, da je pipetiranje škodljivo za celice in bi bilo lahko celo smrtno za določene celične tipe, ki so bolj občutljivi, posebej potem, ko so bili izpostavljeni elektroporaciji.

Elektroporirane celice imajo poškodovane membrane in so bistveno bolj občutljive za pipetiranje, ki na celice pritiska samo s silo. To se pojavlja kot problem npr. pri elektrofuzijskih protokolih, kjer dosežemo medcelični stik po elektroporaciji. Celice je potrebno premikati iz komore k cevi centrifuge z mikropipeto takoj po elektroporaciji.

Majhen volumen

Drug problem je velikost obstoječih komor. Molekule (barvila, plazmidi), uporabljeni pri poskusih, so pogosto dragi in na voljo le v majhnih količinah. Dodatno so celice, ki naj bi jih povezali ali transfektirali, pogosto dragocene in na voljo le v majhnih količinah. Potrebno je torej omogočiti delo z majhnim volumnom.

Za elektroporacijo je pomembno lokalno električno polje. Za nekatere celice, npr. majhne celice, potrebujemo visoko napetost do distančnega kvocienta. To se lahko doseže samo z majhno razdaljo med elektrodama, ker so generatorji elektičnih impulzov omejeni pri napetosti, ki jo lahko generirajo. Problem majhnih distančnih komor ali kivet je raba le-teh brez občutne izgube volumna vzorca. Težko je napolniti takšne komore brez zračnih mehurčkov, ki v znatni meri spremenijo električno razporeditev polja v vzorcu. Napolniti komoro ali kiveto s celično suspenzijo brez zračnih mehurčkov in dobiti ven celično suspenzijo po elektroporaciji je težko, če ne nemogoče. Tudi čiščenje je težavno. Potrebno je omogočiti učinkovito praznjenje, napolnitev in čiščenje majhnega prostora med elektrodama.

Po ameriškem patentnem spisu US6492175 obstaja pretočni sistem, ki omogoča delo z majhnimi volumni in zmanjšuje mehanske manipulacije, vendar omogoča samo obdelavo celic z impulzi v eni ali dveh nasprotnih smereh.

Različne smeri impulzov

Večina obstoječih elektrodnih sistemov dovoljuje uporabo impulzov samo v eni ali večinoma v dveh nasprotnih smereh. Bipolarni impulzi so opisani v mednarodni patentni prijavi WO92/06185. V zadnjih nekaj letih je bilo dokazano, da uporaba impulzov v različnih smereh povzroči učinkovitejšo permeabilizacijo in gensko elektrotransfekcijo. To je pomembno tudi pri celični elektrofuziji in vsaditvi proteinov v membrano. Razlog za to je večja površina elektroporirane membrane, ki se jo lahko doseže s takšnimi impulzi brez bistvene izgube glede celičnega preživetja.

Standardna možnost za povečanje površine elektroporirane membrane celic je povečanje električne moči, kar nezadržno vodi do precejšnjega zmanjšanja celičnega preživetja. Različne

smeri impulzov pa povečujejo območje permeabilizirane membrane, ne da bi znatno vplivale na celično preživetje. Treba je zagotoviti možnost elektrofuzije celične suspenzije, ki bi jo lahko elektroporirali v različnih smereh. Možnost elektroporacije mora biti dana, potem ko zagotovimo celični kontakt ali pred tem.

Patent US6746441 opisuje pretok skozi aparat s komorami z vrtljivimi električnimi polji, ki jih generirata dve ali več kot dve (štiri ali šest) elektrodi. Vendar je to pretok skozi sistem za *ex vivo* gensko terapijo, ki ne dopušča operacij majhnega volumna. Patent US2005048651 opisuje koničaste elektrode, ki vsebujejo tudi različne vrste prevodnih površinskih elektrod. Le-te so predvidene za prehajanje različnih substanc iz notranjosti konice do tarč (celic itd.), ki so zunaj konice in so sinhronizirane na način, da uporabimo električne impulze. Vendar pa ni predvideno, da bi celice vsadili v lumen koničastih elektrod in jih le-tam električno obdelali.

Sočasna elektroporacija za elektrofuzijo

Precejšen problem predstavlja postopek za fuzijo dveh različnih celičnih vrst. To se npr. dogaja pri hibridoma tehnologiji za pridobivanje monoklonalnih protiteles, pri kateri se morajo limfociti B združiti s fuzijskimi partnerji mieloma. Slednji je lahko dvakrat tako velik kot limfociti. Skupna električna obdelava katerekoli od obeh celičnih vrst v tem primeru ni optimalna. Ločena elektroporacija in celično kontaktiranje, ki sledita elektroporaciji, pa sta potrebna za optimalen rezultat fuzijskega postopka. Isti problem je prisoten pri kateremkoli celičnem paru, ki je različno občutljiv za električno polje iz kateregakoli razloga razen različne velikosti.

Kiveta po mednarodni patentni prijavi WO03/050232 vsebuje vsadke podporne strukture, ki drži porozno membrano in omogoča lažjo celično fuzijo na membranski osnovi. V takšni kiveti se obe celični vrsti elektroporirata hkrati. V tem primeru se celice manjše velikosti ali suboptimalno permeabilizirajo ali pa se večje celice poškodujejo. Enak je položaj s sistemoma v skladu z DE10359189 in DE10359190. Tudi v US4882281 in US513470 sta opisani aparaturi za elektroporacijo, s katerima se izognemo mehanski obdelavi, ker celice obdelujemo v posodah s kulturami, čeprav je za nadaljnjo fuzijo ločeno elektroporiranih celic prenos celic še vedno potrebno izvesti s pipetiranjem.

Narava fuzijskega postopka zahteva, da se mora celični kontakt vzpostaviti v kratkem času po elektroporaciji, ko so celične membrane še vedno v tako imenovanem fuzogenem stanju. Pipetiranje celic iz dveh ločenih komor je dodatno k temu, da se inducira mehanski stres, zaradi česar se celice poškodujejo, tudi počasno in predstavlja precejšen problem pri doseganju celičnega kontakta v kratkem času, ki je potreben za učinkovito celično elektrofuzijo.

Polprevodniška notranjost elektrodne koničaste komore

Pred kratkim je bilo dokazano, da je celično preživetje najnižje blizu elektrod. Razlog za to so elektrokemične reakcije, ki nastanejo na meji med elektrodo in medijem. V DE20302861U1 je bilo zato predlagano, da bi elektrode pokrili s tankim slojem prevleke, ki bi bila biološko ustrezna, tako da bi obdržali celice stran od te meje.

Pojavlja pa se drug problem, ki zadeva homogenost in porazdelitev električnega polja med elektrodama. Uporabljeno električno polje (z določenimi električnimi impulzi) ni homogeno na celotnem prostoru med elektrodama, ampak le v srednjem delu tega prostora. Samo celice v srednjem delu so izpostavljene želenemu električnemu polju.

Problem, ki še ni rešen, je elektroporacija vnaprej definiranih majhnih volumnov celic v suspenziji. To bo zmanjšalo stroške ali omogočilo poskuse genske transfekcije, vsaditve proteinov in celične fuzije, kadar je količina proteinov, plazmidov ali celic omejena.

Predmet pričujočega izuma leži v uspešni elektroporaciji celic z impulzi, ki dosežejo celico v različnih smereh, s čimer je hkrati z možnostjo hitre obdelave celic dosežena minimalna mehanska obremenjenost celic.

Nadaljnji predmet sedanjega izuma je, da zgradimo aparaturo za elektroporacijo, ki bi omogočala celično fuzijo, *in vitro*. Nadalje je predmet sedanjega izuma postopek za fuzijo dveh različnih vrst celic, ki ga omogoča ločena ektroporacija z različnimi vrednostmi električnih parametrov.

Po pričujočem izumu je možno predvideti tudi načrt notranjosti koničaste komore z vgrajenimi elektrodami s prevodnostjo, ki je primerljiva s prevodnostjo medija celične suspenzije. To zagotavlja zadrževanje celic na centralnem področju komore in dosego želenega homogenega električnega polja na tem področju.

POVZETEK IZUMA

Po sedanjem izumu je možno celice zadržati v osrednjem predelu lumna z uporabo npr. polprevodniškega materiala ali sestavljenega materiala prevodnosti, ki je primerljiv s prevodnostjo medija celične suspenzije v lumnu komore z vgrajenimi elektrodami. Na ta način zagotovimo homogenost polja zaradi prevodnosti, ki je podobna prevodnosti medija celične suspenzije.. Torej je prvi cilj sedanjega izuma, da bi po le-tem pripravili komoro z vgrajenimi elektrodami za elektroporacijo majhnih kontroliranih volumnov celic z minimalno mehansko obdelavo in posledično minimalno mehansko obremenitvijo.

Opisani izum omogoča hitro obdelavo različnih vrst celic na različne načine z elektriko, t.j. z različnimi vrednostmi parametrov električnega polja. Izum nadalje daje možnost uporabe električnih impulzov v več smereh, s čimer se poveča membransko področje elektroporiranih celičnih membran.

KRATEK OPIS SLIK

Sl. 1 je shematski prikaz prečnega prereza skozi koničasto komoro z vgrajenimi elektrodami, na pipetru 4.; elektrodi 2 sta nameščeni na notranjo stran ohišja 1 in električno povezani z zunanjostjo 3;

Sl. 2 predstavlja pogled prečnega prereza koničaste komore z vgrajenimi elektrodami;

Sl. 3 prikazuje možne smeri električnega polja v lumnu komore z vgrajenimi elektrodami v eni legi elektrod;

Sl. 4 prikazuje koničasto komoro z vgrajenimi elektrodami, delno napolnjene z materialom 6 in prevodnostjo, ki je primerljiva s prevodnostjo medija celične suspenzije.

PODROBEN OPIS IZUMA

Koničasta komora z vgrajenimi elektrodami sestoji iz ohišja 1, elektrod 2 in električnih konektorjev 3 za povezavo z zunanjostjo. Ohišje 1 je izdelanoiz neprevodnega materiala, kot je polimetil-metakril (PMMA), ali plastičnih materialov. Elektrodi 2 in električni konektorji 3 so izdelani iz električno prevodnega materiala, kot so kovine ali njihove zlitine, ali npr. grafita.

Gornji del 1a ohišja 1 koničaste komore z vgrajenimi elektrodami je zasnovan tako, da se prilega pipetru 4. Pipeter 4 navadno posrka 1 µl to 100 µl tekočine. Vendar pipeter 4 ni predmet tega izuma. Zunanja oblika spodnjega dela 1b ohišja 1 je koničen, tako da se ga laže uporablja s standardno laboratorijsko opremo, kot so centrifugalne cevi. Po vsem ohišju 1 je po sredini odprtina 5. Skozi to odprtino 5 se celična suspenzija posesa v komoro igelne elektrode in se po opravljeni elektroporaciji izpiha iz koničaste komore z vgrajenimi elektrodami s pipetrom 4. Ko se celična suspenzija posesa, se le-to da v odprtino, kjer sta nameščeni elektrodi 2. Odprtina 5 med elektrodama določa največji volumen enakomerno obdelanih celic. Maksimalni volumen celične suspenzije, ki se ga da vstaviti, tako leži v razmerju, ki je omejeno s konstrukcijskimi možnostmi. Konstrukcija dovoljuje maksimalno prostornino od 10 µl do 2500 µl, večinoma od 10 µl do 1000 µl. Vendar lahko realno prostornino enakomerno obdelanih celic izberemo ustrezno za vsak poskus preprosto z nastavitvijo pipetra.

Oblika prereza odprtine 5 med elektrodama je predvsem odvisna od števila elektrod 2. Če se uporabita dve elektrodi 2, je prečni prerez odprtine 5 načelno pravokoten. Če se uporabijo tri ali več elektrod 2, je prerez odprtine 5 načeloma enakostranične oblike s številom stranic, kakršno je število elektrod 2. Torej, če se uporabljajo tri elektrode, je oblika prečnega prereza odprtine 5 načeloma enakostranični trikotnik; če se uporabijo štiri elektrode 2, je oblika prečnega prereza odprtine 5 načeloma enakostranični četverokotnik oz. kvadrat, itd. Če se uporabijo tri elektrode ali več, so stranice odprtine 5 rahlo konkavne zaradi minimizacije nehomogenosti električnega polja v odprtini 5. Ta konkavnost lahko znaša do 20 % dolžine stranice.

Več elektrod 2 je nameščenih paralelno in simetrično na notranjo površino ohišja 1 in vzdolžno na odprtino 5. Konstrukcija dovoljuje dolžino elektrod 2 od 5 mm do 60 mm, večinoma od 10 mm do 40 mm. Število elektrod 2 lahko variira med dvema do šest elektrod; to število je lahko liho ali sodo. Število elektrod 2 vpliva na število različnih smeri električnega polja, ki ga uporabimo. Npr., štiri elektrode 2, nameščene v kotih kvadranta, dovoljujejo uporabo impulzov v osem različnih smereh (IB in ET, BI in IE, IT, TI, BE, EB, IE in BT, EI in TB). Smeri so razvidne s sl. 3a, 3b in 3c. S številom elektrod se povečuje število različnih smeri električnega polja.

Podrobna zasnova odprtine 5 in elektrod 2 je v veliki meri odvisna od oblike prečnega prereza elektrod 2. Obstajajo tri glavne opcije oblike prečnega prereza elektrod 2: pravokotna, krožna oblika ali na eni strani eliptična, parabolična oz. hiperbolična oblika, in na drugi strani poljubna oblika. Če se uporabita samo dve elektrodi, je oblika prednostno pravokotna za dosego najbolj homogenega električnega polja v odprtini 5, uporabijo pa se lahko tudi druge oblike, omenjene pred tem. Če se uporabita dve elektrodi, je oblika elektrod navadno v obliki kroga, ker jih je laže proizvesti; lahko pa se uporabljajo tudi eliptične, parabolične ali hiperbolične oblike ene strani. Za več kot dve elektrodi pa se lahko uporabi tudi pravokotna oblika, le da je pri tem homogenost električnega polja zelo nizka.

Večino površine omenjenih elektrod 2 navadno vdelamo v material ohišja 1, toda manjši del elektrod 2 po navadi gleda iz materiala ohišja 1. Omenjeni manjši deli so v direktnem kontaktu s celično suspenzijo, ko jo posesamo v odprtino 5 ohišja 1. Kadar uporabimo pravokotni obliki elektrod 2, prednostno vdelamo tri od štirih ravnih presekov elektrode 2 v material ohišja 1 in prednostno eno od štirih ravnin štrli ven iz materiala ohišja 1. Elektrodi 2 pravokotne oblike lahko namestimo simetrično v centre ali prednostno lahko tri ali več elektrod 2 namestimo v kotne točke roba enakostranične oblike odprtine 5. Kadar uporabimo druge oblike elektrod 2, omenjene zgoraj, del površine, vdelane v material ohišja 1, zavisi od števila elektrod 2. Kadar apliciramo dve elektrodi 2 krožne oblike, ležijo njuni centri simetrično s centrom roba oblike prečnega prereza odprtine 5, in prednostno je 180° elektrod 2 vdelanih v material ohišja 1 ter prednostno 180° elektrod 2 gleda ven iz materiala ohišja 1. Kadar so uporabljene tri ali je uporabljenih več elektrod 2 krožne oblike, so njihovi centri pozicionirani na kotnih točkah prečnega prereza oblike odprtine 5, pri čemer so njihovi deli, ki štrlijo iz materiala ohišja 1, prednostno isti kot notranji koti enakostraničnega načrta odprtine 5. Torej, če se uporabijo tri

elektrode 2 krožne oblike, 60° elektrod 2 prednostno gleda ven iz materiala ohišja 1 in je prednostno 300° elektrod 2 vdelanih v material ohišja 1; če so uporabljene štiri elektrode krožne oblike, gleda prednostno 90° elektrod 2 iz ohišja 1 in je prednostno 270° elektrod 2 vdelanih v material ohišja 1, itd. Kadar uporabimo eliptično,
parabolično ali hiperbolično enostranično obliko elektrod 2, morajo biti te specifične oblike usmerjene v center prečnega prereza oblike odprtine 5. Poljubna forma enostranične eliptične, parabolične ali hiperbolične oblike elektrod 2 je prednostno popolnoma vdelana v material ohišja 1. Tako je ta poljubna oblika navadno profil v obliki črke T za dosego močnega kontakta med elektrodama 2 in ohišjem 1. Eliptične, parabolične ali hiperbolične oblike ene strani elektrod 2 prednostno vse gledajo ven iz materiala ohišja 1. Kadar sta uporabljeni dve eliptični, parabolični ali hiperbolični enostranični obliki elektrod 2, sta navadno pozicionirani v center roba prečne oblike odprtine 5. Če so uporabljene tri oblike ene strani elektrod 2 ali je uporabljenih več eliptičnih, paraboličnih ali hiperboličnih enostraničnih oblik elektrod 2, so prve navadno pozicionirane v kotnih točkah prečne oblike odprtine 5.

Premer elektrod 2 in razdalja med njima vplivajo na homogenost električnega polja odprtine 5. Ta vpliv ni tako očiten, kadar uporabimo dve elektrodi 2 pravokotne oblike. Torej je pri dveh elektrodah pravokotne oblike razmerje med premerom in razdaljo med elektrodama 2 poljubno. Premer lahko variira od 0,5 do 7 mm in razdalja med njima lahko variira od 0,5 do 6 mm. Izbira je odvisna od največjega volumna enakomerno obdelanih celic in želenem razmerju med napetostjo in razdaljo. Kot je omenjeno zgoraj, se največji volumen enakomerno obdelanih celic definira kot volumen odprtin 5 med elektrodama in je posledično odvisen od dolžine, premera in razdalje med elektrodama 2. Pri dveh elektrodah pravokotne oblike je največji volumen enakomerno obdelanih celic zmnožek dolžine, premera in razdalje med elektrodama 2. Želeno razmerje med napetostjo in razdaljo je predvsem odvisno od vrste celice in cilja elektroporacije in se določi eksperimentalno. Želeno razmerje med napetostjo in razdaljo variira od 200V/cm do 4000 V/cm, večinoma od 500 V/cm do 1500 V/cm. Generatorji za elektroporacijo običajno generirajo električne impulze do 100 V. Torej mora biti razdalja med elektrodama 2 tako zasnovana, da lahko dosežemo želeno razmerje med napetostjo in razdaljo. Kot primer, če uporabljeni generator za elektroporacijo generira impulze do 200 V in znaša zaželeno razmerje med napetostjo ter razdaljo 1000 V/cm, razdalja med elektrodama 2 ne sme biti večja kot 2 mm. Generator pa ni predmet izuma. Za dve elektrodi 2 krožne oblik lahko premer variira od 0,5 do 5 mm in razdalja med njima lahko variira od 0,5 do 6 mm. Razmerje med premerom in razdaljo

med elektrodama 2 krožne oblike naj bo tako velika, kot je le možno, da bi dosegli najbolj homogeno električno polje v odprtini 5.

Kadar uporabimo tri ali več elektrod 2, naj bo za dosego najbolj homogenega električnega polja linearna prevodnost najkrajše linije sile med električno nasprotnima elektrodama 2 enaka kot linearna prevodnost linije sile med električno nasprotnima elektrodama 2, ki teče skozi center prečnega preseka oblike odprtine 5. Linearna prevodnost je integral gostote toka, ki je razdeljena z električnim poljem nad linijo, ki je v tem primeru linija sile. Električno nasprotni elektrodi sta elektrodi 2, ki sta med elektroporacijo nabiti z različnim električnim potencialom. Elektrodi 2 sta navadno simetrično nabiti z različnim električnim potencialom. Za tri elektrode pravokotne oblike naj bi bilo razmerje med premerom in razdaljo med najbližjima elektrodama 2 približno 0,3. Razdalja med najbližjima elektrodama 2 lahko variira med 0,25 do 3 mm. Za štiri elektrode 2 pravokotne oblike naj bi bilo razmerje med premerom in razdaljo med nasprotnima elektrodama 2 približno 0,3. Razdalja med nasprotnima elektrodama 2 lahko variira med 0,5 do 6 mm. Za pet elektrod 2 pravokotne oblike naj bi bilo razmerje med premerom in razdaljo med najbližjim elektrodama 2 približno 0,5. Razdalja med najbližjima elektrodama 2 lahko variira od 0,25 do 3 mm. Za šest elektrod 2 pravokotne oblike naj bi bilo razmerje med premerom in razdaljo med nasprotnima elektrodama 2 približno 0,2. Razdalja med nasprotnima elektrodama 2 lahko variira med 0,5 do 6 mm. Za tri elektrode 2 krožne oblike naj bi bilo razmerje med premerom in najbližjima elektrodama 2 približno 1,2. Razdalja med najbližjima elektrodama lahko variira od 0,25 do 2,5 mm. Za štiri elektrode krožne oblike naj bi razmerje med premerom in razdaljo med nasprotnim elektrodama 2 znašalo približno 0,7. Razdalja med nasprotnima elektrodama 2 lahko variira od 0,5 do 5 mm. Za pet elektrod 2 krožne oblike naj bi razmerje med premerom in razdaljo med najbližjima elektrodama 2 znašalo 1. Razdalja med najbližjima elektrodama lahko variira od 0,25 do 2,5 mm. Za šest elektrod 2 krožne oblike naj bi razmerje med premerom in razdaljo med nasprotnim elektrodama 2 znašalo približno 0,3. Razdalja med nasprotnima elektrodama 2 lahko variira od 0,5 do 5 mm.

Kadar se uporabijo eliptične, parabolične ali hiperbolične oblike ene strani elektrod 2, se razmerje med parametri oblike ene strani in razdaljo med elektrodama 2 določi numerično. Krožna oblika elektrod 2 se uporabi kot baza v numeričnem modelu. Eliptična, parabolična ali hiperbolična enostranična oblika se potem doda krožni obliki numeričnega modela, tako da je integral "razdalje Manhattan" med dvema oblikama v polarnih koordinatah nad obliko, ki bo v

direktnem kontaktu s celično suspenzijo, najmanjši. Ohišje 1 in odprtina 5 s celično suspenzijo sta na osnovi materialne prevodnosti dodana v numerični model. Nadalje se električno polje med elektrodama 2 eliptične, parabolične ali hiperbolične oblike ene strani izračuna po metodi končnih elementov (FEM). Ocenitev homogenosti električnega polja je izračunana po integralu absolutne napake (IAE) med srednjo vrednostjo električnega polja v odprtini 5 in dejansko vrednostjo električnega polja na določeni točki celotne odprtine 5. Parametre eliptične, parabolične ali hiperbolične oblike ene strani nato iterativno spremenimo, tako da je ocena homogenosti električnega polja minimizirana. Parametri eliptične oblike ene strani so glavna os, krajša os in premik, parametri parabolične oblike ene strani so fokus in premik in parametri hiperbolične oblike ene strani so polovična glavna os, polovična krajša os in premik. Parameter premika je enak premiku oblike iz začetne lege oblike pred minimizacijo ocene homogenosti električnega polja. Na tak način se dobljene oblike potem uporabijo za izdelavo elektrod 2.

Po drugem izvedbenem primeru se zasnova treh elektrod 2 lahko uporabi tudi pri katerikoli komori elektrode za minimizacijo nehomogenega električnega polja med elektrodama. V tem primeru naj bi bilo razmerje med premerom in razdaljo med najbližjima ali nasprotnima elektrodama enako, kot je bilo prej opisano za pravokotno oz. krožno obliko elektrod. Za eliptične, parabolične ali hiperbolične oblike ene strani elektrod naj bi uporabili enake postopke za določitev najprimernejše oblike elektrod glede homogenosti električnega polja med elektrodama v skladu s prejšnjim opisom.

Elektrode so zgoraj povezane z zunanjostjo elektrodne koničaste komore, tako da jih lahko priključimo na generator električnih impulzov. Generatorji navadno generirajo kvadrataste, sinusoidalne in/ali eksponencialne električne impulze do 1000 V s trajanjem do 10 s. Kot je omenjeno zgoraj, generator ni predmet izuma. Električne povezave z zunanjostjo so izvedene z elektrodami v obliki krivulje in/ali dodatno žico 3.

Koničasta komora z vgrajenimi elektrodami za elektroporacijo po izumu je označena s tem, da je odprtina 5 pozicionirana v sredini ohišja 5 in v vzdolžni smeri skozi ohišje 1 in da je od dveh do šest elektrod nameščenih paralelno in simetrično na notranjo površino ohišja 1 in vzdolžno z odprtino 5 ter delno sega do omenjene odprtine 5, in da imata omenjeni elektrodi 2 konektorje 3 za povezavo z zunanjostjo.

V nadaljnjem izvedbenem primeru lahko za minimiziranje električnega polja v celični suspenziji kompaktni polnilec 6 vsadimo v koničasto komoro z vgrajenimi elektrodami ali katerekoli drugo komoro z vgrajenimi elektrodami, kot je prikazano na sl. 4. Kompaktni polnilec 6 sestoji iz prevodnega materiala, ki ima prevodnost, primerljivo prevodnosti medija celične suspenzije (0.001 S/cm do 10 S/cm) tako kot npr. določeni polprevodniški elementi (Si, Ge) in njihove spojine ali zlitine ali spojine s kovinami ali zlitine s kovinami ali katerikoli drugi materiali v trdnem stanju s prevodnostjo v določenem razponu. Dolžina trdnega polnilca 6 je prednostno enaka kot dolžina elektrod. Oblika prečnega prereza trdnega polnilca 6 je prednostno enaka kot oblika prečnega prereza odprtine, tako da kompaktni polnilec 6 sede v odprtino in ima dober stik z elektrodami. Kompaktni polnilec 6 vstavimo v odprtino in pozicioniramo med elektrode. Največji volumen celične suspenzije, ki ga lahko vstavimo, je tako manjši kot odprtina med elektrodami in je enak kot volumen luknje 7, opisane spodaj. Kompaktni polnilec 6 mora biti zasnovan tako natančno, da ga je potrebno hladiti pred vstavljanjem. Posledično mora imeti dober stik z elektrodami, da ne izpade, potem ko se je ogrel. Da bi preprečili izpad trdnega polnilca 6, lahko le-tega tudi prilepimo na ohišje 1. Vzdolžno skozi celotni kompaktni polnilec 6 je v sredini luknja 7, ki je z navedenim materialom ločena od elektrod. Premer luknje 7 lahko variira od 1 mm do premera kroga, ki ga vnesemo v obliko prečnega prereza trdnega polnilca 6, zmanjšanega za 2 mm. V tem primeru je električno polje v luknji 7 skoraj popolnoma homogeno, ker je skoraj celotna nehomogenost porazdeljena znotraj trdnega polnilca 6, ki se nahaja na zunanjih delih prostora med elektrodama. Za koničasto komoro z vgrajenimi elektrodami ali katerokoli drugo komoro z vgrajenimi elektrodami in s kompaktnim polnilcem se prednostno uporablja pravokotna oblika elektrod za dosego dobrega električnega stika med elektrodami in kompaktnim polnilcem.

Koničasta komora z vgrajenimi elektrodami po izumu je označena s tem, da je odprtina 5 pozicionirana v sredini ohišja 1, medtem ko je kompaktni polnilec 6 vstavljen v omenjeno odprtino 5 z luknjo 7 v vzdolžni smeri ohišja 1 in je dve do šest elektrod 2 nameščenih vzporedno in simetrično v stik s površinami ohišja 1 ter trdnega polnilca 6, in imata elektrodi 2 električne elemente 3 za stičišče z zunanjostjo.

Koničasta komora z vgrajenimi elektrodami se preprosto pripne na pipeter 4 ali odpne od le-tega na enak način kot igle, uporabljene za pipetiranje. Po namestitvi koničaste komore z vgrajenimi elektrodami se celična suspenzija vsrka v koničasto komoro z vgrajenimi elektrodami in

priključi se generator za generiranje električnih impulzov. Med pulziranjem se vzpostavi elektroporacija. Po končani pulzaciji se celična suspenzija s pipetrom izpiha iz koničaste komore z vgrajenimi elektrodami. Sedanji izum omogoča elektroporacijo za dosego električne fuzije celic, genske transfekcije celic in elektroporacijo celic.

Čas postopka za pulziranje enega volumna celične suspenzije z omenjeno koničasto komoro z vgrajenimi elektrodami je minimiziran, ker je potrebno precej manj pipetiranja kot pri pulziranju celic v komorah, ki jih je potrebno napolniti z ločenim pipetrom. Polnitev koničaste komore z vgrajenimi elektrodami je enostavna, pri čemer ne nastanejo mehurčki v suspenziji. Minimizirana je torej tudi mehanska obdelava. Čiščenje komore z vgrajenimi elektrodami se tudi enostavno izvede s potiskom čistilne raztopine nekajkrat navzgor in navzdol. Konico lahko steriliziramo z avtoklavom ali drugimi sredstvi v odvisnosti od uporabljenega materiala.

PATENTNI ZAHTEVKI

1. Koničasta komora z vgrajenimi elektrodami za elektroporacijo za namene električne fuzije celic v suspenziji, genske transfekcije celic v suspenziji ali elektroporacije celic v suspenziji, pri kateri je predvidena komora za natančno vstavitev v pipeter, označena s tem, da je odprtina (5) pozicionirana v sredini ohišja (1) in v vzdolžni smeri skozi ohišje (1) in da je od dveh do šest elektrod (2) nameščenih paralelno in simetrično na notranjo površino ohišja (1) in vzdolžno z odprtinio (5) ter delno sega v navedeno odprtino (5), in da imajo omenjene elektrode (2) konektorje (3) za povezavo z zunanjostjo.

2. Koničasta komora z vgrajenimi elektrodami po zahtevku 1, označena s tem, da ima ohišje (1) gornji del (1a) cilindrične oblike in spodnji del (1b) konične oblike, pri čemer je v osi omenjenega ohišja (1) predvidena odprtina (5), ki je na zgornji strani zasnovana tako, da se prilega pipetru.

3. Koničasta komora z vgrajenimi elektrodami po zahtevku 1, označena s tem, da je ohišje (1) izdelano iz neprevodnega materiala.

4. Koničasta komora z vgrajenimi elektrodami po zahtevku 1, označena s tem, da so elektrode (2) vstavljene v material ohišja (1).

5. Koničasta komora z vgrajenimi elektrodami po zahtevku 1, označena s tem, da je oblika elektrod pravokotna, krožna ali z ene strani eliptična, parabolična ali hiperbolična.

6. Koničasta komora z vgrajenimi elektrodami po zahtevku 1, označena s tem, da sta navedeni elektrodi (2) izdelani iz prevodnega materiala.

7. Koničasta komora z vgrajenimi elektrodami po zahtevku 1, označena s tem, da so konektorji (3) za povezavo z zunanjostjo predvideni na zgornjem delu elektrod (2).

8. Koničasta komora z vgrajenimi elektrodami za elektroporacijo za dosego električne fuzije celic v suspenziji, genske transfekcije celic v suspenziji ali elektroporacije celic v suspenziji, pri čemer je predvidena komora za namestitev, prilegajočo se pipetru (4), označena s tem, da je odprtina (5) pozicionirana v sredini ohišja (1) in da je kompaktni polnilec (6) vstavljen v navedeno odprtino (5) z luknjo (7) in je v vzdolžni smeri ohišja (1) in kompaktnega filtra (6) nameščenih od dveh do šest elektrod (2) paralelno in simetrično v notranjost stičišča površin ohišja (1) in kompaktnega polnilca (6) ter da imata navedeni elektrodi (2) konektorje (3) za povezavo z zunanjostjo.

9. Koničasta komora z vgrajenimi elektrodami po zahtevku 8, označena s tem,da ima ohišje (1) gornji del (1a) cilindrične oblike in spodnji del (1b) konične oblike, pri čemer je v osi omenjenega ohišja (1) odprtina (5), predvidena na gornji strani tako, da se prilega pipetru (4).

10. Koničasta komora z vgrajenimi elektrodami po zahtevku 8, označena s tem, da je ohišje (1) izdelano iz neprevodnega materiala.

11. Koničasta komora z vgrajenimi elektrodami po zahtevku 8, označena s tem, da je kompaktni polnilec iz prevodnega materiala, ki je primerljiv prevodnosti medija celične suspenzije.

12. Koničasta komora z vgrajenimi elektrodami po zahtevku 8, označena s tem, da sta elektrodi (2) vstavljeni v material ohišja (1) v stičišču površin ohišja (1) in kompaktnega polnilca (6).

13. Koničasta komora z vgrajenimi elektrodami po zahtevku 8, označena s tem, da je oblika elektrod pravokotna, krožna ali z ene strani eliptična, parabolična ali hiperbolična.

14. Koničasta komora z vgrajenimi elektrodami po zahtevku 8, označena s tem, da sta omenjeni elektrodi (2) izdelani iz prevodnega materiala.

15. Koničasta komora z vgrajenimi elektrodami po zahtevku 8, označena s tem, da so električni kontakti (3) za povezavo z zunanjostjo izdelani na vrhu elektrod (2).

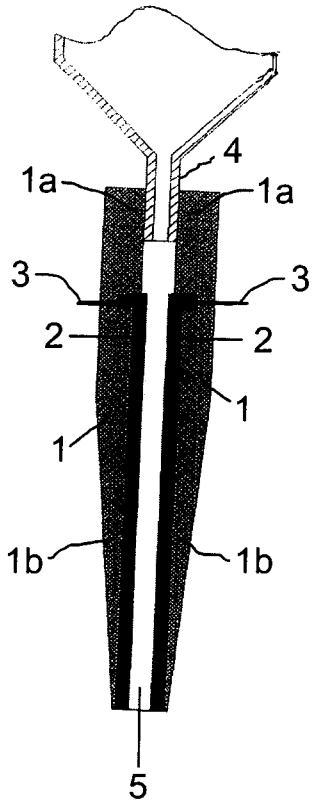

Sl. 1

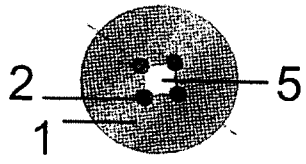

Sl. 2

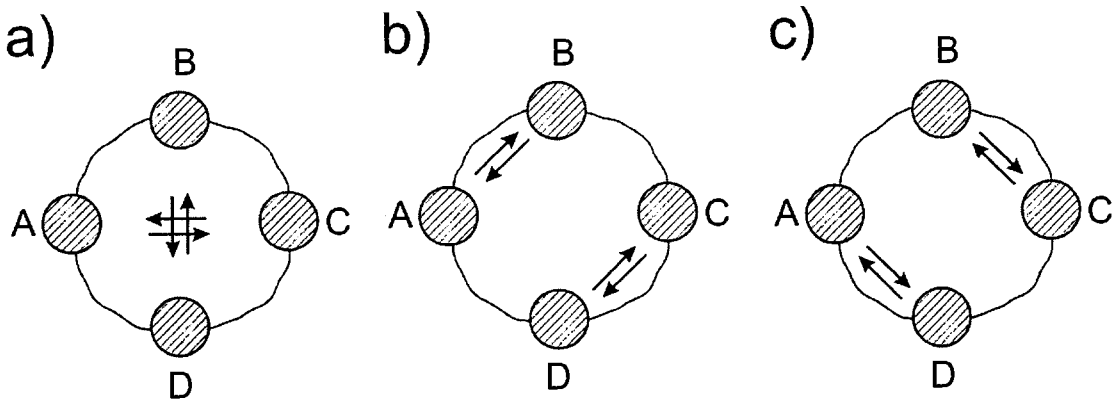

Sl. 3

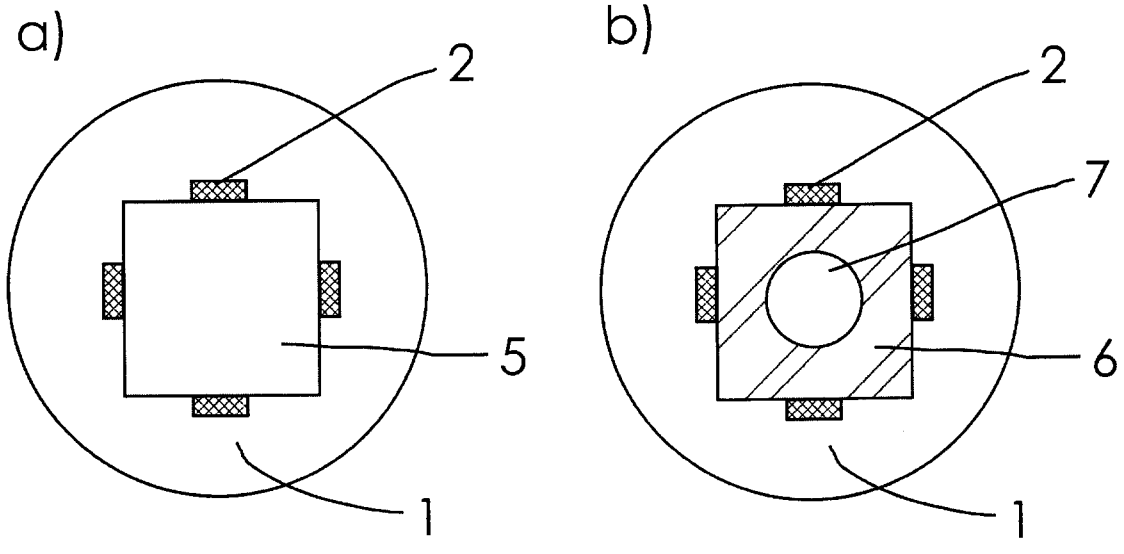

Sl. 4

Izjava

Izjavljam, da sem doktorsko disertacijo izdelal samostojno pod mentorstvom prof. dr. Damijana Miklavčiča, univ. dipl. inž. el. Pomoč ostalih sodelavcev sem v celoti navedel v zahvali.

Matej Reberšek